DERIVING INDUCED PLURIPOTENT STEM CELLS FROM ACUTE MYELOID LEUKEMIA PATIENTS TOWARDS APPLICATIONS OF AUTOLOGOUS THERAPIES AND DISEASE MODELING

BY
DEANNA P PORRAS M.Sc., B.Sc.

A Thesis

Submitted to the School of Graduate Studies

In Partial Fulfillment of the Requirements

For the Degree

Doctor of Philosophy

McMaster University

Descriptive Note

York University BACHELOR OF SCIENCE (2012) Toronto, Ontario (Kinesiology)

York University MASTER OF SCIENCE (2015) Toronto, Ontario (Kinesiology)

DOCTOR OF PHILOSOPHY (2022)

McMaster University, Biochemistry and Biomedical Sciences

Hamilton, Ontario, Canada

TITLE:	Deriving induced pluripotent stem cells from acute myeloid leukemia patients towards applications of autologous therapies and disease modeling
AUTHOR:	Deanna P Porras, M.Sc., B.Sc.
SUPERVISOR:	Dr. Mickie Bhatia
NUMBER OF PAGES:	188

LAY ABSTRACT

A diagnosis of Acute Myeloid Leukemia (AML) varies from patient to patient, as there are many different subtypes of this cancer. This is referred to as 'patient cancer heterogeneity'. AML represents one of the most heterogeneous types of cancers, and unfortunately, only 20% of AML patients survive past five years from diagnosis. AML is a cancer of the blood system that causes the bone marrow to fill up with immature cells that are unable to develop into functional blood cells. The ability to reprogram AML patient cells into induced pluripotent stem cells (iPSCs), which can give rise to any cell in a dish, provides an opportunity to study this disease. Our research proposal is to develop a diverse library of AML patient-derived iPSCs providing a unique alternative approach to interrogate the therapeutic potential, heterogeneity, and molecular basis of AML that "drive" the disease to continue which cannot be captured and studied in existing in vitro or animal models of the disease.

ABSTRACT

Acute myeloid leukemia (AML) is a highly heterogeneous cancer with a poor prognosis. Clinical presentation is characterized by the abundant non-functional immature hematopoietic cells (blasts) in the bone marrow (BM) and peripheral blood (PB) of patients. Untreated, the rapid proliferation of these blasts contributes to hematopoietic system failure within months, leading to death. Although the standard chemotherapy regimen has remained relatively unchanged for decades and has proven to be effective at achieving initial remission induction, most patients succumb to relapse forming the basis of poor long-term survival. Incomplete mechanistic understandings of disease initiation, progression and maintenance of AML have impeded advances in therapy required for the improvement of long-term patient survival rates. This suggests that innovative and new model systems are required to understand the earliest initiation processes of AML disease towards more effective targeted therapy development. The ability to generate induced pluripotent stem cells (iPSCs) from human somatic cells provided a breakthrough in biomedicine to 'capture' diseased cells and their genome in a self-renewing state. Patient-derived human induced pluripotent stem cells (hiPSCs) have the theoretical ability to develop patient-specific (autologous) cell-based therapies and/or produce an endless number of specialized disease-associated cells, allowing replication of pathological characteristics of human disease *in vitro.* Despite the technical challenge of reprogramming human cancer cells due to the high inefficiency of the process compared to healthy samples, whereby iPSCs are often skewed in favor of residual normal cells over cells of the premalignant or malignant clone, **I propose to develop a library of AML patient-derived iPSCs. Moreover, I hypothesize that pluripotent reprogramming can provide a unique alternative approach to dissect heterogeneity and molecular basis of AML that cannot be captured and studied in existing *in vitro* or *in vivo* patient-derived xenograft models. Additionally, I seek to investigate the ability of human iPSCs in the derivation of HSCs as a proof of concept for autologous cell-based therapies.**

ACKNOWLEDGEMENTS

First and foremost, I would like to thank my supervisor Dr. Mick Bhatia. Mick, I honestly cannot put into words my genuine gratitude for everything you have done over the years both personally and scientifically. You truly are an incredible supervisor and have helped me through the extreme highs and lows of this degree. Thank you for not only accepting my "sassinness" and directness, but for being an exceptional mentor. Thank you for being available 24/7 be that responding to my emails at 3:30am or chatting on the phone till 10:30 at night about some exciting data or a new publication that scooped us. I have learned so much from you and I will forever be grateful for that and will carry forward the lessons you taught me.

I would also like to thank my committee members, Drs. Kristin Hope, Brian Leber and Tobias Berg, who have done an excellent job advising me during my graduate studies. I have the utmost respect and admiration of each of you, and I am forever grateful to have had such a positive and supportive team.

To my lab family – the OG members (Borko, Luca, Jenn, Lili, Ryan, Gena, Diana and Meaghan) and the current members (Charisa, Shirley, Sean, Cam, Alice and Amro) and newest members (Cyrielle, Ekta, Aaida, David, Michela and Amy) and any alumni I may have missed – THANK YOU for making my lab experience truly a dream. I will forever cherish the many memories and I am extremely grateful I got to spend the past 6 years surrounded by such an amazing group of people.

I would like to say a special thank you to Dr. Allison Boyd. Thank you for being not only an amazing friend but for being a person I can count on no matter what throughout this challenging process. From our 5-hour phone calls to messaging on WhatsApp at all hours of the day I will forever appreciate your help and guidance during my time in the lab.

To my husband, Trevor Teich – I know I would never have completed this degree without your unconditional support. From reading and editing my reports, to listening to my presentation and providing excellent feedback, this degree in many ways is as much yours as it is mine. I love you with all my heart and cannot wait for our bundle of joy to enter this world in November 2022. When he is old enough, I know we will both encourage him to read this ☺ To the two bundles of joy that we lost towards the end of this degree you both will forever be remembered as a part of this process.

Finally, I would like to thank my family and friends who at times did not think I would complete this degree but still supported and encouraged me to make it to the finish line.

TABLE OF CONTENTS

LIST OF FIGURES AND TABLES

Chapter 1

Chapter 2

Chapter 3

Chapter 4

Chapter 5

LIST OF ABBREVIATIONS

5-Aza	5-Azacytidine
7TF	ERG, HOXA5, HOXA9, HOXA10, LCOR, RUNX1, SPI1
AGM	Aorta-Gonad-Mesonephros
AML	Acute Myeloid Leukemia
APL	Acute Promyelocytic Leukemia
ARMS	Amplification Refractory Mutation System
ATRA	All-Trans Retinoic Acid
bFGF	Basic Fibroblast Growth Factor
BM	Bone Marrow
Cas9	CRISPR associated protein 9
CB	[Umbilical] Cord Blood
CD	Cluster of Differentiation
CFU	Colony Forming Unit
CFU-E	Colony Forming Unit-Erythroid
CFU-G	Colony Forming Unit-Granulocyte
CFU-GEMM	Colony Forming Unit-Granulocyte, Erythroid, Macrophage, Megakaryocyte
CFU-GM	Colony Forming Unit-Granulocyte, Macrophage
CFU-M	Colony Forming Unit-Macrophage
CLP	Common Lymphoid Progenitor
CML	Chronic Myelogenous Leukemia
CMP	Common Myeloid Progenitor
CR	Complete Remission
CRISPR	Clustered Regularly Interspaced Short Palindromic Repeats
CSC	Cancer Stem Cells
ddPCR	Digital Droplet PCR
DMT1	DNA Methyltransferase 1
DNMT	DNA Methyltransferase
DNA	Deoxyribonucleic acid
EB	Embryoid Body
ECC	Embryonal Carcinoma
EHT	Endothelial-to-Hematopoietic
ELN	European Leukemia Net
FAB	French-American-British
FACS	Fluorescence Activated Cell Sorting
FBS	Fetal Bovine Serum
FLT3L	Fms-like tyrosine kinase receptor 3 ligand
FISH	Fluorescence In Situ Hybridization
G-CSF	Granulocyte colony stimulating factor

GMP	Granulocyte Monocyte Progenitor
GvHD	Graft versus Host Disease
GvL	Graft versus Leukemia
hDF	Human Dermal Fibroblast
HE	Hemogenic Endothelium
hESC	Human Embryonic Stem Cell
hiPSC	Human Induced Pluripotent Stem Cell
HLA	Human Leukocyte Antigen
HPC	Human Progenitor Cell
HRM	High Resolution Melting
HSC	Hematopoietic Stem Cell
HSPC	Hematopoietic Stem and Progenitor Cell
HSPCT	Hematopoietic Stem and Progenitor Cell Transplantation
ICM	Inner Cell Mass
IDH	Isocitrate Dehydrogenase
IGF2	Insulin-like Growth Factor 2
IL-3	Interleukin-3
IL-6	Interleukin-6
IMDM	Iscove's Modified Dulbecco's Medium
iMEFs	Irradiated Mouse Embryonic Fibroblasts
iPSC	Induced Pluripotent Stem Cell
ITD	Internal Tandem Repeat
LSC	Leukemia Stem Cell
MDS	Myelodysplastic Syndrome
MEF-CM	Mouse Embryonic Fibroblast Culture Media
MEP	Megakaryocyte/Erythroid Progenitors
mESC	Mouse Embryonic Stem Cell
miRNA	MicroRNA
MNC	Mononucleated Cell
MPB	Mobilized Peripheral Blood
MPP	Multipotent progenitors
MSC	Mesenchymal Stem Cell
NGS	Next Generation Sequencing
NOD	Nonobese Diabetic
NSG	NOD/SCID/IL2Rγ^{null}
OSKM	OCT4, SOX2, KLF4, c-Myc
OSN	OCT4, SOX2, NANOG
PCR	Polymerase Chain Reaction
PML	Promyelocytic Leukemia
PRT	Post-Remission Therapy

PSC	Pluripotent Stem Cell
qRT-PCR	Quantitative Real Time Polymerase Chain Reaction
RBC	Red Blood Cell
RARα	Retinoic Acid Receptor α
RNA	Ribonucleic acid
RNA-seq	RNA sequencing
SCF	Stem Cell Factor
SCID	Severe Combined Immune Deficiency
SCNT	Somatic Cell Nuclear Transfer
SL-IC	SCID leukemia-initiating cells
SR1	Stem Regenin-1
SRC	SCID Repopulating Cells
TGF	Transforming Growth Factor
TF	Transcription Factor
Tpo	Thrombopoietin

DECLARATION OF ACADEMIC ACHIEVEMENT

I contributed to the design and execution of the research presented herein, as well as performed data analysis and writing of all sections of this thesis. Dr. Mickie Bhatia directed and supervised the research projects and aided in the interpretation of results and editing of this thesis. Additional specific contributions by other lab members are noted in Chapters 2 through 4.

CHAPTER 1: INTRODUCTION

1.1 Overview

The work presented in this thesis was inspired by the seminal findings by Takahashi et al., which ushered in an new era of personalized medicine through the discovery of induced pluripotent stem cells (iPSCs) using cellular reprogramming (Takahashi et al., 2007). Accordingly, this dissertation aims to demonstrate that cellular reprogramming of human AML patient somatic cells to iPSCs allows for the generation of personalized sources of normal and dysfunctional blood cells that may form the basis of future cell-based therapies and disease models. As such, the goal of this introductory chapter is to briefly introduce the history of pluripotent stem cells (PSCs) in the context of healthy hematopoietic stem cells (HSCs) and malignant scenarios, specifically acute myeloid leukemia (AML), and summarize the current state of these research fields.

1.2 Hematopoietic stem cells

1.2.1 Hematopoiesis during Development

During mammalian embryogenesis, the hematopoietic system develops in successive waves, representing distinct clonal origins for primitive and definitive stages of hematopoiesis (Orkin & Zon, 2002). The initial primitive wave is transient and dominated by nucleated erythrocytes and myeloid cells (Orkin & Zon, 2008). This primitive stage is ultimately surpassed by definitive hematopoiesis, which gives rise to adult hematopoietic stem cells (HSCs) (Orkin & Zon, 2008; Slukvin, 2013). Definitive HSCs initially appear in the vascular microenvironment of the dorsal aorta in the aortagonad-mesonephros (AGM) region (Medvinsky & Dzierzak, 1996). Emergent HSCs have been observed to bud directly from hemogenic endothelium (HE) cells lining the dorsal aorta (Eilken et al., 2009; Zovein et al., 2008). These cells go on to seed the fetal liver, where they expand dramatically prior to colonizing the bone marrow (BM) at birth (Dzierzak & Speck, 2008; Medvinsky & Dzierzak, 1996). Adult-type definitive HSCs possess the capacity for self-renewal, multi-lineage differentiation, homing and engraftment to hematopoietic territories. Functionally, HSCs are defined by the capacity for long term reconstitution of all blood lineages following transplantation into irradiated adult recipients. With HSCs at the apex, the hematopoietic system is considered to be hierarchically organized, which results in the formation of short-term hematopoietic stem and progenitor cells (HSPCs) that can self-renew for a limited interval and give rise to multipotent progenitors (MPPs) (Morrison et al., 1997; Morrison & Weissman, 1994). In turn, these MPPs, in turn give rise to more committed common lymphoid progenitors (CLPs) or common myeloid progenitors (CMPs) that further differentiate into myelomonocytic (GMPs) and megakaryocyte/erythroid progenitors (MEPs) (Akashi et al., 2000; Kondo et al., 1997). Ultimately, these progenitors terminally differentiate into mature blood cells, each with highly specialized functions. This cascade of differentiation results in amplification of cell number but an accompanying progressive restriction of developmental potential. This restriction in potential is believed to prevent any developmental plasticity that would allow dedifferentiation or fate changes outside of this hierarchical organization under normal in vivo physiological conditions.

1.2.3 Sources of HSPCs and HSCPT

Advances in our understanding of hematopoietic stem and progenitor cell (HSPC) biology has fueled an interest in optimizing HSPC quality and yields from various stem cell sources. To date, HSPC transplantation (HSPCT) remains the most prevalent and efficacious cell therapy and enables complete restoration of the hematopoietic system (myeloid, erythroid and lymphoid lineages) in patients after hematopoietic damaging chemo- and radiation therapy and for treatment of a variety of hematological disorders (Talib & Shepard, 2020). The procedure can be divided into two categories: (1) allogeneic HSCT (allo-HSCT), in which hematopoietic stem and progenitor cells (HSPC) are procured from a healthy donor and used to reconstitute a patient's hematopoietic and immune systems; and (2) autologous HSCT (auto-HSCT), in which the patient's own HSPC are obtained as the donor source for transplantation. The first case of human BM administration and grafting in the form of intravenous infusions was documented in 1957(Thomas et al., 1957), followed by syngeneic infusion of BM between identical twins, one of which had refractory leukemia in 1959 (Thomas et al., 1959). Major milestones in BM transplant have been achieved with the first successful allogeneic transplantation between siblings in a patient who inherited X-linked severe combined immunodeficiency syndrome in 1968 (Gatti et al., 1968), and with the first successful HLA-matched but unrelated donor transplant in 1973, where significant clinical improvement and persistent engraftment was reported more than three years later ("Bone-Marrow Transplant from an Unrelated Donor for Chronic Granulomatous Disease," 1977).

HSPCT has been in clinical practice for greater than 60 years, and is the leading cell-based therapy (Chabannon et al., 2018) with more than 50,000 yearly BM transplants reported (Gratwohl et al., 2010), and the one millionth documented transplant being reached in late December 2012 (Worldwide Network for Blood and Marrow Transplantation). The three major sources utilized for the collection of HSPCs for transplantation include mobilized peripheral blood (MPB), direct aspirates from BM, and umbilical cord blood (CB) harvested at birth. Obtaining HSPCs from BM requires either extracting them directly from within bones or releasing them from the BM into circulation for venous peripheral blood collection. The former requires trephine biopsy needles and is usually taken from the pelvic bone under general anesthesia by a hematologist. The latter is typically achieved with mobilizing agents that disrupt the cellular adhesion of HSPCs and permit their egress into circulation; mobilized peripheral blood (MPB) (Bain, 2001; Petit et al., 2002). As such, mobilization via granulocyte-colony stimulatory factor (G-CSF) leads to the degradation of cellular adhesion molecules tethering HSPCs to the BM increasing their presence in peripheral circulation (Dührsen et al., 1988). The third common source of HSPCs is from umbilical cord blood (CB) (Broxmeyer et al., 1989), which is more highly enriched in functional HSCs than the former two sources (J. C. Wang et al., 1997). These three sources represent the only access to clinical-grade HSCs.

As of 2012 ~58% of transplantations were still of an autologous source, and only 5-6% of transplants were performed for the treatment of non-malignant diseases demonstrating that there is significant room for the range of clinical indications to continue to grow (Talib & Shepard, 2020). Self-tolerance is a major advantage of autologous HSPCT, however even with extensive HSC purification, residual pre- or malignant stem cells contaminate autologous BM or peripheral blood risking relapse (Chabannon et al., 2018; Müller et al., 2012), highlighting a key clinical gap that allogeneic HSPCT could fill. Unfortunately, a major barrier in allogeneic HSPCT is obtaining sufficient human leukocyte antigens (HLAs)-matched donations (Talib & Shepard, 2020). Greater than 30% of patients will not find an HLA-matched donor and this challenge is drastically increased in racially diverse individuals. Poor HLA matches can put transplant recipients at risk of life-threatening acute and/or chronic graft versus host disease (GvHD). GvHD occurs when

donated HSPC give rise to immune cells that recognize the recipient's body as foreign (Ballen, 2015, 2015; Gragert et al., 2014; Pineault & Abu-Khader, 2015; Talib & Shepard, 2020; Zhu et al., 2021). Thus, immunologically superior umbilical CB presents as an appealing alternative source for allo-HSPCs (Gragert et al., 2014; Smith & Wagner, 2009; Zhu et al., 2021). After the initial successful transplant in 1988 in a patient with Fanconi Anemia (Gluckman et al., 1989), umbilical CB samples have rapidly emerged as an effective alternative to the more common sources of HSCs. Nevertheless, explorations into abundant, alternative sources of patient-specific HSPCs for use in future cell-based therapeutics remains a desperate need.

1.2.4 In vitro & in vivo assays of self-renewal

The hematopoietic hierarchy has been meticulously described over the last 60 years utilizing a range of in vitro and in vivo experiments. HSCs cannot be identified morphologically and are only firmly defined based on their functional characteristics, even though they have been linked to distinctive cell surface phenotypes (Bhatia et al., 1997; Notta et al., 2011). To accurately measure and quantify both HSCs and lineage-restricted progenitors, indirect approaches are required to retrospectively study their functional capacity. Till and McCulloch initially described the hematopoietic spleen "colony forming unit" (CFU) in 1961, where by they demonstrated that single clonogenic BM cells were able to self-renew and restore hematopoiesis when transplanted into lethally irradiated recipient mice (Becker et al., 1963; Till & McCulloch, 2012). Further investigation revealed that each colony included up to 10^6 cells, which were the direct genetic offspring of distinct donor cells (Becker et al., 1963; Till & McCULLOCH, 1961). Most importantly, dissociating individual colonies revealed heterogeneous mixtures of maturing, lineage-restricted precursors that could be identified by histological examination (McCulloch, 1983), as well as infrequent cells that could start new splenic colonies if transferred into a new recipient host (Siminovitch et al., 1963). This was a ground-breaking example of how a single cell may produce differentiated and self-renewing offspring, two essential and fundamental characteristics of HSCs.

The first in vitro adaptation of this assay was developed in 1966 when Ray Bradley and Donald Metcalf discovered a small fraction of healthy murine BM cells that were capable of forming clonal colonies when plated in semi-solid growth medium (Bradley & Metcalf, 1966). These primitive BM cells are termed hematopoietic progenitor cells (HPCs), and the viscosity of the medium causes these proliferating progenitors to remain in proximity to their progeny leading to the formation of a colony unit. Thus, HPCs are experimentally defined by their ability to generate mature hematopoietic colonies when subjected to the CFU assay. The in vitro CFU assay was later modified to study human hematopoietic cells (Pike & Robinson, 1970). It is crucial to highlight that colony forming cells are not required to possess significant self-renewal to make colonies and thus the most primitive cells in the hematopoietic hierarchy cannot be functionally quantified using this assay and need a more complex experiment to test for self-renewal; the human-mouse xenograft.

To better mimic human biology in an in vivo system, humanized mouse models have been created and are widely employed in hematopoietic research (Legrand et al., 2006; Shultz et al., 2007; B. Zhang et al., 2009). The creation of immune-deficient mouse strains that would permit multi-lineage repopulation of the human hematopoietic system in a murine host and provide long-term maintenance of CFU populations in vivo was the most significant advancement in our understanding of the biology of human HSCs (Kamel-Reid & Dick, 1988; Lapidot et al., 1992;

McCune et al., 1988). Early xenotransplantation studies of human hematopoietic cells were performed using mice that were homozygous for the severe combined immunodeficiency (SCID) mutation. This mutation prevents the development of cellular or humoral immune responses to human antigens by impairing the ability of lymphocytes to undergo genetic recombination (McCune et al., 1988). The SCID mouse's largest contribution has been in human-mouse xenotransplantation research, which have produced further immune deficient mouse strains (Ito et al., 2012), despite the original authors' recommendation of their SCID mice as a model of impaired T and B cell development. Specifically, this strain was crossed with non-obese diabetic (NOD) mice to create the NOD/SCID strain in an effort to increase the low amounts of engraftment produced by SCID mice (Shultz et al., 2005). NOD/SCID mice exhibit decreased natural killer cell activity and inhibited innate immune function in addition to the lymphocyte abnormalities linked to the SCID strain (Shultz et al., 2005), allowing for more robust human engraftment (Larochelle et al., 1996). Indeed, this strain has remained popular for xenograft applications and enabled the first quantitative measurement of multilineage engraftment (J. C. Wang et al., 1997). By transplanting progressively fewer primitive hematopoietic cells from MPB, BM, and CB into secondary recipient mice, multi-potent repopulating cells, termed SCID repopulating cells (SRC) were defined (Bhatia et al., 1997; J. C. Wang et al., 1997). Despite the functional definition of human HSCs being able to repopulate humans, this thesis refers to SRC as HSC to be consistent with the terminology currently used in the field.

1.3 Embryonic Stem Cells and Pluripotency

1.3.1 Origins and definitions of pluripotent stem cells

The term "pluripotent" refers to a state of cellular developmental potential that can produce all the downstream cells that make up the embryo through the process of differentiation toward the three germ layer lineages. The concept for deriving a pluripotent cell line to study development was born out of an observation of an inbred strain of mice known as “129” which frequently presented with spontaneous testicular tumours called teratomas (Stevens & Little, 1954). Teratomas are tumours that appear as an amorphous mass of adult tissues and organs, including hair, teeth, brain tissue, and bone. In 1958, Leroy C Stevens’ discovered that a small percentage of naturally occurring teratomas could be transplanted repeatedly, indicating that some teratoma cells may have the ability to self-renew (Stevens, 1958). The characteristics of teratomas and their tendency for multi-lineage differentiation indicated to him that the tumours were created from pluripotent, early embryonic-like cells (Stevens, 1960). Stevens’ later provided evidence to support this theory by showing that early embryos injected intraperitoneally or intratesticularly resulted in teratocarcinomas, which are malignant tumours comprised of tissues derived from all three embryonic germ layers (ectoderm, endoderm, and mesoderm), which exist in a disorganized mass and are made up of primarily undifferentiated, self-renewing cells (Stevens, 1970). Although he had not yet produced concrete evidence, Stevens' early works suggested that teratocarcinomas originated from malignant pluripotent embryonal cells that 1) had the ability to differentiate into all three embryonic layers and 2) had the capacity to self-renew after transplantation, as shown by their ability to maintain progressive tumour growth and undifferentiated cell types.

The cells which give rise to teratocarcinomas originate from germ cells in sex organs (ovaries and testis) and are today technically referred to as pluripotent embryonal carcinoma cells (ECC). Malignant ECCs, which could be isolated and cultured in vitro, are the neoplastic

counterparts of the embryonal cells responsible for normal embryogenesis (Kleinsmith & Pierce, 1964; Pierce & Dixon, 1959; Stevens, 1960). Subsequent works in the field questioned the true pluripotent nature of ECCs due to their neoplastic origins, abnormal karyotypes, and variable/limited differentiation potential (Evans, 1972; Kahan & Ephrussi, 1970; Rosenthal et al., 1970; Stevens & Hummel, 1957). Nevertheless, ECCs demonstrated features of pluripotency through their ability to contribute to normal mouse development when injected into blastocysts (Brinster, 1974). This led Martin Evans, Matthew Kaufman, and Gail Martin to consider if normal embryonic cells necessary for the growth of complete organisms could be similarly isolated during early embryogenesis and cultivated in vitro to preserve normal pluripotency in a dish. Instead of using tissue explants from teratomas or teratocarcinomas, both groups sought to produce an in vitro pluripotent cell line directly from the early mouse embryo. While Martin's mouse embryonic stem cell (mESC) lines were created by plating the inner cell masses (ICM) of the mouse blastocyst on a supportive layer of irradiated mouse embryonic fibroblasts (iMEFs), Evans and Kaufman's were created from whole cultured blastocysts (Evans & Kaufman, 1981; Martin, 1981). Both these groups were able to generate mESC colonies that could form teratomas in vivo, differentiate in vitro, and had normal karyotypes. Cultured mESCs were later demonstrated to give rise to an entire mouse by a process called tetraploid complementation more than ten years later, serving as the ultimate pluripotency test (Nagy et al., 1993). This experiment demonstrated conclusively that ESCs could generate every cell type in the mouse and demonstrated their potential use in the development of genetically modified mouse strains (Nagy et al., 1993).

About 17 years after the discovery of mESCs, Jamie Thomson first discovered human embryonic stem cells (hESCs) (Thomson et al., 1998). Like mESCs, hESCs were produced by adapting isolated human blastocyst ICMs to in vitro culture. When implanted into immune deficient mice, the resulting cell lines maintained their ability to develop teratomas with all three germ layers, providing further evidence that they were pluripotent (Thomson et al., 1998). Overall, 59 hESC lines with different characteristics were produced (International Stem Cell Initiative et al., 2007) despite the major scientific difficulties and the ethical discussions about the exploitation of human embryos that were poised after Thomson's discovery (Robertson, 2010). Our research team and many other teams around the world have adopted two of these human ESC lines, H1 and H9 (also known as WA01 and WA09), which are still in use today (International Stem Cell Initiative et al., 2007; Nakanishi et al., 2019).

1.3.2 Maintenance of hPSCs in vitro

Due to their pluripotent capacity, hPSCs can continue to grow and renew themselves indefinitely. However, to preserve pluripotency, certain culture conditions are necessary. At first, undifferentiated hPSC colonies needed to be maintained in vitro on cultures of (iMEFs) (Thomson et al., 1998) but were soon replaced by a feeder-free environments using matrigel extracellular matrix and MEF-conditioned media (MEF-CM) supplemented with basic fibroblast growth factor (bFGF) (Levenstein et al., 2006; C. Xu et al., 2005). Although numerous studies highlighted the significance of bFGF supplementation for the maintenance of hESC self-renewal (Levenstein et al., 2006; C. Xu et al., 2005), our team was the first to describe the functional connection between the addition of bFGF to the culture environment and hESC self-renewal in 2007. In this study, Bendall et al. showed that hESCs generate an autologous niche of human dermal fibroblast (hDFs) that respond to bFGF treatment by producing Insulin-like growth factor 2 (IGF2) and transforming growth factor (TGF)-family members (Bendall et al., 2007). Bendall et al. were able to determine

through careful examination of pluripotent colony initiation capacity, proliferation, survival, and differentiation, that blocking TGF or bFGF signalling at the level of hDFs caused hESCs to differentiate, whereas blocking IGF signalling within the pluripotent cells decreased their proliferation and colony initiation capacity while concurrently causing apoptosis. These results not only describe the functional relationship between extrinsic regulators of hESC and pluripotency, but also contributed to the development of chemically defined, xeno-free culture conditions for hPSCs enabling their use in clinical applications (Chen et al., 2011). Presently, the most widely published feeder-free culture medium for hPSCs is mTeSR manufactured by Stem Cell Technologies (Ludwig, Bergendahl, et al., 2006; Ludwig, Levenstein, et al., 2006).

1.3.3 Molecular hallmarks of pluripotency

In addition to extrinsic regulators, the pluripotency network of transcription factors (TFs) is an inherent molecular circuitry that controls hESCs. This network, which includes but is not limited to OCT4, SOX2, and NANOG (OSN), was predominantly developed in studies of murine development and mESCs. Reduced self-renewal and subsequent differentiation in ESCs are caused by a reduction in the expression of any one of these components. Notably, over-expression of OCT4 or SOX2 results in differentiation (Adachi et al., 2010; Niwa et al., 2000), whereas over-expression of Nanog encourages self-renewal in the absence of essential extrinsic signaling (Chambers et al., 2003). Extrinsic signaling molecules such as bFGF and TGF-β have also been shown to directly regulate and sustain the expression of NANOG, OCT4, and SOX2 (R.-H. Xu et al., 2008). OCT-4, is a TF protein that is encoded by the POU5F1 gene and is part of the POU (Pit-Oct-Unc) family. It is required for the formation of the ICM during embryogenesis, and its loss of expression is embryonic lethal in mice (Nichols et al., 1998). Furthermore, differentiation occurs in hESCs when its expression is reduced by RNA interference (Matin et al., 2004). Likewise, the expression of the homeoprotein NANOG in the ICM is required for the epiblast to properly form and develop prior to generation of the three embryonic germ layers, and its loss of expression in ESCs in vitro results in their differentiation (Chambers et al., 2003; Mitsui et al., 2003). Finally a deficiency for SOX2, an Sry-related HMG box TF, is embryonically lethal and contributes to an aberrant formation of the epiblast from the ICM (Avilion et al., 2003). Boyer et al. identified OCT4, SOX2, and NANOG (OSN) target genes in hESCs using chromatin immunoprecipitation in conjunction with DNA microarrays to learn more about the regulatory circuitry of pluripotency (Boyer et al., 2005). Through this research, Boyer et al. revealed that these three factors co-localize to their own promoter regions as well as a large number of target genes, suggesting that the complex was bound at both active and inactive genes, providing a dual role in activation and repression within the context of hESCs (Boyer et al., 2005). Conversely, a subset of transcriptionally dormant genes that displayed regulatory binding of the complex has been linked to lineage choice and differentiation in the early embryo (Boyer et al., 2005). Taken together, these findings showed OSN's synergistic role to activate their own expression and those of known-self renewal pathways, and to suppress TFs necessary for differentiating from the pluripotent state to preserve the basic regulatory circuitry of pluripotency (Boyer et al., 2005; R.-H. Xu et al., 2008).

By balancing the processes of self-renewal and differentiation, epigenetic regulation adds another level of control over the pluripotent state (Bibikova et al., 2006; W. Xie et al., 2013). According to Bibikova et al., different DNA methylation patterns are present in hPSCs, demonstrating the need for careful regulation and maintenance of these patterns during in vitro self-renewal and replication (Bibikova et al., 2006). As a result, disruption of DNA

methyltransferase 1 (DMT1) disruption, an enzyme involved in DNA methylation, causes cell death in hESCs (Liao et al., 2015) and is embryonically fatal in mice (Li et al., 1992). Furthermore, genes associated with adult lineages are highly methylated, whereas OCT4, NANOG, and genes necessary for cellular function remain highly unmethylated in the pluripotent state until differentiation occurs (Fouse et al., 2008). Ultimately, epigenetic regulation plays an essential role in the maintenance of pluripotency.

1.3.4 Measuring human pluripotent potential

hPSCS are easily recognizable in in vitro cultures given their signature morphological characteristics patterns as flat, spherical colonies, consisting of densely packed cells with large nuclei and minimal cytoplasm (Thomson et al., 1998). In addition to these distinct growth patterns, hPSCs are characterized by a combination of molecular, immunophenotypic, and functional features that have been validated in a wide range of hPSC lines (International Stem Cell Initiative et al., 2007). Given their function in regulating the pluripotent network, OSN's transcriptional and protein-level co-expression is a necessary and prominent indicator of pluripotency (Boyer et al., 2005), whereas the antigens SSEA3, SSEA4, and TRA-1-60 are cell-surface markers found exclusively on hPSCs (International Stem Cell Initiative et al., 2007). Even though these later markers do not play crucial roles in pluripotency (Brimble et al., 2007), their expression permits experimentally valuable live-cell labelling methods for fast identification and immunophenotypic sorting of hPSCs.

hPSCs readily differentiate in culture in the absence of extrinsic growth factor regulation if they become too confluent and compacted together, or upon injection into immune deficient mice where they form teratomas (Thomson et al., 1998). As such, the gold standard functional assay for measuring pluripotent potential is the teratoma assay (Hentze et al., 2009). Importantly, the route of administration, the kind of PSC, and the number of cells are just a few of the variables that can affect teratoma formation. Testing for pluripotent potential involves injecting the test cells into immunodeficient animals in places like the testicles, kidney capsule, hind limb muscle, subcutaneous space, and intraperitoneal spaces (Hentze et al., 2009; Stevens & Little, 1954). After the tumour has been removed and histologically prepared, the tissues from each of the three germ layers—ectoderm, endoderm, and mesoderm—must be observed (Hentze et al., 2009). This indicates the presence of pluripotent precursor cells that were able to give rise to more differentiated tissues at the time of injection. This is known as differentiation potential, the first functionally identified key metric of pluripotent cells. The second indicator of pluripotent cells is their ability to self-renew or create progeny with an identical differentiation potential. While cell division is necessary for self-renewal, cell division by itself does not prove self-renewal. The hPSC that gave rise to a teratoma must be able to divide and maintain equal differentiation potential to effectively exhibit self-renewal. This means that within the primary teratoma, at least one progeny cell exists which could give rise to another teratoma. While the primary teratoma has become the routine test to demonstrate pluripotent potential for PSCs (Takahashi et al., 2007; Takahashi & Yamanaka, 2006), routine testing for self-renewal by secondary transplant is uncommon.

Pluripotent functionality can also be assessed in vitro using embryoid body (EB) or co-culture-based assays in which PSCs are collected into clumps and cultured in lineage-specifying media conditions toward the generation of derivatives of the three embryonic germ layers - a characteristic that, if properly harnessed, has enormous potential for regenerative medicine, and will be discussed later.

1.4 Cellular Reprogramming

1.4.1 Foundational concepts of cellular reprogramming

Somatic cell nuclear transfer & the heterokaryon

In the 1950's, Briggs and King started developing a technique termed somatic cell nuclear transfer (SCNT) to examine whether differentiation imposed irreversible changes on the chromosomes contained within the nucleus (Briggs & King, 1952, 1957). They reasoned that by removing the nucleus from an egg, swapping it out with one from a more mature cell, and simulating fertilisation artificially, they could test whether the mature nucleus would support normal healthy development. This test would shed light on how the nuclei of differentiated cells differ from those in the undifferentiated state found during early embryogenesis. By transplanting nuclei from blastulas (cells of the early stage of frog development considered to be equipotent to single cell embryos) into an enucleated oocyte, they could test whether their manipulations prevented normal development from occurring, prior to assessing normal development from nuclei from differentiated cells. By carefully removing nuclei from *Rana pipiens* frog eggs, and injecting them with partially ruptured blastula cells, such that the nuclei were free to enter the cytoplasm of the oocyte (Briggs & King, 1952), they were able to demonstrate that the process of nuclear transfer afforded normal development, and therefore they could go on to test whether nuclei at different stages of development were capable of the same feat. Next, using endoderm cells as the donor for nuclear transplant experiments, Briggs and King concluded that the developmental potential of DNA within endoderm cells decreases as they differentiate in the developing tadpole, since nuclei from cells taken from mid-neurulae stage (prior to heartbeat development) failed to support the generation of swimming tadpoles (Briggs & King, 1957). However, shortly after their experiments, a young graduate student named John Gurdon was able to clone sexually mature tadpoles and normal adult frogs through nuclear transfer of blastula and differentiated endoderm, including terminally differentiated intestinal epithelium cells (Gurdon, 1960, 1962; Gurdon et al., 1958). Gurdon produced a highly contentious data that was in direct opposition to Briggs and King's theory. Upon establishing reliable methods for performing SCNT in *Xenopus laveis*, Gurdon's data clearly demonstrated that nuclei derived from the intestinal epithelium of feeding tadpoles could support the formation of sexually mature adult frogs using SCNT (Gurdon & Uehlinger, 1966). This was in stark contrast to Briggs and King's findings, whose technically sound results but incorrect interpretation were later attributed to limitations of the *R. pipiens* system (Gurdon, 2006; Gurdon & Uehlinger, 1966). These findings provided definitive evidence that differentiation within specific amphibian tadpoles was not totally governed by mandatory permanent DNA alterations. More importantly, the ability of stochastic factors within the oocyte cytoplasm to reprogramme mature somatic cells back to the pluripotent state gave the first indications that 1) cell state is not always fixed, i.e., seemingly mature somatic cell types can be experimentally reprogrammed to adopt an alternative cell fate, and 2) cytoplasmic factors exert powerful control of gene transcription responsible for cell phenotype and function.

Cell fusion is the experimental process of joining two or more cells through the fusion of their cytoplasm's to produce either a heterokaryon, in which the nuclei are maintained in the cytoplasm as separate entities, or a synkaryon, in which the resulting cell contains a single nucleus harbouring all parent cell chromosomes (Ogle et al., 2005). The former cell hybrid is created when cells of different types or species are fused, and it was the focus of fusion experiments started in the 1960s to determine if elements from non-oocyte cell cytoplasm could also alter cell phenotype.

Henry Harris and John Watkins established the first example of heterokaryon generation through fusing mouse Ehrlich ascites cells and human HeLa cells (Harris & Watkins, 1965). They showed that RNA expression from the mouse and human nuclei continued to contribute to the viability of these hybrid cells, resulting in a phenotype that was different from the contributing parental cells (Harris & Watkins, 1965). Further proof that cell state is not fixed and may be experimentally altered came later from their demonstration that malignant mouse cell phenotypes could be inhibited after fusion to normal mouse fibroblasts but restored after loss of normal chromosomes (Harris et al., 1969). Several studies have since used this experimental system to learn more about cellular reprogramming (Piccolo et al., 2011; Tada et al., 2001), adding to the growing body of evidence that cell fate can be manipulated by cytoplasmic factors that initiate nuclear transcription and remodel the epigenome.

Transcription Factor Reprogramming

The initial discovery that would eventually lead to the first example of TF based cellular reprogramming came about in the lab of Peter Jones. Jones found that cells treated with 5-aza-cytidine (5-Aza) underwent an odd transformation that resulted in the creation of multinucleated striated muscle fibres that spontaneously contracted during a chemotherapeutic drug screen on mouse fibroblasts (Constantinides et al., 1977). Further work by Taylor and Jones' expanded on the reprogramming potential of 5-Aza by showing that after treatment, individual single cell derived clones of mouse fibroblasts generated both striated muscle and fat cells (Taylor & Jones, 1979). These findings demonstrated that, as opposed to the growth of dormant muscle or adipocyte cells, the altered cells were actually the consequence of cellular reprogramming (Taylor & Jones, 1979). Thus, two possible scenarios arose regarding the mechanism of action regarding these experiments 1) regulation of the epigenome allowed for downstream demethylation and activation of muscle genes and/or 2) direct activation of muscle-specific gene programs (Lassar et al., 1986). Deciphering whether either, or both, of these scenarios were the cause of the reprogramming event became the central question of Andrew Lassar. To test both situations, Lassar transfected genomic DNA isolated from converted myoblasts as well as unmethylated DNA coding for muscle proteins that were previously discovered to be elevated after treatment with 5-Aza. The hunt for the factor that was responsible for turning fibroblasts into muscle cells in response to 5-Aza treatment was ultimately launched when it was discovered that only the transfected DNA from existing myoblasts lines did so (Lassar et al., 1986). The ability to transform fibroblasts into myoblasts only through the ectopic expression of the gene MyoD was subsequently proven by screening and transfecting a cDNA library of muscle-specific TFs (Davis et al., 1987). Although this discovery gave rise to TF-mediated reprogramming and offered the first instance of employing defined factors to alter cell fate, it wasn't until the early 2000s that this reprogramming technique was widely acknowledged or utilized in the field (Graf, 2011).

By over-expressing Gata-1 in modified myelomonocytic cell lines, Thomas Graf was one of the first to attempt to use the idea of TF-mediated reprogramming (Kulessa et al., 1995). He demonstrated that myelomonocytic cells were reprogrammed to become thromboblasts and eosinophils when Gata-1 was expressed. Later he would show that mature hematopoietic cells such as B cells could also be reprogrammed by ectopic expression of C/EBPα into macrophages, once again demonstrating the power of TFs to activate programs of genes responsible for cellular fate (H. Xie et al., 2004). Taken together, these early examples of reprogramming highlighted the power of TFs in the regulation of cellular identity, and in doing so would inspire one of the greatest discoveries in biology.

1.4.2 Induced Pluripotent Stem Cells

Through his PhD and postdoctoral work, Dr. Shinya Yamanaka came to learn and master the art of genetically engineering mice through manipulation of mESCs (Yamanaka, 2013). His initial use of mESCs (and later human ESCs) progressed into a fascination with studying the underlying mechanisms of pluripotency. Instead of attempting to differentiate ESCs towards interesting and useful somatic cells for downstream studies, Yamanaka wanted to find a way to create ESCs from somatic cells, since this would circumvent the ethical issues surrounding the derivation of hESCs. Based on pioneering work previously described, the principles of cellular reprogramming were as follows: 1) cell fate can be altered, 2) the pluripotent cytoplasm contains dominant, undefined factors capable of reverting somatic cells back to a state of epigenetic, transcriptional, and functional pluripotency, and 3) the ectopic delivery of TFs represents a powerful molecular tool in which to alter cell fate. Recognizing these principles, Kazutoshi Takahashi and Shinya Yamanaka set forth to define factors responsible for the reprogramming of somatic cells to pluripotency. Through comparison of transcriptional databases from both ESCs and somatic cells, Yamanaka's group generated a list of ESC-specific factors that would be functionally interrogated through derivation of knockout mESCs cells and knockout mice (Yamanaka, 2013). This process eventually led to the identification of 24 factors that appeared to be critical for mESC function, which were then tested for their ability to induce pluripotency (Takahashi & Yamanaka, 2006). Takahashi, the post doc assigned to test the 24 factors, introduced each factor, one by one, through retroviral delivery and observed no activation of pluripotency gene expression or changes in morphology, suggesting that no single factor was able to induce pluripotent status within somatic cells (Takahashi & Yamanaka, 2006). Although no single factor was capable of inducing pluripotency when all 24 factors were introduced together, Takahashi noticed discrete putative reprogrammed colony formations, now referred to as induced pluripotent stem cells (iPSCs). To discern which factors were critical to the colony induction process, Takahashi removed one factor at a time from the pool of 24 and observed whether this resulted in colony formation loss. Eventually it was discovered that OCT4, SOX2, KLF4 and c-Myc (OSKM) were critical for the generation of iPSCs. These iPSCs shared transcriptional, epigenetic, immunophenotypic, and functional hallmarks of pluripotency akin to ESCs, and required the same extrinsic culture conditions (Takahashi & Yamanaka, 2006). Only one year later, both Yamanaka and Jamie Thomson (the developer of hESCs) translated the process to the human system, giving rise to human iPSCs (hiPSCs) (Takahashi et al., 2007; Yu et al., 2007). Interestingly, Thomson had not only reproduced the phenomenon of iPSC reprogramming, but he had done it using a different set of factors that incorporated NANOG and LIN28, suggesting that there could be multiple ways to generate iPSCs through the expression of pluripotency associated factors (Yu et al., 2007; Zhou et al., 2008).

iPSC technology not only achieved what was previously thought to be impossible—changing cell fate and "turning back the clock of development" —but it also was rapidly adopted and robustly reproducible across the globe! Extraordinarily, iPSC technology represented an unprecedented clinical opportunity in its utility to develop products and procedures within the area of personalized regenerative medicine.

1.4.3 Applications of induced pluripotent stem cells

Autologous & Allogeneic cell therapies

Due to their extraordinary capacity for self-renewal and differentiation, iPSCs have the potential to be an endless source of patient-specific (autologous) human cells for use in cell-based therapies. This could supply cell sources that are not clinically available, such as brain cells (D.-S. Kim et al., 2014; S. C. Zhang et al., 2001) and solve the clinical challenges associated with donor (allogeneic) cell sources, such as immune incompatibility/transplant rejection (Copelan, 2006). An early compelling example for the use of human iPSCs with regard to autologous cellular transplantation was shown by Hanna et al., wherein hematopoietic cells derived from iPSCs corrected for a hemoglobin mutation reduced the blood cell defect in a humanized mouse model of sickle cell anemia (Hanna et al., 2007). Impressively, since the discovery of iPSCs, three human transplants of autologous iPSC-derived cells have occurred, with the first transplant taking place in 2014 (Mandai et al., 2017; Schweitzer et al., 2020; Takagi et al., 2019). Despite not receiving immunosuppression, none of the patients in these trials experienced any major adverse events, with the most extended follow-up being 4 years post-transplant, which is an encouraging outcome for the field of personalized medicine.

In contrast to autologous cell therapies, which are patient-specific, allogeneic iPSC-based cell therapies use donor-derived tissues as a starting material and a greater number of allogeneic iPSC-derived cell therapies are also being developed (Blau & Daley, 2019; Yamanaka, 2020). A benefit of allogeneic therapies is the ability to produce multiple dosages simultaneously from a single batch of iPSCs and store them. As a result, it is possible to "scale up" the production process and generate economies of scale, which would in theory lower the cost of each patient dose (Simaria et al., 2014). Additionally, it permits "off-the-shelf" delivery, which streamlines logistics and cuts down on patient wait times (Sullivan et al., 2018; Yamanaka, 2020). Unfortunately, the risk of immunological rejection is a drawback of an allogeneic strategy. Patients must undergo immunosuppression raising their risk of infection and cardiovascular problems (Miller, 2002). Although autologous therapies are considered safer than allogeneic from an immune rejection standpoint (Eliopoulos et al., 2005; Kitala et al., 2016; Song et al., 2020), the immunogenicity of autologous iPSCs is not without controversy. In at least one study, autologous iPSCs transplanted into mice were rejected (Zhao et al., 2011). However, the majority of research have not discovered animal model rejection of autologous iPSCs or iPSC-derived cells (Araki et al., 2013; Guha et al., 2013; Osborn et al., 2020; Schweitzer et al., 2020). Overall, these works illustrate the potential impacts, utilities, and shortcomings of using cellular reprogramming to generate personalized cell sources that avoid immune-rejection and continue to motivate the field toward clinical implementation.

Disease Modeling

The advent of patient-specific reprogramming also allows for the generation of iPSCs from diseased patients, creating opportunities to generate in vitro disease models and large-scale drug screening in disease-specific tissues that are otherwise challenging to obtain. Accordingly, disease-specific iPSCs have been generated from a variety of somatic cells derived from patients with inherited and acquired diseases (Carette et al., 2010; Ebert et al., 2009; Kotini et al., 2017a; Kumano et al., 2012; Marchetto et al., 2010; Sabitha et al., 2021; Tanaka et al., 2015). Most of the time, when iPSCs were differentiated into relevant cell types, they displayed disease characteristics, demonstrating the ability of disease modeling utilizing iPSC technology. For example, iPSC derived motor neurons were successfully used to model and to identify a drug candidate for ALS patients (McNeish et al., 2015). The identified drug target was FDA approved

for the use in patients with epilepsy and was moved into Phase II clinical trials less than two years after initial in vitro experiments. Likewise, degenerative motor neurons with the disease phenotype were produced by fibroblast-derived iPSCs from human patients with hereditary spinal muscular atrophy, a fatal neurological condition brought on by mutations in the SMN1 gene. Later studies employing these defective motor neurons provided preliminary evidence that pharmacological therapy could be effective in treating the condition (Ebert et al., 2009). Similar techniques were used by Stricker et al. to show that malignant neural stem cells from human glioblastoma tumours, an acquired somatic brain cancer characterized by several genomic abnormalities and an aberrant epigenome, could be converted into iPSCs (Stricker et al., 2013). Notably, during reprogramming to pluripotency, the bulk of aberrant epigenomic markers connected to glioblastoma were reset. Despite this resetting, redifferentiation back to the neuronal lineage led to the development of a disease phenotype. This finding demonstrated that reprogramming can still be utilized to create model systems in cancer with defective epigenetic components and that the aberrant epigenome may be caused by genomic abnormalities. Intriguingly, after redifferentiation, epigenetic marks were gradually restored at several gene loci, however, whether the aberrant epigenome was re-established overtime was not further explored (Stricker et al., 2013). It's important to note that developing efficient iPSC models can also be hindered by the inability to generate iPSCs directly from diseased cells. Briefly, though a number of studies have recently demonstrated that reprogramming gastrointestinal cells, chronic myeloid leukemia (CML), glioblastoma, myelodysplastic syndrome, and pancreatic ductal adenocarcinoma cancer cells to pluripotency is possible and can allow for disease modeling (Carette et al., 2010; J. Kim et al., 2013; Kotini et al., 2017a; Kumano et al., 2012; Nagai et al., 2010; Stricker et al., 2013), reprogramming was highly inefficient, with marginal success often observed across primary patient samples. This refractoriness to reprogramming is paradoxical, remains unclear, and limits developing disease models for human cancer. Specific to this thesis, the refractory nature of malignant hematologic disorders such as acute myeloid leukemia (AML) will be discussed a subsequent section.

1.4.4 Hematopoietic differentiation of pluripotent cells

Many research groups have developed protocols which involve temporal administration of growth factors and small molecules, conditioned media, and/or feeder cells, which theoretically guide PSCs along particular pathways of differentiation (Chadwick et al., 2003; Sturgeon et al., 2014; L. Wang et al., 2004); but the ability of hPSCs to give rise to the hematopoietic lineage is further described in this section based on the focus of this thesis.

Derivation of putative HSPCs from hPSCs

Our group provided the first demonstration of the generation of $CD34^{+}CD45^{+}$ HPCs (Chadwick et al., 2003). This was achieved through culture of hESC-derived EBs in media supplemented with bone morphogenetic protein 4 (BMP4) and hematopoietic cytokines: FLT3 ligand (FLT3L), granulocyte-colony stimulating factor (G-CSF), interleukin-3 (IL-3), interleukin-6 (IL-6), and stem cell factor (SCF) (Chadwick et al., 2003). By definition, these HPCs possessed progenitor function in vitro through differentiation to myeloid lineages in the CFU assay (Chadwick et al., 2003), however, long-term reconstitution capacity characteristic of HSPCs was not observed following transplantation in vivo (L. Wang et al., 2005). It was suggested that these findings were attributed to an inability of PSC-derived blood cells to activate molecular programs similar to adult somatic HSPCs (L. Wang et al., 2005); a challenge the field still faces. Over the

years, a number of differentiation strategies have evolved based on the stepwise addition of cytokines and morphogens, such as BMP4, Activin A, and Notch ligands, in serum-free conditions, or differentiation of hPSCs in three-dimensional structures known EBs or co-culture systems with BM stroma/support cells (Chadwick et al., 2003; J. Lee et al., 2017; Sturgeon et al., 2014; Vodyanik et al., 2005).

Though studies from our lab and others have made progress in defining conditions for hPSC differentiation to hematopoietic cells, they have also demonstrated the immense complexity of this process. Notably, the derivation of HSCs from patient-specific hiPSCs is the holy grail in regenerative medicine since HSCT is a curative treatment for hematologic malignancies and innate immunodeficiencies. In an effort to generate HSCs in vitro, researchers have explored the power of lineage conversion via direct reprogramming of somatic cells. Direct reprogramming, also known as direct conversion, discussed previously, is based on the enforced expression of TFs, whose action dictates lineage specification during development (Graf & Enver, 2009). The concept of direct conversion, or directly switching cellular fate without reverting to a pluripotent state, was demonstrated in the pioneering work of both Taylor and Jones (Taylor & Jones, 1979) and Davis (Davis et al., 1987). Since these studies, several groups have gone on to adopt the strategy of directly converting somatic cells to HSCs. In the first direct reprogramming study reported, our lab was first to show that the overexpression of the pluripotency TF OCT4 could induce the generation of multilineage blood progenitors from human neonatal and adult dermal fibroblasts when cultured in hematopoietic permissive culture conditions (Szabo et al., 2010). Similarly, Pereira et al demonstrated that a simple combination of 4 hematopoietic TFs (GATA2, GFI1b, c-Fos, and ETV6) were sufficient to convert murine fibroblasts to hematopoietic progenitors (Pereira et al., 2013). Extensive molecular analysis of the TF-induced fibroblasts demonstrated that the cells experienced an endothelial-to-hematopoietic transition (Pereira et al., 2013), mimicking the in vivo progression of blood development where it is thought that HSCs emerge from a small population of "hemogenic" endothelial cells (Bertrand et al., 2010; Boisset et al., 2010; Zovein et al., 2008). Unfortunately, their functional potential in vivo remained to be fully investigated. In a comparable study, ectopic expression of 5 TFs (ERG, GATA2, LMO2, RUNX1c, and SCL) converted embryonic and adult murine fibroblasts into multilineage hematopoietic progenitors with short-term engraftment potential (Batta et al., 2014). Notably, Batta et al also demonstrated that the emergence of a hematopoietic progenitor was preceded by an endothelial-to-hematopoietic transition (Batta et al., 2014). Using a hybrid strategy, Doulatov et al combined directed differentiation and reprogramming approaches to show that human induced pluripotent stem cells (iPSC) could first be directed to differentiate into hematopoietic progenitors and then 're-specified' back to a stem cell fate with a combination of 5 HSC-specific TFs (HOXA9, ERG, RORA, SOX4, and MYB) (Doulatov et al., 2013). These transcription-factor-re-specified progenitors demonstrated multilineage potential in vitro however they only possessed short-term engraftment potential and were unable to instill multilineage differentiation, specifically lacking lymphoid potential in vivo (Doulatov et al., 2013). Using a similar approach, Riddell et al identified that mature blood cells could be de-differentiated and regain HSC properties utilizing transient expression of 8 TFs (RUNX1T, HLF, LMO2, PRDM5, PBX1, ZFP37, MYCN and MEIS1) (Riddell et al., 2014). In this paper they showed that murine committed lymphoid/myeloid progenitors and mature myeloid cells were successfully reprogrammed into induced-HSCs where the resulting cells were capable of long-term multilineage engraftment and were serially transplantable (Riddell et al., 2014). In a ground-breaking study, colleagues at Harvard reported the generation putative HSPCs with multi-lineage engraftment potential from hPSC-derived HE

by over-expression of 7 TFs (ERG, HOXA5, HOXA9, HOXA10, LCOR, RUNX1 and SPI1) (Sugimura et al., 2017). Specifically, the authors combined morphogen-directed differentiation recapitulating the endothelial-to-hematopoietic (EHT) lineage transition from HE and use of a defined set of TF over-expression in HE cells to mediate the conversion. Even with this most sophisticated protocol to date, human PSC-derived HSCs have not been created in vitro and appear to rely on unspecified extracellular cues from murine transplant recipients (Sugimura et al., 2017).

Despite these failures in demonstrating HSC function from hPSCs, procedures aimed at mimicking in vivo niches have had some limited success. Two independent groups have reported derivation of putative HSC-like cells from hiPSCs utilizing iPSC-derived teratomas as in vivo bioreactors (Amabile et al., 2013; Suzuki et al., 2013). Both studies combined cytokine treatment and OP9 stromal cell co-injection to recapitulate the BM niche environment more closely. Teratoma-mediated hematopoiesis generated derivatives bearing hallmarks of *bona fide* HSCs, namely sustained engraftment and lympho-myeloid differentiation potential after BM homing in xenograft assays. Additionally, one of the studies reported activation of adult programs in differentiated erythrocytes, a mark of definitive hematopoiesis (Suzuki et al., 2013). Overall, continued advances within the area of hematopoietic specification from hPSCs represent a subset of the collective efforts of the field to generate clinically relevant cell types for use in personalized cell-based therapies and disease modelling.

1.5 Acute Myeloid Leukemia

Cancer is the leading cause of death in Canada and is responsible for 28.2% of all deaths. Researchers estimated that there would be 233,900 new cancer cases and 85,100 cancer deaths in Canada in 2022. Moreover, 2 in 5 Canadians are expected to be diagnosed with cancer in their lifetime and approximately 1 in 4 Canadians is expected to die of the disease. In terms of AML, the most recent incidence statistics was reported as 1,090 Canadians being diagnosed with AML, representing a very small percentage of the total cancer incidence. Though this disease does not result in the highest mortality rates in Canada, cancer stem cells (CSC), cells thought to be responsible for disease relapse in many malignancies, due to their preferential ability to evade cytotoxic therapy, were originally described in AML. Additionally, not only has the hierarchical organization of cancer been most thoroughly described in AML, but research on solid tumours, including glioblastoma, breast, and colon, has revealed CSC-driven dynamics that are comparable to AML illness (Atashzar et al., 2020). Thus the gold standard model for CSC dynamics, cancer biology, and drug resistance is still AML as of this writing (Boyd et al., 2018; van Gils et al., 2021). This is extremely significant since numerous early findings in leukaemia research have demonstrated the applicability of well-established ideas to other diseases (Greaves, 2016). Since the first cases of AML were reported in the 1940s (Tefferi, 2008), we now understand that it is a genetically heterogeneous cancer of the hematopoietic system characterized by the inability of immature leukemic cells or "AML blasts" to differentiate into mature cells of the myeloid lineages. This results in the reduction of mature myeloid cells within months, ultimately leading to death (Perl & Carroll, 2007). In this section, I discuss aspects of AML that are relevant to this thesis, including a brief overview of the heterogeneity observed, methods of detecting cytogenetic and molecular aberrations, and the emerging role of epigenetic dysregulation in AML. Lastly, I describe two important assays in AML research, the CFU assay and leukemia stem cell (LSC) assay.

1.5.1 Heterogeneity of acute myeloid leukemia: cytogenetic and molecular aberrations

AML is a heterogeneous disease, characterized by a wide range of genetic abnormalities and genomic alterations that affect clinical outcomes and provide potential targets for drug development. Previously, AML was sub-divided by chromosomal (cytogenetic) and gene-specific (molecular) abnormalities, where 50-60% of all cases were associated with a genetic abnormality (Grimwade et al., 1998). These were first organized into a diagnostic criterion by the French-American-British (FAB) classification which relied heavily on the differentiation status of the leukemia for classification (Bennett et al., 1976). Since more abnormalities were discovered and added onto the list, "The World Health Organization classification of the myeloid neoplasms" was established to classify AML based on cytogenetic and molecular abnormalities (Arber et al., 2016). Additionally, in order to predict the prognosis of AML patients, the updated 2017 European Leukemia Net (ELN) risk stratification guidelines, which combine cytogenetic abnormalities and genetic mutations, are widely used (Döhner et al., 2017). However, some researchers have been looking into how to improve the risk stratification models by incorporating additional prognostic factors into the ELN-2017 guidelines (Pogosova-Agadjanyan et al., 2020). Broadly accepted by physicians as a gold standard, the ELN stratifies patients into three outcome groups: favorable, intermediate, and adverse based on the cytogenetics and the mutation status of ASXL1, CEBPA, FLT3, NPM1, RUNX1, and TP53 (Döhner et al., 2017). The single most adverse factor is a TP53 mutation, commonly associated with complex cytogenetics. The favorable effect of NPM1 and (bi-allelic) CEBPA mutations are considered unaffected by cytogenetic status. A FLT3 internal tandem duplication (ITD) is regarded as unfavorable only if the ratio of mutated to normal alleles (allelic ratio, AR) is >0.5. With increased awareness of the genetic component of AML and advances in next-generation sequencing techniques, a number of molecular aberrations have since been described at the resolution of the gene level through sequencing of over 200 AML patient genomes (Cancer Genome Atlas Research Network, 2013; Welch et al., 2012). These findings provide an additional layer of genetic complexity to AML. It is significant to highlight that despite the large number of driver mutations discovered through cytogenetic analysis and gene sequencing, only a small number, when introduced in healthy human cells, have been shown to initiate disease in humanized mice model recipients (Bursen et al., 2010; Corral et al., 1996; Nagase et al., 2018; Papaemmanuil et al., 2016; Watanabe-Okochi et al., 2008). It is challenging to identify key driver mutations because the majority of these, apart from the MLL-AF9 fusion, are demonstrated to interact synergistically with other mutations to produce disease. As a result, more research is needed to identify the functional disease drivers and develop molecular targets that could successfully treat the disease's underlying causes. Together these research efforts have led to the identification of a remarkable number of cytogenetic and molecular aberrations associated with AML toward improving disease diagnosis, classification, prognosis and therapeutic approaches.

1.5.2 Molecular techniques for the detection of AML cells

Cytogenetic and molecular analysis are the standard techniques to identify and detect abnormalities related to AML. Fluorescence in situ hybridization (FISH) and array comparative genomic hybridization are frequently used to identify cytogenetic aberrations in AML samples, whereas polymerase chain reaction and DNA sequencing-based methods are utilized to discover molecular aberrations. G-banding and/or FISH can be used to probe for and observe cytogenetic abnormalities on a per-cell basis, which is a potent tool for differentiating AML blasts carrying specific leukemia-associated aberrations from healthy cells with no aberrations.

In the 1950's condensed metaphase chromosomes from individual cells were prepared to be visualized under a microscope to count the number of chromosomes (also known as the karyotype) in human cells. It was not long before this "chromosomal spread" method was used on human tumour cells to determine that they had abnormal euploid or aneuploid karyotypes (Hsu & Moorhead, 1957), giving researchers their first look at the potential of using chromosomal spread analysis to distinguish between normal and cancerous cells. The subsequent development of G-banding techniques – Giemsa staining of metaphase chromosomes producing distinct dark (AT rich) and light (GC rich) "band" patterns unique to each chromosome – provided further opportunity to detect abnormal variations in seemingly normal diploid (n=46) karyotypes (Speicher & Carter, 2005). Together, these investigations demonstrated the value of G-banding, a clinical diagnostic method still used to assess the frequency and existence of cytogenetic abnormalities (insertions, deletions, translocations, and -ploidy) in AML samples (Borsatti & Nacheva, 2019). However, because this method necessitates a highly skilled eye, it is impractical for quick adaptation and application in non-clinical contexts.

FISH offers an alternative to classical karyotyping for fast reliable genome assessment ready for use in routine diagnostic settings (Levsky & Singer, 2003). Based on the concept of using fluorescently-labeled probes to target and visualize regions of a chromosome (Bauman et al., 1980), FISH allows users to rapidly identify leukemic cells carrying known leukemia-associated aberrations. For example, chromosomal translocations can be detected when probes that bind to two adjacent genes surrounding a breakpoint region no longer co-localize upon visualization, as is the case with AML-associated translocations involving 11q23.

Alternative methods, such as high-resolution melting (HRM), allele-specific quantitative PCR based on the amplification refractory mutation system technique (ARMS PCR), digital droplet PCR (ddPCR) and next-generation sequencing (NGS), have started to be implemented in detecting mutations specific to AML (Medeiros et al., 2017; Salehzadeh et al., 2019; Wiseman & Somervaille, 2017). For example, ddPCR has been studied as a sensitive and accurate tool for detecting acquired somatic mutations in the isocitrate dehydrogenase 1 and 2 genes (IDH1 and IDH2), whereby IDH2 mutations are found in about 20% of de novo AMLs (Grassi et al., 2020). ddPCR is based on the water-oil emulsion droplet technology that allows fractionating the template DNA into thousands of nanoliter-sized droplets where the amplification occurs. The ddPCR technology, similar to real-time PCR, uses TaqMan probe-based assays, even if results of the reaction are evaluated not in "real-time" but at the "end-point". After amplification, each droplet is analyzed to assess the presence of a positive or negative signal, using the Poisson's statistics to normalize and determine the target concentration in the original sample. The advantages of this technique are represented by the increased signal-to-noise ratio and by the absolute quantification without a need of standard curves. Since cytogenetic and molecular characteristics are important prognostic indicators allowing the identification of distinct subtypes of AML, prognostic stratification, and risk-adapted treatment, novel detection methods will continue to develop.

1.5.3 Epigenetic Dysregulation in AML

In addition to cytogenetic abnormalities, it is well established that the epigenome, which regulates gene expression at the level of chromatin conformation, is aberrant in AML (Goldberg et al., 2007). An extensively studied example of such epigenetic aberration found in AML is DNA methylation (Figueroa et al., 2009). DNA methylation is carried out by enzymes known as DNA methyltransferases (DNMT), such as DNMT1, DNMT3A, and DNMT3B, which catalyze the

conversion of cytosine to 5-methylcytosine. This chemical modification generally occurs in cytosine/guanine rich regions of DNA known as CpG islands that are often found in gene promoters (Bird, 2002), and ultimately represses gene expression (Li et al., 1993). Conversely, the TET family of enzymes are responsible for DNA demethylation required for re-activation of genes (Kohli & Zhang, 2013). In a 2010 publication, based off distinctive methylation profiles, 344 human AML samples were classified into 16 subclasses by Figueroa et al (Figueroa et al., 2010). Interestingly, this research showed that various cytogenetic and molecular abnormalities were connected to various epigenetic states. Later studies that utilized 200 AML genomes and epigenomes for next-generation whole exome sequencing and DNA methylation analyses supported these conclusions and further linked specific epigenetic profiles to underlying cytogenetic and molecular aberrations (Cancer Genome Atlas Research Network, 2013). Taken together, these results suggest that specific changes in the epigenome during AML pathogenesis may occur in response to leukemia-associated aberrations. Accordingly, several leukemic mutations affect known regulators of DNA methylation and chromatin modification such as DNMT, TET, and MLL (Cancer Genome Atlas Research Network, 2013). For example, acute promyelocytic leukemia (APL), a subtype of AML, is associated with reciprocal chromosomal translocations involving the retinoic acid receptor α (RARα) locus on chromosome 17, and in most cases, RARα translocates and fuses with the promyelocytic leukemia (PML) gene located on chromosome 15 (Fu et al., 1995). The resulting fusion genes encode the two structurally unique PML-RARα and RARα-PML fusion proteins as well as aberrant PML gene products. Both PML and RARα genes are known to be involved in regular cellular functions: PML is involved in the regulation of cellular proliferation (Salomoni & Pandolfi, 2002), and RARα is integral in myeloid differentiation and regular hematopoietic development (Melnick & Licht, 1999). It was shown that the PML-RARα product works in tandem with DNA methyltransferases (DNMTs) to induce hypermethylation in PML-RARα targets, and that PML-RARα product seems to be a necessary component for the development of a hypermethylated phenotype (Di Croce et al., 2002). For instance, mice possessing DNMT3a1 but lacking the PML-RARα product did not display a hypermethylated phenotype, while leukemic mice possessing both the PML-RARα product and DNMT3a1 presented with the hypermethylated phenotype (Subramanyam et al., 2010). Notably, retinoic acid reverses this hypermethylated phenotype (Di Croce, 2002), indicating that utility of all-trans retinoic acid (ATRA), which has a high treatment rate capable of inducing complete remission (CR) in APL patients (Degos & Wang, 2001), in part due to the epigenetic nature of its mechanism of action. Though AML has been shown to have mutations in epigenetic regulators, 44% of which are found in DNA methylation related genes, and 43% of which encoded chromatin modifiers or cohesion-complex genes (Cancer Genome Atlas Research Network, 2013), causal links between leukemia-associated aberrations and the abnormal AML epigenome remain poorly resolved. Therefore, the study of epigenetics in the context of AML has become a fast-growing area of research in the field (Cai & Levine, 2019).

1.5.4 Current therapies of AML

For a long time, the first-line treatment for AML has been standard induction chemotherapy, which consists of an anthracycline and cytarabine commonly referred to as “7+3”. The “7+3” chemotherapy regimen, consists of 7 days of cytarabine and 3 days of anthracycline in varying doses to maximize efficacy while minimizing treatment related mortality which is especially of concern in the elderly. Although most patients experience CR with this treatment,

many also experience relapses due to adaptive resistance or have refractory disease (primary resistance). Unfortunately, the persistence of therapy-resistant leukemia cells causes AML to recur and it is reported that relapse affects about 50% of all patients who achieved remission after initial treatment. Leukemic stem cells (LSCs), leukemia cells with stem cell characteristics found in minimal residual disease, are assumed to be the cause of relapse. These leukemia "persister" cells are thought to be created by intra-leukemic heterogeneity and non-genetic variables that cause plasticity in therapeutic response. Recently, major advances in molecular and cell biology have improved our understanding of the pathophysiology of AML and expanded targeted treatment options. These advances have provided personalized treatment options for many patients and may provide future opportunities to pre-empt the development of AML. Currently, a few targeted therapies are being used in the clinic to treat selective molecular abnormalities of AML. The most successful of these and the only therapy used as a sole treatment with no chemotherapy is based on a cytogenetically distinct subtype of AML referred to as APL. APL was first described as a highly aggressive form of hematologic disorder with an abysmal survival of only weeks (Wang & Chen, 2008). ATRA and arsenic trioxide (ATO), a differentiation therapy targeting AML disease demarcated by PML-RARα fusion protein product has changed the prognosis drastically with remission and cure rates of 80 and 90 percent respectively (Dos Santos et al., 2013; Wang & Chen, 2008). Interestingly, the differentiation potency of ATRA was determined even before the molecular basis of leukemic transformation was elucidated.

Since then, targeted therapies have been developed for FLT3 mutations and IDH1/2 mutations. FLT3 mutations are among the most frequently detected in patients with AML. Two types of FLT3 mutation exist, internal tandem duplications (ITDs) resulting in the duplication of nucleotide sequences with differing lengths and insertion sites, and single nucleotide variants in the tyrosine kinase domain (TKD). Both types of mutation lead to constitutive activation of the receptor and its downstream signalling pathways, such as PI3K/AKT/mTOR, RAS/MAPK and STAT5 (Döhner et al., 2021). The clinical development of FLT3 inhibitors has been one of the most active fields in precision medicine for AML (Smith, 2019). First-generation agents, such as midostaurin, sorafenib and lestaurtinib, are broad spectrum tyrosine kinase inhibitors (TKIs) with only modest and transient anti-leukemic activity as single agents. The efficacy of midostaurin in combination with intensive induction and consolidation chemotherapy followed by a 1-year maintenance phase was evaluated in a phase III trial (Stone et al., 2017). Midostaurin significantly increased overall survival (OS) and event-free survival, however, these increases remained modest (4-year OS 51% versus 44% for placebo), and treatment was not curative for approximately half of these patients. Next-generation FLT3 inhibitors, such as gilteritinib, quizartinib and crenolanib, are more selective and have shown promising activity as single agents in early phase trials (Cortes et al., 2018; Perl et al., 2017). Furthermore, somatic gain of function mutations in Isocitrate dehydrogenase 1 (IDH1) and IDH2 exist in approximately 20% of patients with newly diagnosed AML (Bullinger et al., 2017). IDH1 or IDH2 are NADP+ dependent enzymes that catalyze the oxidative decarboxylation of isocitrate to αketoglutarate (αKG) and are key components of the Krebs cycle. The first selective inhibitors of mutant IDH1 and IDH2, to enter clinical development were ivosidenib and enasidenib. These inhibitors have been evaluated for their effects in patients with resistant and/or relapsed IDH1/IDH2 mutant AML, and the results have verified their capacity to operate as single agents, stimulate cellular differentiation, and produce therapeutic responses in a sizable fraction of patients (DiNardo et al., 2018; Stein et al., 2017, p. 2).

An alternative therapeutic approach that is still in its early days is the development of immunotherapies for patients with AML. Several antibody-based, as well as cell-based

immunotherapies, have demonstrated clinical activity across a diverse range of AML genotypes and have enabled certain forms of resistance to molecularly targeted therapies to be overcome. An example of this is Gemtuzumab ozogamicin (GO) which consists of a humanized anti-CD33 monoclonal antibody conjugated with calicheamicin. This antibody-drug conjugate enables the targeted delivery of a cytotoxic payload to leukemia cells since calicheamicin induces double-stranded DNA breaks and subsequent cell cycle arrest and apoptosis. Several studies have investigated the potential role of GO as a maintenance therapy in AML. For example, GO, in combination with high-intensity chemotherapy, has been shown to increase survival in patients with newly diagnosed AML aged 50–70 years, with particular activity in core binding factor and intermediate cytogenetic risk forms of AML, including NPM1 mutant disease, all of which are generally characterized by high levels of CD33 expression (Castaigne et al., 2012; Lambert et al., 2019). Overall, despite the identification of numerous molecular and immunological therapeutic targets and the ongoing development of numerous targeted therapies, significant obstacles still stand in the way of both the effective clinical application of these therapies and their critical evaluation in AML patients.

1.5.5 The development of experimental models of AML

AML is functionally organized in a manner that resembles normal hematopoiesis, whereby the disease is initiated and sustained by a rare population of LSCs that gives rise to dysfunctional AML progenitors incapable of normal differentiation to mature myeloid cells (Bonnet and Dick, 1997; Lapidot et al., 1994). In vitro and in vivo model systems and assays have been instrumental in developing our current understanding of this disease. In this section we highlight two main assays for characterizing AML, the clonogenic progenitor assay and the LSC assay.

Clonogenic Progenitor Assay

As mentioned in the above sections, the clonogenic progenitor or CFU assay was first developed in 1966 by Ray Bradley and Donald Metcalf when they observed a small fraction of healthy murine BM cells were capable of forming clonal colonies when seeded in semi-sold growth medium (Bradley & Metcalf, 1966). Metcalf later adapted this assay to both the human and leukemic systems by measuring the capacity of myelomonocytic leukemia progenitors to form colonies (AML-CFU) (Metcalf et al., 1969). Interestingly, this assay revealed that AML progenitors were capable of initiating the differentiation process but were unable to achieve full morphological maturation and instead produced immature “blast”-like colonies, providing the first in vitro demonstration of a differentiation blockade, phenocopying the primary disease (Metcalf et al., 1969). The concept from this assay have now been improved to efficiently detect HPCs and AML progenitors through the formation of monocytic, granulocytic, erythrocytic, megakaryocytic, and blast colonies (Griffin & Löwenberg, 1986; Wognum et al., 2013), but the principles of the assay remain the same. Together, these studies demonstrated the utility of the CFU assay in identifying and measuring normal and AML progenitors, as well as a framework for modelling the AML differentiation blockage (Moore et al., 1973; Sachs, 1987). The use of the CFU assay, in combination with morphological and cytogenetic assessments, as a means of distinguishing normal and leukemic cells was heavily investigated in this thesis and was crucial to the conclusions drawn.

Humanized Mouse AML Xenotransplant

While the CFU assay provided a testing ground to quantify the frequency of AML progenitors and the severity of their differentiation blockade, it is not informative of their functional long-term self-renewal capacity. Accordingly, researchers set out to identify and characterize the leukemic cells responsible for disease initiation. Since it was hypothesized that leukemia was organized in a similar fashion to the normal hematopoietic system, researchers reasoned that primitive AML cells could initiate leukemia in a mouse similar to the ability of normal HSPCs to initiate normal hematopoiesis (Kamel-Reid & Dick, 1988; Mosier et al., 1988). Initial efforts to transplant primary AML cells into SCID mice were challenged by the inability to create orthotopic xenografts by intravenous transplantation (Sawyers et al., 1992). However, this limitation was overcome by supplementing SCID mice with human cytokine injections following transplantation (Lapidot et al., 1992), and by the eventual application of the more permissive NOD/SCID strain (Bonnet & Dick, 1997). This hypothesis was subsequently proven by demonstrating that a distinct population of AML cells (1 in 250,000) was able to trigger and recapitulate patient leukemia when transplanted into SCID recipient mice (Lapidot et al., 1994). Importantly, like their healthy SRC counterparts (Bhatia et al., 1997), SCID leukemia-initiating cells (SL-ICs) were restricted to the $CD34^+CD38^-$ phenotypic population, with little to no engraftment activity within $CD34^+CD38^+$ or $CD34^-$ cells. Moreover, engrafted human cells lacked evidence of healthy hematopoiesis based on the exclusively myeloid composition of reconstituted cells (Bonnet & Dick, 1997), and the consistent identification of patient-specific chromosomal abnormalities (Lapidot et al., 1994). In additional to the modest differentiation potential observed, xenografted AML cells also maintained self-renewal capacity through serial transplantation and CFU assessment (Bonnet & Dick, 1997; Lapidot et al., 1994).

The finding that $CD34^+CD38^-$ cells could engraft NOD/SCID mice and maintain CFU capacity, but that $CD34^+CD38^+$ populations were restricted to CFU formation was initially suggestive of a hierarchical organization in AML (Lapidot et al., 1994). This hypothesis was further reinforced by lentiviral marking studies, which established that like the healthy hematopoietic system (Guenechea et al., 2001), the clonal lineages that compose the SL-IC pool possess variable capacities for self-renewal (Hope et al., 2004). Together, these seminal studies provided the first experimental evidence in support that AML is organized in a functional hierarchy with a rare subset of primitive LSCs generating and maintaining the tumor through differentiation and self-renewal in a manner similar to their normal HSPC counterparts (Bonnet & Dick, 1997; Hope et al., 2004; Lapidot et al., 1994). As such, the LSC assay – the ability of a leukemic cell to initiate and maintain disease in a mouse recipient – is the current gold-standard in the field for assessing the self-renewal and disease initiation capacity of AML cells.

1.6 iPSC models of AML

Although monogenic inherited blood diseases were the first to be modeled with iPSCs (Hanna et al., 2007), malignant hematologic disorders such as AML have been more challenging to obtain. Unlike inherited genetic diseases, where disease-causing mutations are present in the germline to be passed to all somatic cells, most AML genetic lesions arise postnatally and accumulate sequentially in the somatic HSC compartment. Accordingly, while iPSC models of inherited monogenic diseases can be derived by reprogramming any accessible cell type, derivation of AML-iPSCs requires reprogramming hematopoietic leukemic cells themselves and

not skin fibroblasts etc. from the AML patient. In 2017 Kotini et al. and Chao et al. demonstrated that iPSCs can be reprogrammed from AML samples and give rise to LSCs that robustly engraft and cause acute disease in mice (Chao et al., 2017; Kotini et al., 2017a). These findings suggested that oncogenic mutations captured within AML-iPSCs can specify the LSC epigenetic state during differentiation. Although some reports have successfully reprogrammed myeloid malignancies over the past few years, we and others have shown leukemic cells are relatively refractory to reprogramming (Chao et al., 2017; Kotini et al., 2017a; J.-H. Lee et al., 2017; Yamasaki et al., 2020), similar to other highly proliferative malignant cells (Gandre-Babbe et al., 2013; Hosoi et al., 2014; Hu et al., 2011; Kumano et al., 2012). This results in an experimental predominance of normal iPSCs from patient hematopoietic BM and PB-derived tissue devoid of clinically defined leukemic mutations (Chao et al., 2017; Hoffman et al., 2017; J. Kim et al., 2013; Kotini et al., 2017a; J.-H. Lee et al., 2017; Muñoz-López et al., 2016; Raya et al., 2009; Yamasaki et al., 2020). This refractoriness to reprogramming is paradoxical, and the refractory nature of leukemic cells is unclear. While this introduces a challenge to reprogram some leukemic cells directly, it creates an opportunity to capture and interrogate preleukemic and leukemic intermediates that may be too rare to detect in other assays. For example, by measuring the engraftment potential of HSPCs derived from low-risk Myelodysplastic syndromes (MDS)-iPSCs (MDS-iPSCs), high-risk MDS-iPSCs, and AML-iPSCs, Kotini et al demonstrated that only the AML-iPSCs were able to give rise to leukemia in vivo, and could be maintained long term in vitro (Kotini et al., 2017a). MDS are a heterogenous group of clonal bone marrow disorders characterized by cytopenia, bone marrow dysplasia, ineffective hematopoiesis, and a high risk for transformation to AML (Bejar, 2014; Ogawa, 2019). Similarly, Chao et al. compared the engraftment potential of KRAS G13D-mutant and wild-type AML-iPSC subclones derived from the same patient. AML cells derived from KRAS mutant iPSCs engrafted, while the KRAS wild type cells did not (Chao et al., 2017). Building off of their 2017 paper, Papapetrou's group isolated two different AML-iPSC derived hematopoietic populations termed iLSC and iBlasts and demonstrated that only iLSCs could initiate leukemia in vivo (Wesely et al., 2020). Further characterization of the iLSCs revealed RUNX1 as a critical player in the maintenance of the iLSC population. Attenuating RUNX1 protein by 50% in the iLSC population abolished their ability to engraft or to survive long term in vitro (Wesely et al., 2020). These studies collectively show how patient-derived iPSC models can inform leukemogenesis.

One strategy to circumvent reprogramming barriers in the generation of AML-iPSCs is to engineering mutations directly into healthy iPSCs by using CRISPR/Cas9. For example, a high-risk MDS patient sample reprogrammed by Kotini et al. yielded iPSCs derived from normal cells or from a high-risk MDS clone (Kotini et al., 2017a). The normal iPSC line was genetically edited to introduce a truncating mutation in ASXL1 gene, which encodes a protein involved in chromatin remodeling, and a further deletion of 7q in the ASXL1 mutant clone. This yielded patient-derived iPSC lines representative of each stage of disease progression, from normal to pre leukemic to MDS. More recently, the same authors developed a CRISPR/Cas9-based system to more simply introduce precise chromosomal deletions in iPSCs (Kotini & Papapetrou, 2020). In summary, even though reprogramming barriers can make it difficult to derive all disease clones in a patient, normal or preleukemic subclones can be genetically edited to create a group of clones with the same genetic background that mimic the disease's progression.

1.7 Summary of Intent

AML is a highly heterogeneous cancer with a poor prognosis. Clinical presentation is characterized by abundant non-functional immature hematopoietic cells (blasts) in the BM and PB of patients. Untreated, the rapid proliferation of these blasts contributes to hematopoietic system failure within months, leading to death. Although the standard chemotherapy regimen has remained relatively unchanged for decades and has proven to be effective at achieving initial remission induction, most patients succumb to relapse forming the basis of poor long-term survival. Despite the clinical need to move toward targeted treatments, novel therapeutics optimized using existing models of AML fail to prevent relapse. Moreover, AML patients who achieve CR after induction therapy require post remission therapy (PRT) to remain disease free. For patients in CR, HSCT is considered curative. Incomplete mechanistic understandings of disease initiation, progression and maintenance of AML have impeded advances in therapy required for the improvement of long-term patient survival rates. This suggests that innovative and new model systems are required to understand the earliest initiation processes of AML disease towards more effective targeted therapy development.

The ability to generate iPSCs from human somatic cells provided a breakthrough in biomedicine to 'capture' diseased cells and their genome in a self-renewing state. Patient-derived hiPSCs have the theoretical ability to develop patient-specific (autologous) cell-based therapies and produce an endless number of specialized disease-associated cells, allowing replication of pathological characteristics of human disease in vitro. Despite the technical challenge of reprogramming human cancer cells due to the high inefficiency of the process compared to healthy samples, whereby iPSCs are often skewed in favor of residual normal cells over cells of the premalignant or malignant clone, **I propose to develop a library of AML patient-derived iPSCs. Moreover, I hypothesize that pluripotent reprogramming can provide a unique alternative approach to dissect heterogeneity and molecular basis of AML that cannot be captured and studied in existing *in vitro* or *in vivo* patient-derived xenograft models.**

Although some reports have successfully reprogrammed myeloid malignancies over the years, we and others have shown leukemic cells are relatively refractory to reprogramming similar to other highly proliferative malignant cells. This results in an experimental predominance of normal iPSCs from patient hematopoietic BM and PB-derived tissue devoid of clinically defined leukemic mutations which our lab has previously successfully generated. However, prior to interrogating how best to refine the reprogramming process for the generation of the library**, we first sought to investigate the ability of two AML patient-derived iPSC lines devoid of somatic leukemic aberrations as a means of generating SRC as a proof of concept for the use of hiPSCs as a potential autologous source of HSCs (Figure 1).**

HSCs are functionally defined by their self-renewal activity and multi-lineage differentiation potential and thus possess an enormous therapeutic potential for HSCT. To date, HSCT remains the most efficacious cell therapy and enables the complete restoration of the hematopoietic system (myeloid, erythroid, and lymphoid lineages). In the context of AML, the generation of AML patient-specific HSCs that are devoid of the leukemic aberration(s) that affect the patient's hematopoietic tissue would provide a transformative approach in establishing a healthy autologous source of transplantable HSCs. HSCs arise from a type of endothelial cell called HE and are experimentally detected by transplantation into SCID mice or other immune-deficient mouse recipients, termed SCID-Repopulating Cells (SRC). Recently, using a defined set of TFs two landmark studies recapitulated the endothelial-to-hematopoietic lineage transition (EHT) to generate putative mouse HSCs or human SRCs using HEs derived from PSC. **Therefore, using HEs derived from iPSCs reprogrammed from AML patient skin fibroblasts and BM**

cells devoid of somatic leukemic aberrations, I tested whether forced expression of the previously defined set of TFs would enable derivation of autologous sources of HSPCs in vitro and in vivo. In this study **(Chapter 2)**, we discovered the low potential of human PSCs to generate bona fide HSPCs, but overall concluded a lack of understanding of how these TFs act, on which cell types they act on (e.g., HSC vs. common lymphoid progenitors or common myeloid progenitors), and the nature of niche signals that direct the specification of HSPCs from hPSC-derived HE cells in vivo.

We next sought to investigate what is necessary to improve the overall reprogramming efficiency of AML into a pluripotent state. Despite the unknown 'barriers' that exist with successful reprogramming including the admixture of co-isolating normal and clonal leukemic cells in the BM and PB of AML patients, **I hypothesize that their clonal heterogeneity holds the potential to be leveraged to derive both disease and normal iPSC lines in the same reprogramming process to generate paired isogenic and AML-iPSCs from individual AML patients (Figure 2). Moreover, immuno-phenotyping before reprogramming is a natural extension of previous work done in our lab, but no one has contrasted and compared both during reprogramming.** Using our refined methods for reprogramming AML cells, a total of 15 out of 22 AML patient samples representing a wide variety of cytogenic abnormalities of this disease were successfully reprogrammed **(Chapter 3)**. This allowed us to derive genetically matched normal control isogenic lines and capture rare clones of AML disease in bona fide AML induced pluripotent stem cell (AML-iPSC) which were confirmed to possess leukemic-specific genetic aberrations specific to the primary samples they were isolated from. Furthermore, using fluorescence activated cell sorting (FACS), we show that AML and healthy reprograming is linked to the differentiation state of diseased tissue. Our efforts provided the basis for further optimization of AML-iPSC generation, and a unique library of 131 mutant and healthy iPSCs of which 77 AML-iPSC lines from a total of 7 AML patients were generated, representing the largest AML-iPSC library to date.

To validate our AML-iPSCs library, **the previously reported ability of AML-iPSCs to maintain features of their cells of origin was assessed by performing hematopoietic differentiation assays (Figure 3)**. In contrast to isogenic control lines from the same patients, AML-iPSC lines demonstrate a block in differentiation measured by functional colony-forming unit (CFU) generation and fail to develop into primitive ($CD34^+/CD45^+$) or mature blood cells ($CD45^+$). These results were consistent across three distinct hematopoietic differentiation methodologies tested for human PSC: (1) cytokines and BMP4 treatment of embryoid bodies (2) endothelial-hematopoietic transition (EHT) and (3) OP9 co-culture supporting that this was not an artifact of *in vitro* differentiation **(Chapter 4)**. Notably, these findings are reminiscent of the hematopoietic blockade observed in AML characterized by an inability to generate mature blood cells. This supports the concept of retaining epigenetic memory of the reprogrammed AML cells and is similar to the observation of enhanced blood formation from iPSCs made from healthy hematopoietic cells (K. Kim et al., 2010; J.-H. Lee et al., 2014). However, despite harbouring cytogenetic mutations originating from donor patient disease cells, some AML-iPSC clones from the same patient demonstrated hematopoietic differentiation capacity to similar degrees as healthy iPSCs, thereby serving as ideal controls for future molecular comparison between iPSCs lines with differing hematopoietic capacity.

In conclusion, this global body of work shows that it is possible to use cellular reprogramming to generate normal and dysfunctional HSPCs from AML patient somatic cells. These foundational observations should motivate additional studies aimed at systematically

understanding the fundamental molecular drivers of AML disease, identification of new targets, and development of new biomarkers to predict and prevent relapse toward improving AML patient quality of life and long-term survival rates.

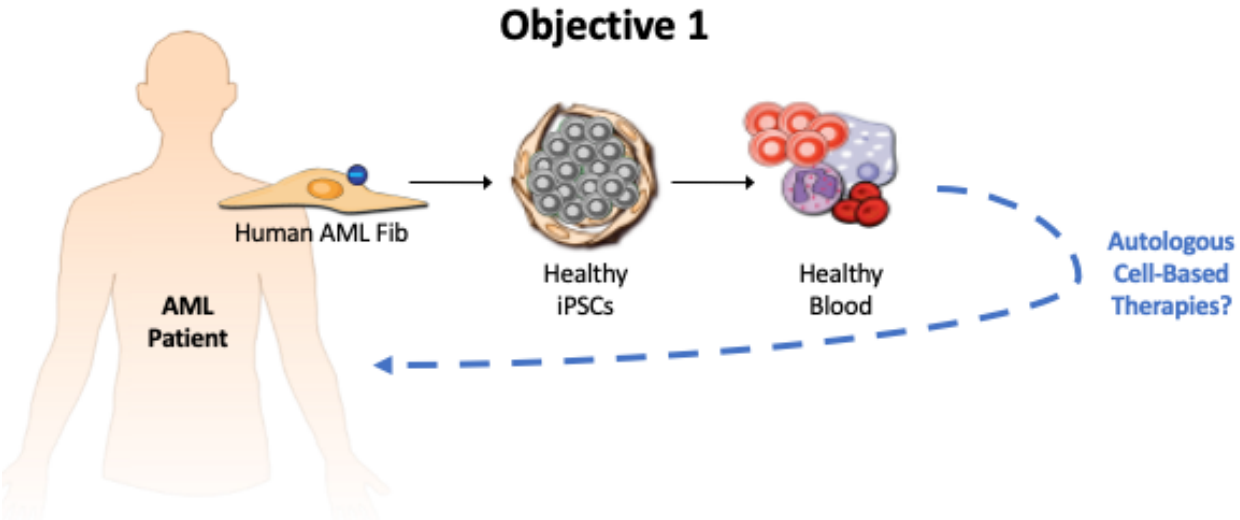

Figure 1. Objective 1
Using iPSCs reprogrammed from AML patient skin fibroblasts and BM cells devoid of somatic leukemic aberrations, I sought to generate putative SCID repopulating cells (HSCs) by development of hemogenic endothelial cells (HEs) through forced expression of a previously defined set of TFs as a proof of concept for the use of PSCs for autologous hematopoietic stem cell transplantations (HSCTs).

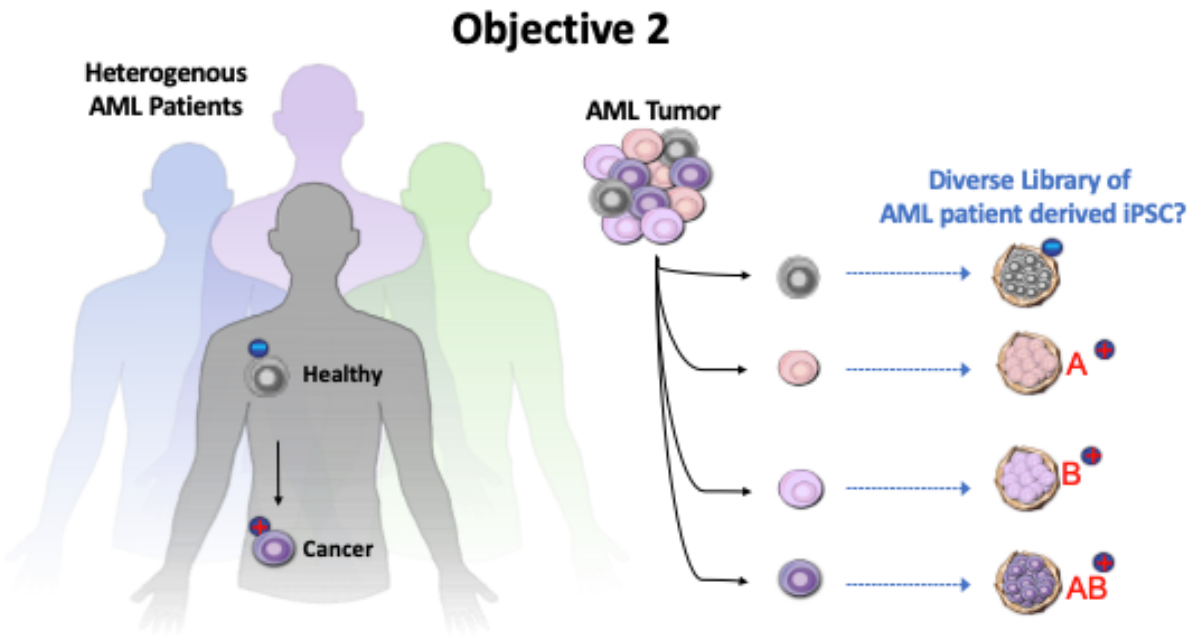

Figure 2. Objective 2
Develop a large diverse library of AML patient derived iPSCs from a heterogenous set of patients.

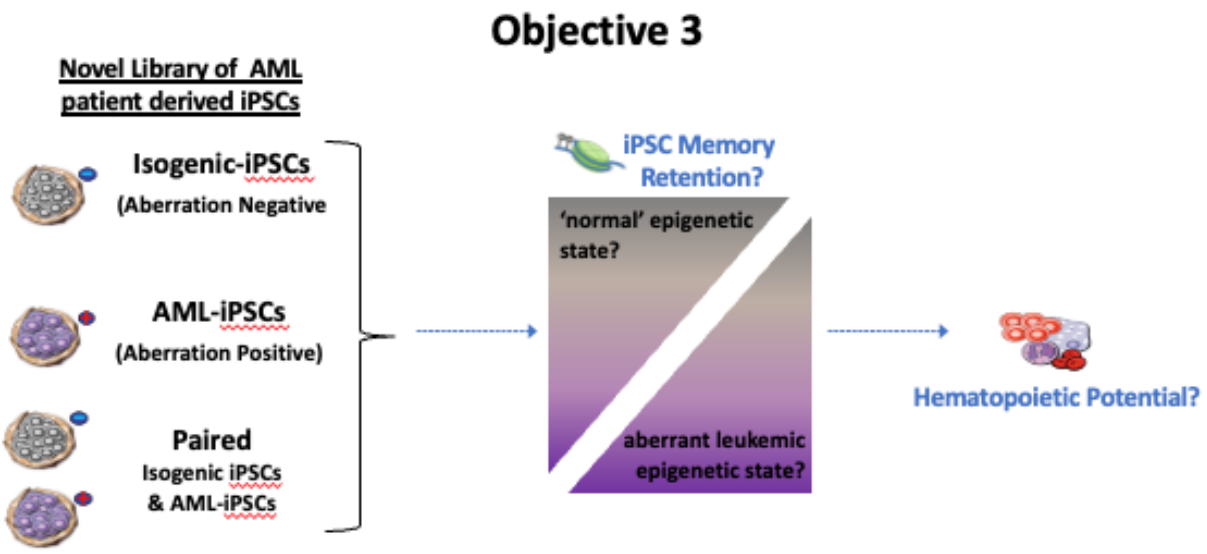

Figure 3. Objective 3
Through the generation of our novel AML patient derived iPSC library which captures both intra- and inter-patient heterogeneity, I sought to interrogate whether an aberrant leukemic epigenetic landscape inherent to de novo human AML is captured in AML-iPSCs (when the cytogenetics of the primary patient are present in the iPSC line derived.

Chapter 2: Challenges in cell fate acquisition to Scid-Repopulating Activity from hemogenic endothelium of hiPSCs derived from AML patients using forced transcription factor expression

Preamble

This chapter is an original published article. It is presented in its published form.

Cells **2022,** 11(12), 1915; https://doi.org/10.3390/cells11121915

Author contributions: D.P.P, J.C.R., B.T., and D.G. performed experiments. A.L.B., aided with the CB transplant assay. D.P.P, J.C.R. and M.B. designed experiments and interpreted data. D.P.P and B.T. cloned constructions. D.P.P and M.B wrote the manuscript. M.B. directed the study.

Author contributions in greater detail: I designed the study and wrote the manuscript along with input from Dr. Jenn Reid and my supervisor Dr. Mick Bhatia. I performed all western blotting, qRT-PCR and lenti viral generation and transduction of all transcription factor and control constructs. Transcription factor inducible constructs were generated by Dr. Borko Tanasijevic with input and assistance from myself. Dr. Jenn Reid performed RT-PCR experiments on bone marrow harvests for human DNA detection. Dr. Allison Boyd performed all CB transplant assays. All animal harvest were performed by me, Dr. Jenn Reid and on occasion Diana Golubeva. Animals treated by daily oral gavage were treated by Dr Jenn Reid and myself. Similarly *in vitro* culture of all hPSC lines and flow cytometric experiments were performed by myself and Dr. Jenn Reid. Dr. Mick Bhatia directed the entire study and assisted in manuscript preparation.

Challenges In Cell Fate Acquisition To Scid-Repopulating Activity From Hemogenic Endothelium Of Hipscs Derived From AML Patients Using Forced Transcription Factor Expression

Authors: Deanna P. Porras [1,†], Jennifer C. Reid [1,†], Borko Tanasijevic [1], Diana Golubeva [1], Allison L. Boyd [1] and Mickie Bhatia [1,2,*]

Affiliations:
[1]Department of Biochemistry and Biomedical Sciences, McMaster University, Hamilton, ON L8N 3Z5, Canada; porrasd@mcmaster.ca (D.P.P.); reidjc2@mcmaster.ca (J.C.R.);
tanasb@mcmaster.ca (B.T.); golubeda@mcmaster.ca (D.G.); boydal2@mcmaster.ca (A.L.B.)
[2]Michael G. DeGroote School of Medicine, McMaster University, 1200 Main Street West, MDCL 5029, Hamilton, ON L8N 3Z5, Canada
*Correspondence: mbhatia@mcmaster.ca; Tel.: +1-(905)-525-9140 (ext. 28687)
[†]These authors contributed equally to this work.

Academic Editors: Françoise Porteu and Halvard B. Bönig

Cells 2022, 11(12), 1915; https://doi.org/10.3390/cells11121915
Received: 27 March 2022 / Revised: 5 June 2022 / Accepted: 8 June 2022 / Published: 13 June 2022 (This article belongs to the Special Issue Generation of Hematopoietic Stem/Progenitor Cells from Pluripotent Stem Cells for Cellular Therapy)

Highlights

- Derivation of hemogenic endothelium from a broad range of hPSCs, including AML derived iPSCs
- Forced expression of 7TFs enhances progenitor capacity from iPSCs derived from AML patients
- TF induction in hPSC-derived hemogenic endothelium lack robust SCID Repop-ulating Activity.

Keywords : AML; acute myeloid leukemia; HSPC; hematopoietic stem/progenitor cell; iPSC; induced pluripotent stem cell; HE; hemogenic endothelium; TF; transcription factor; hPSC-HSPCs; human pluripotent stem cell (hPSC)-derived HSPCs; Xenotransplantation

Abstract

The generation of human hematopoietic stem cells (HSCs) from human pluripotent stem cells (hPSCs) represents a major goal in regenerative medicine and is believed would follow principles

of early development. HSCs arise from a type of endothelial cell called a "hemogenic endothelium" (HE), and human HSCs are experimentally detected by transplantation into SCID or other immune-deficient mouse recipients, termed SCID-Repopulating Cells (SRC). Recently, SRCs were detected by forced expression of seven transcription factors (TF) (ERG, HOXA5, HOXA9, HOXA10, LCOR, RUNX1, and SPI1) in hPSC-derived HE, suggesting these factors are deficient in hPSC differentiation to HEs required to generate HSCs. Here we derived PECAM-1-, Flk-1-, and VE-cadherin-positive endothelial cells that also lack CD45 expression (PFVCD45^{-}) which are solely responsible for hematopoietic output from iPSC lines reprogrammed from AML patients. Using HEs derived from AML patient iPSCs devoid of somatic leukemic aberrations, we sought to generate putative SRCs by the forced expression of 7TFs to model autologous HSC transplantation. The expression of 7TFs in hPSC-derived HE cells from an enhanced hematopoietic progenitor capacity was present in vitro, but failed to acquire SRC activity in vivo. Our findings emphasize the benefits of forced TF expression, along with the continued challenges in developing HSCs for autologous-based therapies from hPSC sources.

1. Introduction

Hematopoietic stem cells (HSCs) are functionally defined by their self-renewal activity and multi-lineage differentiation potential [1,2,3]. Consequently, human HSCs possess enormous therapeutic potential in the context of HSC transplantation (HSCT) [4,5,6]. To date, HSCT remains the most prevalent and efficacious cell therapy and enables the complete restoration of the hematopoietic system (myeloid, erythroid, and lymphoid lineages) in patients after hematopoietic damaging chemo- and radiation therapy, as well as for treatment of a variety of hematological disorders such as Acute myeloid leukemia (AML). AML is a clonal disorder characterized by the accumulation of immature myeloid progenitors (AML blasts) in the bone marrow (BM) and peripheral blood of patients. The overproduction of AML blasts and inability to differentiate depletes and affects production of other normal blood cells resulting in a variety of symptoms, including anemia and infection [7]. Although the induction of remission and subsequent post-remission therapies for AML are generally effective, relapse of the disease attributes to poor long-term survival rates [8]. However, the use of HSCT is known to be curative and may, in part, be due to the replacement of leukemic stem cells (LSC)s with healthy, newly transplanted HSCs [9]. This suggests that although the majority of HSCT in AML patients are allogenic and are accompanied with benefits of graft versus leukemia (GVL) [10], autologous HSCT has significant benefits and a potential impact on disease survival. An alternative source of HSCs would be directly applicable to AML disease management and several other disorders, where pluripotent stem cells (PSCs) have been noted as an ideal renewable source [11] capable of generating these highly sought-after cells.

The generation of HSCs from pluripotent sources requires an understanding of development biology involving HSC genesis in the mammal. HSCs emerge in the second and definitive wave of hematopoiesis derived from the endothelial microenvironment of the dorsal aorta within the aorta–gonad–mesonephros (AGM) region [12,13,14]. Accordingly, endothelial markers are expressed in early hematopoietic cells, underscoring the direct link of hematopoietic and endothelial cells from a common endothelial precursor [15,16]. Lineage-tracing studies provided direct evidence for a specialized hemato-endothelial precursor, that has been broadly termed a hemogenic endothelium (HE) [17,18]. HE cells migrate to the fetal liver where they expand dramatically, and then migrate to the BM at birth and sustain hematopoiesis throughout

adulthood [14,19]. The developmental origins and molecular cues driving hematopoiesis and subsequent HSC formation have been investigated to recapitulate this process in vitro for HSC generation from embryonic stem cells (ESCs). Specifically, the ability to generate human induced pluripotent stem cells (hiPSCs) [20] that share phenotypic, molecular, and functional hallmarks with human ESCs, provides opportunities to mimic developmental programs in vitro through the utilization of growth factors that regulate similar signaling cascades. Unfortunately, similar to the initial pioneering attempts to generate HSCs from human PSCs, extensive investigation and more sophisticated procedures to derive transplantable HSCs from hPSC sources have been consistently unsuccessful when strictly using morphogens and cytokines [21,22,23,24,25]. This is likely due to the complex coordinated orchestration and reception of temporally and spatially dynamic signaling pathways (NOTCH, FGF (fibroblast growth factor), EGF (epidermal growth factor), Wingless/WNT, HEDGEHOG, BMP/TGF, HIPPO, cytokine/JAK/STATs, TNF/IFN/NFB, JNK, and RAR) crucial to hematopoietic development [26].

HSCs are operationally defined based on their ability to give rise to the reconstitution (self-renewal) of all blood lineages (multi-lineage) following transplantation into patients, clinically speaking, and immunodeficient mice, experimentally. Currently, the severe combined immunodeficiency (SCID)-repopulating cell (SRC) assay has been considered a gold standard for the surrogate assessment of human HSC activity [27,28]. The generation of abundant alternative sources of HSCs remain an elusive, but critical need for expanded HSC applications. In the context of AML, the generation of AML patient-specific HSCs that are devoid of the leukemic aberration(s) that affect the patient's hematopoietic tissue would provide a transformative approach in establishing a healthy autologous source during the management of AML patients [29]. Robust long-term engraftment of hPSC-derived SRCs remains a major goal to the clinical and scientific communities alike [25,30]. Recently, two landmark studies recapitulated the endothelial-to-hematopoietic lineage transition (EHT) to generate putative mouse HSCs [31] or human SRCs [32] from the Rafii and Daley groups, respectively. In the case of human PSCs-derived SRCs, both morphogen-directed differentiation and defined transcription factor (TF) over-expression were required to mediate the conversion [32]. Interestingly, engraftment was only achieved when HE precursor cells were programmed by TFs in vivo, suggesting that extracellular cues were essential for the subsequent specification of putative HSCs from hPSCs at this specific stage of cellular differentiation. Using iPSCs reprogrammed from AML patient skin fibroblasts [29] and BM cells devoid of somatic leukemic aberrations [33], we sought to generate putative SRCs by the development of HEs, and forced expression of previously defined TFs as a proof of concept for the use of PSCs for autologous HSCTs.

2. Material & Methods

2.1. Human iPSC Lines

The derivation of the human hiPSC-1 (normal iPSC from AML #15331 BM N1) and hiPSC-2 (normal iPSC from AML #28787 fib N18) used in this study has previously been described [29,33].

2.2. hPSC Culture

Experiments were performed using human ESC line (H9), hiPSC-1, and hiPSC-2, maintained on matrigel (BD, Mississauga, ON, Canada) in mouse embryonic fibroblast-conditioned media (MEF-CM) with 8 ng/mL basic fibroblast growth factor (bFGF), as previously described [34].

Media were changed daily and cells were passaged as clumps weekly using collagenase IV. In a subset of experiments, hPSCs were transitioned to mTeSR media (Stem Cell Technologies, Vancouver, BC, Canada) and maintained on matrigel with daily media changes. hPSC colonies cultured in mTeSR media were dissociate with 0.05% Trypsin for 5 min at 37 °C, pipetted thoroughly with p1000 to form small aggregates, and subsequently washed twice with PBS+2%FBS media for further experimentation (i.e., EB differentiation).

2.3. hPSC EB Differentiation

hPSCs were differentiated using two distinct methods: (1) using cytokines and BMP4 protocol in which hPSCs were treated with 200 U/mL collagenase IV (Invitrogen, Burlington, ON, Canada), scraped into clumps, and transferred into suspension culture to form embryoid bodies (EB), as previously described [34]; and (2) using cytokines and "supplemented StemPro-34" media in 10 cm plates of EZSPHERE (EZSPHERE TM, ASAHI GLASS CO; Well Size (μm) Diameter: 400–500, Depth: 100–200; No. of Well 14,000/dish) at a density of 5 million/dish, as previously described [32]. Experiments were conducted under normoxia (5% CO_2 incubator) unless stated otherwise. In select cases, cells were maintained in hypoxic (5%O_2/5% CO_2/90% N_2) culture conditions.

2.4. hPSC EHT Differentiation

Both MEF-CM-cultured hPSCs and mTeSR-cultured hPSCs were dissociated, as described above, on either EB day 10 or EB day 8, respectively (EHT day 0). Dissociated EBs were immediately processed for isolation of HE cells, as previously described [30]. Briefly, cells were resuspended in 1 mL of PBS+2%FBS and incubated with human CD34 MicroBead kit for 1 h (Miltenyl Biotec, Inc., Somerville, MA, USA; Cat# 130-046-702). After incubation, cells were washed again with PBS+2%FBS and human CD34+ cells were isolated by magnetic cell isolation (MACS) using LS columns (Miltenyl Biotec, Inc., Somerville, MA, USA; Cat# 130-042-401) according to the manufacturer's instructions. Next, sorted human CD34+ cells were resuspend in supplemented StemPro-34 media, containing Y-27632 (10 μM), TPO (30 ng/mL), IL-3 (10 ng/mL), SCF (50 ng/mL), IL-6 (10 ng/mL), IL-11 (5 ng/mL), IGF-1 (25 ng/mL), VEGF (5 ng/mL), bFGF (5 ng/mL), BMP4 (10 ng/mL), and Flt-3L (10 ng/mL), hereafter called EHT media. All reagents were purchased from the suppliers listed in the referenced study. Cells were seeded at a density of 25–50 × 10^3 cells per well onto thin-layer Matrigel-coated 24-well plates.

2.5. Lentiviral Gene Transfer

The following ORFs were purchased from Genecopoeia (GeneCopoeia, Inc., Rockville, MD, USA): (Table 1).

Table 1. Transcription Factor ORFs

Description	Biological (Y/N)/BSL Level	Cat #
ERG (transcript variant 1) ORF clone	Y, level 1	EX-Z1500-Lv165
LCOR (transcript variant 3) ORF clone	Y, level 1	EX-E2088-Lv165
HOXA10 ORF clone	Y, level 1	EX-Z5789-Lv165
HOXA5 ORF clone	Y, level 1	EX-F0180-Lv165

Description	Biological (Y/N)/BSL Level	Cat #
HOXA9 ORF clone	Y, level 1	EX-P0078-Lv165

Upon personal communication and collaboration with Dr. Sugimura, RUNX1c (splicing variant 1, which is most recognized in hematopoietic development process) and ERG splicing variant 1 (NM_182918.3) were selected since some of the TFs previously published have multiple transcript variants (RUNX1, ERG, and LCOR) and were not specified in the publication. ORFs were not purchased for either RUNX1c or SPI1, but instead were obtained from Cord blood or reference cDNA. All TFs were first subcloned into a non-inducible pHIV backbone vector (Addgene; example pHIV(IRES)EGFP vector #21373, Addgene, Watertown, MA, USA) and then upon sequence verification further subcloned into the Lentiviral Tet-On 3G Inducible Expression Systems. Our TRE3G Vector system contains a TRE3G tetracycline-inducible promoter and our EF1a-Tet3G Vector expresses the Tet-On 3G transactivator protein from the human EF1 alpha promoter, enabling expression in the presence of tetracycline or the derivative of tetracycline, doxycycline (dox), when co-expressed. Lentivirus was produced from HEK 293FT cells with 2nd generation pMD2.G and psPAX2 packaging plasmids. Viral supernatants were harvested 72 h after transfection and concentrated by Amicon Ultra-15 (Ultracel-100) Centrifugal Filter Units (Millipore, Burlington, ON, Canada). The multiplicity of infection (MOI) was calculated by a dilution series on Hella cells. At day 3 of EHT culture, experimental cells were transduced with lentivirus in EHT culture media supplemented with Polybrene (8 μg/mL). All infections were carried out, as previously described [32], in a static volume of 250 μL in 24-well plate. The multiplicity of infection (MOI) for each transcription factor was 20. 12 h post-infection, and 250 μL of fresh EHT media was supplemented to dilute polybrene. Next, cells were either harvested for transplantation experiments (see xenotransplantation section) or parallel wells were kept for an additional three days of culture ± doxycycline (Sigma-Aldrich, St. Louis, MO, USA, Cat # D9891) to measure infection efficiency by percentage of positive fluorescent proteins by flow cytometry.

2.6. Xenotransplantation

Immunodeficient NOD.Cg-Prkdcscid Il2rgtm1Wjl/SzJ (NSG) mice were bred in a barrier facility and all experimental protocols were approved by the Animal Research Ethics Board of McMaster University. On the same day of HE cells transduction, mice were sublethally irradiated (315 rads) 12 h before transplantation. HE cells were transplanted by intra-femoral (IF) injection into each recipient NSG mouse, as previously described [24]. Experimental cell sources and cell doses for all transplants are discussed later. Mice were administered doxycycline in mouse drinking water (1 g/L doxycycline hyclate; Sigma, Cat # D9891) in light protected (tinted) bottles, which were replaced every few days, and via irradiated rodent diet food (0.625 g/kg doxycycline hyclate; ENVIGO, Indianapolis, IN, USA, Cat # 01306) for 2 weeks. We did observe that a combination of radiation and doxycycline (by food or water) lead to high morbidity rates and significant body weight loss (Figure S4B) and, therefore, we added 10 g/L sucrose to drinking water with doxycycline in combination with 0.5 mL saline subcutaneous injections for the first week post-transplant. To ensure mice maintained adequate doxycycline exposure and healthy body weights, mice were also daily gavaged with doxycycline. On day of harvest, BM from the injected (Inj) and contralateral (Ctl) femurs were collected separately and processed as previously described [25]. Cells were recovered separately by mechanical dissociation in IMDM Gibco (Thermo Fisher Scientific, Waltham, MA, USA) supplemented with 3% FBS (HyClone FBS, Mississauga, ON,

Canada), and 1 mM EDTA (Invitrogen, Waltham, MA, USA). Immediately following harvest, RBCs were lysed using ammonium chloride, MNCs were counted, and then MNCs were analyzed by flow cytometry. BM cells from NSG mice injected IF with empty control vector (TRE3G-eGFP, Addgene, Watertown, MA, USA), were used as the negative controls. Both male and female mice were used as recipients and were distributed across all transplant groups, with no overt differences observed. No statistical method was used to predetermine sample size.

2.7. Colony Forming Unit (CFU) Assay

hPSC-derived HPCs were plated at 5.0 × 102 cells/0.5 mL in Methocult H4434 (StemCell Technologies, Vancouver, BC, Canada) to assess clonogenic colony-forming unit (CFU) capacity, as previously describe [25]. Cells were incubated at 37 °C for 14 days and manually scored. Each CFU well represents an independent biological assay, as input cells and MethoCult formulations were individually prepared for testing in single wells. CFU were stained with calcein green (Invitrogen, Waltham, MA, USA) in Hank's Buffered Salt Solution (HBSS) for 30 min and imaged with the Operetta High Content Imaging System (PerkinElmer, Guelph, ON, Canada).

2.8. Western Blotting

Cells were lysed with RIPA buffer (0.5% NP-40, 0.1% sodium deoxycholate, 150 mM NaCl, 50 mM Tris-Cl, pH 7.5) containing protease inhibitors. The protein concentration was determined using DC protein assay (Bio-Rad, Hercules, CA, USA), and equal amounts of protein were separated on 6–12% SDS-PAGE Gels and transferred to PVDF membrane (Invitrogen, Waltham, MA, USA). Nonspecific protein binding was blocked using either 3% Bovine Serum Albumin (BSA) or 5% powdered milk in Tris-buffered saline with 0.1% Tween-20 (TBST) at room temperature for 1 h followed by incubation with primary antibodies diluted in the blocking solution, overnight at 4 °C. The following morning, the membranes were washed with TBST and incubated with horseradish peroxidase-conjugated secondary antibodies (anti-mouse, NA931V, and anti-rabbit, NA934V, Amersham) for 1 h at room temperature. Membranes were then washed and imaged. Images were developed using the Immobilon Western Kit (Millipore, Burlington, MA, USA) and detected on a ChemiDoc imaging system (Bio-Rad, Hercules, CA, USA), and Bio-rad (version S.0.2.3.0, Rochester, NY, USA) was used to quantify protein content. GAPDH (1:10,000, no. ab9484, Abcam, Cambridge, United Kingdom) was used as a loading control. (Table 2).

Table 2. Primary antibodies

Antibody	Company	Cat #
Rb mAb to RUNX1	Abcam	ab92336
Rb mAb to PU.1/SPI1	Abcam	ab76543
Rb mAb to HOXA5	Abcam	ab140636
HOXA9 (rabbit polyclonal IgG)	EMD Millipore Corp	07–178
HOXA10	Abcam	ab191470
Rb mAb to ERG	Abcam	ab92513
Rb mAb to LCOR	Abcam	ab171086

Antibody	Company	Cat #
Ms mAB to GAPDH	Abcam	ab8245

2.9. RT-qPCR

Total RNA purification was performed using RNeasy Mini Kit (QIAGEN, Hilden, Germany), according to manufacturer's instructions. Purified RNA was quantified on a Nanodrop 2000 Spectrophotometer (Thermo Scientific, Waltham, MA, USA). For RT-qPCR, cDNA was synthesized from 1 µg of total RNA using SuperScript III FirstStrand Synthesis System (Life Technologies, Carlsbad, CA, USA). RT-qPCR was carried out as previously described [35], using PowerUp SYBR Green Master Mix (Thermo Fisher Scientific, Waltham, MA, USA), utilizing manufacturer's recommended cycling conditions on ViiA7 Real-time PCR system (Applied Biosystem, Waltham, MA, USA). (Table 3).

Table 3. Primers

Gene Name	Gene Forward (5′–3′)	Reverse (5′–3′)
RUNX1c	CGT ACC CAC AGT GCT TCA TGA	GGC ATC GTG GAC GTC TCT AGA
SPI1	GCC AAA CGC ACG AGT ATT ACC	GGG TGG AAG TCC CAG TAA TGG
HOXA5	ACC CCA GAT CTA CCC CTG GAT	CGG GCC GCC TAT GTT G
HOXA9	ATG AGA GCG GCG GAG ACA	CCA GTT GGC TGC TGG GTT A
HOXA10	AAA GCC TCG CCG GAG AA	GCC AGT TGG CTG CGT TTT
ERG	GAA CGA GCG CAG AGT TAT CGT	TGC CGC ACA TGG TCT GTA CT
LCOR	CTC AGT CAG AAC CTA GCG AAC AAG	GCC AGC ACA TGG ACT TTT CTT A
GAPDH	CCA CAT CGC TCA GAC ACC AT	GCG CCC AAT ACG ACC AAA T

2.10. Conventional PCR

Genomic DNA was extracted by DNA Micro Kit (Qiagen, Hilden, Germany) following manufacturer's protocol and analyzed by conventional PCR. (Table 4).

Table 4. Conventional PCR primer sequences

Human DNA	Gene Forward (5′–3′)	Reverse (5′–3′)
alpha-satellite, chromosome 17	GGGATAATTTCAGCTGACTA AACAG	TTCCGTTTAGTTAGGTGCAGTTAT C
TRE3G-TF-FP	CTG GAG CAA TTC CAC AAC AC	

Human DNA	Gene Forward (5′–3′)	Reverse (5′–3′)
RUNX1c		CAA CGC CTC GCT CAT CTT
SPI1		GGA GCT CCG TGA AGT TGT TC
HOXA5		AGA TCC ATG CCA TTG TAG CC
HOXA9		CTT GGA CTG GAA GCT GCA C
HOXA10		CAG CTC TGC AGC CCG TAG
ERGv1		GTT CCT TGA GCC ATT CAC CT
LCOR		GGT CCA GAG GTG AGT CTT GG

2.11. Flow Cytometry

For all live staining experiments, <1 × 106 cells/200 µL were incubated with antibodies for 30 min at 4°C, and then washed before flow cytometry. To exclude non-viable cells, 7AAD (Beckman Coulter, Pasadena, CA, USA) was used. Flow cytometry was performed using the LSRII Flow Cytometer with FACSDiva software (BD, Mississauga, ON, Canada) and analyzed by FlowJo software (version 10.8.0; BD, Mississauga, ON, Canada). (Table 5).

Table 5. Antibody Details

Antigen	Reactivity	Conjugated	Clone	Supplier
CD34	Human	APC-Cy7	581	BD Horizon Cat # 343514
CD31	Human	FITC		BD Horizon Cat # 555445
FLK1	Human	APC	89106	BD Horizon Cat # 560495
VE-cadherin	Human	PE-Cy7	16B1	BD Horizon Cat # 25-1449-41
CD45	Human	V450	2D1	BD Horizon Cat # 642275
CD43	Human	PE	1G10	BD Horizon Cat # 560199
CD235a	Human	PE	GA-R2	BD Horizon Cat # IM22114
CD45	Human	APC	2D1	BD Horizon Cat # 340943

2.12. Gene Expression Profiling

Expression levels of RNA-seq and microarray data were obtained from series matrix sheets in the GEO repository (NCBI), described in the table below this section (Table 6). All data are available in a publicly accessible repository. Gene expression analysis was conducted using Partek Gene Suite (v6.6, Partek Inc., Chesterfield, MO, USA). Log2 transformation of RNA-seq data was completed, as previously described in Nature by Nakamura et al. [36], as a common technique to enable basic comparisons between RNA-seq and microarray datasets. Furthermore, the mean probe intensity was used for genes with multiple probes in the microarray data. Datasets were merged by common gene symbols. Batch effect was removed using Batch effect Remover in Partek Gene Suite across different studies that were selected as they also included FACS-purified cord blood phenotypic HSC samples tested in parallel with hPSC-derived cells. All genes were used in principal component analysis (PCA) and unsupervised hierarchical clustering. Gene set

enrichment analysis (GSEA, Broad Institute, Inc., Massachusetts Institute of Technology, and Regents of the University of California, v4.0.3) was performed with default settings, using the gene expression matrix from Sugimura et al., from GEO (NCBI): GSE83719. Gene list names were obtained from the Molecular Signatures Database (MSigDB, Broad Institute, Inc., Massachusetts Institute of Technology, and Regents of the University of California) as grp files (Table 6).

Table 6. Gene expression sample details

Lab Source	GEO ID	Symbol in Study	Samples Used	Sample IDs	Platform Technology	Total Annotated Genes
Bhatia	GSE3823	circle	18	U133A; GSM87705 to GSM87716, GSM87729 to GSM87734	HG U133A	13,462
Daley	GSE49938	diamond	17	GSM1210379 to GSM1210384, GSM1210388 to GSM1210392, GSM1210401 to GSM121406	HG U133A Plus2	23,520
Daley	GSE83719	triangle	5	All; GSM2214010 to GSM2299187	Illumina NextSeq 500	25,855

2.13. Statistical Analysis

Data are presented as mean ± standard error of mean (SEM). Prism software (GraphPad Prism, San Diego, CA, USA, version 9.3.1) was used for all statistical analyses, and the criterion for statistical significance was $p < 0.05$. In all figures, n indicates biological replicates. Statistics are described in figure legends.

3. Results

3.1. Molecular Comparison of Human HE Derivation from Pluripotent Cell

Since no distinguishing cell surface markers have been described to identify HE [37], yet transcription-factor-mediated expression in hPSC-derived HE has recently been shown to confer the ability to generated SRCs [32], we sought to directly compare the phenotypic markers of previously characterized primitive endothelial-like cells. Specifically, we compared cells that are responsible for hematopoietic output, and thus functionally represents hemogenic precursors arising from hPSCs [38] to a more recent derivation approach utilized by Sugimura et al. (Figure 1A) [32], relying on EB formation [39,40]. HEs have previously been shown to be detectable as early as day seven of EB development, and have been defined as PECAM-1-, FLK-1-, and VE-cadherin-positive endothelial cells that also lack CD45 expression (PFVCD45−) HE cells [38,41,42]. In comparison, utilizing an adapted protocol to derive HE from hPSCs that was previously verified to have hematopoietic potential [39], HE cells are phenotypically characterized

by the FLK+CD34+CD43−CD235A− expression by Sugimura et al. (Figure 1B) [32]. PFVCD45− cells had one overlapping expression marker with HE derived by Sugimura et al., FLK-1 (fetal liver kinase 1, also known as a kinase insert domain-containing receptor, KDR and vascular endothelial growth factor receptor 2 (VEGFR2) (Figure 1A) which has previously been described as a positive marker for HE cells [43]. Notably, PFVCD45− cells also have more phenotypes associated with endothelial surface markers (Figure 1A) in comparison to HE cells derived using an alternative PSC differentiation methodology (Figure 1B). Side-by-side morphological comparisons of hPSC-derived hemato-endothelial progenitor cells revealed a similar monolayer after EB dissociation and culture (Figure 1C). Methods to derive PFVCD45− cells capture the HE signatures of FLK+CD34+CD43−CD235A− cells (Figure 1D) [38], though to a lesser extent. However, the means to select HEs using the PFVCD45− provides a potentially superior approach to purification amongst differentiating hPSCs using positive selection vs. less definite negative selection based on the absence of the marker. To this point, phenotypic expression was analyzed and all surface markers by flow cytometry were common of HEs, independent of the methodology used for derivation (Figure 1E); however, higher CD31/VE-cadherin markers were observed with HE derived using Sugimura et al.'s methodology across experimentations (Figure S1A). These observations remained the same under hypoxic conditions of HE derivation (Figure S1B), which has previously been suggested as an important state in adult BM HSC niches to defend against oxidative stress [44,45,46], but in fact when quantitively analyzed, has no bearing on the molecular phenotype of HEs differentiated from hPSCs. To determine whether global transcriptome analysis would demarcate these HE populations, we next used gene expression profiles from hPSC progenies from several sources and procedures, including 7TF overexpression [30,32,47], and compared these to publicly available datasets of primitive hematopoietic populations enriched for HSC/HPCs (CD45+CD34+CD38−), including BM, MPB, CB, and fetal blood (FB) sources (Figure 1F). Despite being derived using different in vitro differentiation protocols, PFVCD45− HE cells clustered with HE cells previously reported from other groups (Figure 1G), suggesting that human hPSC-derived HEs are functionally and molecularly fairly similar, independent of differentiation methods which merely change the efficiency and frequency of the derivation from hPSCs (Figure 1E). Furthermore, 7TF hPSC-HSPCs clustered closer to HE cells than to hematopoietic stem and progenitor cells (HSPCs), implying an incomplete conversion to an HSC-like state (Figure 1G). As a positive control, using the gene expression matrix provided by Sugimura et al., GSEA analysis comparing the genes of interest in the key cell types of interest were reproduced. Similar to their previous findings, Figure S1B shows that the 7TF hPSC-HSPCs are more highly enriched than hPSC-derived HEs for Integrin genes. Additionally, using two well-established gene lists for HSCs [48,49], we found that both gene lists were highly similar in their results and were more highly enriched in CB than 7TF and HE (Figure S1B). Interestingly, the difference between CB and HE was smaller than the difference between CB and 7TF. Furthermore, HE cells were more highly enriched in HSC genes than the 7TF hPSC-HSPCs, again suggesting an incomplete conversion of 7TF to an HSC-like state (Figure 1G and Figure S1B). Based on these results, we sought to apply these methods of HE derivation from hPSCs toward a proof-of-principle experimentation to determine if normal HSPCs can be generated from hiPSCs obtained from AML patient cells devoid of leukemic aberrations [29] upon 7TF overexpression [32].

3.2. Derivation of HE from AML Patient-Specific iPSCs into Endothelial-to-Hematopoietic Transition (EHT) Conditions for Forced 7TF Expression

In cases where AML patients fail chemo-induced remission, HSC transplantation provides an impactful treatment option [50,51,52]. As such, the generation of AML patient-specific HSCs that are devoid of the leukemic aberration(s) would provide an ideal source in which to obtain a healthy autologous blood source for transplantation. The potential of using reprogramming to generate healthy HSCs from an AML patient has yet to be explored and it remains unclear whether the generation of AML-patient HSCs is even possible or capable of bestowing surrogate properties such as SRC capacity. By definition, HE is a transient, specialized endothelium with the capacity to generate hematopoietic cells through a gradual process of endothelial-to-hematopoietic transition (EHT) [53,54]. Based on this, we evaluated the potential of generating normal HSPCs from AML patient-derived iPSCs adhering to the specific methods used by Sugimura et al., in which HE cells are cultured in EHT medium and have previously been shown to be conducive to TF reprogramming (Figure 2A) that resulted in SRC activity [32]. We selected two patient samples (AML 15331 and 28787) to generate iPSCs [29,33] for use in this study. AML genetic interrogation of ≥4 iPSC lines per sample previously revealed that all colonies were derived from blood cells (AML 15331) or skin fibroblasts (AML 28787) devoid of leukemic aberration t(9;11)(p22;q23) [55], and thus were classified as normal iPSCs derived from AML patients. Therefore, they represent an ideal source in which to interrogate the potential of deriving autologous HSCs and progenitors. We found that both iPSC lines produced HE phenotypes (Figure 2B), though hiPSC-2 yielded higher frequencies of positive HE phenotypes CD31, FLK1, and VE-cadherin in comparison to hiPSC-1 at EHT day 0 (Figure S2A). To accurately control the quality of HE cells derived using our normal iPSCs derived from AML patients upon EHT induction, we reassessed both the HE panels of phenotypes (a combination of FLK+CD34+CD43−CD235A− cells and our PFVCD45− cells). Consistent with Sugimura et al., we routinely observed an HE phenotype in both iPSC lines upon CD34+ population enrichment based on magnetic cell isolation and an extended culture with hematopoietic cytokines that are believed to encourage EHT on fibronectin-coated plates (Figure 2C; EHT day 3). These results provided a platform in which we were confident in interrogating whether normal iPSCs derived from AML patients can produce SRCs devoid of leukemia-associated aberrations upon the forced expression of specific TFs having successfully derived an HE phenotype.

PFVCD45− HE cells can be cultured and expanded for a length of time, but unfortunately, produce hematopoietic progenitors incapable of engraftment potential [24,38]. Thus, having demonstrated that hESC-derived HEs are functionally and molecularly similar, independent of differentiation methods prior to EHT induction (Figure 1), we adapted our protocol and designed a merged approach whereby we performed our classical method of hematopoietic differentiation [38] followed by subsequently culturing in EHT medium, as described previously [32], using hESCs (Figure S2B). We questioned whether adapting our methods would bestow long-term engraftment upon TF reprogramming on hESC-derived HE cells, having previously yielded negative potential [24,38]. Cells were culture and EB formed as previously described [34]. However, we isolated HE based on the magnetic cell isolation of a CD34+ population at day 10 of EB formation (EHT day 0; Figure S2C), and then subsequently cultured in EHT medium for 3 days. Using this adapted protocol, we found similar levels of enrichment for the HE phenotypic panel on EHT day 3 (Figure 2D). Moreover, the phenotypic expression remained unaltered under hypoxic conditions (Figure S2D) consistent with our previous results (Figure S1B). Overall, our results show that both methodologies, either mirroring the protocol directly from Sugimura et al.,

(Figure 2A) or our newly adapted protocol (Figure S2B), derive similar phenotypic HE cells (Figure 2C,D) from hPSCs, suggesting that both outcomes of in vitro EHT are conducive to TF reprogramming.

3.3. Generation and Forced Expression of 7TF under HE In Vitro Differentiation Conditions from hPSCs

Based on the ability to generate HE from both normal iPSCs from AML patients and hESCs, along with the recent breakthrough study reported in Nature [32] which recapitulated the EHT lineage transition from HE to generate SRCs, we hypothesized that the introduction of these defined HSC-specific TFs may endow hPSC-derived HE with the potential to engraft multi-lineage hematopoiesis in vivo. Thus, we subcloned the following TFs: RUNX1c, SPI1, HOXA5, HOXA9, HOXA10, ERG-transcript variant 1 (ERGv1; shorter), and LCOR-transcript variant 3 (LCORv3; longest) into a lentiviral Tet-On 3G inducible expression system. These resulting vectors were validated by biological testing for expression and transduction into target cells (Figure 3A and Figure S3). These TF constructs were carefully engineered with distinguishing fluorescent proteins (FPs: eGFP; BFP2; and mKusabiraOrange2, mKO2) to be co-expressed with individual TF constructs due to the presence of an internal ribosome entry site (IRES) cassette, making our system a unique inducible reporter system by the inclusion of doxycycline (Dox). Lentiviral ectopic expression of select individual TFs demonstrated functional expression validity (Figure 3B). In order to include hematopoietic phenotyping, in addition to multiplexing our fluorescent reporter system, we categorized the 7TFs into groups utilizing three FPs: (1) the likely essential two TFs RUNX1 and SPI1 (green, eGFP), based on overlapping TFs used between the Sugimura et al. and Lis et al. groups; (2) the HoxA genes, HOXA5, 9, and 10 (blue, BFP2); (3) and ERGv1 and LCOR (orange, mKO2), both associated with oncogenesis [56,57,58,59]. We transduced hPSC-derived HE cells at day 3 of EHT culture for 24 h, and subsequently added fresh EHT medium supplemented with dox (Figure 3C). The induction of TF expression post-transduction was successful (Figure 3D), and the concomitant emergence of CD34+CD45+ hematopoietic cells occurred (Figure 3E). These results demonstrate that transduction with a defined set of 7TFs promotes a hematopoietic phenotype from hPSC-derived hemogenic endothelium, independent of the methodologies used. Additionally, these results confirm the validity of the systems and provide the foundation for interrogating the biology and mechanism of TF regulation for hPSC-guided development towards hematopoietic progenitor capacity.

3.4. Progenitor Capacity from hPSC-Derived HE with 7TF Expression

To investigate the functional outcome of the temporal expression of the 7TFs under EHT conditions, we transduced HE cells, as detailed in Figure 3, and assayed for the clonogenic progenitor capacity after 3 days of culture post-exposure to the delivery virus. As previously described, we compared two distinct protocols and approaches: (1) Sugimura et al. and (2) our adapted protocol which encompassed merging methods (Wang et al. [38] adapted) to derive hemogenic endothelium from hPSCs on normal iPSCs derived from AML patients and hESCs, respectively (illustrated in Figure 4A). As predicted, we routinely observed enhanced hPSC-derived hematopoietic colony-forming unit (CFU) morphology in hPSC HE-derived cells treated in the presence of dox (Figure 4B) when cultured for 14 days in vitro in both hESC and AML-iPSC. To control for variations in the CD34+CD45+ frequency (Figure 3D), we determined the total CFU output and lineage distribution per 40,000 cells seeded. A higher functional progenitor capacity was observed in both hPSC lines (H9s and BM-derived normal AML-iPSC) transduced

with the 7TF in the presence of dox (Figure 4C). These results indicate that AML-iPSCs possess a normal differentiation capacity towards the hematopoietic progenitors and lineage development, and 7TF expression augments the putative hematopoietic progenitor output from iPSCs derived from AML-patient fibroblasts. Based on this successful induction to increase the progenitor output from AML-derived iPSCs, we sought to measure the in vivo SRC activity using these established methods and approaches.

3.5. SRC Engraftment Potential of TF-Induced Hemogenic Precursors Derived from Healthy iPSCs Established from AML Patients

While we have previously verified that AML patient-derived iPSCs can generate hematopoietic progenitors with an in vitro myeloid lineage maturation capacity [29,33], multi-lineage reconstitution potential could not be evaluated in vivo, due to a lack of bona fide HSC generation methods available at the time. Similarly, we have historically been unsuccessful in deriving the long-term engraftment of SRCs using hESCs [25]. Using our inducible transgene system (Figure 3), hPSC-derived HE cells were infected on day 3 of EHT culture with 7TFs, and after 24 h, the transduced cells were injected intrafemorally into sub-lethally irradiated immune-deficient NOD LtSz-scidIL2Rγnull (NSG) mice to interrogate hPSC-derived SRCs' potential. As illustrated in Figure 5A, mice received doxycycline in their drinking water and diet for 2 weeks to induce transgene expression, after which doxycycline was withdrawn and hematopoietic chimerism was assessed over time. All mice were subsequently harvested at 8 weeks post-transplantation and the injected femur (IF), contralateral femur (CF) BM, and peripheral blood (PB) were assessed to determine any potential migration capacity in vivo (Figure 5A).

To assess the induction efficiency of the 7TF in cells that were transplanted into recipient mice, a portion of the cells remained in the culture post-lentiviral removal and were phenotypically characterized by flow cytometry. FP expression, indicative of TF expression and hematopoietic frequency, were measured at EHT day 7, and demonstrated an expression of TFs as well as an emergence of a CD34+CD45+ phenotype (Figure 5B). Next, we transplanted three sets of HE-7TF-derived cells obtained from either normal iPSCs derived from AML patients using the Sugimura et al., protocol (hiPSC-1 and hiPSC-2), or HE-7TF-derived cells obtained from the hESC using our adapted protocol (H9 cell line; Figure S4A). Additionally, a control set of HE cells were transplanted in which HE cells were transduced with an empty control vector. It was previously reported that the stem cell frequency of HE-7TF cells was approximately 1 in 10,000 cells, calculated by a limiting dilution assay using the software ELDA [32]. Thus, we transplanted varying levels of HE-7TF-derived cells, ranging from 50,000 cells up to 400,000 cells, encompassing a total of 35 experimental mice and 12 control mice (Figure 5C). Early in the experimentation, we observed some mice with a low body weight and determined that radiated mice were not drinking sufficient water, potentially as a side effect of radiation sickness in conjunction with supplementing dox in their diet (Figure S3B) [60], occasionally resulting in premature death (Figure 5C). We thus decided to supplement mice with 1mg/mL doxycycline hyclate and 10 mg/mL sucrose via daily gavage to ensure mice obtained a sufficient dose of dox during the two-week administration, as well as avoiding endpoint monitoring based off a significant drop in the mouse's body weight, relatively to its starting weight (see methods section for additional information). Human engraftment was evaluated after 8 weeks using human CD34 and CD45 antibodies from the injected femurs and contralateral femurs of recipient mice. The frequency of human hematopoietic cell chimerism was extremely rare and could not be fully captured by flow cytometric analysis across all hPSC HE-7TF-derived cells (Figure 5D).

Similarly, when blood chimerism was assessed at both four weeks and six weeks, no human hematopoietic cell chimerism was observed (data not shown). One mouse did display human CD45+ detection (Figure S4C), though the levels and frequency were not on par with previous reports [32]. Notably, CB cells transplanted in a separate experiment in the same IF manner displayed significant engraftment potential in comparison to all sets of HE-7TFs when evaluating total human CD45+ BM chimerism (Figure 5E; separate scale used to highlight striking difference in chimerism). All sets of HE-7TFs yielded engraftment levels indistinguishable from the negative control mice, in which no cells were transplanted, but BM was harvested as an additive control measure (Figure 5E; black vs. all other colors). Similarly, blood chimerism produced next to no human CD45+ detection (Figure 5F), suggesting little to no migration potential capacity in vivo. In lieu of the previously described radiation sickness, one mouse had to be harvested early to due significant weight loss and resulted in a singly intriguing yet unreproduced result. Human hematopoietic phenotyping of one 7TF-transplanted mouse, harvested at the ethical endpoint on day 12 post-transplant, demonstrated striking human CD45+ BM chimerism in both its injected femur and contralateral BM (Figure 5G). Impressively, HE-7TF cells derived from hiPSC-2 displayed a human origin when assessed by PCR (Figure 5H), in which a faint band of human chromosome 17 was detected, in comparison to DNA extracted from the BM of a negative control mouse that was harvested in parallel. Unfortunately, HE-7TF cells derived from hiPSC-2 were not sufficient to confer a similar level of detection in the contralateral femur, or in any other mouse, or at any longer timepoints. Notably, it was not possible to confirm that we completely reproduced all aspects of the original report due to variation in both the targeted cell type, e.g., AML patient-derived iPSCs, and variation in the transduction efficiencies and stoichiometry of TF expression that was not fully described previously. Overall, our results suggest a deficient acquisition of functional SRCs from hPSC-derived hemogenic endothelia upon transcription factor induction independent of the methodology used to derive the cells using various sources of hPSCs.

4. Discussion

Since their discovery, human embryonic stem cells (hESCs) have offered great promise as a near-unlimited source of a variety of therapeutically relevant cell types, due to their ability for indefinite self-renewal and their potential to form all somatic cell types [61]. Subsequently, the derivation of hiPSCs from adult somatic cells not only established a paradigm shift in our understanding of the developmental potential of terminally differentiated cells in demonstrating the ability to drastically be altered by a relatively simple genetic approach, but has also provided a foundation for novel autologous cell-based therapies to be explored [20,62]. Over the years, extensive investigations of new methods for the derivation of HSCs from hPSC sources have suggested that robust transplantable HSCs were around the corner. The first report on such attempts showed limited success of HSC properties from resulting primitive hematopoietic cells [24]. Almost 20 years later, various groups have reported dozens of methods and approaches for the derivation of HSCs from hPSCs, including complex developmental programs of definitive and primitive hematopoiesis, co-culture methods, embryonic hematopoietic phenotypes, and sequential growth factor treatments to mimic native niches and unique regulating signaling cascades [21,22,23,25,63,64,65,66,67,68]. Despite the augmentation of hematopoietic progenitors, accelerating timing, and ease of protocols, e.g., less expensive and numerous factors, those studies capable of testing the SRC/HSC capacity consistently remained unsuccessful. This left the clinical prospects of therapeutic benefit elusive. Our current study further demonstrates that the current

understanding of HSC genesis from hPSCs remains naive and is incapable of discerning methods for the pre-clinical and clinical study design for HSCs from hPSCs. In addition, we propose the field question the current understanding of the causal and functional impact of published regulators of hematopoietic specification from hPSCs that is not restricted to developmental biology. This is supported by our experience in human PSCs that is similar to murine PSCs where bone-marrow-derived HSCs are still used for the study of HSC biology due to the inconsistency and difficulty of deriving HSC from PSCs, even in the mouse system.

Despite the failures in demonstrating robust HSCs from hPSCs, procedures aimed at mimicking in vivo niches have had some limited success. Serially transplantable hPSC-derivatives have been reported, although with modest levels of chimerism and a lack of definitive hematopoiesis, as judged by primitive erythroid characteristics and limited lymphoid potential [23,66,69]. Two independent groups have reported a derivation of putative HSC-like cells from hiPSCs utilizing iPSC-derived teratomas as in vivo bioreactors [70,71]. Both studies combined cytokine treatment and OP9 stromal cell co-injection to recapitulate the BM niche environment more closely. Teratoma-mediated hematopoiesis generated derivatives bearing the hallmarks of bona fide HSCs, namely sustained engraftment, and the lympho-myeloid differentiation potential after BM homing in xenograft assays. These combined studies were not successful at demonstrating the two hallmark properties of HSPCs, but both strongly contributed to the overall goal of generating hPSC-HSPCs by suggesting a crucial role of the niche in providing inductive cues for functional HSPC development.

Most recently, the transcription factor-mediated specification of HSPCs has been extensively studied. Reports utilizing murine fibroblasts identified a combination of four transcription factors (Gata2, Gfi1b, cFos, and Etv6) capable of inducing endothelial precursors that, upon culture modifications, generated HSPC-like cells, although the engraftment potential of the resulting cells was not evaluated [72]. Additional studies have focused on either lineage-restricted precursors or committed progenitors of the hematopoietic system as the starting cell population for reprogramming. A hybrid study, combining hPSC differentiation into precursor cells with a subsequent re-specification of the resulting cells, described a set of five transcription factors (HOXA9, ERG, RORA, SOX4, and MYB), which imparted self-renewal and multilineage potential in vitro and short-term engraftment potential in vivo on these cells [30]. Murine committed lymphoid/myeloid progenitors and myeloid effector cells have been successfully reprogrammed into induced-HSCs (iHSCs) utilizing the transient expression of eight transcription factors (Run1t1, Hlf, Lmo2, Prdm5, Pbx1, Zfp37, Mycn, and Meis1) [73]. The resulting cells exhibited self-renewal and multilineage differentiation potential at the clonal level and were serially transplantable [73]. Another study exploited the current underlying ideas behind the endothelial-to-hematopoietic transition that results in the formation of definitive HSCs within the developing embryo to generate human multipotent progenitors (hMPPs) from non-hemogenic endothelial cells using four transcription factors (FOSB, GFI1, RUNX1, and SPI1) [74]. Reprogramming was critically dependent on the instructions provided by the specialized serum-free vascular niche; generated hMPPs were capable of long-term primary and secondary multilineage engraftment [74]. Notably, two breakthrough studies reported in Nature recapitulated the EHT lineage transition from HE to generate putative functional mouse and human HSCs, from the Rafii and Daley groups, respectively, that were able to reconstitute recipient mice [31,32]. In the case of human PSC-derived HSPCs, both morphogen-directed differentiation and defined TF over-expression were required to mediate the conversion [32]. Interestingly, engraftment was only achieved when hPSC-HE precursors were programmed by TFs in vivo, again suggesting and fully

consistent with unidentified extracellular cues that are essential for the subsequent specification of hPSC-to-HSPCs. When taken into consideration that independent groups have reported a limited derivation of hPSC-HSPCs in vivo using teratoma formation, and now, most recently, HSC engraftment of 7TF-HE cells being achieved by in vivo programming, this further highlights that extracellular cues from the in vivo BM niche are crucial.

Overall, our study reveals the potential of hPSCs to generate bona fide HSPCs, but highlights our lack of understanding of how these TFs act, on which cell types they act on (e.g., HSC vs. common lymphoid progenitors or common myeloid progenitors), and the nature of niche signals that direct the specification of HSPCs from hPSC-derived HE cells. Importantly, as not all aspects can be reproduced from one report to another report identically, we would like to emphasize that our observed results included here do not dismiss the studies of Sugimura et al., but rather our own work found it difficult to generate SRC using a similar model system and approach. Moreover, although our results show that both methodologies derive phenotypic HE cells (Figure 2) from hPSCs, and both outcomes of in vitro EHT were conducive to TF reprogramming, we recognize that in vivo experimentation would have potentially been informative using H9 hESCs, used by Sugimura et al., as we initially did in the experimental results shown in Figure 1. Since H9s were not used in the same manner as for Sugimura et al., for various in vitro and in vivo experimentations, as this was not the goal or target of the authors in our current study, we cannot conclude that our in vitro culture or lenti-viral system contributed to negligible in vivo chimerism using iPSCs derived from AML patients.

5. Conclusions

We propose that more emphasis should be placed on methodological improvements, including robust data collection and evaluation, together with the complete disclosure of protocols and publication of all outcomes, be that favorable or negative results. Experimental replication (as best as possible) and validation should be achieved at the pre-clinical stage to maximize the prospects of successful clinical translation.

Supplementary Materials

The following supporting information can be downloaded at: https://www.mdpi.com/article/10.3390/cells11121915/s1, Figure S1. Comparison of HE phenotype under normoxic or hypoxic conditions. Figure S2. Timeline of HE derivation using adapted protocol. Figure S3. Molecular validation of 7TF induction. Figure S4. Data from transplantation experiments.

Author Contributions

D.P.P., J.C.R., B.T. and D.G. performed experiments. A.L.B., aided with the CB transplant assay. D.P.P., J.C.R. and M.B. designed experiments and interpreted data. D.P.P. and M.B. wrote the manuscript. M.B. directed the study. All authors have read and agreed to the published version of the manuscript.

Funding

D.P.P. was supported by the Jans Graduate Scholarship in Stem Cell Research, the Michael G. DeGroote Doctoral Scholarship, and the Ontario Graduate Scholarship. J.C.R. was supported by the Canadian Institutes of Health Research (CIHR) Doctoral Award, the Michael G. DeGroote

Doctoral Scholarship, and an Ontario Graduate Fellowship. D.G. was supported by the Jans Graduate Scholarship in Stem Cell Research. This work was supported by a research grant to M.B. from the CIHR Foundation Grant FRN 159925 to M.B. and approved by the Stem Cell Oversight Committee in Canada. Support to M.B. came from the Canada Research Chair Program CRC Tier 1 in Human Stem Cell Biology and Michael G. DeGroote Chair in Stem Cell Biology.

Institutional Review Board Statement
This study and all experimental protocols were conducted in accordance with the Animal Research Ethics Board of McMaster University (AUP: 19-11-29).

Informed Consent Statement
Not applicable.

Data Availability Statement
Expression levels of RNA-seq and microarray data were obtained from series matrix sheets in the GEO repository (NCBI). (Table 6).

Acknowledgments
We want to thank Ronan Foley and Brian Leber for providing primary human AML samples that were previously reprogrammed. We would also like to thank B.T. for their assistance with subcloning, D.G. for in vivo experimental assistance, and S. Raha and M. Wong for procedures related to hypoxia. We would also like to acknowledge J.C.R. and A.L.B. in editing and reviewing the manuscript.

Conflicts of Interest
The authors indicate no potential conflict of interest.

References

1. Doulatov, S.; Notta, F.; Eppert, K.; Nguyen, L.T.; Ohashi, P.S.; Dick, J.E. Revised Map of the Human Progenitor Hierarchy Shows the Origin of Macrophages and Dendritic Cells in Early Lymphoid Development. Nat. Immunol. **2010**, 11, 585–593.
2. Notta, F.; Doulatov, S.; Laurenti, E.; Poeppl, A.; Jurisica, I.; Dick, J.E. Isolation of Single Human Hematopoietic Stem Cells Capable of Long-Term Multilineage Engraftment. Science **2011**, 333, 218–221.
3. Hope, K.; Bhatia, M. Clonal Interrogation of Stem Cells. Nat. Methods **2011**, 8, S36–S40.
4. Kondo, M.; Wagers, A.J.; Manz, M.G.; Prohaska, S.S.; Scherer, D.C.; Beilhack, G.F.; Shizuru, J.A.; Weissman, I.L. Biology of Hematopoietic Stem Cells and Progenitors: Implications for Clinical Application. Annu. Rev. Immunol. **2003**, 21, 759–806.
5. Kørbling, M.; Estrov, Z. Adult Stem Cells for Tissue Repair—A New Therapeutic Concept? N. Engl. J. Med. **2003**, 349, 570–582.
6. Sureda, A.; Bader, P.; Cesaro, S.; Dreger, P.; Duarte, R.F.; Dufour, C.; Falkenburg, J.H.F.; Farge-Bancel, D.; Gennery, A.; Kröger, N.; et al. Indications for Allo- and Auto-

SCT for Haematological Diseases, Solid Tumours and Immune Disorders: Current Practice in Europe, 2015. Bone Marrow Transplant. **2015**, 50, 1037–1056.
7. Löwenberg, B.; Downing, J.R.; Burnett, A. Acute Myeloid Leukemia. N. Engl. J. Med. **1999**, 341, 1051–1062.
8. Shipley, J.L.; Butera, J.N. Acute Myelogenous Leukemia. Exp. Hematol. **2009**, 37, 649–658.
9. Boyd, A.L.; Campbell, C.J.V.; Hopkins, C.I.; Fiebig-Comyn, A.; Russell, J.; Ulemek, J.; Foley, R.; Leber, B.; Xenocostas, A.; Collins, T.J.; et al. Niche Displacement of Human Leukemic Stem Cells Uniquely Allows Their Competitive Replacement with Healthy HSPCs. J. Exp. Med. **2014**, 211, 1925–1935.
10. Dickinson, A.M.; Norden, J.; Li, S.; Hromadnikova, I.; Schmid, C.; Schmetzer, H.; Jochem-Kolb, H. Graft-versus-Leukemia Effect Following Hematopoietic Stem Cell Transplantation for Leukemia. Front. Immunol. **2017**, 8, 496.
11. Salci, K.R.; McIntyre, B.A.; Bhatia, M. Foundational Concepts of Cell Fate Conversion to the Hematopoietic Lineage. Curr. Opin. Genet. Dev. **2013**, 23, 585–590.
12. Dzierzak, E.; Bigas, A. Blood Development: Hematopoietic Stem Cell Dependence and Independence. Cell Stem Cell **2018**, 22, 639–651.
13. Zambidis, E.T.; Sinka, L.; Tavian, M.; Jokubaitis, V.; Park, T.S.; Simmons, P.; Péault, B. Emergence of Human Angiohematopoietic Cells in Normal Development and from Cultured Embryonic Stem Cells. Ann. N. Y. Acad. Sci. **2007**, 1106, 223–232.
14. Medvinsky, A.; Dzierzak, E. Definitive Hematopoiesis Is Autonomously Initiated by the AGM Region. Cell **1996**, 86, 897–906.
15. Bertrand, J.Y.; Chi, N.C.; Santoso, B.; Teng, S.; Stainier, D.Y.R.; Traver, D. Haematopoietic Stem Cells Derive Directly from Aortic Endothelium during Development. Nature **2010**, 464, 108–111.
16. De Bruijn, M.F.T.R.; Ma, X.; Robin, C.; Ottersbach, K.; Sanchez, M.-J.; Dzierzak, E. Hematopoietic Stem Cells Localize to the Endothelial Cell Layer in the Midgestation Mouse Aorta. Immunity **2002**, 16, 673–683.
17. Eilken, H.M.; Nishikawa, S.-I.; Schroeder, T. Continuous Single-Cell Imaging of Blood Generation from Haemogenic Endothelium. Nature **2009**, 457, 896–900.
18. Zovein, A.C.; Hofmann, J.J.; Lynch, M.; French, W.J.; Turlo, K.A.; Yang, Y.; Becker, M.S.; Zanetta, L.; Dejana, E.; Gasson, J.C.; et al. Fate Tracing Reveals the Endothelial Origin of Hematopoietic Stem Cells. Cell Stem Cell **2008**, 3, 625–636.
19. Dzierzak, E.; Speck, N.A. Of Lineage and Legacy: The Development of Mammalian Hematopoietic Stem Cells. Nat. Immunol. **2008**, 9, 129–136.
20. Takahashi, K.; Tanabe, K.; Ohnuki, M.; Narita, M.; Ichisaka, T.; Tomoda, K.; Yamanaka, S. Induction of Pluripotent Stem Cells from Adult Human Fibroblasts by Defined Factors. Cell **2007**, 131, 861–872.
21. Kaufman, D.S.; Hanson, E.T.; Lewis, R.L.; Auerbach, R.; Thomson, J.A. Hematopoietic Colony-Forming Cells Derived from Human Embryonic Stem Cells. Proc. Natl. Acad. Sci. USA **2001**, 98, 10716–10721.
22. Vodyanik, M.A.; Bork, J.A.; Thomson, J.A.; Slukvin, I.I. Human Embryonic Stem Cell-Derived CD34+ Cells: Efficient Production in the Coculture with OP9 Stromal Cells and Analysis of Lymphohematopoietic Potential. Blood **2005**, 105, 617–626.

23. Tian, X.; Woll, P.S.; Morris, J.K.; Linehan, J.L.; Kaufman, D.S. Hematopoietic Engraftment of Human Embryonic Stem Cell-Derived Cells Is Regulated by Recipient Innate Immunity. Stem Cells Dayt. Ohio **2006**, 24, 1370–1380.
24. Wang, L.; Menendez, P.; Shojaei, F.; Li, L.; Mazurier, F.; Dick, J.E.; Cerdan, C.; Levac, K.; Bhatia, M. Generation of Hematopoietic Repopulating Cells from Human Embryonic Stem Cells Independent of Ectopic HOXB4 Expression. J. Exp. Med. **2005**, 201, 1603–1614.
25. Reid, J.C.; Tanasijevic, B.; Golubeva, D.; Boyd, A.L.; Porras, D.P.; Collins, T.J.; Bhatia, M. CXCL12/CXCR4 Signaling Enhances Human PSC-Derived Hematopoietic Progenitor Function and Overcomes Early In Vivo Transplantation Failure. Stem Cell Rep. **2018**, 10, 1625–1641.
26. Perrimon, N.; Pitsouli, C.; Shilo, B.-Z. Signaling Mechanisms Controlling Cell Fate and Embryonic Patterning. Cold Spring Harb. Perspect. Biol. **2012**, 4, a005975.
27. Dick, J.E. Normal and Leukemic Human Stem Cells Assayed in SCID Mice. Semin. Immunol. **1996**, 8, 197–206.
28. Doulatov, S.; Notta, F.; Laurenti, E.; Dick, J.E. Hematopoiesis: A Human Perspective. Cell Stem Cell **2012**, 10, 120–136.
29. Salci, K.R.; Lee, J.-H.; Laronde, S.; Dingwall, S.; Kushwah, R.; Fiebig-Comyn, A.; Leber, B.; Foley, R.; Dal Cin, A.; Bhatia, M. Cellular Reprogramming Allows Generation of Autologous Hematopoietic Progenitors From AML Patients That Are Devoid of Patient-Specific Genomic Aberrations. Stem Cells Dayt. Ohio **2015**, 33, 1839–1849.
30. Doulatov, S.; Vo, L.T.; Chou, S.S.; Kim, P.G.; Arora, N.; Li, H.; Hadland, B.K.; Bernstein, I.D.; Collins, J.J.; Zon, L.I.; et al. Induction of Multipotential Hematopoietic Progenitors from Human Pluripotent Stem Cells via Respecification of Lineage-Restricted Precursors. Cell Stem Cell **2013**, 13, 459–470.
31. Lis, R.; Karrasch, C.C.; Poulos, M.G.; Kunar, B.; Redmond, D.; Duran, J.G.B.; Badwe, C.R.; Schachterle, W.; Ginsberg, M.; Xiang, J.; et al. Conversion of Adult Endothelium to Immunocompetent Haematopoietic Stem Cells. Nature **2017**, 545, 439–445.
32. Sugimura, R.; Jha, D.K.; Han, A.; Soria-Valles, C.; da Rocha, E.L.; Lu, Y.-F.; Goettel, J.A.; Serrao, E.; Rowe, R.G.; Malleshaiah, M.; et al. Haematopoietic Stem and Progenitor Cells from Human Pluripotent Stem Cells. Nature **2017**, 545, 432–438.
33. Lee, J.-H.; Salci, K.R.; Reid, J.C.; Orlando, L.; Tanasijevic, B.; Shapovalova, Z.; Bhatia, M. Brief Report: Human Acute Myeloid Leukemia Reprogramming to Pluripotency Is a Rare Event and Selects for Patient Hematopoietic Cells Devoid of Leukemic Mutations. Stem Cells Dayt. Ohio **2017**, 35, 2095–2102.
34. Chadwick, K.; Wang, L.; Li, L.; Menendez, P.; Murdoch, B.; Rouleau, A.; Bhatia, M. Cytokines and BMP-4 Promote Hematopoietic Differentiation of Human Embryonic Stem Cells. Blood **2003**, 102, 906–915.
35. Orlando, L.; Tanasijevic, B.; Nakanishi, M.; Reid, J.C.; García-Rodríguez, J.L.; Chauhan, K.D.; Porras, D.P.; Aslostovar, L.; Lu, J.D.; Shapovalova, Z.; et al. Phosphorylation State of the Histone Variant H2A.X Controls Human Stem and Progenitor Cell Fate Decisions. Cell Rep. **2021**, 34, 108818.
36. Nakamura, T.; Okamoto, I.; Sasaki, K.; Yabuta, Y.; Iwatani, C.; Tsuchiya, H.; Seita, Y.; Nakamura, S.; Yamamoto, T.; Saitou, M. A Developmental Coordinate of Pluripotency among Mice, Monkeys and Humans. Nature **2016**, 537, 57–62.

37. Lange, L.; Morgan, M.; Schambach, A. The Hemogenic Endothelium: A Critical Source for the Generation of PSC-Derived Hematopoietic Stem and Progenitor Cells. Cell. Mol. Life Sci. **2021**, 78, 4143–4160.
38. Wang, L.; Li, L.; Shojaei, F.; Levac, K.; Cerdan, C.; Menendez, P.; Martin, T.; Rouleau, A.; Bhatia, M. Endothelial and Hematopoietic Cell Fate of Human Embryonic Stem Cells Originates from Primitive Endothelium with Hemangioblastic Properties. Immunity **2004**, 21, 31–41.
39. Ditadi, A.; Sturgeon, C.M.; Tober, J.; Awong, G.; Kennedy, M.; Yzaguirre, A.D.; Azzola, L.; Ng, E.S.; Stanley, E.G.; French, D.L.; et al. Human Definitive Haemogenic Endothelium and Arterial Vascular Endothelium Represent Distinct Lineages. Nat. Cell Biol. **2015**, 17, 580–591.
40. Ditadi, A.; Sturgeon, C.M. Directed Differentiation of Definitive Hemogenic Endothelium and Hematopoietic Progenitors from Human Pluripotent Stem Cells. Methods **2016**, 101, 65–72.
41. McIntyre, B.A.S.; Ramos-Mejia, V.; Rampalli, S.; Mechael, R.; Lee, J.-H.; Alev, C.; Sheng, G.; Bhatia, M. Gli3-Mediated Hedgehog Inhibition in Human Pluripotent Stem Cells Initiates and Augments Developmental Programming of Adult Hematopoiesis. Blood **2013**, 121, 1543–1552.
42. Lee, J.B.; Werbowetski-Ogilvie, T.E.; Lee, J.-H.; McIntyre, B.A.S.; Schnerch, A.; Hong, S.-H.; Park, I.-H.; Daley, G.Q.; Bernstein, I.D.; Bhatia, M. Notch-HES1 Signaling Axis Controls Hemato-Endothelial Fate Decisions of Human Embryonic and Induced Pluripotent Stem Cells. Blood **2013**, 122, 1162–1173.
43. Nishikawa, S.I.; Nishikawa, S.; Hirashima, M.; Matsuyoshi, N.; Kodama, H. Progressive Lineage Analysis by Cell Sorting and Culture Identifies FLK1+VE-Cadherin+ Cells at a Diverging Point of Endothelial and Hemopoietic Lineages. Dev. Camb. Engl. **1998**, 125, 1747–1757.
44. Testa, U.; Labbaye, C.; Castelli, G.; Pelosi, E. Oxidative Stress and Hypoxia in Normal and Leukemic Stem Cells. Exp. Hematol. **2016**, 44, 540–560.
45. Suda, T.; Takubo, K.; Semenza, G.L. Metabolic Regulation of Hematopoietic Stem Cells in the Hypoxic Niche. Cell Stem Cell **2011**, 9, 298–310.
46. Miharada, K.; Karlsson, G.; Rehn, M.; Rörby, E.; Siva, K.; Cammenga, J.; Karlsson, S. Hematopoietic Stem Cells Are Regulated by Cripto, as an Intermediary of HIF-1α in the Hypoxic Bone Marrow Niche. Ann. N. Y. Acad. Sci. **2012**, 1266, 55–62.
47. Lee, J.; Dykstra, B.; Spencer, J.A.; Kenney, L.L.; Greiner, D.L.; Shultz, L.D.; Brehm, M.A.; Lin, C.P.; Sackstein, R.; Rossi, D.J. MRNA-Mediated Glycoengineering Ameliorates Deficient Homing of Human Stem Cell-Derived Hematopoietic Progenitors. J. Clin. Investig. **2017**, 127, 2433–2437.
48. Jaatinen, T.; Hemmoranta, H.; Hautaniemi, S.; Niemi, J.; Nicorici, D.; Laine, J.; Yli-Harja, O.; Partanen, J. Global Gene Expression Profile of Human Cord Blood-Derived CD133+ Cells. Stem Cells Dayt. Ohio **2006**, 24, 631–641.
49. Eppert, K.; Takenaka, K.; Lechman, E.R.; Waldron, L.; Nilsson, B.; van Galen, P.; Metzeler, K.H.; Poeppl, A.; Ling, V.; Beyene, J.; et al. Stem Cell Gene Expression Programs Influence Clinical Outcome in Human Leukemia. Nat. Med. **2011**, 17, 1086–1093.

50. Cioch, M.; Jawniak, D.; Wach, M.; Mańko, J.; Radomska, K.; Borowska, H.; Szczepanek, A.; Hus, M. Autologous Hematopoietic Stem Cell Transplantation for Adults With Acute Myeloid Leukemia. Transplant. Proc. **2016**, 48, 1814–1817.
51. Simancikova, I.; Bojtarova, E.; Hrubisko, M.; Farkas, F.; Horvathova, D.; Sopko, L.; Batorova, A.; Mistrik, M. Autologous Hematopoietic Stem Cell Transplantation for Acute Myeloid Leukemia—Single Center Experience. Neoplasma **2017**, 64, 738–744.
52. Zittoun, R.A.; Mandelli, F.; Willemze, R.; de Witte, T.; Labar, B.; Resegotti, L.; Leoni, F.; Damasio, E.; Visani, G.; Papa, G. Autologous or Allogeneic Bone Marrow Transplantation Compared with Intensive Chemotherapy in Acute Myelogenous Leukemia. European Organization for Research and Treatment of Cancer (EORTC) and the Gruppo Italiano Malattie Ematologiche Maligne Dell'Adulto (GIMEMA) Leukemia Cooperative Groups. N. Engl. J. Med. **1995**, 332, 217–223.
53. Kissa, K.; Herbomel, P. Blood Stem Cells Emerge from Aortic Endothelium by a Novel Type of Cell Transition. Nature **2010**, 464, 112–115.
54. Sturgeon, C.M.; Ditadi, A.; Awong, G.; Kennedy, M.; Keller, G. Wnt Signaling Controls the Specification of Definitive and Primitive Hematopoiesis from Human Pluripotent Stem Cells. Nat. Biotechnol. **2014**, 32, 554–561.
55. Schoch, C.; Schnittger, S.; Klaus, M.; Kern, W.; Hiddemann, W.; Haferlach, T. AML with 11q23/MLL Abnormalities as Defined by the WHO Classification: Incidence, Partner Chromosomes, FAB Subtype, Age Distribution, and Prognostic Impact in an Unselected Series of 1897 Cytogenetically Analyzed AML Cases. Blood **2003**, 102, 2395–2402.
56. Salek-Ardakani, S.; Smooha, G.; de Boer, J.; Sebire, N.J.; Morrow, M.; Rainis, L.; Lee, S.; Williams, O.; Izraeli, S.; Brady, H.J.M. ERG Is a Megakaryocytic Oncogene. Cancer Res. **2009**, 69, 4665–4673.
57. Tomlins, S.A.; Rhodes, D.R.; Perner, S.; Dhanasekaran, S.M.; Mehra, R.; Sun, X.-W.; Varambally, S.; Cao, X.; Tchinda, J.; Kuefer, R.; et al. Recurrent Fusion of TMPRSS2 and ETS Transcription Factor Genes in Prostate Cancer. Science **2005**, 310, 644–648.
58. Sorensen, P.H.; Lessnick, S.L.; Lopez-Terrada, D.; Liu, X.F.; Triche, T.J.; Denny, C.T. A Second Ewing's Sarcoma Translocation, t(21;22), Fuses the EWS Gene to Another ETS-Family Transcription Factor, ERG. Nat. Genet. **1994**, 6, 146–151.
59. Jalaguier, S.; Teyssier, C.; Nait Achour, T.; Lucas, A.; Bonnet, S.; Rodriguez, C.; Elarouci, N.; Lapierre, M.; Cavaillès, V. Complex Regulation of LCoR Signaling in Breast Cancer Cells. Oncogene **2017**, 36, 4790–4801.
60. Cawthorne, C.; Swindell, R.; Stratford, I.J.; Dive, C.; Welman, A. Comparison of Doxycycline Delivery Methods for Tet-Inducible Gene Expression in a Subcutaneous Xenograft Model. J. Biomol. Tech. JBT **2007**, 18, 120–123.
61. Thomson, J.A.; Itskovitz-Eldor, J.; Shapiro, S.S.; Waknitz, M.A.; Swiergiel, J.J.; Marshall, V.S.; Jones, J.M. Embryonic Stem Cell Lines Derived from Human Blastocysts. Science **1998**, 282, 1145–1147.
62. Yu, J.; Vodyanik, M.A.; Smuga-Otto, K.; Antosiewicz-Bourget, J.; Frane, J.L.; Tian, S.; Nie, J.; Jonsdottir, G.A.; Ruotti, V.; Stewart, R.; et al. Induced Pluripotent Stem Cell Lines Derived from Human Somatic Cells. Science **2007**, 318, 1917–1920.
63. Choi, K.-D.; Vodyanik, M.A.; Slukvin, I.I. Generation of Mature Human Myelomonocytic Cells through Expansion and Differentiation of Pluripotent Stem Cell-Derived Lin-CD34+CD43+CD45+ Progenitors. J. Clin. Investig. **2009**, 119, 2818–2829.

64. Kennedy, M.; Awong, G.; Sturgeon, C.M.; Ditadi, A.; LaMotte-Mohs, R.; Zúñiga-Pflücker, J.C.; Keller, G. T Lymphocyte Potential Marks the Emergence of Definitive Hematopoietic Progenitors in Human Pluripotent Stem Cell Differentiation Cultures. Cell Rep. **2012**, 2, 1722–1735.
65. Risueño, R.M.; Sachlos, E.; Lee, J.-H.; Lee, J.B.; Hong, S.-H.; Szabo, E.; Bhatia, M. Inability of Human Induced Pluripotent Stem Cell-Hematopoietic Derivatives to Downregulate MicroRNAs in Vivo Reveals a Block in Xenograft Hematopoietic Regeneration. Stem Cells Dayt. Ohio **2012**, 30, 131–139.
66. Narayan, A.D.; Chase, J.L.; Lewis, R.L.; Tian, X.; Kaufman, D.S.; Thomson, J.A.; Zanjani, E.D. Human Embryonic Stem Cell-Derived Hematopoietic Cells Are Capable of Engrafting Primary as Well as Secondary Fetal Sheep Recipients. Blood **2006**, 107, 2180–2183.
67. Chang, K.-H.; Nelson, A.M.; Cao, H.; Wang, L.; Nakamoto, B.; Ware, C.B.; Papayannopoulou, T. Definitive-like Erythroid Cells Derived from Human Embryonic Stem Cells Coexpress High Levels of Embryonic and Fetal Globins with Little or No Adult Globin. Blood **2006**, 108, 1515–1523.
68. Chicha, L.; Feki, A.; Boni, A.; Irion, O.; Hovatta, O.; Jaconi, M. Human Pluripotent Stem Cells Differentiated in Fully Defined Medium Generate Hematopoietic CD34- and CD34+ Progenitors with Distinct Characteristics. PLoS ONE **2011**, 6, e14733.
69. Ledran, M.H.; Krassowska, A.; Armstrong, L.; Dimmick, I.; Renström, J.; Lang, R.; Yung, S.; Santibanez-Coref, M.; Dzierzak, E.; Stojkovic, M.; et al. Efficient Hematopoietic Differentiation of Human Embryonic Stem Cells on Stromal Cells Derived from Hematopoietic Niches. Cell Stem Cell **2008**, 3, 85–98.
70. Suzuki, N.; Yamazaki, S.; Yamaguchi, T.; Okabe, M.; Masaki, H.; Takaki, S.; Otsu, M.; Nakauchi, H. Generation of Engraftable Hematopoietic Stem Cells from Induced Pluripotent Stem Cells by Way of Teratoma Formation. Mol. Ther. J. Am. Soc. Gene Ther. **2013**, 21, 1424–1431.
71. Amabile, G.; Welner, R.S.; Nombela-Arrieta, C.; D'Alise, A.M.; Di Ruscio, A.; Ebralidze, A.K.; Kraytsberg, Y.; Ye, M.; Kocher, O.; Neuberg, D.S.; et al. In Vivo Generation of Transplantable Human Hematopoietic Cells from Induced Pluripotent Stem Cells. Blood **2013**, 121, 1255–1264.
72. Pereira, C.-F.; Chang, B.; Qiu, J.; Niu, X.; Papatsenko, D.; Hendry, C.E.; Clark, N.R.; Nomura-Kitabayashi, A.; Kovacic, J.C.; Ma'ayan, A.; et al. Induction of a Hemogenic Program in Mouse Fibroblasts. Cell Stem Cell **2013**, 13, 205–218.
73. Riddell, J.; Gazit, R.; Garrison, B.S.; Guo, G.; Saadatpour, A.; Mandal, P.K.; Ebina, W.; Volchkov, P.; Yuan, G.-C.; Orkin, S.H.; et al. Reprogramming Committed Murine Blood Cells to Induced Hematopoietic Stem Cells with Defined Factors. Cell **2014**, 157, 549–564.
74. Sandler, V.M.; Lis, R.; Liu, Y.; Kedem, A.; James, D.; Elemento, O.; Butler, J.M.; Scandura, J.M.; Rafii, S. Reprogramming Human Endothelial Cells to Haematopoietic Cells Requires Vascular Induction. Nature **2014**, 511, 312–318.

Figures

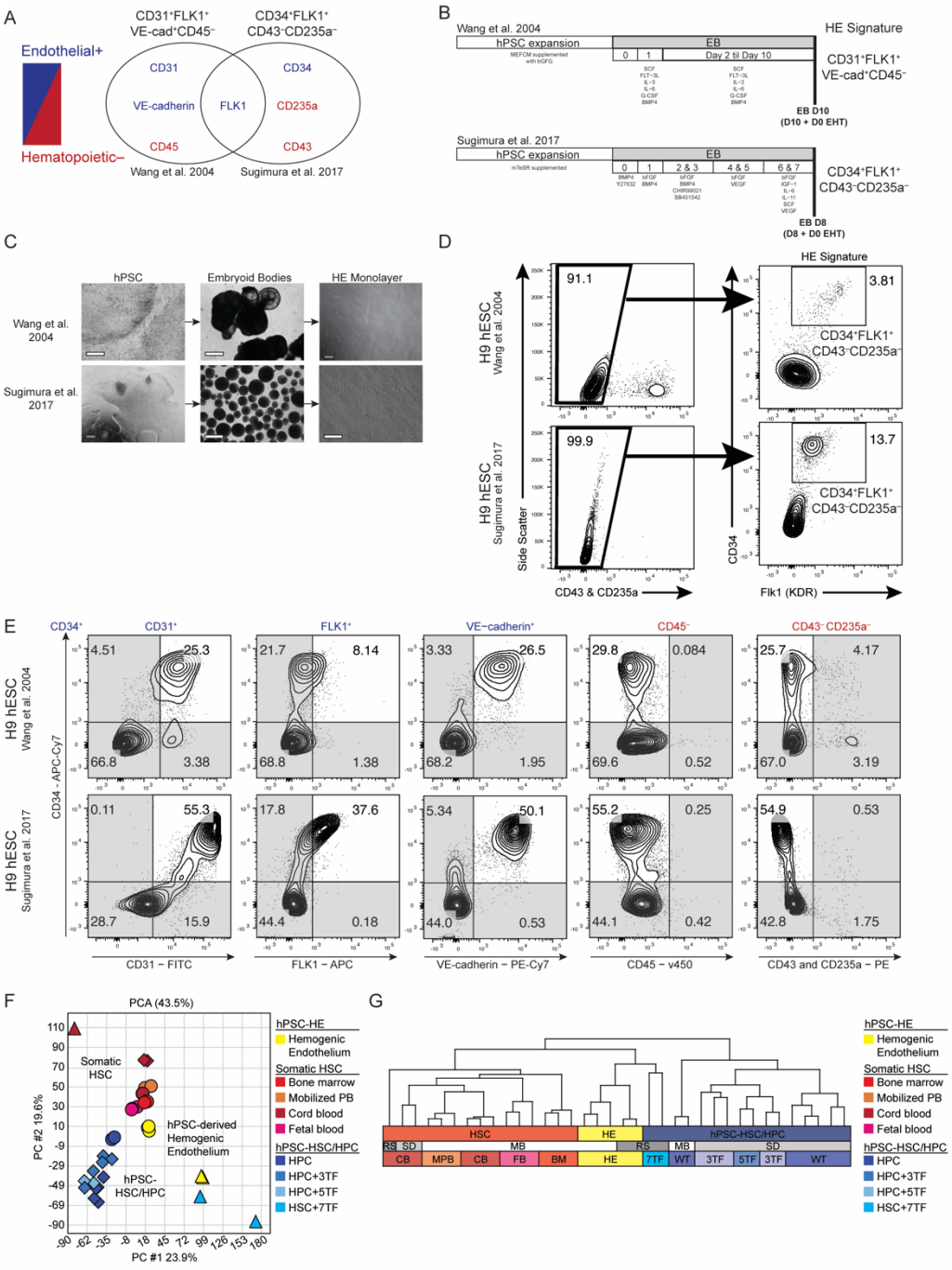

Figure 1. Co-expressed surface markers of hPSC-derived hemogenic endothelium
(A) Overlap of hemogenic endothelium (HE) phenotype with shared antigens from Wang et al. [38], and Sugimura et al. [32]. (B) Morphological comparison of HE derived from hPSC differentiated into embryoid bodies (EBs) using Wang et al. [38] (top), and Sugimura et al. [32] (bottom). Both protocols yield HE cells that adhere to the culture plate and grow post-dissociation of hEBs. White scale bar represents 500 mm; black scale bar represents 30 mm. (C) Timeline of HE derivation from hEBs using two distinct methodologies previously mentioned. (D) Flow

cytometry of Sugimura et al., HE signature (CD34+Flk1+CD43−CD235A−) on differentiation day 10 generated using the Bhatia (Wang et al. [38]; top) and Daley (Sugimura et al., [32]; bottom) methods. (E) Overlap of HE phenotype with shared antigens combined in one flow cytometry panel on day 8 hEB (EHT day 0) derived from Sugimura et al. [32], protocol or day 10 hEBd (EHT day 0) Wang et al. [38], protocol. Despite distinct hEB culture conditions, both methodologies produce similar frequency of HE phenotypic markers. (F) Shared molecular signature of HE across Daley and Bhatia lab. A principal component analysis (PCA) correlation biplot comparing gene expression of FACS-purified HSCs (BM, N n = 3; CB, n = 7; FB, n = 3; MPB, n = 3; and hPSC(+7TF)-HSC, n = 2) and hPSC-HE(HE, n = 2) and hPSC-HPCs (wt, n = 7; 3TF, n = 3; and 5TF, n = 2) from a combined dataset including GSE83719 (Sugimura et al. [32]) and GSE49938 (Doulatov et al. [30]). (G) Unsupervised hierarchical clustering of samples described in F. Abbreviations (top row): hematopoietic stem cell, HSC; hemogenic endothelium, HE; in vitro human pluripotent stem cell-derived hematopoietic progenitor cells, in vivo human pluripotent stem cell-derived hematopoietic stem cell, hPSC-HSC/HPC; (middle row): Mick Bhatia, MB; Ryohichi Sugimura, RS; Sergei Doulatov, SD; (bottom row): cord blood, CB; mobilized peripheral blood, MPB; fetal blood, FB; bone marrow, BM; hPSC-HE, HE; hPSC(+7TF)-HPC, 7TF; wildtype, WT; hPSC(+3TF)-HPC, 3TF; hPSC(+5TF)-HPC, 5TF.

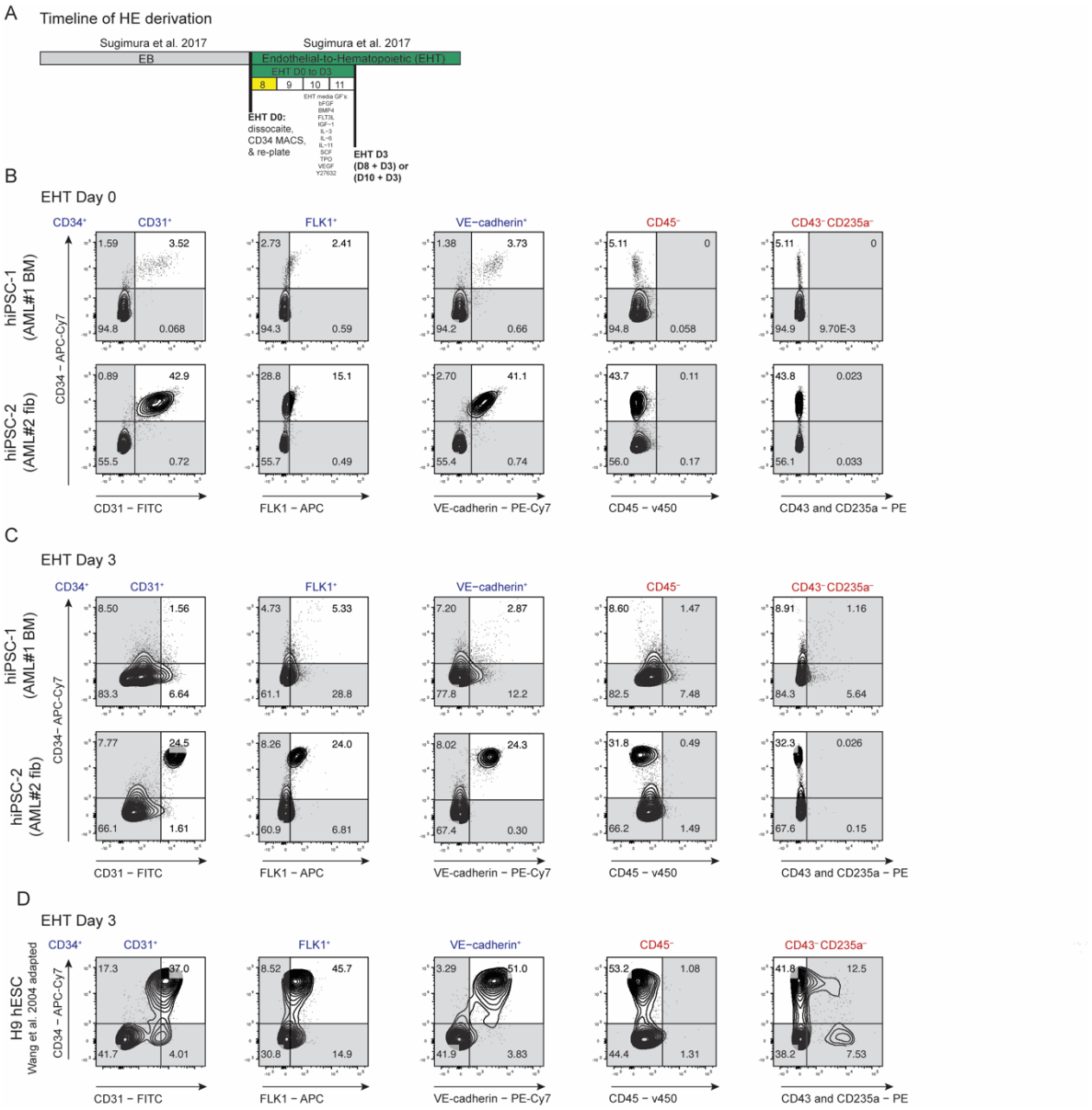

Figure 2. Endothelial-to-hematopoietic transition (EHT) of AML patient-specific iPSCs

(A) Schematic depicting simplified timeline of HE derivation used on various hPSCs. HE cells were isolated through dissociation of hEBs and enriched by positive selection of CD34+ through Magnetic-Activated Cell Sorting (MACS) at day 8 (or day 10) and then further cultured in Endothelial-to-Hematopoietic Transition (EHT) medium for the indicated number of days (Sugimura et al. [32]). (B) Flow analysis of HE phenotype on EHT day 0 post-CD34+ MACS enrichment in two AML-iPSC lines, hiPSC-1 (AML-iPSC derived from reprogramming AML patient 15331 bone marrow cells) and hiPSC-2 (AML-iPSC derived from reprogramming AML patient #2 fibroblast cells). (C) Flow analysis of HE phenotype on day 3 of EHT on hiPSC-1 and hiPSC-2. (D) HE phenotype of hESC line H9s derived using Wang et al. [38], methodology depicted on one flow cytometry panel.

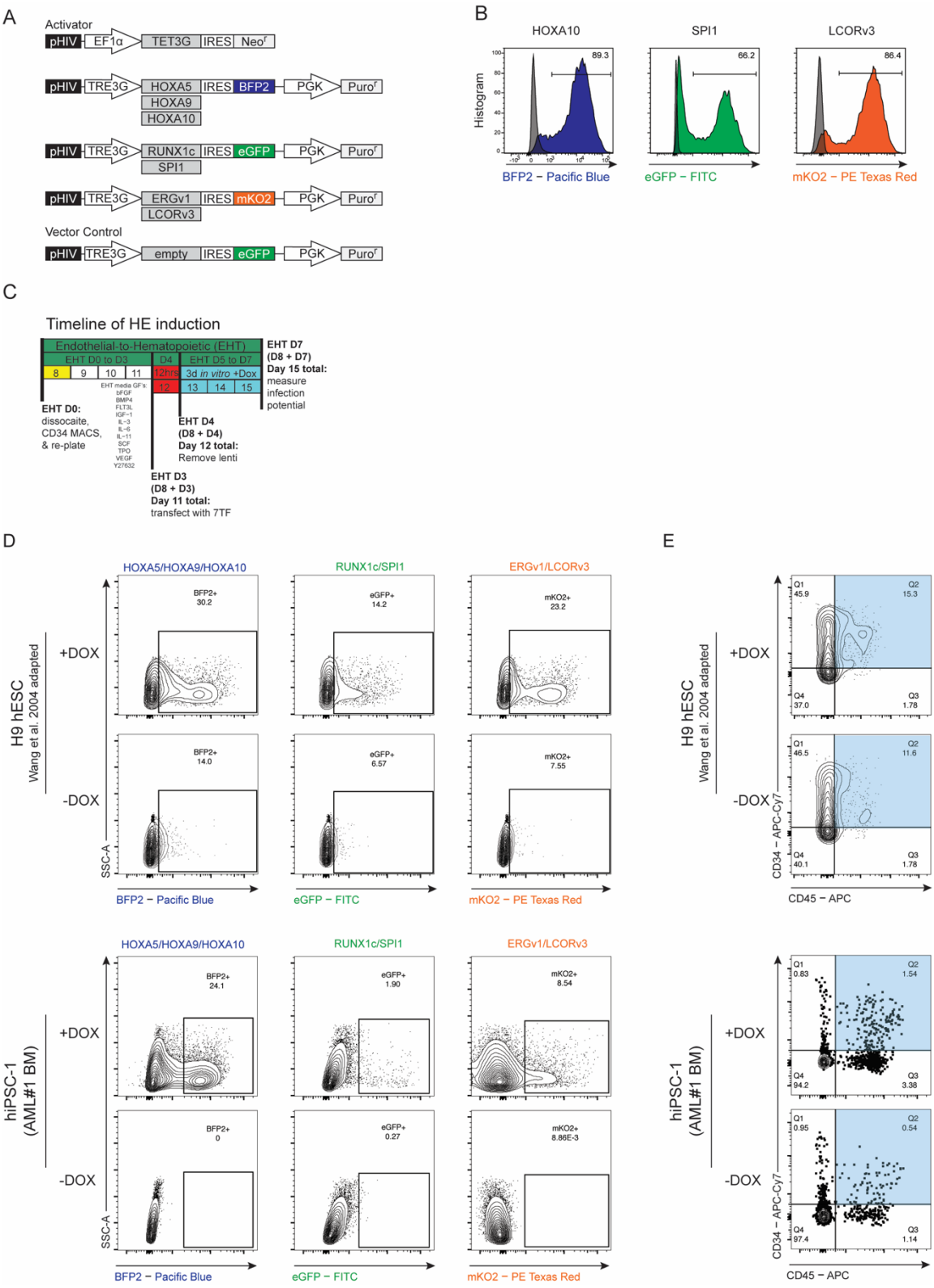

Figure 3. Generation and forced expression of 7TF under HE conditions in AML-iPSCs

(4) Schematic representation of the Doxycycline-inducible system utilized throughout experiments with a defined set of seven hematopoietic transcription factors (TF). Human TFs were cloned into pHIV-TREG vector, which has an internal ribosome entry site (IRES) translation link to distinct fluorescent proteins BFP2, mKusabiraOrange2 (mKO2), or eGFP. (B) Doxycycline induction of individual TFs in HE cells. Fluorescent proteins are representative single stains of select TFs. (C) Schematic depicting temporal forced expression of 7TF on HE derived from hPSC in the presence of doxycycline in EHT medium maintained in vitro, as well as empty vector control. (D) Representative transduction efficiency of TFs comprising all three fluorescent protein channels (Wang et al. [38]). € Doxycycline induction of 7 TF-transduced HE, maintained in vitro 3 days beyond the day of transduction. Acquisition of a larger hematopoietic phenotype (CD34+CD45+) observed in HE cells treated with Doxycycline vs. untreated cells (Wang et al. [38]).

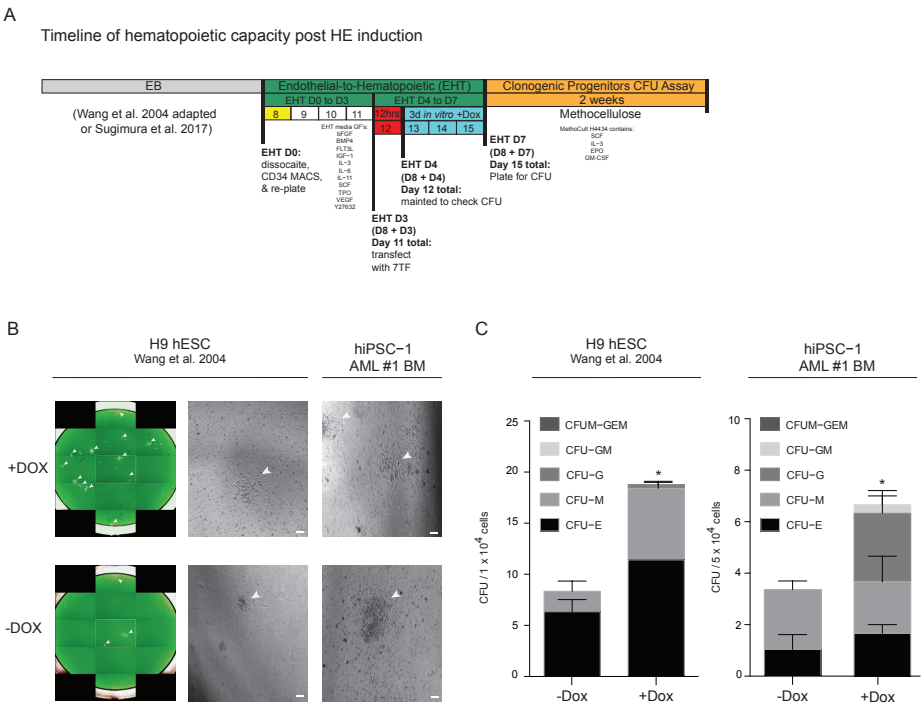

Figure 4. Progenitor capacity from hPSC-derived HE upon 7TF initiation

(A) Schematic depicting temporal forced expression of 7TF to assess clonogenic progenitor or "colony forming unit" (CFU) assay on HE derived from hPSCs (Sugimura et al. [32] and Wang et al. [38]). (B) Representative whole-well CFU images of hPSC lines stained by calcein-green (475 ex; 525 em) fluorescence on day 14 of cultures. Images were acquired at 2× using Operetta High Content Screening (Perkin Elmer) by means of calcein-green am staining. Whole-well images were stitched in Columbus Image Data Storage and Analysis System version 2.9.0 (Perkin Elmer). Scale bar 2 µm. White arrow heads highlight colonies formed (Wang et al. [38]). (C) Total number of hematopoietic colony forming units (CFUs) and number of colony subtypes CFU-Erythroid, CFU-Granulocyte, CFU-Monocyte/macrophage, and CFU-GM and CFU-GEMM (Wang et al. [38]). Unpaired Student t-test was performed for statistical analysis * = $p < 0.05$. All data shown are mean ± SEM (N = 3–4).

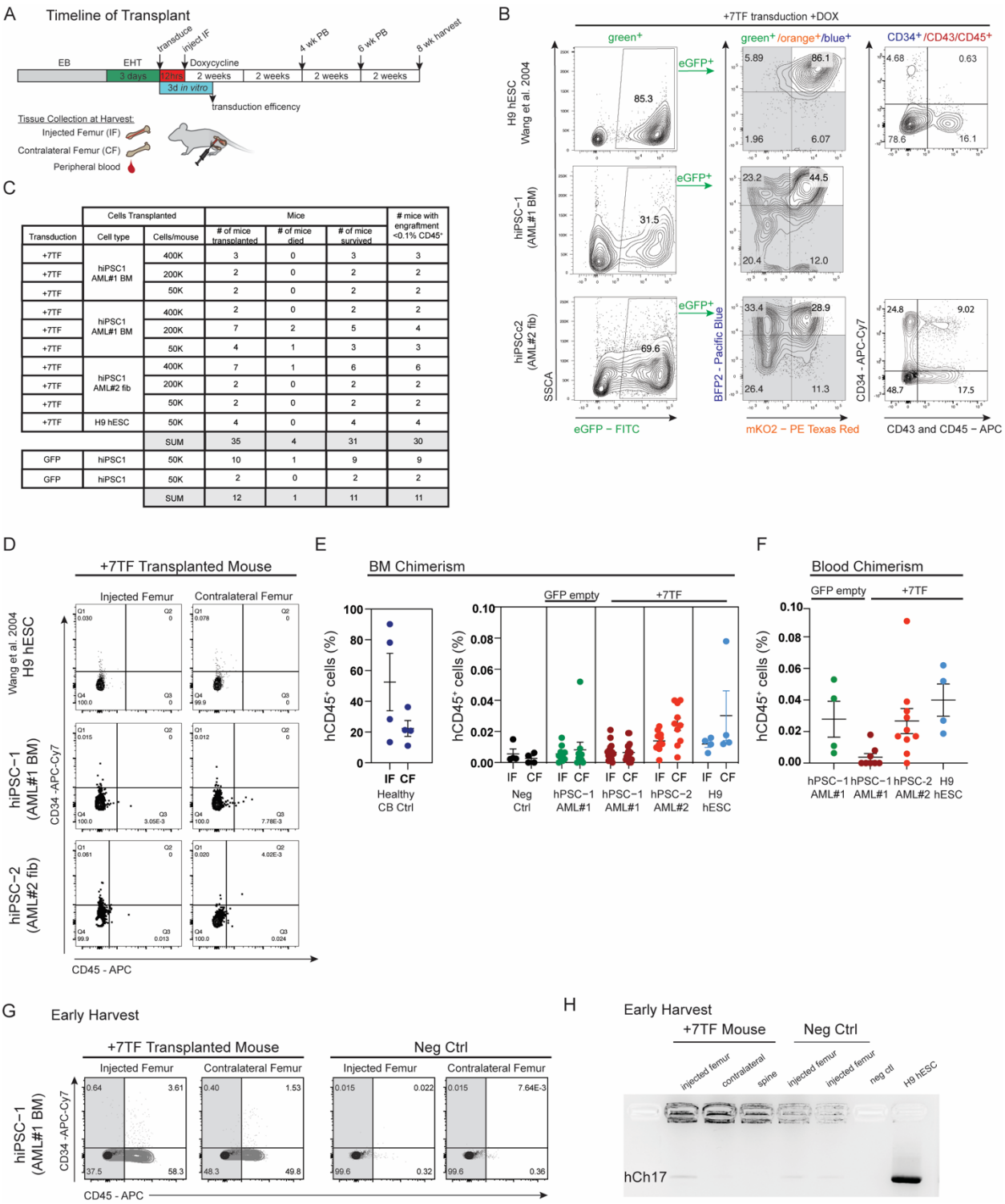

Transduction	Cells Transplanted: Cell type	Cells/mouse	Mice: # of mice transplanted	# of mice died	# of mice survived	# mice with engraftment <0.1% CD45+
+7TF	hiPSC1 AML#1 BM	400K	3	0	3	3
+7TF		200K	2	0	2	2
+7TF		50K	2	0	2	2
+7TF	hiPSC1 AML#1 BM	400K	2	0	2	2
+7TF		200K	7	2	5	4
+7TF		50K	4	1	3	3
+7TF	hiPSC1 AML#2 fib	400K	7	1	6	6
+7TF		200K	2	0	2	2
+7TF		50K	2	0	2	2
+7TF	H9 hESC	50K	4	0	4	4
		SUM	35	4	31	30
GFP	hiPSC1	50K	10	1	9	9
GFP	hiPSC1	50K	2	0	2	2
		SUM	12	1	11	11

Figure 5. Early harvest of transplanted mouse reveals human hematopoietic chimerism

(A) Schematic depicting timeline of transplantation experiments. Hemogenic endothelium cells infected at day 3 EHT were incubated for 24 h and intrafemorally (IF) injected into mice. Doxycycline was provided for 2 weeks in vivo after transplantation into sub-lethally irradiated

immune-deficient NSG mice. Three days post-transfection, transduction efficiency of transplanted cells were assessed. Tissues collected during each harvest was as follows: injected femur, contralateral femur, and peripheral blood via cheek bleeds. (B) Representative transduction efficiency flow plots of fluorescent proteins multiplexed by flow cytometry. Doxycycline induction of 7 TF-transduced hemogenic endothelium, maintained in vitro 6 days beyond the day of transplant. Acquisition of hematopoietic phenotype ($CD34^{+}CD45^{+}$) observed post-transduction (Wang et al. [38]). (C) Table summarizing the numbers of mice, cell doses transplanted, and chimerism outcome. (D) Representative flow plots of bone marrow of NSG mouse engrafted with HE-7 transcription factor analyzed at 8 weeks for scid-repopulating cells (hCD34+hCD45+). N numbers represent transplanted mice (Wang et al. [38]). (E) BM chimerism of NSG mice engrafted with HE-7 transcription factor analyzed at 8 weeks for human hCD45+. Data shown as mean ± SEM (N = 3–18); each dot represents a separate mouse. Mice transplanted with cord blood (CB) were harvested at 6 weeks during a separate round of experimentation. Mice that were not transplanted with hPSCs are referred to as negative control (neg ctrl). Mice that were transplanted with HE transduced with an empty eGFP vector are referred to as hPSC-1 + eGFP. (F) Blood chimerism of NSG mice engrafted with HE-7 transcription factor were analyzed at 8 weeks by cheek bleeds. (G) Representative flow plots showing human chimerism after transplant. Human hematopoietic phenotyping of 7TF-transplanted mouse harvested at day 12, in parallel with a negative control mouse. (H) Genomic DNA extracted from harvested tissue and probed for human sequences by conventional PCR (hCh17; alpha-satellite chromosome 17).

Supplementary Figures

Supplementary Figure 1

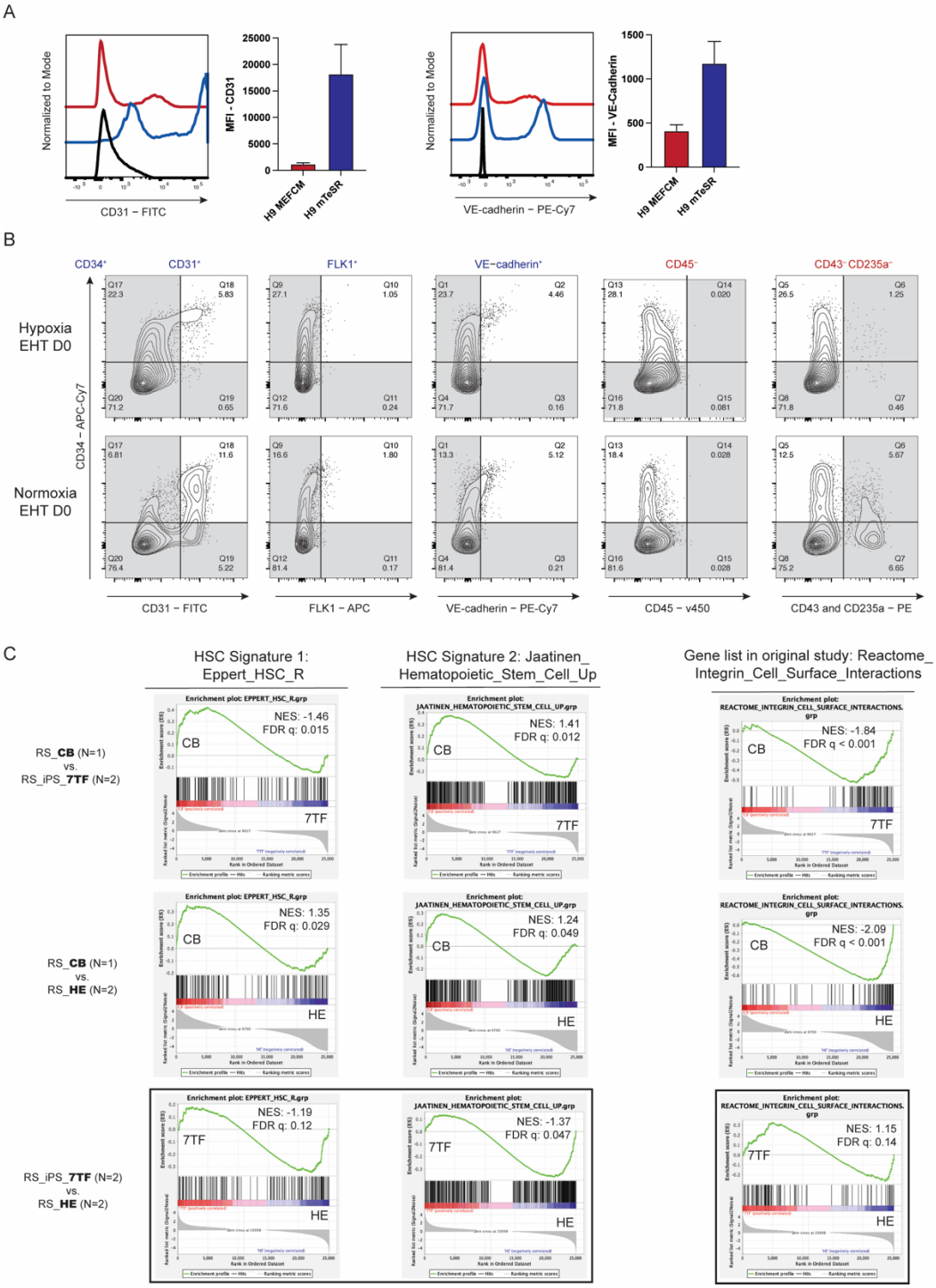

Supplemental Figure S1.

Comparison of HE phenotype under normoxic or hypoxic conditions. (A) Histogram and corresponding bar graphs reporting flow cytometry analysis determined by MFI (mean fluorescence intensity) of CD31 or VE-Cadherin respectively. H9 MEFCM denotes HE derivation by using Wang et al., 2004 methodology. H9 mTeSR denotes derivation by using Sugimura et al., 2017 methodology. (B) Embryoid body differentiation in normoxia (5%CO2) or hypoxia (5%CO_2/5%O2/90% N_2) conditions. (C) Gene set enrichment analyses (GSEA) comparing gene expression profiles of the following samples from Sugimura et al.: CB, 7TF and HE. NES, normalized enrichment score; FDR, false discovery rate.

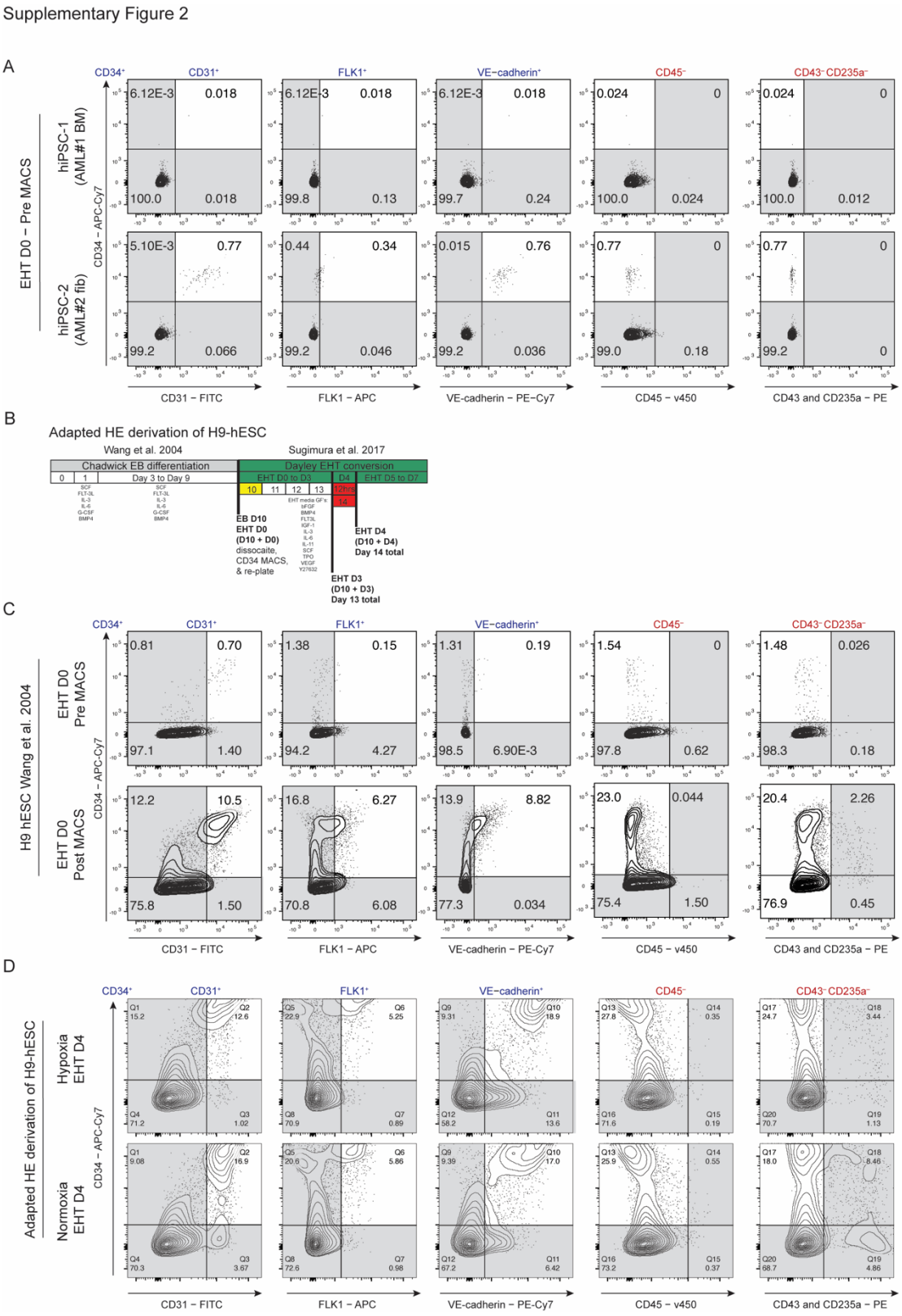

Supplemental Figure S2.

Timeline of HE derivation using adapted protocol. (A) Flow analysis of HE phenotype on EHT day 0 pre $CD34^+$ MACS enrichment in two AML-iPSC lines, hiPSC-1 (AML-iPSC derived from reprogramming AML patient 15331 bone marrow cells) and hiPSC-2 (AML-iPSC derived from reprogramming AML patient #2 fibroblast cells). (B) Schematic depicting timeline used for HE derivation by merging Wang et al., 2004 EB differentiation and Sugimura et al., 2017 endothelial-to-hematopoietic transition medium. (C) Flow analysis of HE phenotype on EHT day 0 pre and post CD34+ MACS enrichment of hESC (H9) using our adapted protocol. (D) Endothelial-to-hematopoietic transition differentiation in normoxic (5%CO_2) or hypoxic (5%CO_2/5%O_2/90% N_2) conditions at EHT day 4.

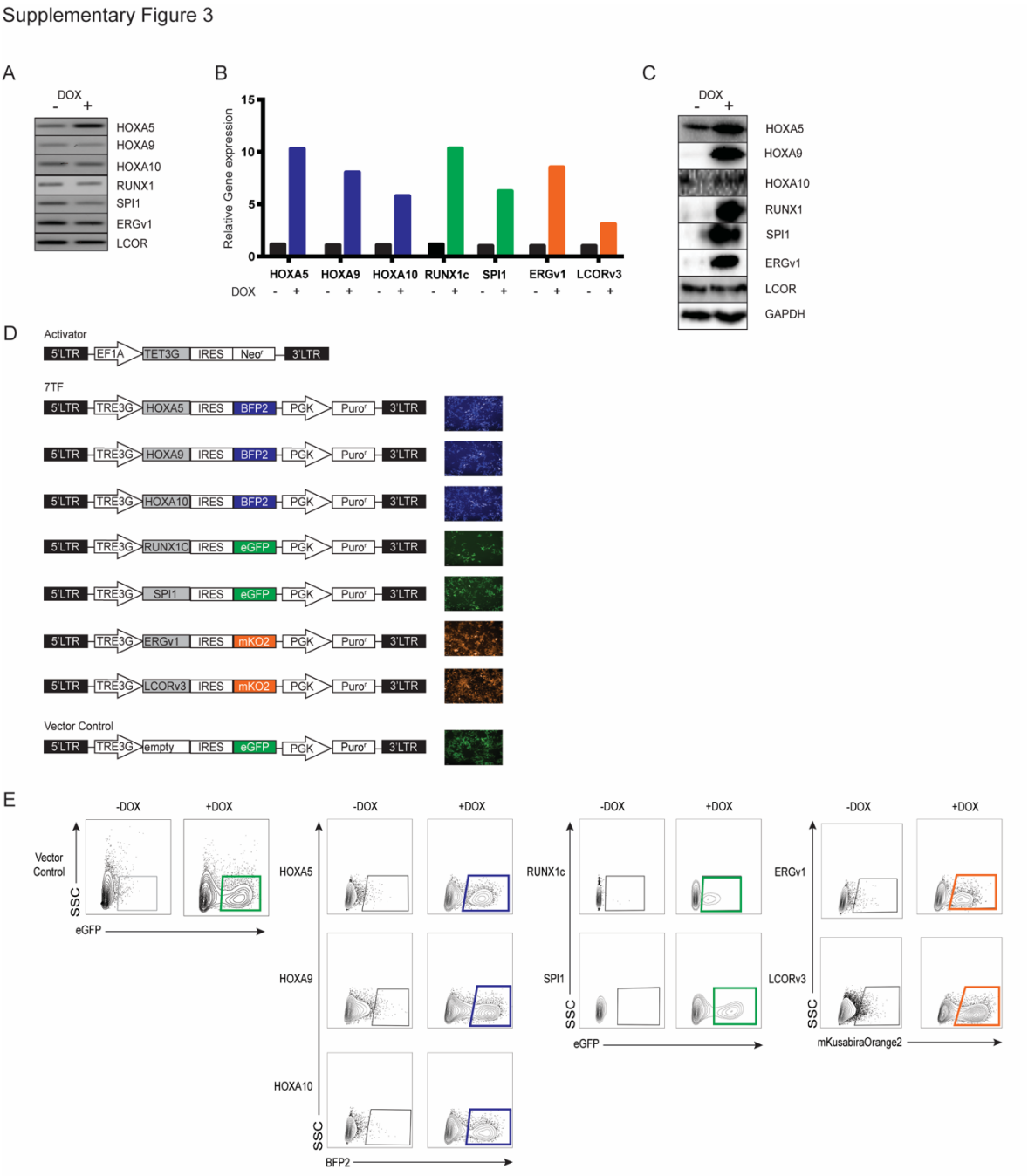

Supplemental Figure S3.

Molecular validation of 7TF induction. (A) Validation of transcription factor by PCR (genomic integration) and (B) doxycycline induction of gene (qPCR) and (C) protein (WB) expression of TF on HEKs. (D) Vector constructs and representative fluorescent images of individual transcription factors acquired using the PerkinElmer Operetta High Content Imaging System. (E) Demonstration of fluorescent protein expression by flow cytometry on HEKs in the presence or absence of doxycycline.

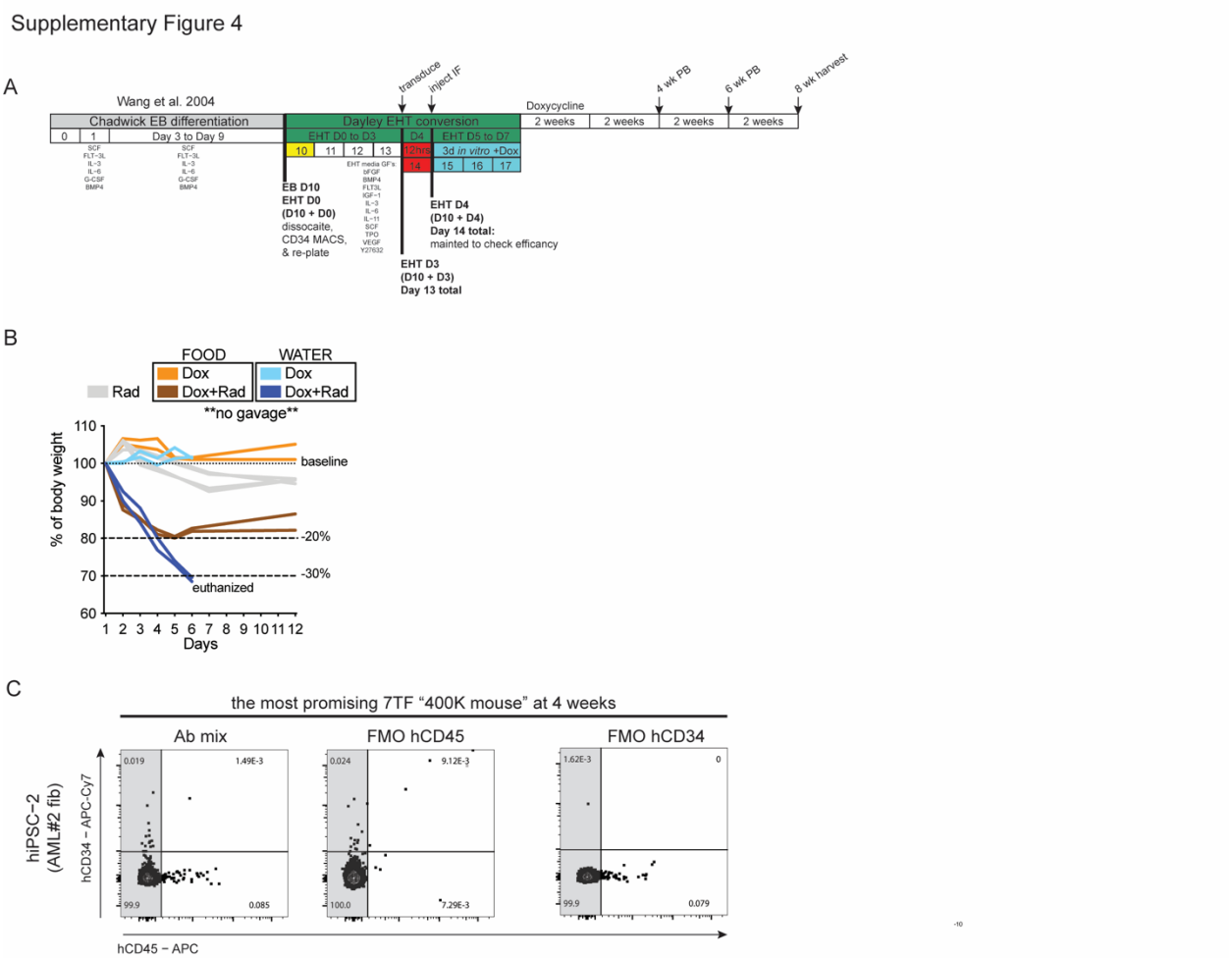

Supplemental Figure S4.

Data from transplantation experiments. (A) Schematic depicting timeline of transplantation experiments utilizing adapted procedure for HE derivation by merging Wang et al., 2004 EB differentiation and Sugimura et al., 2017 endothelial-to-hematopoietic transition medium. (B) Observed issue resulting from combination of radiation and doxycycline (by food or water) leading to high morbidity rates. To mitigate this problem, 10g/L of sucrose was added to drinking water with doxycycline. Additionally, daily gavage was performed with dox & sucrose water, starting on the day of transplant. See methods for further details. (C) Representative flow plot of peripheral blood chimerism of "best" 400K mouse from hiPSC-2 = normal iPSC from AML #28787 fib clone N18.

Chapter 3: Reprogramming of Acute Myeloid Leukemia Patients Cells Harboring Cancer Mutations Requires Targeting of AML hierarchy

Preamble

This chapter is a submitted manuscript. It is presented in its submitted form.

Author contributions: D.P.P, D.G, M.D performed experiments. J.R and A.L.B., aided with the transplant assay design. D.P.P, D.G, M.D and M.B. designed experiments and interpreted data. D.P.P and M.B wrote the manuscript. M.B. directed the study.

Author contributions in greater detail: D.G reprogrammed 15 primary AML samples, performed FISH analysis, prepped a single sample for Affymetrix HD CytoScan microarry and performed a teratoma assay. JR assisted with bone marrow aspirates and teratoma harvest. D.P.P wrote the manuscript, reprogrammed primary 7 AML samples via the assistance of M.D. and assisted with the culture, expansion, and cryopreservation of all AML-patient derived iPSCs. D.G and M.D provide reprogramming efficacy values and D.P.P provided interpretation and analysis of these values. D.G, D.P.P and M.D all prepped samples for karyotypic analysis, and ddPCR which was conducted by the Centre for Applied Genomics at the Hospital for Sick Children. D.G and D.P.P both performed flow cytometry analysis of pluripotent markers of AML-patient derived iPSCs. A.L.B provided insight into the transplant assay design and assisted with clinical annotation of AML patient samples selected for reprogramming.

Reprogramming of Acute Myeloid Leukemia Patients Cells Harboring Cancer Mutations Requires Targeting of AML hierarchy

Authors: Diana Golubeva[1†], Deanna P Porras[1†], Meaghan Doyle[1], Jennifer C Reid[1], Borko Tanasijevic[1], Allison L Boyd[1] and Mickie Bhatia[1,2,*]

Addresses
[1]Department of Biochemistry and Biomedical Sciences, McMaster University, Hamilton, ON L8N 3Z5, Canada;
golubeda@mcmaster.ca (D.G.); porrasd@mcmaster.ca (D.P.P.); reidjc2@mcmaster.ca (J.C.R.); tanasb@mcmaster.ca (B.T.); boydal2@mcmaster.ca (A.L.B.)
[2]Michael G. DeGroote School of Medicine, McMaster University, 1200 Main Street West, MDCL 5029, Hamilton, ON L8N 3Z5, Canada

[*]Correspondence: mbhatia@mcmaster.ca; Tel: +1-(905)-525-9140 (ext. 28687)

[†] These authors contributed equally to this work

RUNNING HEAD TITLE: Targeting of AML hierarchy in derivation of AML-iPSCs

AUTHOR CONTRIBUTIONS:

1. Diana Golubeva: Conception and design, collection and/or assembly of data, data analysis and interpretation
2. Deanna P Porras: Conception and design, collection and/or assembly of data, data analysis and interpretation, manuscript writing, final approval of manuscript
3. Meaghan Doyle: collection and/or assembly of data, data analysis and interpretation
4. Jennifer C Reid: collection and/or assembly of data, data analysis and interpretation
5. Borko Tanasijevic: collection and/or assembly of data
6. Allison L Boyd: data analysis and interpretation, administrative support, provision of study material or patients
7. Mickie Bhatia: Conception and design, financial support, administrative support, provision of study material or patients, manuscript writing, final approval of manuscript

SIGNIFICANCE STATEMENT:
Establishment of an unprecedented library of 79 AML-induced pluripotent stem cell (AML-iPSC) lines harboring driver mutations from a broad range of AML patients to increase capture of disease heterogeneity for modeling.

KEYWORDS (3-10 keywords)

1. acute myeloid leukemia (AML),
2. hematopoietic stem/progenitor cell (HSPC)
3. induced pluripotent stem cell (iPSC)

4. xenotransplantation
5. AML-induced pluripotent stem cell (AML-iPSC)
6. reprogramming

Abstract

High throughput screening of acute myeloid leukemia (AML) patient cells is challenging based on intrinsic characteristics of human AML disease and patient specific conditions required to sustain AML cells in culture. Further complexities of inter-and intra-patient heterogeneity, and 'contaminating' residual healthy cells increase the challenges. Derivation of induced pluripotent stem cells (iPSCs) from human somatic cells have provided approaches for the development of patient-specific models of disease biology, including AML recently. Although reprogramming patient-derived cancer cells to pluripotency allows for aspects of disease modeling, the major limitation preventing applications and deeper insights using AML-iPSCs is the rarity of success and limited subtypes of AML disease that can be captured by reprogramming to date. Here, we tested and refined methods including de novo, xenografting, naïve vs prime states and prospective isolation for reprogramming AML cells using a total of 22 AML patient samples representing the wide variety of cytogenetic abnormalities. These efforts allowed us to derive genetically matched healthy control (isogenic) lines and capture clones found originally in AML patients. Using fluorescence activated cell sorting, we show that AML and healthy reprogramming is linked to the differentiation state of diseased tissue, where use of myeloid marker CD33 compared to the stem cell marker, CD34, reduces reprogramming capture of AML clones. Our efforts provide a platform for further optimization of AML-iPSC generation, and a unique library of 129 mutant and healthy iPSCs derived directly from AML patients for study by the broader scientific community.

1. Introduction

Cancer is the leading cause of death in developed countries, firmly linked to genetics as well as environmental factors [1]. Cancer is considered a multi-step disease involving several stages of development toward full malignancy, requiring a better understanding of the diverse genetic and epigenetic steps in the alteration from healthy to diseased cells. Acute myeloid leukemia (AML) is one of the most heterogeneous cancers with diversity observed at the levels of genetics, epigenetics, and clonal organization across AMLs patients [2]. This heterogeneity is believed to be the basis of difficulty in predicting patient responses to chemotherapy and related disease relapse [3–6]. Although some genomic DNA mutations carry prognostic value, these rarely provide a means for targeted therapeutic intervention, and their functional contributions to disease initiation, progression, and maintenance are largely unknown7–9 creating further challenges in developing novel therapeutics [10].

AML patients share a disease phenotype where dysfunctional cells accumulate in the myeloid compartment of the hematopoietic system and are blocked in their ability to differentiate and fully mature. AML results in the rapid accumulation of non-functional, immature hematopoietic cells in the BM and peripheral blood (PB) of patients leading to hematopoietic system failure [11]. These aberrantly differentiated cells compete in the BM niche with healthy cells [12] where they also assemble in an hierarchy similar to normal hematopoiesis. In a non-diseased state, the healthy hematopoietic system has rare hematopoietic stem and progenitor cells

(HSPCs) residing at the apex [13,14] to simultaneously maintain HSPC populations and undergo appropriate differentiation into to all mature lymphoid and myeloid blood cells [15]. Unfortunately, primitive AML and healthy HSPCs cells share similar phenotypes [12]. Therefore, it is difficult to prospectively isolate diseased vs. healthy primitive cells from each other for interventional studies or experimentally analysis. Accordingly, development for more diverse model systems able to capture and distinguish AML from healthy counterparts, as well as observe rare clonal and epigenetic diversity of AML disease evolution are needed.

Human-induced pluripotent stem cells (hiPSCs) represent a potential platform to achieve such goals. In the last decade, thousands of hiPSCs have been generated from healthy donors and from patients afflicted with various diseases [16–19]. Patient-derived hiPSCs have the potential to produce an endless number of specialized disease-associated cells and organoids, allowing researchers to replicate some pathological characteristics of human disease in vitro. Indeed, such models have already aided in the discovery of molecular processes of pathogenesis, paving the way for new treatments for some diseases [20]. Although monogenic inherited blood diseases were readily modeled with iPSCs, malignant hematologic disorders such as AML have been more challenging to obtain. Unlike inherited genetic diseases, where disease-causing mutations are present in the germline to be passed to all somatic cells, most AML genetic lesions arise postnatally and accumulate sequentially in the somatic hematopoietic stem cell (HSC) compartment. Accordingly, while iPSC models of inherited monogenic diseases can be derived by reprogramming any accessible cell type, derivation of AML-iPSCs requires reprogramming hematopoietic leukemic cells themselves and not skin fibroblasts or other cell types that would represent germline mutations of AML patients [21,22].

Although some reports have successfully reprogrammed myeloid malignancies over the years, we and others have shown leukemic cells are relatively refractory to reprogramming and represent only a small minority of the diversity of genetic phenotypes observed in AML patients [22–26]. AML's refractory behavior to reprogramming is similar to other highly proliferative malignant cells [27–30]. This results in an experimental predominance of normal iPSCs from patient tissue devoid of clinically defined mutations [22–25,30–34]. Here, we interrogate strategies to selectively reprogram AML and healthy cells from AML patients to increase successful reprogramming of bona fide aberration-containing AML cells. Using prospective purification, we show that AML and healthy reprogramming correlates to the stage of hematopoietic differentiation. In total, we report the development of a library of 77 AML-induced pluripotent stem cell (AML-iPSC) lines from AML patients. We also report 52 genetically normal iPSC lines developed from these patients, for a total of 129 distinct and functionally and phenotypically characterized iPSC lines and has allowed for isogenic paired lines to be generated within this library of AML patient iPSCs.

2. Material & Methods

2.1 Primary Patient Samples

Healthy human hematopoietic cells were isolated from mobilized peripheral blood of adult donors. Primary AML specimens were obtained from peripheral blood apheresis or BM aspirates of consenting AML patients. AML samples and adult sources of healthy hematopoietic tissue were provided by Juravinski Hospital and Cancer Centre and London Health Sciences Centre (University of Western Ontario). All samples were obtained from informed consenting donors in

accordance with approved protocols by the Research Ethics Board at McMaster University and the London Health Sciences Centre, University of Western Ontario.

2.2 Patient Derived Xenografts

AML samples were thawed and CD3 depleted using EasySep Human CD3 Positive Selection Kit II (STEMCELL Technologies) and EasySep Magnet (STEMCELL Technologies). Immune-deficient NOD LtSz-scidIL2Rγnull (NGS) mice were bred in a barrier facility and all experimental protocols were approved by the Animal Research Ethics Board of McMaster University. NGS mice 6-10 weeks of age were sub lethally irradiated at 315 Rads using a ^{137}Cs γ-irradiator 24-hours prior to transplantation. 5-15x10^6 cells were intravenous (IV) injected and BM aspirates were performed to identify human chimerism prior to harvesting. BM was harvested from legs and spines 6-12 weeks post engraftment and cells recovered by mechanical dissociation as previously described [35] and analyzed by flow cytometry.

2.3 Reprogramming of Primary AML Samples

2.3.1 Fluorescent Activated Cell Sorting (FACS)

Samples were thawed using 100% FBS and PBS supplemented with 3% FBS (HyClone FBS, Mississauga, ON, Canada), and 1 mM EDTA (Invitrogen, Waltham, Massachusetts, USA) referred to as PEF. Cells were counted, and a fraction of the cells were set aside to be sorted using Fluorescence Activated Cell Sorting (FACS). Cells to be sorted were stained using the following antibodies at a 1:100 concentration: CD33-APC, CD34-FITC, CD45-v450 (BD Biosciences) and CD3- PE (Beckman Coulter). Cells were stained at 10 million cells per mL, for 45 minutes at 4 °C. Subsequently, cells were then stained with 7-amino actinomycin D (7-AAD, Becton Dickinson) at 1:50 to exclude nonviable cells. Fluorescence Minus One controls and single stains of each antibody on compensation beads were used to ensure that gates were properly set, and sorted populations were pure. Cells were sorted using an Aria II flow cytometer (Beckman Coulter) into separate tubes for several target different populations, depending on what populations existed or had a substantial number of cells. This includes $CD45^+CD34^+CD33^+$, $CD45^+CD34^+CD33^-$, and $CD45^+CD34^-CD33^+$. Collected cells were kept on ice during sorting, then centrifuged at 1500 rpm for 5 minutes, pooled and counted for viability and total cell count.

2.3.2 Reprogramming

All AML or mobilized peripheral blood (MPB) samples were reprogrammed in media consisting of StemSpan SFEM II (STEMCELL Technologies) supplemented with 100 ng/mL stem cell factor (SCF), 100 ng/mL Fms-related tyrosine kinase 3 ligand (FLT3-L), and 20 ng/mL thrombopoietin (TPO), all from R&D Systems, 8μg/mL polybrene (Sigma-Aldrich) and 0.75 μM StemRegenin 1 (SR1) (STEMCELL Technologies), referred to as "reprogramming media". The factors used to reprogram the primary AML cells were delivered using a non-transmissible form of the Sendai virus, from the Cytotune iPS 2.0 Sendai Reprogramming Kit (ThermoFisher Scientific). This kit consists of three viruses: hKOS, hc-Myc and hKlf4. Volume of virus used was variable depending on the lot number of the virus kit and its titer, but the general ratio used for these viruses is 5:5:3 (ThermoFisher Scientific). Any cells to be reprogrammed were counted, aliquoted and centrifuged at 1500 rpm for 5 minutes. Cells were resuspended in reprogramming media with the appropriate volume of each virus added and plated at 200,000 cells per 24-well in 250 uL per well, in an ultra-low attachment plate (Corning). For each sample and population, at least two separate wells were reprogrammed as a technical replicate, or more if the number of cells and reprogramming resources

allowed. Cells were transduced and incubated at 37 °C for 48 hours, after which the cells in each 24-well were collected into individual Eppendorf tubes and centrifuged in BSL2+ containers for 5 minutes at 1500 rpm. Cells were plated into Leukemia Inhibitory Factor (LIF), and 2 small molecule inhibitors (2i) of MEK and GSK (LIF2i media), which is SR media consisting of DMEM/F12 (1:1) (Gibco), 20% KOSR (Gibco), 1x NEAA (Gibco), 1 mM L-glutamine (Gibco), 0.1 mM β-mercaptoethanol, supplemented with 1 μM MEK inhibitor PD0325901 (Stemgent), 3μM GSK3 inhibitor CHIR 99021 (Sigma-Aldrich) and 10 ng/mL leukemia inhibitor factor (LIF) (Millipore). Each 24-well of cells was counted and plated into one tissue-culture treated 6-well, referred to as the mother plate. 6-wells were coated with 0.5% gelatin (Millipore Sigma) and seeded with 180,000 irradiated mouse embryo fibroblast (iMEF) cells 24 hours prior to seeding the transduced AML cells. iMEFs were seeded in MEF media, which consists of KO-DMEM (Gibco), 10% FBS. 1% NEAA, 1% Sodium pyruvate, 2 mM L-Glutamine, and 0.1 mM β-mercaptoethanol. Reprogrammed cells were carefully fed every other day with LIF2i media, beginning on day two or three from plating them into the 6-wells, until colonies arose to be selected and expanded as individual clones (2-3.5 weeks post transduction).

2.3.3 Clone Expansion

Each clone derived from individual colonies was expanded separately, after two to three and a half weeks post transduction. Once enough colonies arose in the mother plate, colonies were stained using a live cell imaging kit (TRA-1-60 Alexa Fluor488 Conjugate Kit for Live Cell Imaging (Invitrogen), according to manufacturer's instructions. From the mother plates, colonies were picked individually with a p200 filtered tip, and plated into a 12-well tissue culture treated plate, referred to as passage zero (p0). Each 12-well was coated with 0.5% gelatin before being seeded with 100,000 iMEFs 24 hours prior to picking clones. iMEFs were seeded in MEF media previously described. 24 hours after individual colonies were plated into 12-wells, the media was carefully aspirated, and fed with 1.5 mL of LIF2i media. Cells were then fed each day with LIF2i media, and manually passed every 5-7 days to a new plate, increasing the number of wells or size of the well as needed to expand the clones. Between the second (p2) and third (p3) passage of the clones, they were transitioned to SR Media supplemented with 8 ng/mL basic fibroblast growth factor (bFGF) (VWR). 24 hrs after passing, the cells were transitioned by feeding with two thirds LIF2i media and one third SR media + bFGF, then two thirds SR media + bFGF 48hrs from the initial pass date. SR media + bFGF was used to feed the cells on day three from the initial pass date of p2 or p3 and onwards. Cells reprogrammed using exclusively bFGF did not require this transition and were solely cultured in SR media + BFGF from the initial p0. Cells were cryopreserved in 1 mL of freeze media, consisting of DMEM/F12 (1:1) (Gibco), 30% KOSR (Gibco), and 10% DMSO (Sigma Aldrich).

2.4 Aberration Detection of iPSC lines/clones

2.4.1 Droplet PCR

DNA was isolated from each iPSC clone by passing a subset of colonies from the clone to a tissue-culture treated plate coated with 1:15 Matrigel (Corning). The colonies were expanded for 2-3 days before DNA isolation and were fed every day with SR media + bFGF. Upon collection, the colonies were treated with Collagenase IV (Thermo Fisher Scientific) for 10 minutes at 37 °C then cell dissociation buffer (Gibco) for 10 minutes at 37 °C. Colonies were then washed from the plate and spun down for 5 minutes at 1500 rpm. Cells were resuspended in PEF (3% FBS), filtered, and counted. Cells were then centrifuged for 5 minutes at 1500 rpm and resuspended in 200 uL of cold

PBS. DNA was isolated using DNeasy Blood & Tissue Kit according to the manufacturer's protocol (Qiagen). DNA was eluted in ultra-pure water and stored at -80°C. DNA samples were aliquoted at 50 ng/uL in 10 uL and diluted in ultra-pure water to be shipped to The Centre for Applied Genomics (TCAG) Genetic Analysis Facility (Toronto) for droplet digital PCR (ddPCR). For each probe used, a mobilized peripheral blood sample was sent as a negative control, and the original primary AML sample associated with the iPSC clones was sent as a positive control. Primers were designed using RefSeq transcripts and https://mutalyzer.nl/positionconverter.

2.4.2 Karyotyping

Cells were cultured and expanded until four 80% confluent 6-wells of a clone were obtained. At that point, these cells were passed into two T25 Tissue-culture flasks, which were pre-gelatinized for 30 minutes at 37°C and seeded with 350,000 iMEFs each, 24 hours prior to passing the iPSCs. One day after passing, cells were washed and fed with SR media + bFGF. The following day, the flasks were filled with SR media + bFGF, sealed, and shipped to the karyotyping facility via priority shipping overnight. Once received, the cells were harvested and screened for abnormalities, and sent for a full karyotyping if abnormalities were present. Karyotyping of all samples was completed by TCAG Cytogenomics Facility (Toronto) following standard protocols.

2.4.3 Cytogenomics

Comparative genomic hybridization using Cytoscan HD Array (Thermo Fisher) was performed by TCAG, at The Hospital for Sick Children (SickKids), Toronto, Ontario, Canada. Cytoscan analysis was performed using Chromosome Analysis Suite (NetAffx 33.1, h19) using default settings.

2.4.4 Fluorescent in Situ Hybridization (FISH)

Primary AML cells and iPSCs were synchronized by adding 0.1 μg/mL KaryoMAX Colcemid (ThermoFisher) to cell media for 3-4 hours. Cells were collected as single cell suspension. iPSCs were dissociated using cell dissociation buffer (Gibco) for 5-10 minutes at 37°C. Cells were incubated in a hypotonic solution of 0.075 M KCl for 15 minutes at 37°C. Cell were then fixed using 3:1 methanol: glacial acetic acid and pipetted onto a glass slide. Slides were dehydrated using a sequence of 70,80, and 100% EtOH and pre-warmed at 37°C. Probe was also pre-warmed to 37°C. Sample and probe were simultaneously denatured on a hotplate at 75°C for 2 minutes and then placed at 37°C overnight. Slides were then washed, stained with DAPI, visualized, and scored manually. MYH11/CBFB probe (Empire Genomics), and PML/RARα translocation dual fusion probe (Cytocell) were used and scored as recommended by the manufacturer.

2.4 Flow Cytometry

All antibodies used for flow cytometry were titrated to generate signal-based populations consistent with those demonstrated by the antibody manufacturer. All extracellular staining was performed in PEF, where 10 million cells per mL were stained for 45 minutes at 4 °C, washed with 10 volumes of PEF and then stained with 7-amino actinomycin D (7-AAD, Becton Dickinson) at 1:50 to exclude nonviable cells. The following antibodies were used at 1:100 unless otherwise specified as follows: CD45-v450, SSEA3-PE, TRA-1-60-AF647 at 1:1000, CD34-FITC or APC (1:200), mCD45-FITC, CD33-PE or APC, CD3-PE (Beckman Coulter), all from BD Biosciences unless otherwise specified. For pluripotent stem cells, cells were treated with Collagenase IV for 10 min, followed by 10 min treatment with Cell dissociation buffer (Thermo Fisher Scientific) and then filtered through a 40 μm cell strainer. For intracellular staining, cells were fixed using

Cytofix/Cytoperm (BD Biosciences) and Perm/Wash buffer (BD Biosciences) according to the manufacturer's instructions. Prior to performing fixation and permeabilization, cells were stained with Live/Dead Violet discrimination dye at 1:7000 (Life Technologies) for 30 minutes at 4°C in the dark. Intracellular staining was performed in Perm/Wash buffer overnight at 4° in the dark and washed with 10 volumes of PBS prior to analysis. The following antibodies were used at 1:000 for intracellular staining: Alexa Fluor 488 Mouse anti-OCT4 and Alexa Fluor 488 Mouse anti-NANOG. Cells were analyzed with an LSRII Flow Cytometer (BD Biosciences) and resulting data analyzed using FlowJo software version 10.8.0 (FlowJo, LLC). https://fccf.sitehost.iu.edu/pdf/LSRIIBrochure.pdf

2.5 Teratoma Assay

To assess the developmental potential of AML-iPSCs, cells were collected by collagenase IV treatment and injected as clumps into NOD/SCID mice via intratesticular injection (IT). At eight to ten weeks, teratomas were harvested, dissected, and fixed with 4% paraformaldehyde. Samples were embedded in paraffin and processed for H&E staining. Images were acquired using Aperio ScanScope CS digital slide scanner (Leica).

2.6 Statistical analysis

Data are represented as means ± SEM. Prism (6.0c, GraphPad) software was used for all statistical analyses, and the criterion for statistical significance was $P<0.05$. Statistics are described in each figure legend when applicable.

3. Results

3.1 AML Patient Selection Strategy

To date, although primary AML reprogramming has been implicated in multiple studies [22–24,26,36,37] it is apparent that deriving AML-iPSCs is challenging. Interestingly, AML-iPSCs have been shown to reacquire leukemic properties, including AML reconstitution in xenograft models, as well as methylation and gene expression patterns providing indication that AML-iPSC can be used to successfully mimic the disease without the need for continuous use of primary patient samples [24,36]. The study by Kotini and colleagues used AML-iPSCs to model myelodysplastic syndrome (MDS) to AML transition [23], however, a limitation of this work was that the progression of disease stages iPSCs were derived from different patients. Moreover, within the aforementioned study, only 4 patient AML cases have been reprogrammed to iPSCs, 3 of which harbor MLL gene family network alternations which represent only 2% of adult AML patients7 thus failing to capture AML patients' heterogeneity. To overcome this, we sought to develop a library of AML-iPSCs using a large number of heterogeneous AML patient samples with a range of different mutational categories (Table 1). For sample selection, samples were examined to see if they contained known, detectable genetic and/or molecular abnormalities, and if Next Generation Sequencing (NGS) data existed. The presence of various phenotypic markers based on preliminary flow cytometry data obtained from the clinic in which the sample was collected was also considered to ensure that selected samples would be viable for reprogramming. This was to confirm that the populations of interest would yield an adequate number of cells based on the estimated percentage of the cells that contained that population (Table 1; CD34%). Similar to healthy hematopoietic cells, in AML, CD34 marks a more primitive cell compartment [38]. These cells play a role in disease progression and relapse, hold a higher reprogramming potential, and

are relevant in healthy hematopoiesis [39] and thus were prioritized for reprogramming. Additionally, if a sample had two clear populations such as CD34+CD33+ and CD34-CD33+ (discussed later, see Figure 2), this would be an opportunity to reprogram multiple populations from a sample and determine how these markers influence reprogramming, creating more interest for the sample. Samples were also prioritized if specimens were taken at different stages of a patient's disease (such as diagnosis, and relapse) (Table 1; Patient's 16308 & A472). Lastly, samples were selected based on availability and cell quantity. Overall, 22 unique AML samples from 20 distinct patients were selected for reprogramming. By selecting a variety of patient samples with a broad range of genetic aberrations (Table 1), interpretations would not be limited and would strengthen the ability to be applied to AML disease wide conclusions.

3.2 Reprogramming to naïve vs. primed states

Patient samples selected for reprogramming were subsequently categorized based on the percent distribution of cytogenetically and molecularly defined subsets of AML described by Medinger & Passweg [40,41]. Eight out of the fourteen samples yielded classification (Figure 1A) demonstrating representative breadth of molecular heterogeneity of AML disease from the proposed AML-iPSC library of which samples were detectable using ddPCR, Karyotyping, Cytoscan HD Array and FISH (Figure 1A). ddPCR uses digital PCR by separating DNA molecules into individual droplets based on water-oil emulsion droplet technology and amplifies the DNA within each droplet, and analyzed based on Variant Allele Frequency (VAF) representing the number of droplets positive for the mutation compared to control [42], whereas clinical cytogeneticists allowed analysis of human karyotypes involving several megabases of DNA and Karyotyping revealing chromosome number associated with aneuploid conditions, or chromosomal deletions, duplications, translocations, or inversions.

We first subjected AML patient cells to two distinct methods of reprogramming referred to as naïve or primed reprogramming, LIF2i or SR + bFGF respectively (Figure 1B). Uniquely, iPSCs are like embryonic stem cells in terms of their ability to exist in two different states, referred to as the naïve and primed states. Naïve cells are derived from the preimplantation blastocyst inner cell mass, whereas primed cells are derived from post-implantation epiblast cells [43]. They differ in terms of their cell morphology, gene expression, growth factor dependency and presence of X chromosome activity in female cells. Although iPSCs derived from somatic cells maintain epigenetic signatures from their origin cell [44], iPSCs derived into naïve conditions erase this epigenetic memory of their origin cell type, as seen by a reactivation of the X chromosome [43]. Cells in the naïve state can re-establish epigenetic memory by switching to the primed state, and epigenetic memory of iPSCs in the primed state impacts their differentiation by favoring differentiation into the cell type of their origin [44,45]. We have previously shown the refractoriness of reprogramming primary AML samples. Specifically, we demonstrated that a single AML patient sample (AML 15331) was able to reprogram and yield iPSCs with a leukemic aberration matching the primary patient sample only when reprogramming was carried out in naïve conditioned media (LIF2i) [22].

To compare the reprogramming efficiency between naïve reprogramming (LIF2i) and primed (bFGF), we hypothesized that reprogramming in SR+bFGF media would enhance our overall reprogramming efficiency as well as our efficiency at deriving isogenic healthy iPSC clones devoid of leukemic aberrations. Reprogrammed cells were fed every other day with LIF2i media, beginning on day two or three from plating them into 6-wells, until colonies arose to be selected and expanded as individual clones (2-3 week's post transduction) (Figure 1B; see method

section for additional details). Once colonies arose, cultures were stained using a live cell imaging for detection of the PSC marker TRA-1-60 denoting colonies as truly pluripotent (Figure 1C). Colonies were then plucked and expanded for approximately two weeks. For naïve reprogramming, iPSC colonies were subsequently transitioned to SR media supplemented with bFGF (SR +bFGF) following the two weeks. Samples undergoing primed reprogramming did not undergo this transition and were always maintained in SR+bFGF medium (Figure 1B). A two-tailed unpaired t-test was used to compare the two distinct methods of reprogramming and no significant difference was observed amongst the six AML samples tested (Figure 2D). Reprogramming efficiency is calculated as the number of colonies that arose divided by the number of cells reprogrammed (i.e 200,000 cells), per well. Thus, reprogramming efficiency is determined as a frequency on a patient specific manner. Reprogramming efficiency ranged from ~0 to 5.9 (% x10-2), compared to a previously reported efficiency of 10% (% x10-2) for healthy blood cells using Sendai Virus [46]. This highlights the extreme rarity of reprogramming, and a frequency has not been reported in this manner for iPSC from non-cancerous cells, as the rate is so low. However, when samples were collapsed on either methodology used, then stratified based on reprogramming a CD34+ population versus a CD34- population, a significantly greater reprogramming efficiency was achieved by reprogramming the CD34+ population (Figure 1E) similar to previous observations [47]. Despite yielding no significant difference among LIF2i reprogramming and bFGF statistically speaking, a higher number of reprogrammed iPSCs were observed amongst the AML patient samples via LIF2i reprogramming (Figure 1D). Given our previous report only yielded one bona fide AML-iPSC clone using LIF2i22, and others showed low iPSCs skewed often in favor of residual normal cells over cells of the premalignant or malignant clone, we used LIF2i for future reprogramming in this study to ideally achieve a higher yield of AML-iPSC aberration positive AML-iPSC lines.

3.3 Reprogramming Strategy & Pluripotency Validation

Despite the 'barriers' that exist with successful reprogramming including the mixture of co-isolating normal and clonal leukemic cells in the BM and PB of AML patients, their clonal heterogeneity holds the potential to be positively leveraged to derive both disease and normal iPSC lines in the same reprogramming process to derive paired isogenic and AML-iPSCs from individual AML patients (termed 'de novo' samples). AML reprogramming to iPSCs has been shown to be a rare event and limited to extremely rare subtypes of AML [22–24]. To improve the frequency of generating AML-iPSC with aberrations of the patient's somatic leukemic cells, we proposed that reprogramming competency in the AML hierarchy may be unique to specific compartments. Using FACS, we isolated AML patient samples into cells expressing cell surface markers for CD34, CD33, and CD45 which are also used to classify patient disease in the clinic [48,49]. Samples were thus sorted for CD45 expression (CD45+) hematopoietic cells, and then divided into four populations based on expression of CD33 and CD34 (Figure 2A).

In addition to purification of de novo samples, a subset of AML de novo samples were transplanted into immunodeficient mice to determine if leukemic cell progeny of cancer stem cells had adopted changes to reprograming capacity due to a human-mouse xenograft environment. Successful engraftment enabled reprogramming FACS-purified populations to enrich for functionally defined stemness in vivo (Figure 2A). Furthermore, we hypothesized that progeny of leukemic initiating cells (LIC) [38] that engraft these recipient mice, would potentially bestow an enhanced reprogramming efficiency of AML-iPSC and would also allow selective enrichment of leukemic vs. normal hematopoietic cells as LIC dominantly reconstitute in mice. In addition, some

reports have also speculated that AML cells do not reprogram due to the lack of cell division [34], whereas our approach to reprogram active LSCs that engraft mice could allow an increase AML-iPSC generation. We compared reprogramming of AML samples by either de novo reprogramming, xenograft reprogramming, or a combination in which select samples underwent both methods of reprogramming (Figure 2B & 2C). Samples that underwent xenografting were assessed for human engraftment using pan-hematopoietic marker CD45, myeloid marker CD33, B-cell marker CD19 and stem and progenitor cell marker CD34 after eight weeks post injection (Figure 2B). Human chimerism was assessed by human pan-hematopoietic marker, CD45. Myeloid grafts were identified by exclusive expression of CD33 and considered LSC+. Multilineage grafts displayed expression of CD33 and CD19 and were healthy HSCs based engraftment, and devoid of LSCs (LSC-, Figure 2B). To best maximize the rare event of reprogramming known to be enhanced in the CD34+ hematopoietic compartment, we reprogrammed FACS purified primitive (CD45+CD33+CD34+) and more mature myeloid populations (CD45+CD33+CD34-) from each sample [39]. In rare instances, select samples had a CD45+CD33-CD34+ purified and subjected to reprogramming in vitro (Figure 2C). Since healthy hematopoietic cells are known to have reduced reprogramming potential with increased differentiation, CD34 was used to separate cells into more primitive (CD34+) and terminally differentiated (CD34-) cell fractions [47]. To further promote CD34+ cell culture, in vitro reprogramming was attempted together with supplementation of StemRegenin 1 (SR1). SR1 is a small molecule which is well established to promote in vitro expansion of CD34+ cells50 and carried out in naïve conditions media [22], which has been shown to have better success at generating AML-iPSCs (Figure 1). A total of 5 AML samples underwent both de novo and xenograft reprogramming (Figure 2B), and an additional seventeen samples underwent de novo reprogramming (Figure 2C). All iPSC colonies that arose had indistinguishable morphology and expanded similarly when picked and subsequently passaged every six days in comparison to a healthy MPB-iPSC control (Figure 2D). Once cultured for approximately three to four weeks post derivation, iPSC clones were dissociated on day 6 post passage and tested for their expression of external pluripotency markers TRA-1-60 and SSEA3, and internal pluripotency markers OCT3/4, and NANOG. No difference was observed amongst pluripotency markers from AML derived iPSCs and healthy hiPSC controls (Figure 2E). When functionally interrogated for pluripotency using the teratoma assay [51] both methods of deriving iPSCs from AML, de novo reprogramming or xenografting, demonstrated that AML derived iPSCs can give rise to all three germ lineages – endoderm, mesoderm and ectoderm in vivo (Figure 2F).

Overall, despite the historically refractoriness to reprogram, fifteen out of twenty-two samples were successfully reprogrammed the highest number reported to date, yielding a total of 129 AML patient-derived iPSC lines (Supplemental Table 1).

3.4 Classification of Derived iPSCs

To determine if leukemic or isogenic clones were derived, the mutation status of each clone was tested for the presence of established AML patient mutations (DNA aberration) and subsequently classified as either aberration negative or aberration positive (Figure 3A). Of the 129 number iPSC generated, see supplemental table 1, all isolated iPSCs colonies were treated as independent clones, expanded, and cryopreserved at multiple early passages into iPSC lines (Figure 1B). Independent of method, of the 22 patient samples reprogrammed, 7 patient samples (AML 8-10, 12, 18-20) were unsuccessful in generating any iPSCs and were thus not assessed (Figure 3B & Table 2). All clones derived were assessed by methodologies previously reported

and representative results of each methodology are shown in Figure 3. Individual clonal information is described below in detail and provided in supplemental figures. Classification of each clone derived via aberration detection was imperative to determine if reprogramming efficiency had been altered using our distinct novel methods. Moreover, classification would allow for clonal and sub clonal representation to be captured.

Twelve clones derived from AML patient sample A374.1 (AML 1) were tested by G-band karyotyping and determined to all have inv(3) and del(7), along with other mutations detected in the primary sample (Figure 3B & Supplemental Figure 1A). Some clones had identical karyotyping patterns and thus likely originated from the same leukemic clone, for example clones AML1-2 and AML1-4 (Supplemental Figure 1A). Thus, seven unique clones were captured from AML-1. Four clones were derived from AML patient sample A422 (AML 2) and tested using HD CytoScan Array and determined to capture del(7) coinciding to the primary AML sample in all clones (Figure 3C). Of the four clones derived via de novo reprogramming from AML patient sample 13814.1 (AML-3) G-band karyotyping was used for assessment. Of these clones, two clones were found to have unique leukemic aberrations, and two clones were found to have a normal karyotype (Supplemental Figure 1B). Four additional clones via xenograft reprogramming were derived from AML-3. However, karyotypic analysis revealed that these were all aberration negative and therefore presumed to be healthy isogenic clones (AML 1-5 to AML 1-12). Another AML patient sample assessed by karyotype 15328 (AML 6), was also found to be devoid of any leukemic aberrations in comparison to the primary sample (Figure 3B & Supplemental Figure 1C). Lastly, AML A485 (AML 14) was also characterized using G band karyotyping (Supplemental Figure 1D). The expected karyotype included common AML-associated mutations, such as del(7), which are typically associated with a poorer prognosis52. However, the resultant karyotype was abnormal for two out of 6 clones derived, but these clones all had a translocation between chromosomes 3 and 12, with breaks in 3q26 and 12p13 (Supplemental Figure 1D). This mutation was not detected in the primary patient sample. The remaining clones derived from AML 14 all had normal karyotypes (Supplemental Figure 1D) and thus could not be defined as AML in origin.

FISH was used to test AML patient sample 16150 (AML 4), A151.1 (AML 5) and A320 (AML 11) (Figure 3F & Supplemental Figure 2A & 2B). Ten clones derived from AML 4 and three clones derived from AML 5 did not contain inv(16) tested using the CBFβ-MYH11 fusion probe (Figure 3F & Supplemental Figure 2A). Nine clones derived from AML 11 did not contain PML-RARα gene fusion found in the primary patient sample (Supplemental Figure 2B).

AML patient samples A295.1 (AML 7),16534 (AML 15), A494 (AML 16), 16308F (AML 22), A472-3 (AML 17) and A472-1 (AML 21) were probed for mutations using ddPCR. As previously mentioned, ddPCR is a method for performing digital PCR by separating DNA molecules into individual droplets based on water-oil emulsion droplet technology and amplifies the DNA through PCR within each droplet. The data is analyzed based on Variant Allele Frequency (VAF), which shows the number of droplets that were positive for the mutation being probed for in each sample or control [42]. Only a single clone was derived from A295.1 (AML 7) and, when tested using ddPCR for the presence of an isodecentric chromosome 21, it was found to be normal (Figure 3E). AML 16 (A494) contained the point mutation IDH2:c.515G>A, a mutation in the isocitrate dehydrogenase gene involved in intermediary metabolism (IDH2 isocitrate dehydrogenase (NADP(+)) 2 [Homo sapiens (human)] - Gene - NCBI). All eight clones derived and tested contained this mutation, as seen by the fractional abundance of the clones being similar to that of the primary AML sample (Figure 3F). Of the three clones tested of 16534 (AML 15), none of them contained the NPM1c.863_864 ins_TCTG mutation present in the primary AML

sample, which is a mutation in the gene encoding nucleophosmin, which is involved in centrosome duplication, cell proliferation and protein chaperoning (NPM1 nucleophosmin 1 [Homo sapiens (human)] - Gene - NCBI) (Supplemental Figure 3A). A472-3 (AML 17) was reprogrammed twice, and was probed for two different mutations: ASXL1:c2725 A>T and IKZF1:c.476A>G. ASXL1 is a transcriptional regulator involved in chromatin remodeling (ASXL1 gene – Genetics Home Reference - NIH) while IKZF1 encodes a zinc-finger transcription factor also associated with chromatin remodeling (IKZF1 gene - Genetics Home Reference - NIH) (Supplemental Figure 3B & 3C). Of the ten clones tested in the first round of reprogramming this sample, all clones contained the ASXL1 mutation where, one of ten clones contained just the ASXL1 mutation which may allow to capture disease progression (Supplemental Figure 1B; Clone 1.4 absent for IKZF1). This patient (AML 17), also contains a RUNX1 mutation (Table 1; RUNX1:c.656_657insAAGG). RUNX1 is a transcription factor which commonly forms a complex with the cofactor, core binding factor beta (CBFβ), to activate genes that regulate the differentiation of hematopoietic stem cells into myeloid and lymphoid lines (RUNX1 gene - Genetics Home Reference - NIH). Unfortunately, we were unable to validate a successful probe that was able to detect this mutation in the primary patient sample, therefore any clones that were derived were not probed for the RUNX1 mutation. The second time AML 17 was reprogrammed, two different reprogramming methods were done LIF2i vs bFGF respectively (Supplemental Figure 3C). Of the 11 clones derived using primed reprogramming (SR+bFGF), all clones contained the ASXL1 mutation as well as the IKZF1 mutation. Note clones are denoted with the letter F in front to distinguish clones derived using primed reprogramming vs naïve reprogramming denoted by the letter L. Of the 6 clones derived using our standard reprogramming media LIF2i, all clones contained both mutations as well (Supplemental Figure 3C). AML 21 (A472-1), is the diagnosis AML patient sample of A472-3, and harbors the same three mutations as previously described for A472-3, ASXL1:c2725 A>T and IKZF1:c.476A>G and RUNX1:c.656_657insAAGG. Of the ten clones derived using SR media + bFGF to reprogram this sample, three did not contain both mutation (Supplemental Figure 3D; Clone F1.1,F1.7, F1.10 absent for IKZF1). Of the eight clones derived using LIF2i reprogramming media, four clones did not contain both mutations (Supplemental Figure 3D; Clone L1.4, L1.6, L1.11, L1.1 and L1.3 absent for IKZF1). Lastly, one clone was derived from AML 22 (16308F) and it did not contain the point mutation NPM1 c.863_864 ins_TCTG present in the primary AML sample (Supplemental Figure 3E).

Overall, though not all 22 samples donated from AML patients reprogrammed yielded iPSCs, the detection of AML-associated mutations in iPSCs may uniquely represent the heterogeneity of AML and capture the progression of the disease in various lines derived. In terms of detecting aberrations, it is imperative to attempt to probe for as many mutations in a patient sample as possible to better understand the heterogeneity of the disease. Based on these results we successfully generated both aberration positive (AML-iPSC), aberration negative, and paired AML-iPSCs and Isogenic iPSCs for the first time.

3.5 Reprogramming Efficiency correlates to AML Hierarchy

In establishing a novel method of reprogramming via partitioning AML samples based on immuno-phenotyping and FACS we sought to determine if de novo reprogramming versus xenograft reprogramming would yield a greater efficiency in producing AML patient derived iPSCs. Reprograming efficiency is calculated by dividing the number of resulting colonies by the number of input cells [53] which in our cases was 200,000 cells, per well. Five AML samples subjected to both methods of derivation were thus assessed independent of the type of iPSCs

generated, i.e aberration positive (AML-iPSCs) or aberration negative. Of the five samples, only one sample AML 9, was unsuccessful in generating AML patient derived iPSCs (Figure 4A). Intriguingly, the reprogramming efficiency via de novo reprogramming was on average higher in comparison to the same sample that underwent xenograft reprogramming, though not statically significant (Figure 4B). Since there was no significant difference amongst methods of reprogramming, we separated the five individual samples and assessed their individual reprogramming efficiency based on the specific immuno-phenotype population that was subjected to reprogramming. This included the following populations for AML 13814.1 (AML 3) and 16150 (AML 4): CD45+CD34+CD33+, CD45+CD34-CD33+, CD45+CD34+CD33- and CD45+CD34-CD33-. Whereas A374.1 (AML 1) had three populations reprogrammed, CD45+CD34+CD33+, CD45+CD34-CD33+ and CD45+CD34-CD33, and AML A422 (AML 2) only had two populations reprogrammed, CD45+CD34+CD33+and CD45+CD34-CD33+ (Figure 4C). Across all three samples in which a CD45+CD34-CD33- population was reprogrammed, no colonies were derived (Figure 4C). AML 13814 (AML 3) and 16150 (AML 4) both displayed significantly higher reprogramming efficiency in the more primitive population (CD45+CD33-CD34+) in comparison to any other phenotypic population reprogrammed. In contrast, both AML A374.1 (AML 1) and AML A422 (AML 2) had significantly higher reprogramming efficiency in the more mature double positive population (CD45+CD33+CD34+) in comparison to any other phenotypic population successfully reprogrammed (Figure 4C). Interestingly, AML 1 and AML 4 were samples that gave rise to both aberration positive and negative iPSC lines, whereas AML 1 and AML 2 solely gave rise to aberration positive lines (Figure 5A). We next sought to assess the reprogramming efficiency of the samples that solely underwent de novo reprogramming of which the seventeen samples reprogrammed, seven did not produce any iPSC colonies (Figure 4D). Of the seventeen samples, one sample AML A320 (AML 11) was excluded from the analysis since its reprogramming efficiency was extremely high (0.078%; Supplemental Figure 4A) and would thus skew the data since its reprogramming efficiency was even superior to healthy MPB which demonstrated an average of 0.00825% (Supplemental Figure 4B). Using these samples, we sought to discern the relationship between leukemic reprogramming and CD34, thus the efficiency was again stratified on either CD34+CD33+ or CD34+CD33- populations. Though no significant difference was observed, there was on average a higher reprogramming efficiency in the double positive population presumed to contain an increase probability of capturing a leukemic stem or progenitor cell for reprogramming (Figure 4E). Overall, the efficiency of reprogramming of the AML patient samples in this study had a wide and unpredictable range from 0% to 0.078% (Supplemental Figure 4C). Notably, reprogramming blood cells using sendai virus has been reported to have an efficiency of 0.1% [46] and more recently, generation of iPSCs from a variety of human primary fibroblast lines using an RNA-based approach has shown an even higher efficiency of approximately 7% (3132 colonies per well, per 500 input cells per well)[53].

Based on our results obtained and goal of characterizing AML-iPSC based on the presence or absence of driver mutations, we stratified AML patients into four categories (Table 2). Based on this stratification, we next determined whether samples that gave rise to aberration negative iPSC lines solely (Category 1), aberration positive iPSC lines solely (Category 2), or a mixture of both types of lines (Category 3) would yield distinct reprogramming efficiencies (Figure 4F & 4G). Interestingly, samples in which aberration negative colonies were only derived (Category 1) had significantly higher reprogramming efficiency in the CD34+CD33- population. In contrast, samples in which aberration positive colonies were only derived (Category 2) yielded significantly higher reprogramming efficiency in the CD34+CD33+ population (Figure 4F). In rare instances

in which a sample gave rise to both aberration positive containing clones and aberration negative containing clones (Category 3; Paired Isogenic & AML-iPSC clones), the CD34+CD33- subpopulation demonstrated a significantly higher reprogramming efficiency (Figure 4G). This suggests that AML clones reside in a variety of immunophenotypic compartments. However, there is a greater probability of obtaining AML-iPSCs (aberration positive) clones when reprogramming the double positive CD34+CD33+ population. Thus, in future studies, it may be advantageous to use the myeloid marker CD33 in combination with the hallmark stem cell marker (CD34) in deriving AML-iPSCs or disadvantageous if the goal is to produce aberration negative lines (devoid of the primary patient mutation) from an AML patient.

3.6 Stratification of derived iPSC lines

In previous reports from our group and others, AML patient cells have been notoriously difficult to reprogram compared to healthy counterparts. AML either does not produce any reprogrammed colonies or it produces colonies that do not contain leukemic aberrations and thus likely arise from healthy progenitors within the patient sample. Despite these barriers, we successfully reprogrammed fifteen of twenty-two AML samples, of which seven AML samples were found to contain aberrations related to the primary patient sample and thus yielded bona fide AML-iPSC lines (Figure 5A). Having successfully achieved AML-iPSCs from seven diverse AML samples gives us the unique opportunity to use this library for further investigations, and proves the hypothesis that reprogramming primary AML samples to iPSCs is possible, but achieving AML-iPSCs is a rare event, as seen by the frequency (23%) of only 6 out of 22 samples yielding aberration positive clones, 2 of which yielded a combination of both (9%) versus (32%) failing to reprogram or solely generating aberration negative iPSC lines (36%) (Figure 5B). Excitingly, this library of reprogrammed AML patient samples can model 8 different categories of AML-associated mutations (Figure 5C). Previously, the collective efforts from other groups who have published results related to AML-iPSCs excluding our previous work, have only represented two categories: TP53 mutations and MLL fusion genes, using a total of 5 patient samples across 4 publications [23,24,26,36] whereby the same lines have been studied across publications. Intriguingly, samples either gave rise to aberration negative iPSCs (presumed to be isogenic healthy) or aberration positive (AML-iPSCs) solely, except for AML 3 and AML 14 in which both iPSCs were derived (Figure 5C), allowing for the library to be stratified into four distinct categories providing unique opportunities for future studies using a broad and representative library of AML-iPSCs.

4. Discussion

Our study has tested sendai and lentiviral delivery of reprogramming factors, naïve vs. primed conditions, de novo vs. xenograft conditions, and prospective cell purification and fractionation using 20 independent AML patients. Despite the technical challenges of reprogramming human cancer cells, our group has established an unprecedented library of 129 AML patient-derived iPSC of which 77 are leukemia-specific genetically aberrant AML-iPSCs. We also derived aberration-negative iPSCs from a subset of these same AML patients, providing an invaluable isogenic control for future direct molecular comparisons. This library aims to capture both intra- and inter-patient heterogeneity and provides a novel model system for the study of AML biology.

Using a combination of immunophenotyping and FACS, we successfully reprogrammed fifteen AML patients' samples harboring a wide variety of genetic aberrations using non-integrating plasmids from a diverse genetic background. Utilizing our novel approach of phenotyping CD34(+)CD45(+)CD33(+/-) cells prior to reprogramming de novo and xenografted AML patients cells, successful derivation of multiple sub clones and healthy iPSCs lines were derived, the largest library to date. By generating both iPSCs devoid of leukemic mutations (aberration negative), containing leukemic mutations (aberration positive), or paired isogenic and AML-iPSC lines, we were able to stratify our library into three categories that will enable us to evaluate hematopoietic differentiation and intracellular signaling differences between different cytogenic AMLs patient-derived iPSCs in future studies. Moreover, our iPSC lines within Category 1 (devoid of leukemic mutations) may serve as high importance since these lines are excellent candidates for future CRISPR-Cas9 gene editing experimentation. Recently, iPSCs have been utilized to investigate leukemogenesis and to identify compounds targeting AML [24,26,36,54–56]. Previous studies using CRISPR-Cas9 gene editing have demonstrated the possibility to introduce distinct mutations in iPSCs and study stepwise, stage-specific leukemia progression [57]. By using this approach, leukaemia models can be created to compare various mutations (such as missense versus nonsense mutations) in endogenously produced proteins (e.g., RUNX1) [58]. Interestingly, within this category, we observed almost completely successful reprogramming in the CD34+/CD33- population. Thus, future studies interested in deriving AML patient-specific iPSC devoid of clinically defined leukemic mutations would benefit from incorporating such methodologies.

Consistent with previous results, our data indicate that clonal representation of the original cells in the iPSCs is often in favor of normal cells instead of the malignant clones. Moreover, it is reprogramming, and not the in vitro stimulation, that accounts for this bias, which appears to be conferred by AML-associated genetic lesions, but not others, while some genetic abnormalities seem to be incompatible with reprogramming. In contrast, elevated reprogramming efficiency was observed in Category 2 iPSCs in the CD34+/CD33+ population suggesting a greater probability of reprogramming a leukemic stem and/or progenitor cell harboring a leukemic mutation. Thus if bona fide AML-iPSC lines are of a priority to derive, future studies would benefit by utilizing our immunophenotyping approach as a means of overcoming the refractory nature of reprogramming AML patient cells. This refractoriness to reprogramming is paradoxical, and the refractory nature of leukemic cells remains unclear.

The AML-iPSCs model has the potential to study broad disease concepts while eliminating the need to use quantity-limited patient samples, for which the ideal ex vivo culture conditions have recently improved but have not been completely elucidated [50]. Additionally, the ability of AML-iPSCs to break down the disease into clones can provide an avenue to pursue targets of differentiation therapy, the discovery of which has proven to progress to previously unheard-of cure and remission rates of 80 and 90% respectively for acute promyelocytic leukemia (APL) patients [59]. Our group invested in a new campaign to develop techniques to reprogram primary AML leukemic blasts into induced pluripotent stem cells (iPSCs) to serve as a future library for investigating leukemogenesis, whereby implementation of this cellular models may lead to the characterization of rare clonal contributions of genetic and epigenetic abnormalities and lead to a better understanding of AML patient etiology.

ACKNOWLEDGEMENTS : We want to thank Ronan Foley, Brian Leber and Anargyros Xenocostas for providing primary human MPB and AML samples. We would also like to thank

B.T., for their assistance with initial lentiviral transduction; J.R for in vivo experimental assistance and A.L.B for valuable discussions and input. We would also like to acknowledge D.G, M.D and J.C.R in editing and reviewing the manuscript. Finally, we thank the Centre for Applied Genomics at the Hospital for Sick Children for performing all karyotypic screening, droplet digital PCR and Affymetrix HD CytoScan microarray analyzed using ChAS software.

FUNDING : D.P.P. was supported by the Jans Graduate Scholarship in Stem Cell Research, the Michael G. DeGroote Doctoral Scholarship, and the Ontario Graduate Scholarship. D.G. was supported by the Jans Graduate Scholarship in Stem Cell Research. J.C.R. was supported by the Canadian Institutes of Health Research (CIHR) Doctoral Award, the Michael G. DeGroote Doctoral Scholarship, and an Ontario Graduate Fellowship. This work was supported by CIHR foundation grant FRN 159925 to MB approved by the Stem Cell Oversight Committee in Canada. MB holds the Canada Research Chair Program CRC Tier 1 in Human Stem Cell Biology and the Michael G. DeGroote Chair in Stem Cell Biology.

AUTHOR CONTRIBUTIONS : D.P.P, D.G, M.D performed experiments. J.R and A.L.B., aided with the transplant assay design. D.P.P, D.G, M.D and M.B. designed experiments and interpreted data. D.P.P and M.B wrote the manuscript. M.B. directed the study.

INSTITUTIONAL REVIEW BOARD STATEMENT :
This study and all experimental protocols were conducted in accordance with the Animal Research Ethics Board of McMaster University (AUP: 19-11-29).

DISCLOSURE OF POTENTIAL CONFLICTS OF INTEREST : The authors indicate no potential conflicts of interest.

REFERENCES

1. Dagenais GR, Leong DP, Rangarajan S, et al. Variations in common diseases, hospital admissions, and deaths in middle-aged adults in 21 countries from five continents (PURE): a prospective cohort study. Lancet Lond Engl. 2020;395(10226):785-794. doi:10.1016/S0140-6736(19)32007-0
2. Cai SF, Levine RL. Genetic and epigenetic determinants of AML pathogenesis. Semin Hematol. 2019;56(2):84-89. doi:10.1053/j.seminhematol.2018.08.001
3. Cancer Genome Atlas Research Network. Genomic and epigenomic landscapes of adult de novo acute myeloid leukemia. N Engl J Med. 2013;368(22):2059-2074. doi:10.1056/NEJMoa1301689
4. Vardiman JW, Thiele J, Arber DA, et al. The 2008 revision of the World Health Organization (WHO) classification of myeloid neoplasms and acute leukemia: rationale and important changes. Blood. 2009;114(5):937-951. doi:10.1182/blood-2009-03-209262
5. Welch JS, Ley TJ, Link DC, et al. The Origin and Evolution of Mutations in Acute Myeloid Leukemia. Cell. 2012;150(2):264-278. doi:10.1016/j.cell.2012.06.023
6. Mardis ER, Ding L, Dooling DJ, et al. Recurring mutations found by sequencing an acute myeloid leukemia genome. N Engl J Med. 2009;361(11):1058-1066. doi:10.1056/NEJMoa0903840

7. Döhner H, Estey E, Grimwade D, et al. Diagnosis and management of AML in adults: 2017 ELN recommendations from an international expert panel. Blood. 2017;129(4):424-447. doi:10.1182/blood-2016-08-733196
8. Burnett A, Wetzler M, Löwenberg B. Therapeutic advances in acute myeloid leukemia. J Clin Oncol Off J Am Soc Clin Oncol. 2011;29(5):487-494. doi:10.1200/JCO.2010.30.1820
9. Grimwade D, Walker H, Oliver F, et al. The importance of diagnostic cytogenetics on outcome in AML: analysis of 1,612 patients entered into the MRC AML 10 trial. The Medical Research Council Adult and Children's Leukaemia Working Parties. Blood. 1998;92(7):2322-2333.
10. DiNardo CD, Cortes JE. Mutations in AML: prognostic and therapeutic implications. Hematol Am Soc Hematol Educ Program. 2016;2016(1):348-355.
11. Perl AE, Carroll M. Exploiting signal transduction pathways in acute myelogenous leukemia. Curr Treat Options Oncol. 2007;8(4):265-276. doi:10.1007/s11864-007-0043-z
12. Boyd AL, Campbell CJV, Hopkins CI, et al. Niche displacement of human leukemic stem cells uniquely allows their competitive replacement with healthy HSPCs. J Exp Med. 2014;211(10):1925-1935. doi:10.1084/jem.20140131
13. Leary AG, Strauss LC, Civin CI, Ogawa M. Disparate differentiation in hemopoietic colonies derived from human paired progenitors. Blood. 1985;66(2):327-332.
14. Mayani H, Dragowska W, Lansdorp PM. Lineage commitment in human hemopoiesis involves asymmetric cell division of multipotent progenitors and does not appear to be influenced by cytokines. J Cell Physiol. 1993;157(3):579-586. doi:10.1002/jcp.1041570318
15. Bryder D, Rossi DJ, Weissman IL. Hematopoietic stem cells: the paradigmatic tissue-specific stem cell. Am J Pathol. 2006;169(2):338-346. doi:10.2353/ajpath.2006.060312
16. Liu G, David BT, Trawczynski M, Fessler RG. Advances in Pluripotent Stem Cells: History, Mechanisms, Technologies, and Applications. Stem Cell Rev Rep. 2020;16(1):3-32. doi:10.1007/s12015-019-09935-x
17. Takahashi K, Tanabe K, Ohnuki M, et al. Induction of Pluripotent Stem Cells from Adult Human Fibroblasts by Defined Factors. Cell. 2007;131(5):861-872. doi:10.1016/j.cell.2007.11.019
18. Park IH, Arora N, Huo H, et al. Disease-specific induced pluripotent stem cells. Cell. 2008;134(5):877-886. doi:10.1016/j.cell.2008.07.041
19. Yu J, Hu K, Smuga-Otto K, et al. Human induced pluripotent stem cells free of vector and transgene sequences. Science. 2009;324(5928):797-801. doi:10.1126/science.1172482
20. Shi Y, Inoue H, Wu JC, Yamanaka S. Induced pluripotent stem cell technology: a decade of progress. Nat Rev Drug Discov. 2017;16(2):115-130. doi:10.1038/nrd.2016.245
21. Salci KR, Lee JH, Laronde S, et al. Cellular Reprogramming Allows Generation of Autologous Hematopoietic Progenitors From AML Patients That Are Devoid of Patient-Specific Genomic Aberrations. Stem Cells Dayt Ohio. 2015;33(6):1839-1849. doi:10.1002/stem.1994
22. Lee JH, Salci KR, Reid JC, et al. Brief Report: Human Acute Myeloid Leukemia Reprogramming to Pluripotency Is a Rare Event and Selects for Patient Hematopoietic Cells Devoid of Leukemic Mutations. Stem Cells Dayt Ohio. 2017;35(9):2095-2102. doi:10.1002/stem.2655

23. Kotini AG, Chang CJ, Chow A, et al. Stage-Specific Human Induced Pluripotent Stem Cells Map the Progression of Myeloid Transformation to Transplantable Leukemia. Cell Stem Cell. 2017;20(3):315-328.e7. doi:10.1016/j.stem.2017.01.009
24. Chao MP, Gentles AJ, Chatterjee S, et al. Human AML-iPSCs Reacquire Leukemic Properties after Differentiation and Model Clonal Variation of Disease. Cell Stem Cell. 2017;20(3):329-344.e7. doi:10.1016/j.stem.2016.11.018
25. Yamasaki AE, Warshaw JN, Kyalwazi BL, Matsui H, Jepsen K, Panopoulos AD. An iPSC line derived from a human acute myeloid leukemia cell line (HL-60-iPSC) retains leukemic abnormalities and displays myeloid differentiation defects. Stem Cell Res. 2020;49:102096. doi:10.1016/j.scr.2020.102096
26. Hsu J, Reilly A, Hayes BJ, et al. Reprogramming identifies functionally distinct stages of clonal evolution in myelodysplastic syndromes. Blood. 2019;134(2):186-198. doi:10.1182/blood.2018884338
27. Gandre-Babbe S, Paluru P, Aribeana C, et al. Patient-derived induced pluripotent stem cells recapitulate hematopoietic abnormalities of juvenile myelomonocytic leukemia. Blood. 2013;121(24):4925-4929. doi:10.1182/blood-2013-01-478412
28. Kumano K, Arai S, Hosoi M, et al. Generation of induced pluripotent stem cells from primary chronic myelogenous leukemia patient samples. Blood. 2012;119(26):6234-6242. doi:10.1182/blood-2011-07-367441
29. Hosoi M, Kumano K, Taoka K, et al. Generation of induced pluripotent stem cells derived from primary and secondary myelofibrosis patient samples. Exp Hematol. 2014;42(9):816-825. doi:10.1016/j.exphem.2014.03.010
30. Hu K, Yu J, Suknuntha K, et al. Efficient generation of transgene-free induced pluripotent stem cells from normal and neoplastic bone marrow and cord blood mononuclear cells. Blood. 2011;117(14):e109-119. doi:10.1182/blood-2010-07-298331
31. Hoffman GE, Hartley BJ, Flaherty E, et al. Transcriptional signatures of schizophrenia in hiPSC-derived NPCs and neurons are concordant with post-mortem adult brains. Nat Commun. 2017;8(1):2225. doi:10.1038/s41467-017-02330-5
32. Kim J, Hoffman JP, Alpaugh RK, et al. An iPSC line from human pancreatic ductal adenocarcinoma undergoes early to invasive stages of pancreatic cancer progression. Cell Rep. 2013;3(6):2088-2099. doi:10.1016/j.celrep.2013.05.036
33. Raya A, Rodríguez-Pizà I, Guenechea G, et al. Disease-corrected haematopoietic progenitors from Fanconi anaemia induced pluripotent stem cells. Nature. 2009;460(7251):53-59. doi:10.1038/nature08129
34. Muñoz-López A, Romero-Moya D, Prieto C, et al. Development Refractoriness of MLL-Rearranged Human B Cell Acute Leukemias to Reprogramming into Pluripotency. Stem Cell Rep. 2016;7(4):602-618. doi:10.1016/j.stemcr.2016.08.013
35. Reid JC, Tanasijevic B, Golubeva D, et al. CXCL12/CXCR4 Signaling Enhances Human PSC-Derived Hematopoietic Progenitor Function and Overcomes Early In Vivo Transplantation Failure. Stem Cell Rep. 2018;10(5):1625-1641. doi:10.1016/j.stemcr.2018.04.003
36. Wesely J, Kotini AG, Izzo F, et al. Acute Myeloid Leukemia iPSCs Reveal a Role for RUNX1 in the Maintenance of Human Leukemia Stem Cells. Cell Rep. 2020;31(9):107688. doi:10.1016/j.celrep.2020.107688

37. Doulatov S, Papapetrou EP. Studying clonal evolution of myeloid malignancies using induced pluripotent stem cells. Curr Opin Hematol. 2021;28(1):50-56. doi:10.1097/MOH.0000000000000620
38. Lapidot T, Sirard C, Vormoor J, et al. A cell initiating human acute myeloid leukaemia after transplantation into SCID mice. Nature. 1994;367(6464):645-648. doi:10.1038/367645a0
39. Shojaei F, Gallacher L, Bhatia M. Differential gene expression of human stem progenitor cells derived from early stages of in utero human hematopoiesis. Blood. 2004;103(7):2530-2540. doi:10.1182/blood-2003-09-3209
40. Grimwade D, Ivey A, Huntly BJP. Molecular landscape of acute myeloid leukemia in younger adults and its clinical relevance. Blood. 2016;127(1):29-41. doi:10.1182/blood-2015-07-604496
41. Medinger M, Passweg JR. Acute myeloid leukaemia genomics. Br J Haematol. 2017;179(4):530-542. doi:10.1111/bjh.14823
42. Mazaika E, Homsy J. Digital Droplet PCR: CNV Analysis and Other Applications. Curr Protoc Hum Genet. 2014;82:7.24.1-13. doi:10.1002/0471142905.hg0724s82
43. Tran THY, Fukuda A, Aizawa S, et al. Live cell imaging of X chromosome reactivation during somatic cell reprogramming. Biochem Biophys Rep. 2018;15:86-92. doi:10.1016/j.bbrep.2018.07.007
44. Kim K, Doi A, Wen B, et al. Epigenetic memory in induced pluripotent stem cells. Nature. 2010;467(7313):285-290. doi:10.1038/nature09342
45. Lee JH, Lee JB, Shapovalova Z, et al. Somatic transcriptome priming gates lineage-specific differentiation potential of human-induced pluripotent stem cell states. Nat Commun. 2014;5:5605. doi:10.1038/ncomms6605
46. Malik N, Rao MS. A Review of the Methods for Human iPSC Derivation. In: Lakshmipathy U, Vemuri MC, eds. Pluripotent Stem Cells. Vol 997. Methods in Molecular Biology. Humana Press; 2013:23-33. doi:10.1007/978-1-62703-348-0_3
47. Eminli S, Foudi A, Stadtfeld M, et al. Differentiation stage determines potential of hematopoietic cells for reprogramming into induced pluripotent stem cells. Nat Genet. 2009;41(9):968-976. doi:10.1038/ng.428
48. Johnston DL, Meshinchi S, Opheim KE, et al. Progenitor cell involvement is predictive of response to induction chemotherapy in paediatric acute myeloid leukaemia. Br J Haematol. 2003;123(3):431-435. doi:10.1046/j.1365-2141.2003.04633.x
49. Pollard JA, Alonzo TA, Gerbing RB, et al. FLT3 internal tandem duplication in CD34+/CD33- precursors predicts poor outcome in acute myeloid leukemia. Blood. 2006;108(8):2764-2769. doi:10.1182/blood-2006-04-012260
50. Pabst C, Krosl J, Fares I, et al. Identification of small molecules that support human leukemia stem cell activity ex vivo. Nat Methods. 2014;11(4):436-442. doi:10.1038/nmeth.2847
51. Wesselschmidt RL. The teratoma assay: an in vivo assessment of pluripotency. Methods Mol Biol Clifton NJ. 2011;767:231-241. doi:10.1007/978-1-61779-201-4_17
52. Kota V, Saliba RM, Bayraktar UD, et al. Chromosome 7 Abnormalities in Allogeneic Transplantation for AML and MDS. Blood. 2011;118(21):2037. doi:10.1182/blood.V118.21.2037.2037

53. Kogut I, McCarthy SM, Pavlova M, et al. High-efficiency RNA-based reprogramming of human primary fibroblasts. Nat Commun. 2018;9(1):745. doi:10.1038/s41467-018-03190-3
54. Papapetrou EP. Modeling myeloid malignancies with patient-derived iPSCs. Exp Hematol. 2019;71:77-84. doi:10.1016/j.exphem.2018.11.006
55. Ruiz-Gutierrez M, Bölükbaşi OV, Alexe G, et al. Therapeutic discovery for marrow failure with MDS predisposition using pluripotent stem cells. JCI Insight. 2019;4(12). doi:10.1172/jci.insight.125157
56. Chang CJ, Kotini AG, Olszewska M, et al. Dissecting the Contributions of Cooperating Gene Mutations to Cancer Phenotypes and Drug Responses with Patient-Derived iPSCs. Stem Cell Rep. 2018;10(5):1610-1624. doi:10.1016/j.stemcr.2018.03.020
57. Kotini AG, Chang CJ, Chow A, et al. Stage-Specific Human Induced Pluripotent Stem Cells Map the Progression of Myeloid Transformation to Transplantable Leukemia. Cell Stem Cell. 2017;20(3):315-328.e7. doi:10.1016/j.stem.2017.01.009
58. Dannenmann B, Klimiankou M, Oswald B, et al. iPSC modeling of stage-specific leukemogenesis reveals BAALC as a key oncogene in severe congenital neutropenia. Cell Stem Cell. 2021;28(5):906-922.e6. doi:10.1016/j.stem.2021.03.023
59. Coombs CC, Tavakkoli M, Tallman MS. Acute promyelocytic leukemia: where did we start, where are we now, and the future. Blood Cancer J. 2015;5:e304. doi:10.1038/bcj.2015.25

Figures & Tables

Table 1

# of AML Samples Reprogrammed	AML Patient ID #	Source	Clinical Stage	AML #	Genetic/molecular abnormality	LSC	CFU	CD34+ (%)
1	**A374.1**	PB	Diagnosis	**AML 1**	46,XX,add(3),der(3),del(5), del(7), add(18), -20, -22,+mar1,+mar3	Y-myeloid	Y	80.3
2	**A422**	PB	Relapse	**AML 2**	45,XX,-7[19] /46,XX[1]	Y-myeloid	Y -myelo & erythro	88
3	**13814.1**	BM	Diagnosis	**AML 3**	43~46,XY,del(15)(q11.2q15)[cp5]/ 46,XY,+mar1[cp2]/46,XY[11]	Y-multilineage	N	60.1
4	**16150**	*BM*	Diagnosis	**AML 4**	CBFbeta/MYH11 inv(16)	Y-myeloid	Y -myelo & erythro	72.8
5	**A151.1**	PB	De novo AML	**AML 5**	46,XY,inv(16)(p13.1q22)[20]/47,sl,+8[5]	Y-myeloid	Y	30
6	**15328**	BM	Diagnosis	**AML 6**	45~46,XX,der(X)?t(X;11)(q28;q12)[2], -2[3],del(3)(q11.2)[3],-5[2], add(7)(p11.2)[3], -17[3],+3~5mar[3][cp3]	Y-multilineage	*UNK*	85.8
7	**A295.1**	PB	Diagnosis	**AML 7**	trisomy i21	Y-multilineage	Y	67
8	**16158.1**	BM	Diagnosis	**AML 8**	45, XX, del(5), -7	Y-multilineage	Y	92.8
9	**16626**	BM	Refractory AML	**AML 9**	inv (3)	Y-myeloid	Y	45
10	**19447**	PB	Diagnosis	**AML 10**	complex, isolated +8	Y-multilineage	N/A	64
11	**A320-1**	BM	De novo AML	**AML 11**	PML, RARA translacation (APL)	*UNK*	*UNK*	0.1
12	**A477**	Leuka	Diagnosis	**AML 12**	DNMT3A:c.2645G>A, p.(Arg882His) (48.8%)	N	Y - myelo & erythro	88
13	**13051.1**	Leuka	Diagnosis	**AML 13**	NPM+, FLT3-ITD+	N	Y - myelo & erythro	57.3
14	**A485-3**	Leuka	Relapse	**AML 14**	46,XY,del(7)(q22q34)[18]/46,XY[1] and FLT3:c.1794_1795insGGAGGAAACTACGTTGATTTCAGAGAATATGAA, p.(Glu598_Tyr599insGlyGlyAsnTyrValAspPheArgGluTyrGlu) (5.6%)	N	Y - myelo & erythro	92
15	**16534**	PB	Diagnosis	**AML 15**	NPM+, FLT3 ITD +, normal karyotype	N	N	22
16	**A494-1**	PB	De novo AML	**AML 16**	Karyotype: 47,XX,+11[20] and FLT3 –ve IDH2:c.515G>A, p.(Arg172Lys) (49.1%) PTPN11:c.179G>T, p.(Gly60Val) (46.3%)	N	Y - Erythroid	90
17	**A472-1**	BM	Diagnosis	**AML 17**	ASXL1:c.2725A>T, p.(Lys909*) (42.6%) IKZF1:c.476A>G, p.(Asn159Ser) (27.5%) RUNX1:c.656_657insAAGG, p.(Ser220Argfs*9) (27.8%)	*UNK*	Y - myelo & erythro	50
18	**A063**	PB	Diagnosis	**AML 18**	t(4;12)[25/25]	N	N	99
19	**A492-2**	PB	Relapse	**AML 19**	Karyotype: 46,XY,t(2:12)(p23;p13)[20] & FLT3 -ve NPM1:c.863_864insCCTG, p.(Trp288Cysfs*12) (28.6%)	N	N	30
20	**16308A**	PB	Diagnosis	**AML 20**	NPM1+	Y-myeloid	Y - myelo & erythro	57.4
21	**A472-3**	PB	Refractory AML	**AML 21**	ASXL1:c.2725A>T, p.(Lys909*) (42.6%) IKZF1:c.476A>G, p.(Asn159Ser) (27.5%) RUNX1:c.656_657insAAGG, p.(Ser220Argfs*9) (27.8%)	Y - myeloid	Y - Myeloid	20
22	**16308F**	PB	Relapse	**AML 22**	NPM1+	*UNK*	Y - myelo & erythro	33.5

Table 1. Sample characteristics of reprogrammed AML samples

Characteristics of 22 reprogrammed AML samples, including AML patient ID number, primary AML specimen source, clinical stage of disease, genetic/molecular abnormality, leukemic stem cell (LSC) content and engraftment type if applicable, colony forming unit (CFU) capacity and $CD34^+$ percentage. Yes (Y), No (N), Unknown (UNK). Samples with engraftment are described as myeloid or multilineage engraftment. Samples in which CFU capacity was known are described as either containing myeloid and erythroid CFU's (Y - myelo & erythro) or only myeloid (Y - myelo).

Figure 1

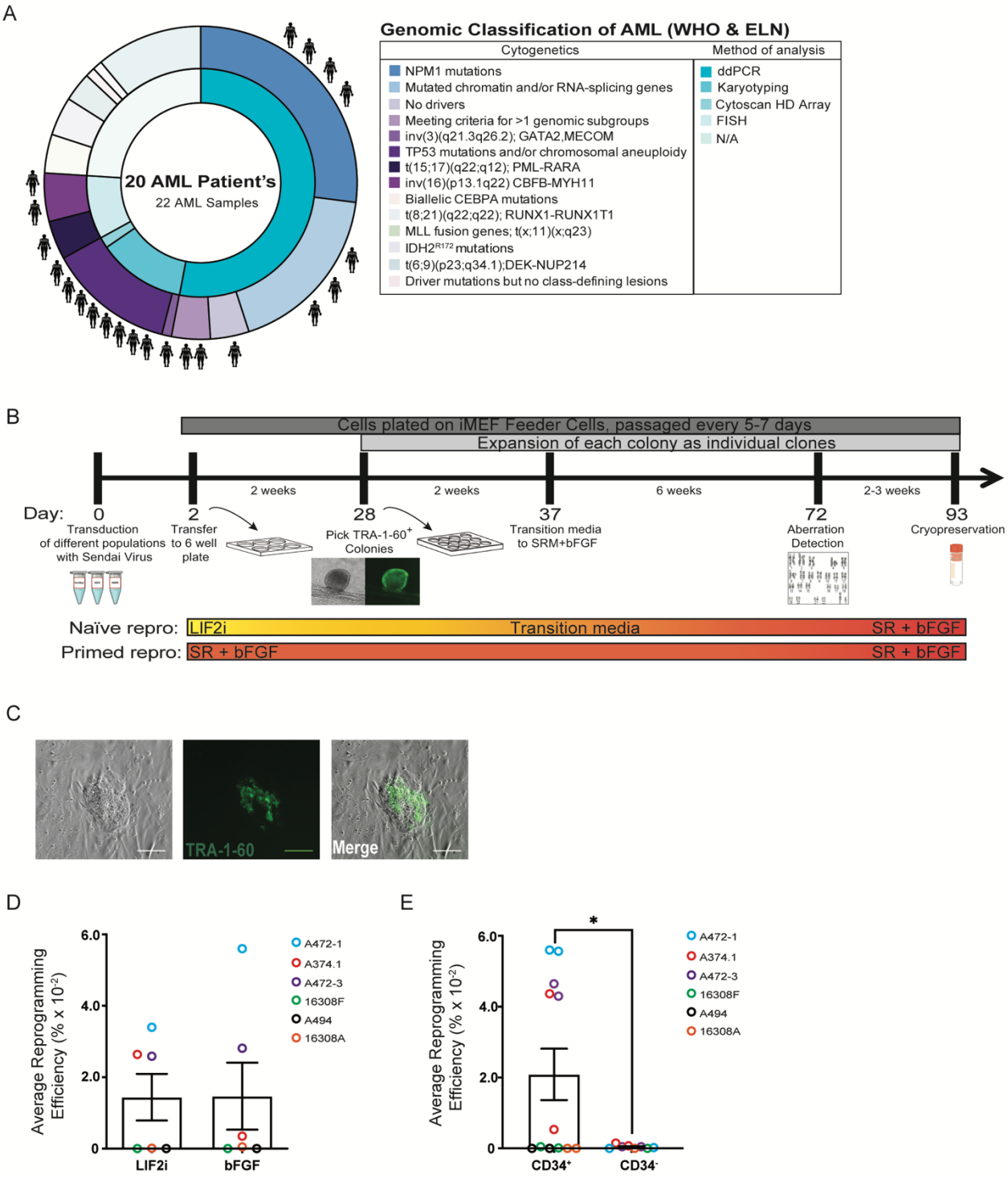

Figure 1. Reprogramming strategy and AML sample section

(A) Size distribution of cytogenetically and molecularly defined subsets of AML described by Medinger & Passweg (Grimwade et al., 2016; Medinger & Passweg, 2017) of the 22 AML patient samples analyzed in this study. Further details concerning patients and samples are included in

Table 1. **(B)** Illustrative workflow depiction of reprogramming strategy using primed (SR+bFGF) versus naïve (LIF2i) reprogramming. Reprogramming is carried out on sorted populations using Sendai virus (SeV) containing polycistronic Klf4-OCT3/4-SOX2, cMyc and KLs4 vectors in naïve (LIF2i) media for 21-28 days until iPSCs arose and then transitioned to primed (SR+bFGF) media. For samples undergoing primed reprogramming, no transitional phase was required as cells were always maintained in SR+bFGF medium. **(C)** Morphology and live cell TRA-1-60 staining of derived iPSC colonies prior to being picked and propagated. Scale bar 500um. **(D)** Average reprogramming efficiency of six AML patient samples reprogrammed by both naïve and primed methodologies (N=6, AML samples; n=3-5, the number of wells reprogrammed as a technical replicate) **(E)** Average reprogramming efficiency of six AML patient samples stratified by reprogramming a $CD34^+$ population or $CD34^-$ population independent of methodology used. Reprogramming efficiency is calculated as the number of colonies that arose divided by 200,000 cells reprogrammed, per well. (N=6, AML samples; n=8-12, the number of wells reprogrammed as a technical replicate). Data shows average with error bars representing $\mp$SEM. All comparisons were made using unpaired student t-test * $p<0.05$.

Figure 2

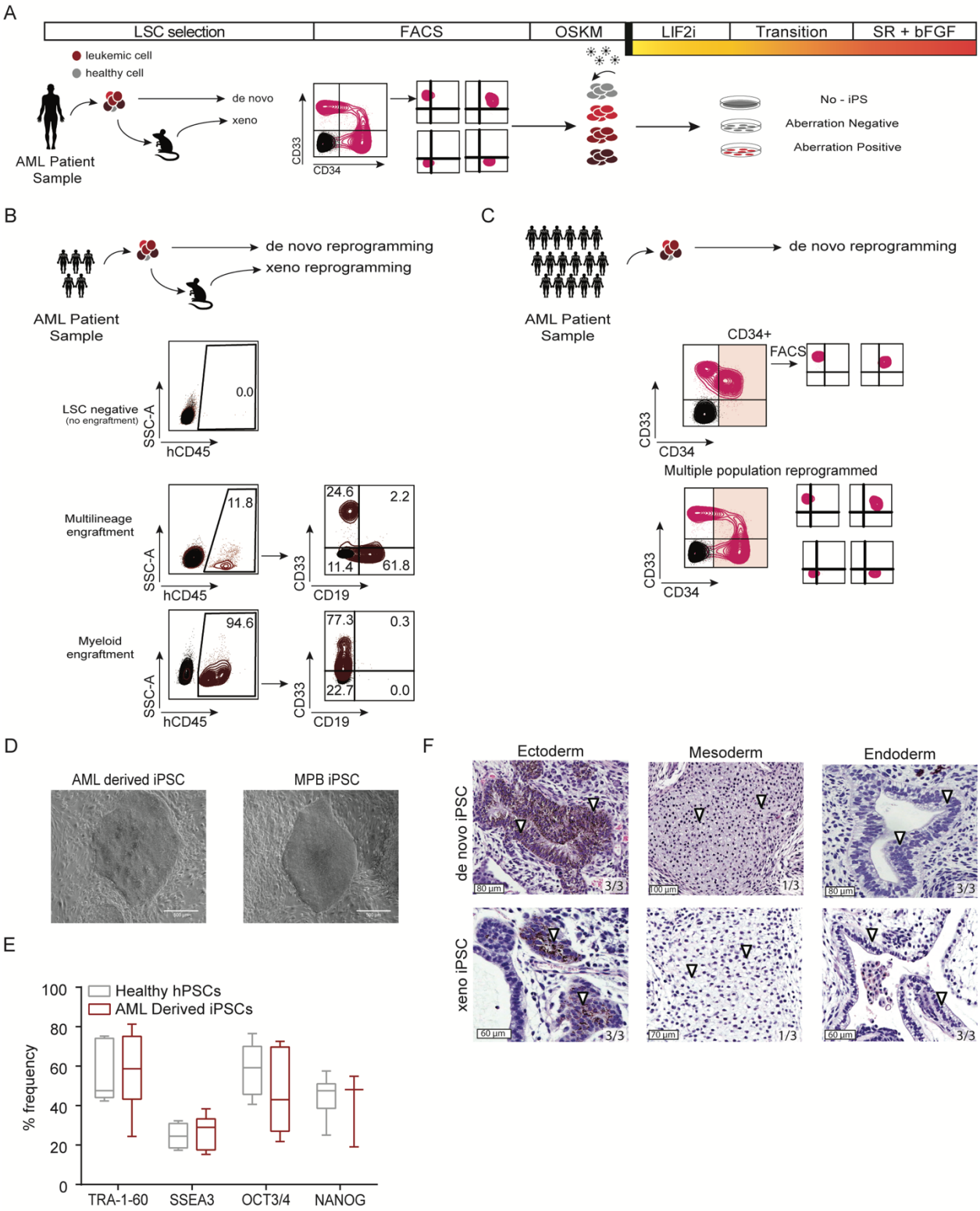

Figure 2. Novel Reprogramming Strategy for LSC Selection

(A) Schematic diagram depicting the way primary AML samples were reprogrammed using fluorescence activated cell sorting (FACS) directly by de novo reprogramming, or post xenograft sorting (xeno reprogramming) on CD45, CD34 and CD33 populations. **(B)** Workflow of select AML samples (AML 1, 2, 3, 4, & 9) that underwent both methodologies of reprogramming to generate iPSC colonies, de novo and xenograft reprogramming respectively. AML samples were engrafted into NSG mice and assessed for human chimerism by pan-hematopoietic marker, CD45. Exclusive myeloid grafts were identified by exclusive expression of CD33 and considered leukemic and LSC^{+}. Multi-lineage grafts displayed expression of CD33 and CD19 and considered to be healthy and LSC^{-}. Samples that were LSC^{+} (Table 1) were candidates for reprogramming for both de novo and xenografted methods. **(C)** Workflow of select AML samples (AML 5-8, 10-22) that underwent de novo reprogramming solely to generate iPSC colonies. Samples in which clear and distinct populations existed underwent reprogramming from multiple populations ($CD34^{+}CD33^{+}$, $CD34^{-}CD33^{+}$, $CD34^{+}CD33^{-}$, $CD34^{-}CD33^{-}$). **(D**) AML derived and MPB-iPSCs imaged using phase-contrast microscopy. Scale bars are 500 μm. Morphologically, clones do not look distinct from each other. **(E)** Percent frequency expression of pluripotency markers SSEA3, TRA-1-60, OCT3/4, and NANOG by flow cytometry in representative iPSC colonies derived from AML patient sample in comparison to healthy control MPB iPSCs. N=1-3, iPSC samples; n=5-7, box and whisker plot showing min to max highlighting median value in center. Statistical analysis done using two-way ANOVA and Tukey's multiple comparison test. **(F)** Teratoma analysis of AML 1- iPSCs lines derived via de novo reprogramming or xenograft reprogramming. Hematoxylin and eosin staining of teratoma sections at 10 weeks. Arrows denote pigmented epithelium (ectoderm), goblet cells (endoderm), and cartilage (mesoderm). Scale bar 100 μm. Frequency of tissue per independent mouse teratomas after 1 scored tissue section is recorded in bottom right corner. N=3 mice transplanted per iPSC line.

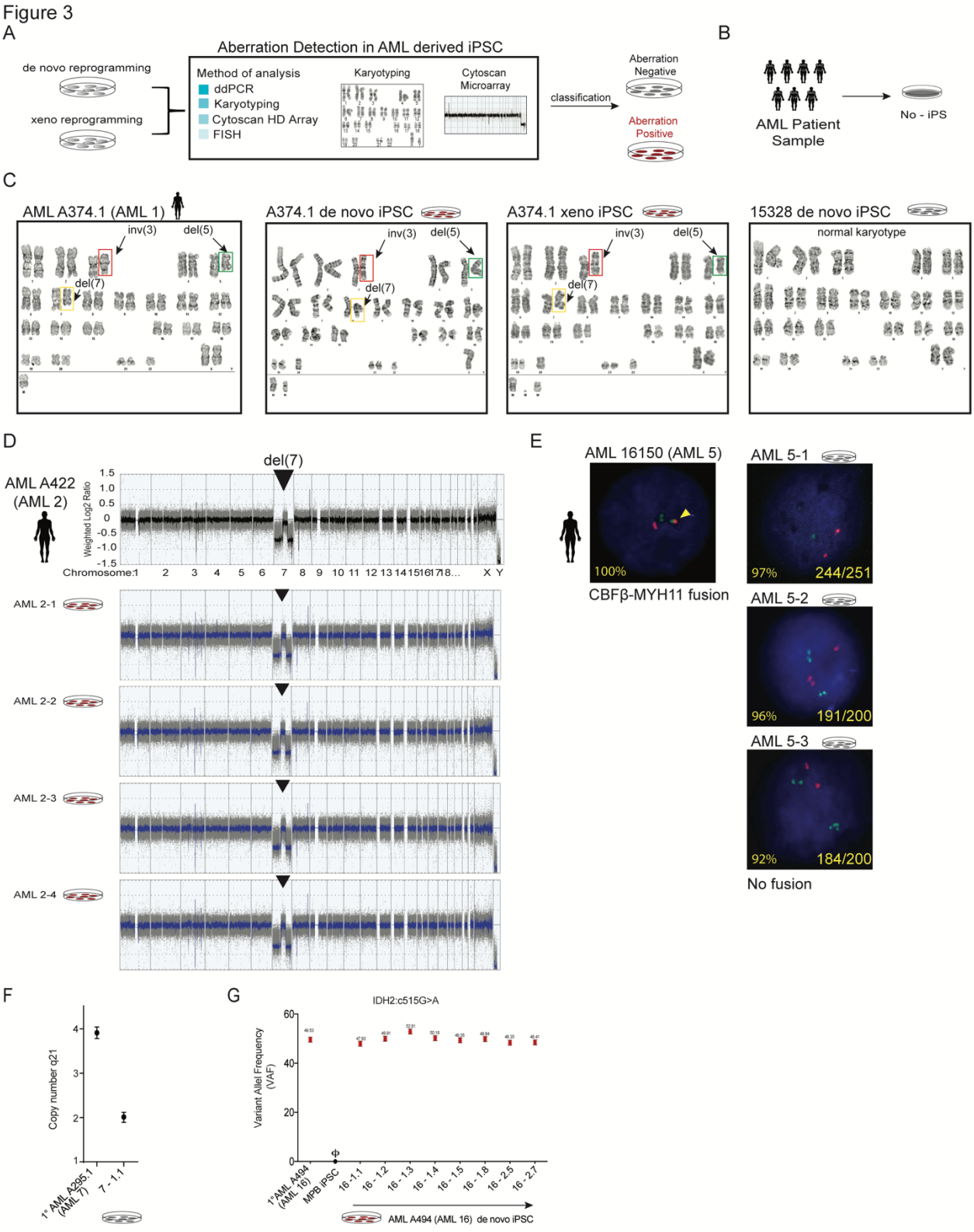

Figure 3. Detection of primary AML mutations in derived iPSC lines

(A) Illustrative depiction of aberration detection in AML derived iPSC lines using selective methods previously described. **(B)** AML patient samples that did not yield any iPSCs **(C)** Karyotype results of primary AML A374.1 (AML 1) and two associated clones derived via de novo reprogramming and xenograft reprogramming showing an abnormal karyotype mirroring the primary sample, as well as karyotype of iPSC clone derived from patient AML 15328 (AML 6) that did not contain any mutations corresponding to the expected karyotype based on the primary AML sample. **(D)** Gene copy number was assessed in AML A422 (AML 2) and derived iPSCs by Affymetrix HD CytoScan microarray and analyzed using ChAS software. All 4 clones contain del(7) present in primary AML 2. **(E)** FISH was performed on AML 16150 (AML 5) using CBFβ-MYH11 hybridization probe. When the gene fusion is present the foci pattern is 1 green, 1 red, 1 red-green. All clones derived from AML 5 show no gene fusion with a 2 green, 2 red pattern. **(F)** AML A295.1 (AML 7) and AML7-iPSC clone assessed by ddPCR for long arm (q) of chromosome 21. Copy number determined relative to control probe. Error bars represent Poisson 95% confidence intervals. **(G)** Droplet digital PCR results of AML A494 (AML 16) iPSC clones 1-8 by comparison to primary AML and healthy controls. Variant Allele Frequency (VAF) is displayed for droplet PCR results, probing for IDH2:c.515G>A. The primary AML sample contained the mutation, and the mobilized peripheral blood (MPB) used as a healthy control did not, as expected. All 8 clones tested contained the mutation, with VAFs similar to that of the primary sample.

Table 2

	iPSC Derived Yes / No	Stratification of iPSC lines derived			AML Patient ID	Source	Clinical Stage	AML #	Genetic/molecular abnormality	# of Isogenic clones derived	# of AML - iPSC clones derived	Total # of clones derived
1	No	Category 0	1	No iPS Derived	16158.1	BM	Diagnosis	**AML 8**	45, XX, del(5), -7	0	0	0
2			2		16626	BM	Refractory AML	**AML 9**	inv (3)	0	0	0
3			3		19447	PB	Diagnosis	**AML 10**	complex, isolated +8	0	0	0
4			4		A477	Leuka	Diagnosis	**AML 12**	DNMT3A:c.2645G>A, p.(Arg882His) (48.8%)	0	0	0
5			5		A063	PB	Diagnosis	**AML 18**	t(4;12)[25/25]	0	0	0
6			6		A492-2	PB	Relapse	**AML 19**	Karyotype: 46,XY,t(2:12)(p23:p13)[20] & FLT3 -ve NPM1:c.863_864insCCTG, p.(Trp288Cysfs*12) (28.6%)	0	0	0
7			7		**16308A**	PB	Diagnosis	**AML 20-1**	NPM1+	0	0	0
1	Yes	Category 1 Aberration Negative	1	Pure Isogenic iPSC Derived Clones	16150	*BM*	Diagnosis	**AML 4**	CBFbeta/MYH11 inv(16)	**10**	0	10
2			2		A151.1	PB	De novo AML	**AML 5**	46,XY,inv(16)(p13.1q22)[20]/47,sl,+8[5]	**3**	0	3
3			3		15328	BM	Diagnosis	**AML 6**	45~46,XX,der(X)?t(X;11)(q28;q12)[2],-2[3],del(3)(q11.2)[3],-5[2], add(7)(p11.2)[3],-17[3],+3~5mar[3][cp3]	**6**	0	6
4			4		A295.1	PB	Diagnosis	**AML 7**	trisomy i21	**1**	0	1
5			5		A320-1	BM	De novo AML	**AML 11**	PML, RARA translacation (APL)	**5**	0	5
6			6		13051.1	Leuka	Diagnosis	**AML 13**	NPM+, FLT3-ITD+	**13**	0	13
7			7		16534	PB	Diagnosis	**AML 15**	NPM+, FLT3 ITD +, normal karyotype	**3**	0	3
8			8		16308F	PB	Relapse	**AML 20-2**	NPM1+	**1**	0	1
9		Category 2 Aberration Positive	1	Pure AML iPSC Derived Clones	A374.1	PB	Diagnosis	**AML 1**	46,XX,add(3),der(3),del(5), del(7), add(18), -20, -22,+mar1,+mar3	0	**12**	12
10			2		A422	PB	Relapse	**AML 2**	45,XX,-7[19] /46,XX[1]	0	**4**	4
11			3		A494-1	PB	De novo AML	**AML 16**	Karyotype: 47,XX,+11[20] and FLT3 –ve IDH2:c.515G>A, p.(Arg172Lys) (49.1%) PTPN11:c.179G>T, p.(Gly60Val) (46.3%)	0	**8**	8
12			4		A472-1	BM	Diagnosis	**AML 17-1**	ASXL1:c.2725A>T, p.(Lys909*) (42.6%) IKZF1:c.476A>G, p.(Asn159Ser) (27.5%) RUNX1:c.656_657insAAGG, p.(Ser220Argfs*9) (27.8%)	0	**18**	18
13			5		A472-3	PB	Refractory AML	**AML 17-2**	ASXL1:c.2725A>T, p.(Lys909*) (42.6%) IKZF1:c.476A>G, p.(Asn159Ser) (27.5%) RUNX1:c.656_657insAAGG, p.(Ser220Argfs*9) (27.8%)	0	**29**	29
14		Category 3 Aberration +/-	1	Isogenic & AML iPSC Derived Clones	13814.1	BM	Diagnosis	**AML 3**	43~46,XY,del(15)(q11.2q15)[cp5]/ 46,XY,+mar1[cp2]/46,XY[11]	**6**	**2**	8
15			2		A485-3	Leuka	Relapse	**AML 14**	46,XY,del(7)(q22q34)[18]/46,XY[1] and FLT3:c.1794_1795insGGAGGAAACTACGTTGATTTCAGAGAATATGAA, p.(Glu598_Tyr599insGlyGlyAsnTyrValAspPheArgGluTyrGlu) (5.6%)	**4**	**4**	8
										52		
											77	
											Total	**129**

Table 2 – Categorization of reprogrammed AML samples

All AML samples reprogrammed were divided into four categories based off the iPSC lines derived. Table includes a summary of the total number of clones derived per AML sample, patient ID #, source of sample, clinical stage, AML # provided in the manuscript, and the genetic/molecular abnormality associated with the primary sample. Category 0, made up of 7 samples, represents samples in which no iPSCs were derived. Category 1 represents 8 samples in which aberration negative iPSCs were solely derived after reprogramming. Category 2 represents 5 samples in which aberration positive iPSCs were solely derived after reprogramming. Category 3 represents 2 samples in which both aberration positive and aberration negative lines were derived there by producing paired isogenic and AML-iPSC lines.

Figure 4

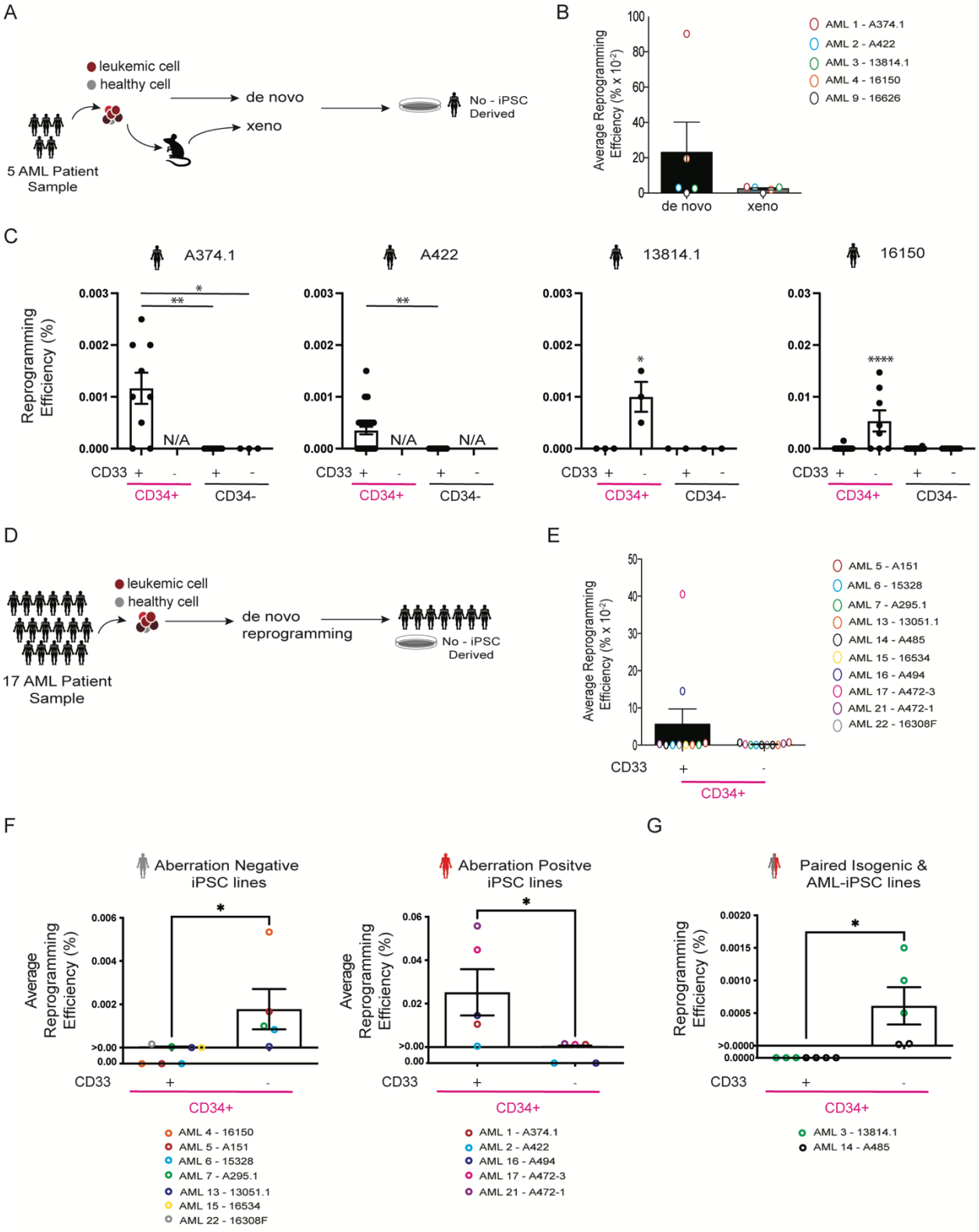

Figure 4. Reprogramming efficiency of AML samples via immunophenotyping on distinct populations

(A) Illustrative depiction of 5 AML samples that underwent both de novo and xenograft reprogramming. Note AML 9 did not give rise to iPSC using either methodology. **(B)** Bar graph in which de novo reprogrammed samples versus xenografted samples are compared. Reprogramming efficiency was firstly calculated by determining the number of colonies that arose divided by the number of cells reprogrammed, per well, per sample. Technical replicates of individual AML samples were then averaged. N=5 AML samples, n=7-22, the number of wells reprogrammed as a technical replicate. **(C)** Reprogramming efficiency of AML samples that were FACS separated by CD34 and CD33 independent of methodology used for reprogramming. Populations that did not exist in the patient sample and thus were not reprogrammed are labeled as N/A. N=1 AML sample, n=2-30, the number of wells reprogrammed as a technical replicate per immunophenotype. **(D)** Illustrative depiction of 17 AML samples that de novo reprogramming. Note AML 8-10, 12, & 18-20 did not give rise to iPSC **(E)** Average reprogramming efficiency based of the immunophenotype $CD34^{+}CD33^{+}$ or $CD34^{+}CD33^{-}$ in samples that underwent de novo reprogramming. Plotted dots represent reprogramming efficiency calculated by taking the average of each individual AML sample. N=10 AML samples, n=3-14, the number of wells reprogrammed as a technical replicate). **(F)** Average reprogramming efficiency based of the immunophenotype $CD34^{+}CD33^{+}$ or $CD34^{+}CD33^{-}$ in samples that produced aberration negative, or aberration positive iPSCs. Plotted dots represent reprogramming efficiency calculated by taking the average of each individual AML sample. N=5-7 AML samples, n=3-20, the number of wells reprogrammed as a technical replicate. **(G)** All reprogramming efficiency based of the immunophenotype $CD34^{+}CD33^{+}$ or $CD34^{+}CD33^{-}$ in samples in which paired isogenic and AML-iPSCs lines were produced. N=2 AML samples, n=5-6, the number of wells reprogrammed as a technical replicate. Data points represent individual values with error bars representing $\mp$SEM. All comparisons were made using either a Two-way ANOVA with Tukey's multiple comparison or an unpaired student t-test * $p<0.05$, ** $p<0.01$

Figure 5

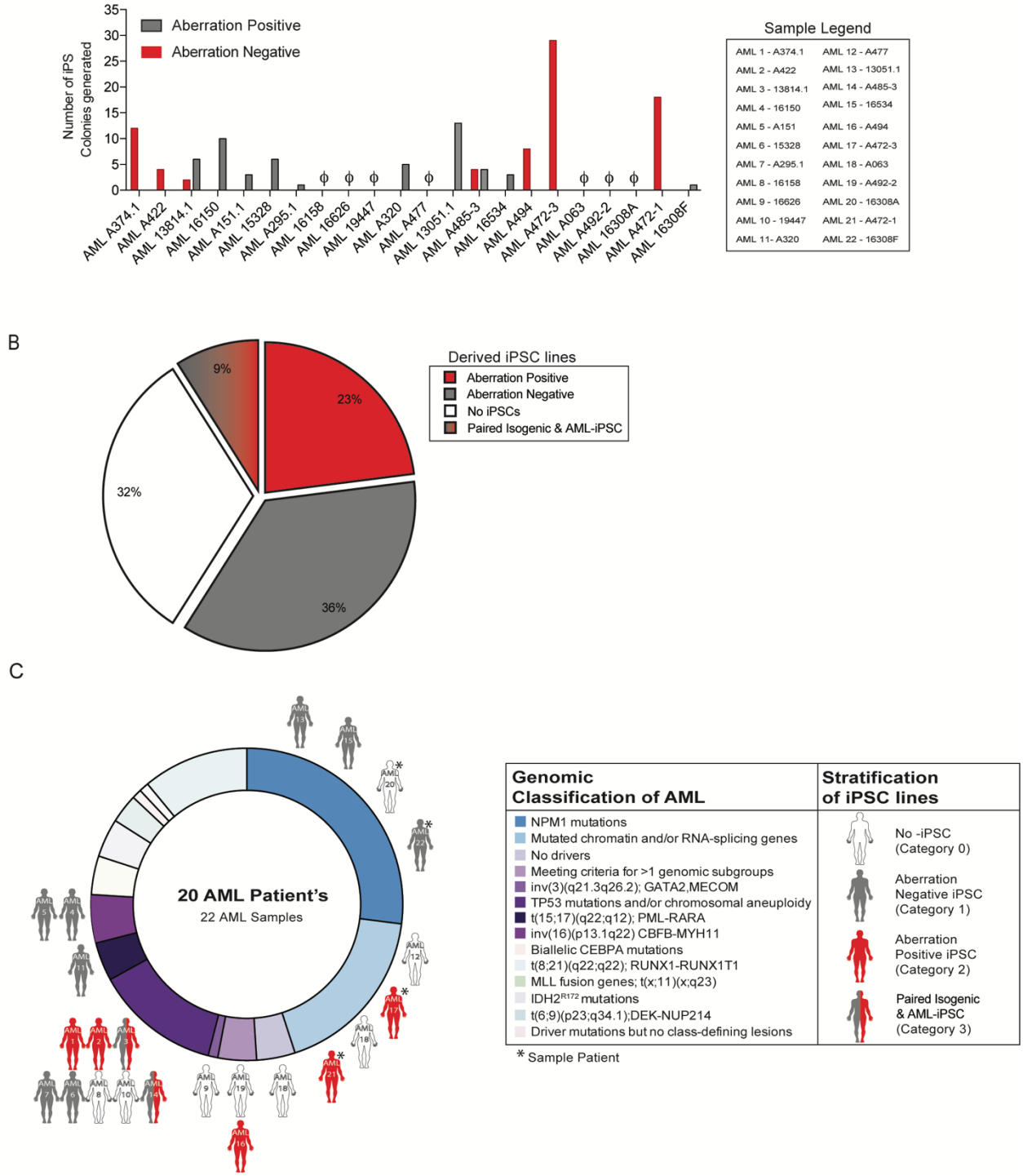

Figure 5. Cytogenetic Summary of iPSC Derived

(A) Graphical representation of the total number of iPSC colonies generated from 22 patient samples that were reprogrammed. All clones (iPSC lines) derived were tested for patient aberrations using FISH, karyotyping HD cytoscan array and ddPCR. **(B)** Percent distribution of

the type of derived iPSC lines within the 4 categories - no iPSC, aberration negative, aberration positive, or mixed (paired isogenic and AML-iPSC). 7/22 samples produced no iPSC colonies, 15/22 produced colonies, of which 5 produced aberration positive lines solely (AML-iPSC) and 7 produced only normal/healthy clones (aberration negative). **(C)** Summary of AML samples reprogrammed by the Bhatia lab, and the category of mutations they fall under. 18 primary AML samples were reprogrammed, representing 7 different categories of mutations.

Supplemental Figures & Table

Supplemental Figure 1A

A

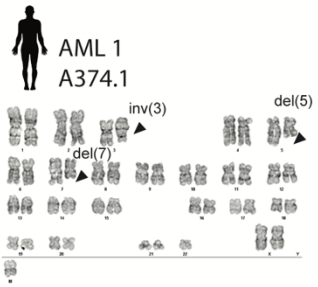

45~47,XX,add(3)(p?21)[28],der(3)?inv(3)(p?13q?21)del(3)(q?22~24)[28],del(5)(q22~31q?35)[28],del(7)(q31~32)[28],add(18)(q21)[28],?add(20)(p12)[28],-22[28],+mar1[28],+mar2[26][cp28]

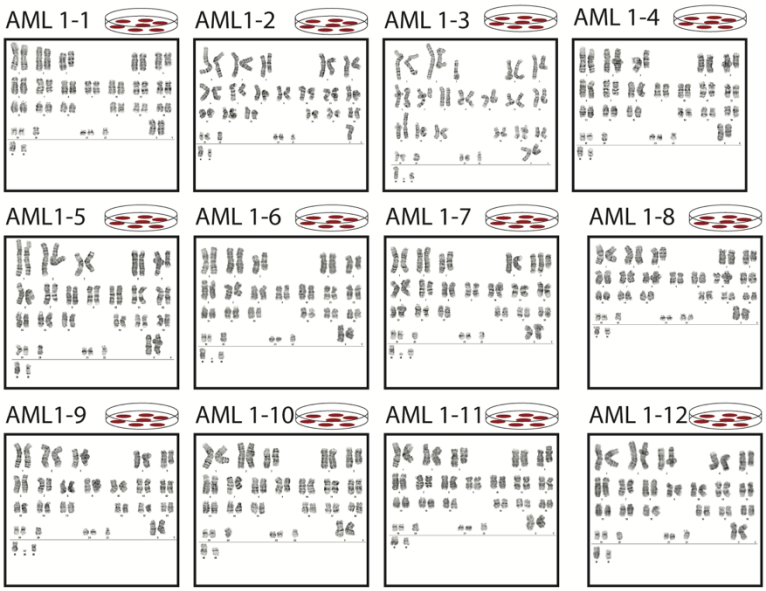

B

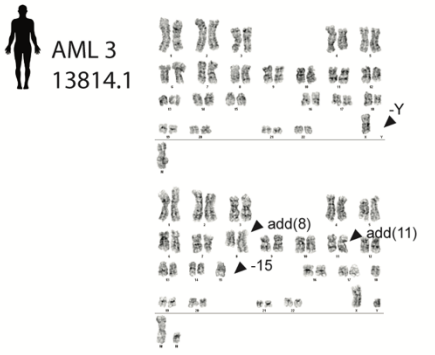

43 or 46,XY,
del(15)(q11.2q15)[cp5]/
46,XY,+mar1[cp2]/46,XY[11]

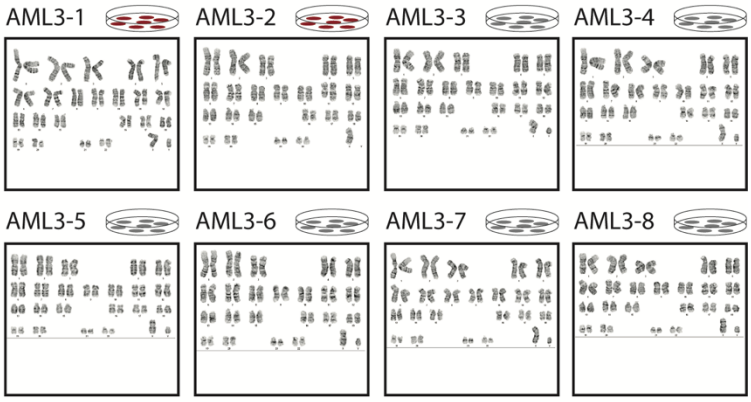

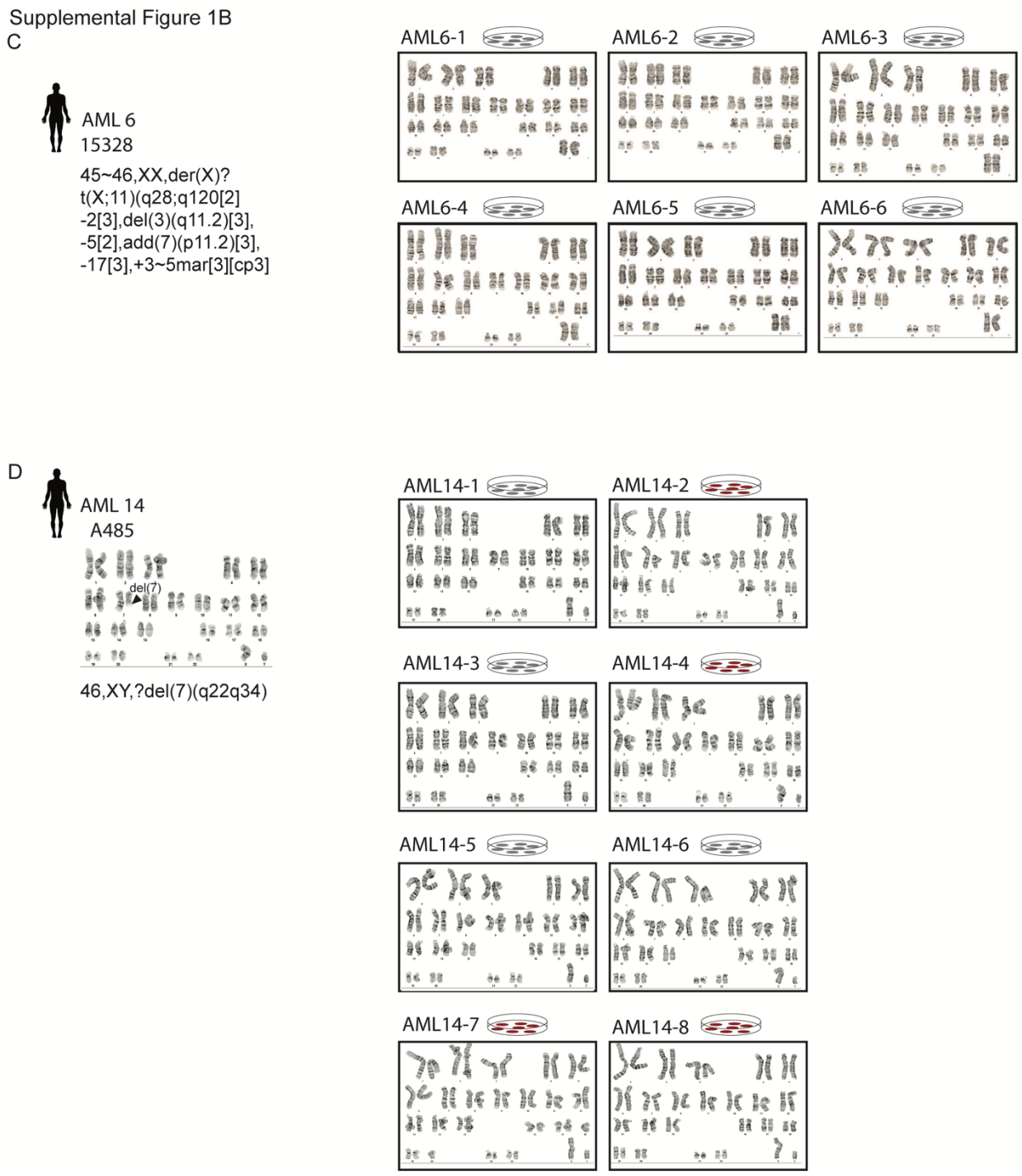

Supplemental Figure 1. Detection of primary AML mutations using G-band karyotyping in derived iPSCs

(A) Using G-banding, it was found that AML A374.1 (AML 1) clones 1-1 to 1-12 were found to have chromosomal aberration seen in primary AML A374.1 shown on the left. Red colonies in petri dish denote aberration positive iPSCs. **(B)** Primary AML 13814.1 (AML 3) clones 3-1 and

3-2 were found to have leukemic aberration, whereas clones 3-3 to 3-8 were found to be normal by G-band karyotyping. Karyotyping was conducted twice on the primary AML 13814.1 sample and representative images and karyotypic information are shown on the left. Red colonies in petri dish represent aberration positive iPSCs whereas grey colonies in petri dish represent aberration negative iPSCs. **(C)** AML 15328 (AML 6) gave rise to exclusively normal iPSCs as all 6 clones did not contain aberrations found in primary sample. **(D)** Karyotype results of AML 14 (A485-3) in which clones 14-1, 14-3, 14-5, and 14-6 (grey colonies in petri dish) shows a normal karyotype, indicating that the iPSC clone did not contain any mutations corresponding to the expected karyotype based on the primary AML sample. Clones 14-2, 14-4, 14-7 and 14-8 (red colonies in petri dish) shows an abnormal karyotype, with a translocation between chromosomes 3 and 12, with breaks in 3q26 and 12p13.

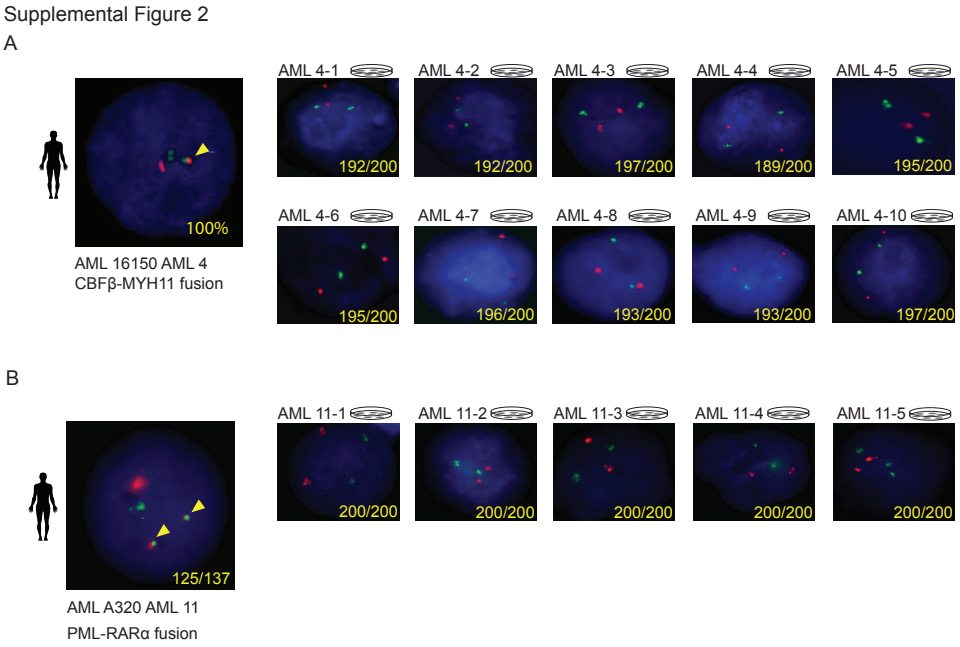

Supplemental Figure 2. Detection of primary AML mutations using FISH in derived iPSCs

(A) FISH was performed on AML 16150 (AML 4) using CBFβ-MYH11 hybridization probe. When the gene fusion is present the foci pattern is 1 green, 1 red, 1 red-green. All clones derived from AML 4 show no gene fusion with a 2 green, 2 red pattern, where as the primary sample demonstrates gene fusion. **(B)** FISH was performed on AML A320 (AML 11) and derived iPSCs using PML-RARα dual hybridization probe. Primary AML demonstrates gene fusion foci pattern of 1 green, 1 red and 2 green-red. All clones demonstrate no gene fusion with the normal, 2 green, 2 red foci pattern. Yellow arrows point to green-red foci. Yellow numbers the bought right corner indicate the number of nuclei with the shown pattern out of the total number of nuclei scored.

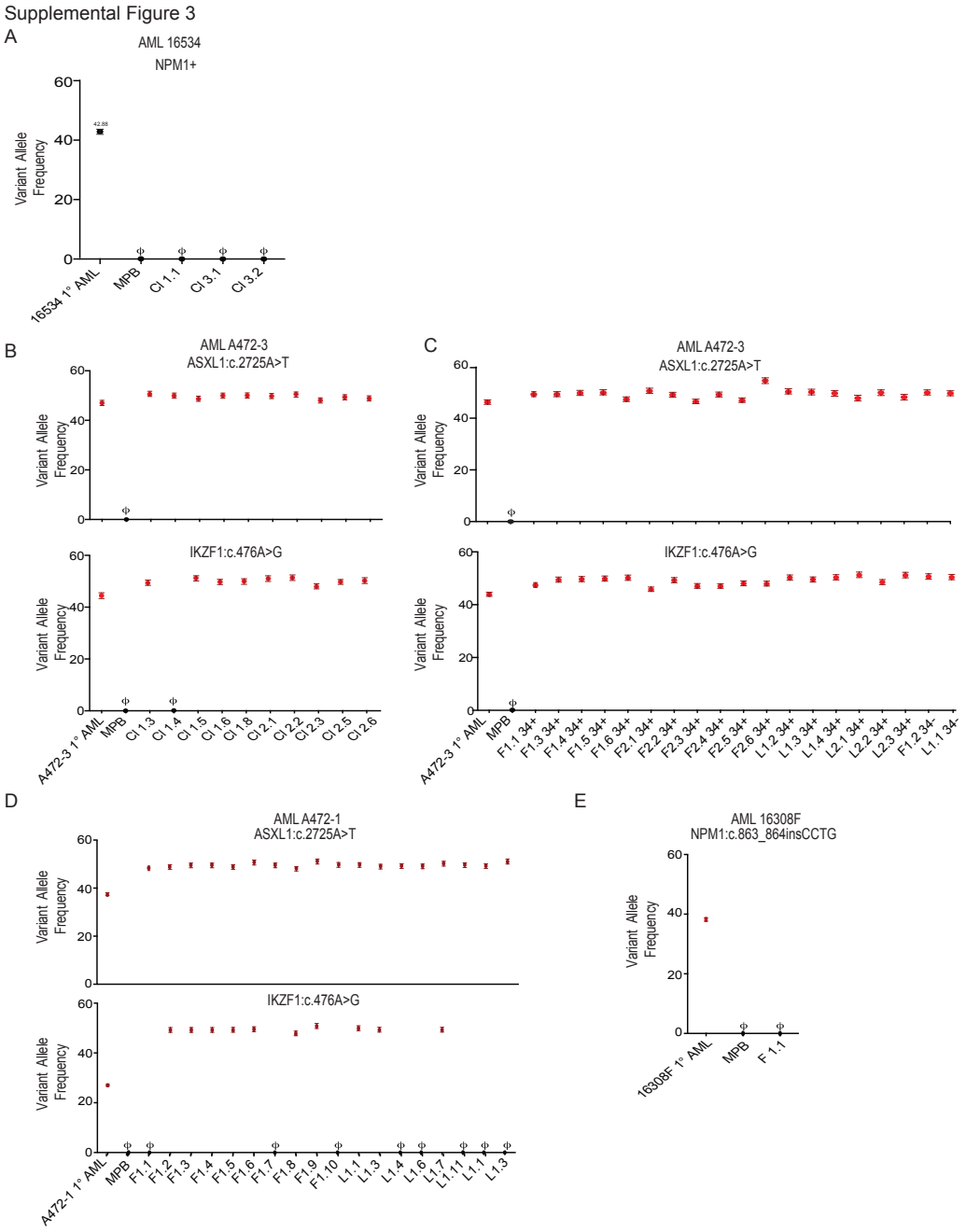

Supplemental Figure 3. Detection of primary AML mutations using ddPCR in derived iPSCs

(A) Droplet PCR results of AML 16534 (AML 15) iPSC clones 1.1, 3.1 and 3.2 by comparison to primary AML 16534 and healthy mobilized peripheral blood (MPB) iPSC control. Variant Allele Frequency (VAF) is displayed for droplet PCR results, probing for NPM1 c.863_864 ins_TCTG. The primary AML sample contained the mutation and the mobilized peripheral blood (MPB) healthy control did not, as expected. None of the three tested clones contained the mutation present in the patient sample, as seen by the VAF of 0. **(B)** Droplet PCR results of AML A472-3 (AML 17; Refractory AML) 10 iPSC clones by comparison to primary AML and healthy controls *(First round of reprogramming).* Variant Allele Frequency (VAF) is displayed for droplet PCR results, probing for ASXL1:c.2725A>T (top graph) and IKZF1:c.476A>G (bottom graph). The primary AML sample contained the mutation, and the MPB iPSC healthy control did not, as expected. 9 out of 10 clones tested contained both mutations (ASXL1 & IKZF1), with VAFs similar to that of the primary sample with the exception of one clone (clone 1.4) which did not contain the IKZF1 mutation as seen by the VAF of 0. AML A472-3 (AML 17) also has the mutation RUNX1:c.656_657insAAGG, however we were unable to successfully design a probe and therefore it remains to say if any of the 10 clones derived also contain the RUNX1 mutation. **(C)** Droplet PCR results of AML A472-3 (AML 17; Refractory AML) iPSC clones derived using different reprogramming media *(bFGF vs LIF2i; second round of reprogramming)*. Variant Allele Frequency (VAF) is again displayed for droplet PCR results, probing for ASXL1:c.2725A>T and IKZF1:c.476A>G. The primary AML sample contained the mutation and the MPB iPSC healthy control did not. All clones tested regardless of reprogramming media used to derive iPSCs contained both mutations (ASXL1 & IKZF1), with VAFs similar to that of the primary sample. It remains to say if any of the 17 clones derived also contain the RUNX1 mutation. **(C)** Droplet PCR results of AML 16 (A494) iPSC clones 1-8 by comparison to primary AML and healthy controls. Variant Allele Frequency (VAF) is displayed for droplet PCR results, probing for IDH2:c.515G>A. The primary AML sample contained the mutation and the mobilized peripheral blood (MPB) healthy control did not, as expected. All 8 clones tested contained the mutation, with VAFs similar to that of the primary sample. **(D)** Droplet PCR results of AML A472-1 (AML 22; Diagnosis AML sample of AML 17) iPSC clones derived using different reprogramming media (*bFGF vs LIF2i*). Variant Allele Frequency (VAF) is displayed for droplet PCR results, probing for ASXL1:c.2725A>T and IKZF1:c.476A>G. The primary AML sample contained both mutation and the control did not. 7/10 clones reprogrammed with SR+bFGF media contained both mutations (ASXL1 & IKZF1), with VAFs similar to that of the primary sample. 4/10 clones reprogrammed with LIF2i media contained both mutations (ASXL1 & IKZF1), with VAFs similar to that of the primary sample. It remains to say if any of the 18 clones derived also contain the RUNX1 mutation. **(E)** Droplet PCR results of single clone F1.1 derived from AML 16308F (AML 22) using different reprogramming media *(bFGF vs LIF2i).* Clone F1.1 displayed an absence for NPM1 c.863_864 ins_TCTG by VAF whereas the primary AML sample contained the mutation and the healthy control did not.

A

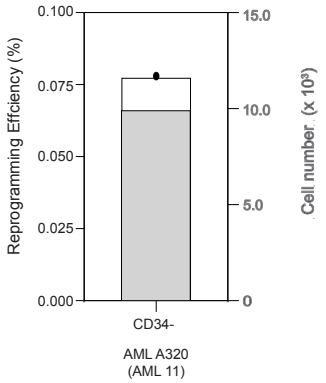

B

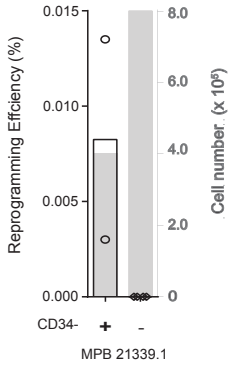

C

	FACS Population Reprogrammed		
Sample ID#	CD34+CD33+	CD34-CD33+	CD34+CD33-
AML 1_A374.1	0.044	0.001	N/A
AML 2_A422	0.00042	N/A	N/A
AML 3_13814.1	0	0	0.001
AML 4_16150	0	0	0
AML 5_A151.1	0.0025	N/A	N/A
AML 6_15328	0	N/A	0.001
AML 7_A295.1	0	N/A	0.001
AML 8_16158	0	N/A	N/A
AML 9_16626	0	0	N/A
AML 10_19447	0	N/A	N/A
AML 11_A320	N/A	N/A	0.078
AML 12_A477	N/A	N/A	0
AML 13_13051.1	0	N/A	0.0045
AML 14_A485	0	N/A	0.000025
AML 15_16534	0.0005	N/A	N/A
AML 16_A494	0.0145	N/A	N/A
AML 17_A472-3	0.0391	N/A	N/A
AML 18_A063	0	N/A	N/A
AML 19_16308A	0	0	N/A
AML 20_A492	0	0	N/A
AML 21_A472-1	0.056	0.0015	N/A
AML 22_16308F	0.00017	0	N/A

Supplemental Figure 4. Reprogramming Efficiency

(A) Reprogramming efficiency of AML A320 (AML 11) where a single well was reprogrammed depicted in black, plotted on left axis. Total cells that were attempted to be reprogrammed per population (1000) are shown on right axis in grey. **(B)** Reprogramming efficiency of MPB 21339.1 where each attempt is depicted in black, plotted on left axis. Total cells that were attempted to be reprogrammed per population are shown on right axis in grey. N=1 primary sample reprogrammed, n= 2-4 the number of wells reprogrammed as a technical replicate. Error bars represent ± SEM. **(C)** Summary of all reprogrammed samples in terms of the efficiency of reprogramming by immunophenotype population. Populations marked N/A show populations that were not reprogrammed for a particular sample either because the population did not exist, or not enough cells were able to be obtained for reprogramming. This does not separate clones that contain patient mutations from clones that did not.

Supplemental Table 1

# of AML Samples Reprogrammed	AML Patient ID #	Source	Clinical Stage	AML #	IPS Derived (Yes / No)		Genetic/molecular abnormality	Total # of clones
1	16158.1	BM	Diagnosis	AML 8	No	1	45, XX, del(5), -7	0
2	16626	BM	Refractory AML	AML 9		2	inv (3)	0
3	19447	PB	Diagnosis	AML 10		3	complex, isolated +8	0
4	A477	Leuka	Diagnosis	AML 12		4	DNMT3A:c.2645G>A, p.(Arg882His) (48.8%)	0
5	A063	PB	Diagnosis	AML 18		5	t(4;12)[25/25]	0
6	A492-2	PB	Relapse	AML 19		6	Karyotype: 46,XY,t(2:12)(p23;p13)[20] & FLT3 -ve NPM1:c.863_864insCCTG, p.(Trp288Cysfs*12) (28.6%)	0
7	16308A	PB	Diagnosis	AML 20-1		7	NPM1+	0
8	16150	*BM*	Diagnosis	AML 4	Yes	1	CBFbeta/MYH11 inv(16)	**10**
9	A151.1	PB	De novo AML	AML 5		2	46,XY,inv(16)(p13.1q22)[20]/47,sl,+8[5]	**3**
10	15328	BM	Diagnosis	AML 6		3	45~46,XX,der(X)?t(X;11)(q28;q12)[2],-2[3],del(3)(q11.2)[3],-5[2], add(7)(p11.2)[3],-17[3],+3~5mar[3][cp3]	**6**
11	A295.1	PB	Diagnosis	AML 7		4	trisomy i21	**1**
12	A320-1	BM	De novo AML	AML 11		5	PML, RARA translacation (APL)	**5**
13	13051.1	Leuka	Diagnosis	AML 13		6	NPM+, FLT3-ITD+	**13**
14	16534	PB	Diagnosis	AML 15		7	NPM+, FLT3 ITD +, normal karyotype	**3**
15	16308F	PB	Relapse	AML 20-2		8	NPM1+	**1**
16	A374.1	PB	Diagnosis	AML 1		9	46,XX,add(3),der(3),del(5), del(7), add(18), -20, -22,+mar1,+mar3	**12**
17	A422	PB	Relapse	AML 2		10	45,XX,-7[19] /46,XX[1]	**4**
18	A494-1	PB	De novo AML	AML 16		11	Karyotype: 47,XX,+11[20] and FLT3 –ve IDH2:c.515G>A, p.(Arg172Lys) (49.1%) PTPN11:c.179G>T, p.(Gly60Val) (46.3%)	**8**
19	A472-1	BM	Diagnosis	AML 17-1		12	ASXL1:c.2725A>T, p.(Lys909*) (42.6%) IKZF1:c.476A>G, p.(Asn159Ser) (27.5%) RUNX1:c.656_657insAAGG, p.(Ser220Argfs*9) (27.8%)	**18**
20	A472-3	PB	Refractory AML	AML 17-2		13	ASXL1:c.2725A>T, p.(Lys909*) (42.6%) IKZF1:c.476A>G, p.(Asn159Ser) (27.5%) RUNX1:c.656_657insAAGG, p.(Ser220Argfs*9) (27.8%)	**29**
21	13814.1	BM	Diagnosis	AML 3		14	43~46,XY,del(15)(q11.2q15)[cp5]/ 46,XY,+mar1[cp2]/46,XY[11]	**8**
22	A485-3	Leuka	Relapse	AML 14		15	46,XY,del(7)(q22q34)[18]/46,XY[1] and FLT3:c.1794_1795insGGAGGAAACTACGTTGATTTCAGAGAGAATATGAA, p.(Glu598_Tyr599insGlyGlyAsnTyrValAspPheArgGluTyrGlu) (5.6%)	**8**
							Total	**129**

Supplemental Table 1. AML samples which successfully yielded AML patient derived iPSC

Table summarizing samples that were successfully reprogrammed and the total number of clones they individually produced. A total of 129 AML patient-derived iPSCs were derived. 7 of the 22 samples were unsuccessful in reprogramming.

Chapter 4: Pluripotent reprogramming of acute myeloid leukemia from heterogeneous patient-specific DNA mutations demonstrates an exclusive block in hematopoietic lineage specification

Preamble

This chapter is unpublished data

AUTHOR CONTRIBUTIONS: D.P.P, M.D, A.Q, D.G and K.V performed experiments. A.E and A.Q aided in image capture of immunofluorescences and cytospins. D.P.P and M.B designed experiments and interpreted the data. D.P.P and M.B wrote the manuscript. M.B directed the study.

Author contributions in greater detail: D.P.P cultured all AML-patient derived iPSCs, and differentiated all iPSC reported in the manuscript to blood, cardiomyocytes and hepatocytes. D.P.P also performed flow analysis, and immunofluorescences staining for cardiomyocytes, early ectoderm and hepatocytes on all iPSC lines described in the manuscript. D.P.P assembled all data, provided interpretation and wrote the manuscript. On occasion M.D, A.Q, assisted with hematopoietic differentiation of iPSCs to increase technical replicates. Specifically, A.Q assisted mainly with OP9 co-culture differentiation and M.D assisted with EHT differentiation. D.G performed EB hematopoietic differentiation on select iPSC lines. A.Q also assisted with flow cytometry, image capture of whole well CFUs and cytospins. K.V performed all neural differentiation and quantification of all immunofluorescent images. A.E assisted with capture of cardiomyocytes and on occasion whole well CFUs and cytospins images.

Pluripotent reprogramming of acute myeloid leukemia from heterogeneous patient-specific DNA mutations demonstrates an exclusive block in hematopoietic lineage specification

Deanna P Porras[1], Meaghan Doyle[1], Amy Qiao[1], Kinga Vojnits[1], Diana Golubeda[1], Amro Elrafie[1] and Mickie Bhatia[1,2]

Addresses
[1]Department of Biochemistry and Biomedical Sciences, McMaster University, Hamilton, ON L8N 3Z5, Canada;

porrasd@mcmaster.ca (D.P.P.)
golubeda@mcmaster.ca (D.G.) or diana.a.golubeva@gmail.com
mdoyle2024@meds.uwo.ca (M.D.)
qiaoa1@mcmaster.ca (A.Q.)
vojnitsk@mcmaster.ca (K.V.) or kinga.vojnits@ubc.ca
elrafiea@mcmaster.ca (A.E)
mbhatia@mcmaster.cas

[2]Michael G. DeGroote School of Medicine, McMaster University, 1200 Main Street West, MDCL 5029, Hamilton, ON L8N 3Z5, Canada

[*]Correspondence: mbhatia@mcmaster.ca; Tel: +1-(905)-525-9140 (ext. 28687)

RUNNING HEAD TITLE: Human AML-iPSCs regain leukemic characteristics upon differentiation

AUTHOR CONTRIBUTIONS:

1. Deanna P Porras: Conception and design, collection and/or assembly of data, data analysis and interpretation, manuscript writing, final approval of manuscript
2. Meaghan Doyle: Collection and/or assembly of data, data analysis and interpretation
3. Diana Golubeva: Collection and/or assembly of data, data analysis and interpretation
4. Amy Qiao: Collection and/or assembly of data, data analysis and interpretation
5. Kinga Vojnit: Collection and/or assembly of data, data analysis and interpretation
6. Amro Elrafie: Collection and/or assembly of data
7. Mickie Bhatia: Conception and design, financial support, administrative support, provision of study material or patients, manuscript writing, final approval of manuscript

KEYWORDS (3-10 keywords)

1. acute myeloid leukemia (AML),
2. induced pluripotent stem cell (iPSC)
3. AML-induced pluripotent stem cell (AML-iPSC)
4. Hematopoietic differentiation
5. Pluripotent differentiation

Abstract

Acute myeloid leukemia (AML) represents a cancer of the myeloid lineages of the hematopoietic system. Design of targeted therapeutics for AML requires an understanding of the impact of patient-specific DNA aberrations among inter and intra-heterogeneous disease. Here, we underwent a campaign to fully characterize the hematopoietic development of a library of induced pluripotent stem cells (iPSCs) derived from AML patients harboring leukemic mutations. Of 20 iPSC lines interrogated, 18/20 demonstrated a block in hematopoietic differentiation measured by phenotypic and functional colony-forming unit (CFU) assays. A smaller subset of 2/20 AML-iPSC lines harbouring cytogenetic mutations originating from donor patient disease cells, demonstrate hematopoietic differentiation capacity to similar degrees as healthy iPSCs or iPSCs derived from AML patients devoid of DNA aberrations. This pattern of hematopoietic differentiation was consistent across three distinct hematopoietic differentiation methodologies, including cytokine-treated embryoid bodies, endothelial-hematopoietic transition induction and stromal co-culture. The AML-iPSCs blocked in hematopoietic differentiation were fully competent for lineage differentiation representing ectodermal and endodermal germ layers, and other lineages derived from mesoderm, indicating the defect in pluripotent cell fate potential was hematopoietic lineage specific. These findings were observed using isogenic AML-iPSCs lines from the same patient, suggesting a blockade in hematopoietic differentiation involves mechanisms that are not affected by genomic background. Our study reveals a hematopoietic differentiation block of AML-iPSCs, akin to enhanced hematopoietic capacity from iPSC derived from hematopoietic cord blood cells, raising the possibility that AML specific epigenetic control is retained within AML-iPSCs.

1. INTRODUCTION

The ability to generate iPSCs from human somatic cells provided a breakthrough in biomedicine (Takahashi et al. 2007) to genetically capture diseased cells and their entire genome in a self-renewing state. It has been reproducibly established that human iPSCs can be generated from somatic blood or skin cells by forced expression of the Yamanaka factors OCT4, SOX2, KLF4, and MYC (Takahashi and Yamanaka 2006; Takahashi et al. 2007). Resulting pluripotent cells retain the somatic cell genome, including genetic lesions/variations. Several groups have demonstrated a preservation of somatic tissue-specific DNA methylation of established human iPSC (J.-H. Lee et al. 2014; Kim et al. 2010; Nazor et al. 2012; Bar-Nur et al. 2011). Intriguingly, the resulting iPSCs also retain a differentiation bias towards their tissue of origin, which correlates with the preserved epigenetic state of that tissue origin. For example, independent groups have demonstrated a correlation in iPSCs derived from blood cells of enhanced hematopoietic differentiation capacity compared to ESCs or iPSC derived from non-blood cell sources but retain a normal cell fate propensity to other lineages (J.-H. Lee et al. 2014; Kim et al. 2010). This phenomenon has been termed “epigenetic memory” whereby the tissue of origin may influence directed differentiation of the reprogrammed cell.

For cancers such as myeloid leukemia, studies using patient-derived iPSCs to date have suggested the ability to model aspects of the leukemic process (Kotini et al. 2017; Chao et al. 2017; Wesely et al. 2020). However minimal AML-iPSC lines have been generated and are derived from one or two patients, thus not allowing the ability to capture AML patients’ heterogeneity. AML is notoriously heterogenic, with diversity observed at the genetic, epigenetic, and clonal architectural level across clinically distinct AMLs. This leads to difficulty in predicting responses to

chemotherapy and relapse (Cancer Genome Atlas Research Network 2013; Vardiman et al. 2009; Welch et al. 2012; Mardis et al. 2009). Collective international studies show that only 40% of AML patients younger than age 60 survive more than five years (Burnett, Wetzler, and Löwenberg 2011). Although some genomic DNA mutations carry prognostic value and more rarely, reveal potential for targeted therapeutic intervention, their functional contributions to disease initiation, progression, and maintenance remain largely unknown. Thus, it is difficult to target these observed genomic variations towards the development of novel treatment strategies (Döhner et al. 2017; Burnett, Wetzler, and Löwenberg 2011; Grimwade et al. 1998). In addition, many point mutations in AML are loss-of-function mutations, which are difficult to therapeutically modulate (DiNardo and Cortes 2016). Accordingly, model systems able to capture and observe clonal and epigenetic diversity of AML disease evolution would need to be established to gain a better molecular understanding of the molecular basis of AML disease.

Despite the technical challenge of reprogramming human cancer cells due to the high inefficiency of the process compared to healthy samples (J.-H. Lee, Salci, et al. 2017; Muñoz-López et al. 2016), we have recently established an unprecedented library of 77 AML-induced pluripotent stem cell (AML-iPSC) lines (Golubeva, D. 2022 *Reprogramming of Acute Myeloid Leukemia Patients Cells Harboring Cancer Mutations Requires Targeting of AML hierarchy*. Biochemistry & Biomedical Sciences, McMaster University). From the patient cohort used, AML-iPSC clones were confirmed to possess leukemic-specific genetic aberrations specific to the patient samples used to derive the iPSCs. These efforts also provided aberration-negative iPSCs from a subset of same AML patients, providing an invaluable genomic isogenic control for direct molecular comparisons independent of background DNA. The total collection was derived from 15/20 AML patients, extending our capture of intra- and inter-patient heterogeneity. Here, we sought to functionally interrogate AML-iPSC lines from the library in attempt to determine the cell fate potential from a pluripotent state including, specifically, the hematopoietic differentiation capacity of the iPSCs, as AML pathophysiology is defined by perturbations in lineage specification.

2. MATERIALS AND METHODS

2.1 Reprogramming of Primary AML Samples

Over 130 iPSC lines were generated from a genetically diverse set of 20 AML patients (Golubeva, D. 2022 *Reprogramming of Acute Myeloid Leukemia Patients Cells Harboring Cancer Mutations Requires Targeting of AML hierarchy*. Biochemistry & Biomedical Sciences, McMaster University). Patient-derived iPSCs that retained the original patient mutations and cytogenetic abnormalities were classified as AML-iPSCs (aberration positive). A subset of patient iPSC lines did not demonstrate the original abnormalities, termed isogenic iPSCs (aberration negative), and one patient generated both, termed paired (Isogenic iPSCs & AML-iPSCs). Mobilized peripheral blood iPSCs (MPB iPSCs), cord blood iPSCs (CB iPSCs) and the human embryonic stem cell (hESC) line H9, were used as healthy control human pluripotent stem cells (hPSCs).

2.2 hPSC Culture

All hPSC cell lines were maintained in an undifferentiated state and passed every 7 days onto a layer of irradiated mouse embryonic fibroblasts (iMEF) in medium that contains DMEM-F12, KnockOut Serum Replacement (KOSR), 1 mM non-essential amino acids (NEAA), 1 mM L-glutamine, and β-mercaptoethanol (SR medium). In a subset of experiments, hPSCs were

transitioned to mTeSR media (Stem Cell Technologies, Vancouver, BC, Canada) and maintained on matrigel with daily media changes. hPSC colonies cultured in mTeSR media were dissociate with 0.05% Trypsin for 5 min at 37 °C, pipetted thoroughly with p1000 to form small aggregates, and subsequently washed twice with PBS + 2% FBS media for further experimentation. Experiments were performed using human ESC line H9, MPB-iPSC, and AML patient derived iPSCs previously reported (Golubeva, D. 2022 *Reprogramming of Acute Myeloid Leukemia Patients Cells Harboring Cancer Mutations Requires Targeting of AML hierarchy*. Biochemistry & Biomedical Sciences, McMaster University). In a subset of experiments, CB-induced PSCs (J.-H. Lee et al. 2014) were additionally tested. Daily morphological evaluation of cells was performed with light microscopy with routine monitoring of pluripotency marker expression (TRA-1-60 and OCT4) by flow cytometry.

2.3 Hematopoietic differentiation using embryoid body formation

hPSCs were first overlayed with matrigel prior to embryoid bodies (EB) formation. On day 0 of EB formation, cells were treated with 200 U/mL collagenase IV (Invitrogen, Burlington, ON, Canada), scraped into clumps, and transferred into EB suspension culture as previously described (Chadwick et al. 2003). EB medium consisted of KO-DMEM, 20% FBS, 1 mM NEAA, 1 mM L-glutamine, and 0.1 mM β-mercaptoethanol and aggregates were allowed to form overnight at 37°C in normoxic conditions (5% CO_2). On day 1, EB's were collected into 50 mL centrifuge tubes and spun for 5 minutes at 129 g. The pellet was resuspended in EB medium supplemented with a cocktail of hematopoietic growth factors (300 ng/mL SCF, 300 ng/mL FLT3L, 10 ng/mL IL-3, 10 ng/mL IL-6, 50 ng/mL G-CSF) and BMP-4 (25 ng/mL). Media supplemented with the cytokine cocktail was changed every 4 to 5 days until day 21 when cells are collected and prepared for analysis. On the day of harvest, EBs were incubated with Collagenase B for 2 hours at 37 °C at 5% CO_2 before being centrifuged and incubated with cell dissociation buffer for 10 minutes in a 37°C water bath. PEF media, consisting of PBS with 3% FBS and 1mM EDTA, was used to wash cells which were then filtered through a 100 μM cell strainer, counted, and stained with antibodies for flow cytometry or used to perform colony-forming unit (CFU) assays.

2.4 Endothelial-to-hematopoietic transition (EHT) hematopoietic differentiation

hPSCs were treated with SR media supplemented with 10 μM Y-27632 for 1 hour before being harvested using TrypLE Select Enzyme. The single cells were collected using a differentiation medium composed of 75% IMDM, 25% DMEM, 0.5x N-2 supplement, 0.5x B-27 supplement minus Vitamin A, 0.28 mM ascorbic acid, 0.46 mM monothioglycerol, 0.09 mM folic acid, and 0.05% AlbuMAX I, and counted to seed 6,000 cells per 100 μL in a 96-well ultra-low attachment plate. The plates were centrifuged at 1500 rpm for 5 minutes to generate spin EBs. As previously reported (Reid et al. 2018), upon personal communication with Dr. Lee, ascorbic acid (0.28 mM) and folic acid (0.09 mM) were used at concentrations lower than originally reported (J. Lee et al. 2017). 10ng/mL BMP-4, 50ng/mL VEGF, 25ng/mL bFGF, and 3ng/mL Activin A were added at indicated days as previously described (J. Lee et al. 2017). On day 4, EBs were dissociated into single cells using TrypLE Select Enzyme and plated onto fibronectin-coated 6-well tissue culture-treated plates. Fibronectin is a large macromolecular glycoprotein that provides anchorage for fibroblasts and hematopoietic progenitor cells and is a proliferative stimulus in vitro (Weinstein et al. 1989). Differentiation medium was supplemented with 500 uM 8-bromo-cyclic AMP sodium salt, 25 ng/mL bFGF, 10 ng/mL BMP-4, 10 μM SB431542, and 50 ng/mL VEGF. On day 10, the basal medium was switched to StemSpan SFEM supplemented with 500 uM 8-bromo-cyclic AMP

sodium salt, 100 ng/mL Flt3L, 100 ng/mL SCF, 20 ng/mL IL-6, and 50 ng/mL TPO until day 12 where only non-adherent cells were collected using PEF medium for phenotypic analysis via flow cytometry or CFU assays. All reagents were purchased from the suppliers listed in the original study.

2.5 OP9 Stromal cell line coculture for hematopoietic differentiation

OP9 cells were plated onto gelatinized 10 cm dishes in the OP9 growth medium as previously described (Choi, Vodyanik, and Slukvin 2011). After the OP9 dishes became confluent, the medium was changed, and the cells were cultured for an additional 10 days with medium changes occurring every 3 to 4 days to form a dense monolayer embedded in the extracellular matrix. For hematopoietic differentiation, two wells of undifferentiated iPSC lines were treated with 1 mg/mL of collagenase IV for 10 minutes before being collected as small cell aggregates by scraping. The hPSC cells were passaged as clumps on to over-confluent OP9 at a density of 1.0×10^6 cells per 10 cm dish in the differentiation medium of α-MEM, 20% FBS, 1 mM NEAA, 1 mM L-glutamine, 100 μM monothioglycerol, and 0.1 mM β-mercaptoethanol. The cocultures were incubated for 12 days at 37 °C in normoxic conditions (5% CO_2) with half-medium changes occurring on days 4, 6, 8, and 10. Single-cell suspension was done on day 12 by treating the cocultures with collagenase IV for 40 minutes at 37 °C, followed by treatment with 0.05% trypsin / 0.5 mM ethylenediaminetetraacetic acid (EDTA) for 15 minutes at 37 °C. Preparation for phenotypic analysis and functional analysis was performed as previously described (Reid et al. 2018).

2.6 Flow Cytometry

Single-cell suspensions in PEF media were stained with antibodies specific for CD31, CD34, CD43, and CD45 (Table 1). Live cells were distinguished from dead cells using 7-Aminoactinomycin D (7-AAD). Fluorescence Minus One (FMOs) were used as negative controls for accurate gating of positive populations. Data was collected using CytoFLEX Flow Cytometer and analysis was performed using FlowJo software (version 10.8.0).

Table 1. Primary Antibodies

Name	Fluorochrome	Company	Catalogue Number
Mouse Anti-Human CD31	FITC	BD Bioscience	555445
Mouse Anti-Human CD34	PE	BD Bioscience	550761
Mouse Anti-Human CD43	APC	BD Bioscience	560198
Mouse Anti-Human CD45	V450	BD Bioscience	642275
Mouse Anti-Human CD45	Pacific-Blue	Invitrogen	69-0451-82

2.7 Colony-forming unit (CFU) assay

CFU assays were performed in 6- or 12-well non-treated plates using 2 or 0.5 mL/well of MethoCult H4434 Classic semi-solid medium consisting of methylcellulose, FBS, bovine serum albumin (BSA), β-mercaptoethanol, stem cell factor (SCF), interleukin 3 (IL-3), erythropoietin (EPO), and granulocyte-macrophage colony-stimulating factor (GM-CSF). Cells from all three methodologies were plated at a density of 50,000 cells/well in either duplicate or triplicate on day 21 for the EB hematopoietic protocol and day 12 for both the 2D cytokine (EHT differentiation)

and OP9 coculture hematopoietic protocol. Cells were incubated at 37 °C for 14 days and manually scored based on their colony morphology as granulocyte (CFU-G), macrophage (CFU-M), granulocyte-macrophage (CFU-GM), erythroid (CFU-E), and megakaryocyte (CFU-GEMM) colonies. CFUs were stained with calcein green (Invitrogen) in Hank's Buffered Salt Solution (HBSS) for 30 min and imaged with the Operetta High Content Imaging System (PerkinElmer). Whole-well images were stitched in Columbus Image Data Storage and Analysis System version 2.9.0 (Perkin Elmer). A minimum of 40 cells was required for designation as a colony.

2.8 Cytospins

Cells were collected from CFU assays for morphological analysis by plucking individual colonies using a 200 µL pipette and spun onto glass slides using the Shandon Cytospin 3 cytocentrifuge (Block Scientific, Inc). Differential staining was performed with Shandon Kwik-Diff Stain Kit (Thermo Scientific) following the manufactures instructions. Images taken were analyzed using ImageScope.

2.9 Neural Differentiation

For neural differentiation, hPSCs clones were harvested by collagenase IV treatment and EBs were generated with EB medium without cytokines. 24 hours after suspension culture, EBs were plated onto poly-L-lysine/laminin-coated plates (BD Biosciences) in neural differentiation medium composed of DMEM/F12 supplemented with B27 and N2 (Thermo Fisher Scientific), EGF (25 ng/ml, R&D Systems), and bFGF (8 ng/ml). Cell culture medium was changed every 3 days. After 10 days, neurospheres were collected, dissociated into single cells by Accutase treatment and plated onto poly-ornithine and laminin coated plates. For mature neuron differentiation, cells were cultured in Neurobasal medium supplemented with N2 (1%), B27-RA (2%), non-essential amino acids (1%), brain-derived neurotrophic factor (20 ng/mL), glial cell-derived neurotrophic factor (20 ng/mL), dibutyryl cyclic adenosine monophosphate (1 uM), and ascorbic acid (200 uM). Cells were cultured for 15 days with half media change every other day.

2.10 Hepatocytic differentiation

For hepatocyte differentiation, mTeSR-cultured hPSCs were dissociated, as described above. hPSCs were subsequently seeded onto Matrigel-coated plates, and then cultured for 5 days with 8 ng/ml bFGF and then replaced with RPMI supplemented with 1 x B27, activin 1 (100 ng/ml), hepatocyte growth factor (10 ng/ml) and 1 mM CHIR99021 (GSK3 inhibitor) for 3 days of endoderm formation as previously described (Chen et al. 2012). Medium was subsequently replaced with knockout-DMEM with 20% knockout-SR, 1 mM L-glutamine, 1% nonessential amino acids, 0.1 mM β-mercaptoethanol and 1% dimethyl sulfoxide for 4 days. For hepatocyte maturation, the cells were cultured in hepatocyte maturation media consisting of Iscove's modified Dulbecco's medium (IMDM) containing 20 ng/ml Oncostatin M, 0.5 mM dexamethasone and 50 mg/ml ITS premix as previously reported (J.-H. Lee et al. 2014; Chen et al. 2012).

2.11 Cardiomyocyte differentiation

Cardiomyocyte differentiation was performed based on a previous report (J.-H. Lee, Laronde, et al. 2017; Takashima et al. 2014). Briefly 10,000 cells were plated per U-bottom well in MEFCM containing 8 ng/mL bFGF and 10 µM Y-27632. At day 3 media was replaced with DMEM/F12, 20% FBS, 1 mM L-glutamine, 1 mM NEAA, 0.1 mM β-mercaptoethanol, and 50 ug/mL ascorbic

acid. Aggregates were seeded on gelatin-coated wells at day 7 and differentiation medium was changed every 2 days.

2.12 Immunofluorescence

Briefly, cells were fixed in 4% paraformaldehyde and stained with appropriate antibodies. If permeation was needed, cells were fixed using the BD Cytofix/Cytoperm kit (BD Bioscience) and then stained in perm/wash buffer (BD Biosciences) according to the manufacturer's instructions with the following Abs: Smooth Muscle Actin 1:100 (Millipore), FOXA2 1:100, GATA4 1:100 and *β*-Tubulin-III 1:100. Unconjugated antibodies were visualized with appropriated Alexa fluorochrome conjugated secondary antibodies (1:1000).

2.13 Image Analysis

Neurite outgrowth was analyzed using the NeuronJ plugin (Meijering et al. 2004) from the ImageJ package Fiji (Schindelin et al. 2012). NeuronJ is a commonly used tool for semiautomatic tracing and measurement of neurites in ImageJ and is faster than manual tracing without sacrificing accuracy (Meijering et al. 2004). Images to optimize tracing were first prepared and saved as 8-bit images (NeuronJ can only read 8-bit images). To confirm that neurites stand out against the background the contrast of images were adjusted. To correct the uneven background, the "Subtract Background" command using a rolling ball with a radius of *N* pixels (*N* is a constant 50 in this study) is applied to the original image. Tracing was done by selecting the *add tracings* button and performed from the starting point of the neurite and branches. After all neurites were traced and labelled with distinct colors, they were measured by selecting the *Measure tracings* icon.

To quantify and compare successful endoderm and mesoderm differentiation, the percentage of cells in a sample stained with the fluorescent probe of interest was quantified by using ImageJ Analyze Particles Measure Plugin. Contrast of images was adjusted, and uneven background corrected with the "Subtract Background" command using a rolling ball with a radius of *N* pixels (*N* is a constant 50 in this study) was applied to the original image. After threshold selection, watershed function, and size and circularity adjustment, single cells were measured and number, area, size, and intensity density reported.

2.13 Statistical analysis

Statistical analysis was performed with GraphPad Prism version 6 software. Comparisons between different groups were performed using a one-way analysis of variance (ANOVA) test and Tukey multiple comparison test or a two-way analysis of variance (ANOVA) test and Tukey multiple comparison test. A $P < 0.05$ was considered statistically significant for all analyses and all data are reported with the mean ± standard error of the mean (SEM). In select figures, flow cytometry and CFU data are shown as normalized relative to the control healthy iPSCs.

3. RESULTS

3.1 The majority of AML-iPSCs lack hematopoietic differentiation capacity compared to healthy iPSCs or iPSC devoid of leukemic aberrations from AML patients

To validate a portion of our novel AML-iPSCs library (Figure 1A) (Golubeva, D. 2022 *Reprogramming of Acute Myeloid Leukemia Patients Cells Harboring Cancer Mutations Requires*

Targeting of AML hierarchy. Biochemistry & Biomedical Sciences, McMaster University), the previously reported ability of AML-iPSCs to maintain features of their cells of origin (Kotini et al. 2017; Chao et al. 2017; J.-H. Lee, Salci, et al. 2017) was assessed by performing hematopoietic differentiation assay (Supplemental Figure 1A). Using an established protocol (Chadwick et al. 2003), we assessed the differentiation capacity of a selection of aberration negative iPSC lines and aberration positive iPSC lines to generate primitive hematopoietic progenitor cells detected by human-specific $CD34^+/CD45^+$ expression and mature blood ($CD45^+$) using flow cytometry (Figure 1B-E).

To establish a unique genotype-to-phenotype connection of differentiated AML patient-derived iPSC lines, we first performed hematopoietic differentiation on iPSC lines from unrelated healthy individuals to determine a baseline of hematopoietic differentiation potential (Supplementary Figure 1). Since line-to-line variation in phenotypes and other cellular and molecular properties can pose trouble in the field of disease modeling with iPSCs, we sought to overcome this concern by implementing appropriate controls, sufficient replicates, and robust interrogation of various hematopoietic phenotypic populations. Specifically, we assessed a mobilized peripheral blood iPSC (MPB-iPSC) and neonatal cord blood iPSC (CB-iPSC) lines for the presence of hemogenic precursors ($CD34^+/CD31^+$), primitive blood cells marked by human specific $CD34^+/CD45^+$ and mature blood ($CD45^+$) using flow cytometry. Importantly, all healthy hPSC control lines demonstrated equivalent frequencies of all phenotypic populations quantified (Supplemental Figure 1B) and colony forming unit (CFU) progenitor output and lineage distribution (Supplemental Figure 1C) respectively. These results are consistent with previous reports across a broad range of methodologies to produce phenotypic or functional progenitors from hPSCs (Doulatov et al. 2013; J.-H. Lee, Salci, et al. 2017; Reid et al. 2018). Additionally, we routinely observed similar hPSC-derived hematopoietic CFU morphology across healthy control lines when cultured for 14 days in vitro (Supplemental Figure 1D & 1E).

Altogether, three of eight AML patients in which aberration negative iPSC lines were solely derived (Figure 1B), and five of five different AML patients, of which aberration positive iPSCs lines were solely derived (Figure 1C), underwent hematopoietic differentiation. To account for potential phenotypic variation due to genetic background, multiple iPSC lines from the same individual were contrasted to lines from different patients. For example, AML 4 (AML 16150), in which a total of 10 aberration negative iPSC lines were derived (Figure 1A), had three representative lines undergo differentiation in comparison to AML 5 (AML A151.1) and AML 11 (A320-1) in which only one iPSC line was differentiated per patient (Figure 1B). Similarly, multiple aberration positive iPSC lines from the same AML patient were differentiated and compared to multiple aberration positive iPSC lines from different patients, allowing both intra-patient and inter-patient variation interrogation (Figure 1C). Aberration negative iPSC lines demonstrated no hematopoietic phenotypic variation across multiple hematopoietic populations in comparison to healthy hPSC lines (Figure 1B & 1D; grey iPSC lines in comparison to the dashed line representing healthy control hPSCs), except for AML 11 clone 11-1 which demonstrated a lower frequency of hematopoietic progenitor cells. Additionally, no intra-patient variation was observed among the three aberration negative iPSC lines of AML 4 (Figure 1B & 1D; AML 4 clones 4-1 to 4-3). Excluding the outlier clone (AML 11-1), these results suggest that any epigenetic memory retention of the cellular origin of the established iPSC is presumably normal and similar, if not the same, as healthy hPSCs. In contrast to aberration negative iPSC lines, majority of aberration positive iPSC lines failed to develop into primitive or mature blood cells (Figure 1C & 1E), apart from AML 1 clone 1-5 which demonstrated a superiority in terms of

mature blood formation in comparison to healthy hPSCs (Figure 1E). This failure of majority of AML-iPSCs is reminiscent of the hematopoietic blockade observed in AML characterized by an inability to generate mature blood cells.

We next assessed the progenitor capacity of AML patient derived iPSCs by performing functional colony-forming unit (CFU) assays. Consistent with the phenotypic results, aberration negative iPSCs demonstrated functional hematopoietic differentiation capacity to similar degrees amongst both healthy lines and other aberration negative iPSC lines, again with the exceptions of AML 11 clone 11-1 (Figure 1F). When assessing the CFU progenitor capacity of iPSCs that retain the original patient mutations and cytogenetic abnormalities, referred to as aberration positive iPSCs, we again found a significantly reduced progenitor capacity in majority of AML-iPSCs in comparison to healthy hPSCs (Figure 1G). The impaired hematopoietic differentiation of multiple AML-iPSC clones is not surprising as it has been reported previously (J.-H. Lee, Salci, et al. 2017; Kotini et al. 2017). However, this poses an interesting question of whether the hematopoietic differentiation block is a result of genetic or epigenetic components that are also responsible for the lack of complete myeloid differentiation similar to the primary disease. Intriguingly, one AML-iPSC line from patient A374.1 (AML 1-5) displayed similar $CD34^+/CD45^+$, superior total $CD45^+$ phenotypic frequencies of hematopoietic potential (Figure 1C & 1E; AML 1-5), and robust progenitor activity in comparison to healthy hPSCs (Figure 1G; AML 1-5). Moreover, in select AML-iPSC in which a reduced progenitor capacity was observed, a myeloid restricted phenotype was observed, as little to no erythroid CFUs were detected (Figure 1G). Whereas aberration negative iPSC and control hPSCs gave rise to both myeloid and erythroid colonies (Figure 1F). Overall, this data suggests that in patient-derived iPSCs in which the leukemic aberration is retained (AML-iPSC), hematopoietic differentiation capacity is compromised and that this is presumably due to genetics, epigenetics, or a combination of the two.

3.2 Functional leukemic progenitors can be derived from AML-iPSC and demonstrate self-renewal capacity measured by serial replating

Though majority of AML-iPSCs displayed undetectable to negligible functional progenitor potential, measured by CFU, select clones did have a sufficient number of colonies to interrogate. Specifically, colonies derived from AML 17 (A472-1) and AML 21 (A472-3) iPSCs lines. In order to prove that colonies arising from hematopoietic differentiation of AML-iPSC clones were bonafide leukemic progenitors and not healthy cells, individual colonies were collected from methylcellulose after the progenitor CFU assay and genomic DNA was extracted using QIAamp DNA Micro Kit (QIAGEN) according to the manufacturer's instructions (Figure 2A). Prior to plucking colonies, the hematopoietic functional capacity of select AML-iPSC clones was captured by whole-well CFU images by means of calcein green am staining (Figure 2B). Droplet PCR was then performed on individual CFU-Monocyte/macrophage (CFU-M) colonies derived from AML A472-3 AML-iPSC clones (21-1, 21-3, 21-4) and AML A472-1 AML-iPSC clones (17-2). Figure 2C depicts Variant Allele Frequency (VAF) for droplet PCR results probing for ASXL1:c.2725A>T and IKZF1:c.476A>G on 3-4 individual CFU-M colonies (M1-M4) per AML-iPSC clone. Notably, individual CFU-M colonies have similar VAFs to that of primary patient sample AML 17-A472-3 and AML 21-A472-1 (Figure 2C). Whereas CFU-M colonies arising from a healthy hESC H9 line did not contain either mutation. These results correspond with the original mutations detected in AML-iPSC previously reported (Golubeva, D. 2022 *Reprogramming of Acute Myeloid Leukemia Patients Cells Harboring Cancer Mutations Requires Targeting of AML hierarchy*. Biochemistry & Biomedical Sciences, McMaster University), thus

demonstrating that the hematopoietic progeny derived from AML-iPSCs retain the original patient mutations and cytogenetic abnormalities. In addition, we observed the reestablishment of leukemic features in the cellular morphology of hPSC-derived hematopoietic cells from AML-iPSC clones, mirroring *de novo* AML (Figure 2D). We next assessed whether hematopoietic cells derived from AML-iPSC can give rise to secondary CFU's (Figure 2E), which could suggest that a leukemic stem/progenitor cell population may be present via a serial replating assay. Cells were plated in semisolid methylcellulose media following established protocols (Salci et al. 2015). On day 14, progenitor capacity of leukemic progenitors derived from AML-iPSC clones were evaluated in comparison to control iPSCs by collecting the whole well of primary CFU and re-seeding cells into fresh methylcellulose media for an additional 14 days. In line with previous reports (Chao et al. 2017), AML-iPSC colonies successfully replated and produced primary and secondary CFUs, suggesting a more extensive proliferative potential of HSPCs in comparison to healthy hPSCs which are devoid of progenitor self-renewal ability, and failed to generate secondary CFU's (Figure 2F).

3.3 Paired Leukemic & Isogenic-iPSCs Exhibit Differential Hematopoietic Differentiation Patterns

We next sought to assess iPSCs derived from a single AML patient in which both aberration negative and aberration positive iPSCs were generated (AML 3 – 13814.1; Figure 1A) allowing simultaneous interrogation of both intra-patient variation and paired isogenic and AML-iPSCs. Two of two aberration negative iPSCs (isogenic) and two of six aberration positive (AML-iPSCs) derived from AML 3 – 13814.1 underwent our established hematopoietic differentiation assay (Chadwick et al. 2003) (Supplemental Figure 1A). Intriguingly, despite harbouring cytogenetic mutations found in the primary AML sample, AML 3 clone 3-1 demonstrated hematopoietic differentiation capacity to similar degrees as both Isogenic-iPSCs line (clone 3-3 and 3-4) & healthy hPSCs in contrast to AML 3 clone 3-2 which demonstrated an attenuation in differentiation capacity measured by negligible hematopoietic progenitor and mature blood cell frequency (Figure 3 A & B), indicative of our predicted hematopoietic blockade. In line with the phenotypic differentiation capacity previously observed from aberration negative iPSC (Figure 1B & 1D), AML 13814.1 clone 3-3 and 3-4 (both absent for a leukemic aberration) also resembled normal hematopoietic differentiation (Figure 3A & 3B). These findings were also consistent when assessing functional hematopoietic progenitor capacity where healthy lines and aberration negative iPSC lines displayed similar degrees of mixed lineage CFUs (Figure 3C). However, consistent with the phenotypic results, the aberration positive AML-iPSC line clone 3-1 again displayed hematopoietic progenitor potential on par with healthy hPSCs whereas it's matched cytogenetic clone (3-2) demonstrated an aberrant myeloid-restricted colony phenotype (Figure 3C), suggesting in some cases that these mutations do not play a lasting role in AML disease behaviour. We next examined whether our paired AML-iPSC lines would demonstrate a morphological discrepancy in the HSPCs derived. In lieu of maintaining the cancerous genetic lesion(s) of the primary patient sample, AML 3-1 did not appear to phenocopy a blast-like morphology akin to the primary AML and exhibited more features of myeloid maturation, similar to its paired isogenic iPSC lines, suggesting an absence of leukemic differentiation blockade (Figure 3D). AML 3-2 however, displayed more leukemic features. These observations suggests that despite retaining oncogenic lesions of the primary AML, paired malignant AML-iPSCs exhibit differential hematopoietic capacity suggesting that any blockade in hematopoietic differentiation results from an aberrant hematopoietic-specific transcriptional program and/or aberrant chromatin landscape captured in

select AML-iPSCs. Moreover, this data highlights the uniqueness of individual iPSC clones that allow potential characterization of separable inter- and intra-patient clones that are expandable.

3.4 AML-iPSCs retain germ layer differentiation capacity in vitro for non-hematopoietic lineages

To investigate whether AML-iPSCs give rise to normal, non-tumorigenic cell types in the presence of various cytogenetic aberrations retained during reprogramming, we differentiated paired isogenic and AML-iPSC clones into neural (ectoderm), hepatocytes (endoderm) and cardiomyocytes (mesoderm) (Figure 3A). Neural lineage differentiation was evaluated in two stages; the initial analysis encompassed formation of neural tube-like rosette structures within 5-7 days of differentiation followed by differentiation into neurons, which represent one of three major cell types found in the central nervous system (Reynolds and Weiss 1992; Zhang et al. 2001). All clones tested successfully gave rise to neural precursors (rosette cells; data not shown) as well as expressed the pan-neuronal marker βIII Tubulin to similar levels to that of control healthy mobilized peripheral blood iPSCs (MPB-iPSCs) and the hESC line H9's when qualitatively assessed (Figure 3B). We also differentiated additional AML-iPSC lines independent of the paired sample and found no observable differences in neural differentiation capacity in comparison to control hPSC lines (Supplemental Figure 2A). Next, paired iPSCs were differentiated into hepatocytes through culture in endoderm supportive media followed by hepatocyte maturation media containing hepatocyte growth factor as previously described (J.-H. Lee et al. 2014; Chen et al. 2012). No clear expression differences were observed for early lineage-associated markers, FoxA2 and GATA4, between healthy PSC controls and AML patient derived iPSCs (Supplemental Figure 2B), or the early hepatocyte marker Alpha-fetoprotein (AFP) (Figure 3D & Supplemental Figure 2C).

Since AML is well known to have an aberrant epigenetic state (Figueroa et al. 2009; 2010) and it has been proposed that iPSCs retain a memory of the tissue of origin (J.-H. Lee et al. 2014; Kim et al. 2010), which in this case is AML, it is possible that despite gaining pluripotency, AML-iPSCs retain an aberrant leukemic epigenetic state which interferes with differentiation programs independently or in combination with genetic mutations specific to the mesodermal lineage. Notably, we demonstrated an aberrant hematopoietic potential in select AML-iPSC (Figure 1 & 2) and thus sought to differentiate our library to another meso-derived tissue, specifically cardiomyocytes. All AML patient-derived iPSCs were differentiated based on a previous report whereby embryoid body aggregates are seeded on gelatin-coated wells at day 7 of differentiation and subsequently cultured in cardiomyocyte-specific supportive media (Takashima et al. 2014). Both paired isogenic and AML-iPSCs (Figure 4D), as well as multiple iPSC lines per patient per AML patient-derived iPSC lines (Supplementary Figure 3), yielded qualitatively similar expression levels of smooth muscle actin (SMA) in comparison to healthy control PSCs.

Since we interrogated the lineage differentiation potential of additional AML-iPSC lines in (Supplemental Figure 2 & 3) in combination with our paired iPSC lines, we quantitively assessed all three germ layers and again observed that both neurite total length and neurite number, amongst aberration negative iPSC, aberration positive iPSCs (AML-iPSCs) and healthy hPSC control lines revealed no distinction amongst differentiation capacity (Figure 3E). Consistent with the ectoderm germ layer differentiation potential, no distinct differentiation capacity was observed amongst quantification of AFP^+ cells (Figure 3D) and SMA^+ cells (Figure 3E) indicating that these cultures are capable of normal differentiation down non-hematopoietic lineages. Overall, this data, in combination with the distinct hematopoietic blockade observed in the majority of AML-iPSCs,

highlights the potential of an aberrant epigenetic landscape captured within AML-iPSC lines. However, tissue-specific lineage differentiation distinct to the cellular origin of the derived iPSC lines (non-hematopoietic lineages) are unaffected.

3.5 AML-iPSCs are blocked for hematopoietic lineage specification independent of in vitro differentiation induction approach

To further validate our proposed hypothesis of a leukemic epigenetic memory retention within AML-iPSCs line, we decided to perform distinct methodologies to derive hiPSC-HSPCs beyond our previously reported EB cytokines and BMP4 based treatment (Chadwick et al. 2003). Specifically, iPSCs underwent a co-culture with OP9's, the mouse bone marrow stromal line (Choi, Vodyanik, and Slukvin 2011), and a 2D endothelial-hematopoietic transition (EHT) cytokine based protocol (J. Lee, Dykstra, et al. 2017) respectively (Figure 5A & 5B). Mesenchymal stromal cells (MSC) are an important component of the bone marrow hematopoietic stem cell (HSC) niche for homing and long-term maintenance of hematopoiesis through secretion of soluble factors and cell-cell contact (Jing et al. 2010). The advantage of using the OP9 system is that it is efficient in inducing blood formation from iPSCs in a short period of time (9-12 days) and without added cytokines. Similarly, the EHT method developed by the Rossi group is a short 12 day protocol and facilitates the production of hematopoietic progenitor cells by activating hematopoietic transcriptional programs in hemogenic endothelium resulting in a transition to a hematopoietic fate (Canu et al. 2020; Ottersbach 2019). In the protocol reported by Lee et al., mesoderm induction and endothelial specification occur in the first 4 days of hematopoietic differentiation before cells are plated onto fibronectin for adherent culture for endothelial-to-hematopoietic transition. Subsequently, endothelial-like structures produce hematopoietic cells floating in suspension by day 12 of differentiation when subjected to hematopoietic cytokines (J. Lee, Dykstra, et al. 2017). Select AML-iPSC that previously yielded a differential hematopoietic capacity were solely subjected to these additional distinct methodologies. Specifically, AML 1-12 and AML 3-1 AML-iPSC lines in which hematopoietic capacity was on par to healthy hPSCs and aberration negative/isogenic iPSCs, and AML 1-2 and AML 3-2 which displayed a blockade in hematopoietic differentiation (Figure 1 & Figure 3). Despite the cancerous genetic lesion(s) of the primary patient sample being retained within AML-iPSC lines AML 1-12 and AML 3-1, these lines displayed a consistent capacity for hematopoietic differentiation amongst the three methodologies tested for hPSCs (Figure 5C & 5D). Moreover, AML-iPSC lines AML 1-2 and AML 3-2 demonstrated an attenuation in progenitor differentiation capacity measured by lower to absent CFU potential (Figure 5E & 5F) & produced negligible phenotypic hematopoietic differentiation capacity (Figure 5C & 5D) indicative of our predicted hematopoietic blockade from AML-iPSCs. In addition, we again observed leukemic features in the cellular morphology of hPSC-derived hematopoietic cells from AML-iPSC clones in which minimal progenitor CFU-M colonies were produced (Figure 5G) supporting that this was not an artifact of in vitro differentiation. Relative hematopoietic phenotypic and functional capacity was also observed when aberration negative iPSCs were subjected to both methodologies in comparison to control hPSCs (Supplemental Figure 4). Taken together, these results suggest AML-iPSC differentiation blockade is exclusive to the hematopoietic lineage and independent of environmental influences in vitro.

4. DISCUSSION

The concept of an "epigenetic memory" in iPSCs poses the question of whether a leukemic cell epigenome can be similarly retained upon derivation of iPSCs from AML patients. Here, we predicted that resulting AML-iPSCs would manifest an opposite epigenetic memory of iPSC derived from blood cells, e.g., a block in hematopoietic development potential. This block would be like the developmental block of myeloid lineage in AML disease, leading to the clinically observed accumulation of immature cells in AML patients. As AML is a stem cell disease, this inherited block from AML cells would appear differently in resulting iPSCs that are not restricted to hematopoietic stem cell (HSC) potential in the patient but rather stem cells in a pluripotent state. Thus, the blockade would appear at the germ layer (mesoderm) or onset of hematopoietic cell fate decisions in AML-iPSCs. Notably, despite retaining the oncogenic lesion, in this study we show that AML-iPSCs can make non-hematopoietic cell types with seemingly normal morphology and function. This is presumably due to the widespread remodeling of chromatin that occurs upon reprogramming and the establishment of a robust and dominate pluripotent cell state. In contrast, differentiation of these AML-iPSC lines to hematopoietic cells restores their malignant phenotypes. These results highlight that a blockade in hematopoietic differentiation (oncogenic result of AML) requires both a cancerous genome and the appropriate cell lineage, determined by a cell type-specific transcriptional program and/or chromatin landscape that is exclusively captured in majority of AML-iPSCs. Thus, biological differentiation outcomes are likely controlled by lineage-specific programming (not germ layer specification) within AML-iPSCs.

Line-to-line variation in phenotypes troubles utilizing AML-iPSC modeling in the field, but this can be overcome with appropriate controls, sufficient replicates, and robust differentiation protocols, hence our decision to attempt various hematopoietic differentiation protocols to definitively show attenuation in hematopoietic programs of AML-iPSC lines is not an artifact of the methodology used to derive HSPCs. Specifically, we show that the majority of AML-iPSC clones demonstrated attenuation in functional differentiation capacity measured by lower to absent CFU potential & produced negligible phenotypical hematopoietic progenitors and mature blood cells indicative of our predicted hematopoietic blockade from AML-iPSCs. Although intra- and inter-line variation is not unique to the iPSC field, one should keep in mind that every iPSC line comes from a single cell of a starting population, which may or may not be representative of the majority of the population, and that propagation in culture can result in acquisition and propagation of genetic and chromosomal abnormalities that may change cellular properties. Although genetic variation has been shown to be a contributor of differences in differentiation potential and cellular phenotypes among iPSC lines, epigenetic differences – either pre-existing or established during reprogramming – can also contribute to variable behavior among lines of the same genetic composition. Importantly, our results support the notion that an epigenetic memory retained by the primary cell reprogrammed influences a blockade in hematopoietic potential demonstrated by consistent attenuation of hematopoietic potential seen in inter- and intra-patient derived AML-iPSC lines, independent of their respective cytogenetics. Moreover, hematopoietic progeny derived from AML-iPSCs retain primary patient mutations and may display variable levels (lower to absent) of hematopoietic differentiation potential. Taken together, this data highlights the uniqueness that our iPSC clones provide, by allowing for characterization of separable clones and suggest that this model may also capture clonal evolution through malignant transformation of an individual AML patient.

Using our unique library, we were also able to interrogate AML-iPSCs with varying hematopoietic differentiation potential and their paired matching normal/isogenic clones, providing the perfect platform to investigate the mechanisms responsible for the deficiency of

hematopoietic differentiation with potential to link this to the primary patient disease. In particular, we demonstrate that in the presence of leukemic mutations, AML-iPSCs have an aberrant myeloid-restricted phenotype, suggesting that a leukemic epigenetic memory is retained from the cellular origin of established patient-derived hiPSCs phenocopying the primary disease of the established patient-derived hiPSCs. In contrast, isogenic iPSCs, in which there is an absence of leukemic mutations, yielded similar hematopoietic capacity to healthy hPSCs, suggesting a normal/healthy epigenetic memory is retained from the cellular origin. Overall, our current study implicates epigenetic modification of histone status as markers of cellular memory within reprogrammed pluripotent cells.

It is well established that epigenetic modifications comprise a class of heritable, non-genetic methylation, histone modification, and chromatin remodeling (Allis and Jenuwein 2016) and are crucial for cell differentiation and hematopoiesis in healthy hematopoietic stem cells (Rodrigues, Shvedunova, and Akhtar 2021). Abnormalities in epigenetic mechanisms that impair healthy hematopoiesis are thought to play a role in the transformation of normal hematopoietic cells into their leukemogenic counterparts (Hu and Shilatifard 2016). Indeed, epigenetic dysregulation is a recognized characteristic of AML that is implicated in the pathophysiology of the disease (Melnick 2010; Shih et al. 2012). Aberrant DNA methylation, histone modifications, and chromatin accessibility are observed in AML both in the presence and absence of mutations in key epigenetic regulatory factors (Ntziachristos, Abdel-Wahab, and Aifantis 2016; Wouters and Delwel 2016). These observations suggest that epigenetic dysregulation may independently contribute to leukemogenesis. Unfortunately, the reversibility of epigenetic modifications and relative contributions of leukemic genetic and epigenetic programs to pathogenesis in AML are still poorly understood. Given the importance of the epigenome, future studies would benefit from exploring the causative role of leukemic genetic/epigenetic mutations captured in our AML-iPSC library governing the variable hematopoietic differentiation capacity.

AUTHOR CONTRIBUTIONS: AUTHOR CONTRIBUTIONS: D.P.P., M.D., A.Q., D.G. and K.V. performed experiments. A.E. and A.Q. aided in image capture of immunofluorescences and cytospins. D.P.P. and M.B. designed experiments and interpreted the data. D.P.P. and M.P. wrote the manuscript. M.B. directed the study.

ACKNOWLEDGMENTS: We want to thank Ronan Foley, Brian Leber and Anargyros Xenocostas for providing primary human MPB and AML samples that were used for the creation of our AML patient derived iPSC library. We would also like to thank V.K., for assistance with quantification of immunofluorescence images.

FUNDING: D.P.P. was supported by the Jans Graduate Scholarship in Stem Cell Research, the Michael G. DeGroote Doctoral Scholarship, and the Ontario Graduate Scholarship. D.G. was supported by the Jans Graduate Scholarship in Stem Cell Research. J.C.R. was supported by the Canadian Institutes of Health Research (CIHR) Doctoral Award, the Michael G. DeGroote Doctoral Scholarship, and an Ontario Graduate Fellowship. This work was supported by CIHR foundation grant FRN 159925 to MB approved by the Stem Cell Oversight Committee in Canada. M.B. holds the Canada Research Chair Program CRC Tier 1 in Human Stem Cell Biology and the Michael G. DeGroote Chair in Stem Cell Biology.

INSTITUTIONAL REVIEW BOARD STATEMENT: This study and all experimental protocols were conducted in accordance with the Animal Research Ethics Board of McMaster University (AUP: 19-11-29).

DISCLOSURE OF POTENTIAL CONFLICTS OF INTEREST: The authors indicate no potential conflicts of interest.

REFERENCES

1. Allis, C. David, and Thomas Jenuwein. 2016. "The Molecular Hallmarks of Epigenetic Control." *Nature Reviews. Genetics* 17 (8): 487–500. https://doi.org/10.1038/nrg.2016.59.
2. Bar-Nur, Ori, Holger A. Russ, Shimon Efrat, and Nissim Benvenisty. 2011. "Epigenetic Memory and Preferential Lineage-Specific Differentiation in Induced Pluripotent Stem Cells Derived from Human Pancreatic Islet Beta Cells." *Cell Stem Cell* 9 (1): 17–23. https://doi.org/10.1016/j.stem.2011.06.007.
3. Burnett, Alan, Meir Wetzler, and Bob Löwenberg. 2011. "Therapeutic Advances in Acute Myeloid Leukemia." *Journal of Clinical Oncology: Official Journal of the American Society of Clinical Oncology* 29 (5): 487–94. https://doi.org/10.1200/JCO.2010.30.1820.
4. Cancer Genome Atlas Research Network. 2013. "Genomic and Epigenomic Landscapes of Adult de Novo Acute Myeloid Leukemia." *The New England Journal of Medicine* 368 (22): 2059–74. https://doi.org/10.1056/NEJMoa1301689.
5. Canu, Giovanni, Emmanouil Athanasiadis, Rodrigo A. Grandy, Jose Garcia-Bernardo, Paulina M. Strzelecka, Ludovic Vallier, Daniel Ortmann, and Ana Cvejic. 2020. "Analysis of Endothelial-to-Haematopoietic Transition at the Single Cell Level Identifies Cell Cycle Regulation as a Driver of Differentiation." *Genome Biology* 21 (1): 157. https://doi.org/10.1186/s13059-020-02058-4.
6. Chadwick, Kristin, Lisheng Wang, Li Li, Pablo Menendez, Barbara Murdoch, Anne Rouleau, and Mickie Bhatia. 2003. "Cytokines and BMP-4 Promote Hematopoietic Differentiation of Human Embryonic Stem Cells." *Blood* 102 (3): 906–15. https://doi.org/10.1182/blood-2003-03-0832.
7. Chao, Mark P., Andrew J. Gentles, Susmita Chatterjee, Feng Lan, Andreas Reinisch, M. Ryan Corces, Seethu Xavy, et al. 2017. "Human AML-IPSCs Reacquire Leukemic Properties after Differentiation and Model Clonal Variation of Disease." *Cell Stem Cell* 20 (3): 329-344.e7. https://doi.org/10.1016/j.stem.2016.11.018.
8. Chen, Yu-Fan, Chien-Yu Tseng, Hsei-Wei Wang, Hung-Chih Kuo, Vincent W. Yang, and Oscar K. Lee. 2012. "Rapid Generation of Mature Hepatocyte-like Cells from Human Induced Pluripotent Stem Cells by an Efficient Three-Step Protocol." *Hepatology (Baltimore, Md.)* 55 (4): 1193–1203. https://doi.org/10.1002/hep.24790.
9. Choi, Kyung-Dal, Maxim Vodyanik, and Igor I. Slukvin. 2011. "Hematopoietic Differentiation and Production of Mature Myeloid Cells from Human Pluripotent Stem Cells." *Nature Protocols* 6 (3): 296–313. https://doi.org/10.1038/nprot.2010.184.

10. DiNardo, Courtney D., and Jorge E. Cortes. 2016. "Mutations in AML: Prognostic and Therapeutic Implications." *Hematology: The American Society of Hematology Education Program* 2016 (1): 348–55.
11. Döhner, Hartmut, Elihu Estey, David Grimwade, Sergio Amadori, Frederick R. Appelbaum, Thomas Büchner, Hervé Dombret, et al. 2017. "Diagnosis and Management of AML in Adults: 2017 ELN Recommendations from an International Expert Panel." *Blood* 129 (4): 424–47. https://doi.org/10.1182/blood-2016-08-733196.
12. Doulatov, Sergei, Linda T. Vo, Stephanie S. Chou, Peter G. Kim, Natasha Arora, Hu Li, Brandon K. Hadland, et al. 2013. "Induction of Multipotential Hematopoietic Progenitors from Human Pluripotent Stem Cells via Respecification of Lineage-Restricted Precursors." *Cell Stem Cell* 13 (4): 459–70. https://doi.org/10.1016/j.stem.2013.09.002.
13. Grimwade, D., H. Walker, F. Oliver, K. Wheatley, C. Harrison, G. Harrison, J. Rees, et al. 1998. "The Importance of Diagnostic Cytogenetics on Outcome in AML: Analysis of 1,612 Patients Entered into the MRC AML 10 Trial. The Medical Research Council Adult and Children's Leukaemia Working Parties." *Blood* 92 (7): 2322–33.
14. Hu, Deqing, and Ali Shilatifard. 2016. "Epigenetics of Hematopoiesis and Hematological Malignancies." *Genes & Development* 30 (18): 2021–41. https://doi.org/10.1101/gad.284109.116.
15. Jing, Duohui, Ana-Violeta Fonseca, Nael Alakel, Fernando A. Fierro, Katrin Muller, Martin Bornhauser, Gerhard Ehninger, Denis Corbeil, and Rainer Ordemann. 2010. "Hematopoietic Stem Cells in Co-Culture with Mesenchymal Stromal Cells--Modeling the Niche Compartments in Vitro." *Haematologica* 95 (4): 542–50. https://doi.org/10.3324/haematol.2009.010736.
16. Kim, K., A. Doi, B. Wen, K. Ng, R. Zhao, P. Cahan, J. Kim, et al. 2010. "Epigenetic Memory in Induced Pluripotent Stem Cells." *Nature* 467 (7313): 285–90. https://doi.org/10.1038/nature09342.
17. Kotini, Andriana G., Chan-Jung Chang, Arthur Chow, Han Yuan, Tzu-Chieh Ho, Tiansu Wang, Shailee Vora, et al. 2017. "Stage-Specific Human Induced Pluripotent Stem Cells Map the Progression of Myeloid Transformation to Transplantable Leukemia." *Cell Stem Cell* 20 (3): 315-328.e7. https://doi.org/10.1016/j.stem.2017.01.009.
18. Lee, Jong-Hee, Sarah Laronde, Tony J. Collins, Zoya Shapovalova, Borko Tanasijevic, Jamie D. McNicol, Aline Fiebig-Comyn, et al. 2017. "Lineage-Specific Differentiation Is Influenced by State of Human Pluripotency." *Cell Reports* 19 (1): 20–35. https://doi.org/10.1016/j.celrep.2017.03.036.
19. Lee, Jong-Hee, Jung Bok Lee, Zoya Shapovalova, Aline Fiebig-Comyn, Ryan R. Mitchell, Sarah Laronde, Eva Szabo, Yannick D. Benoit, and Mickie Bhatia. 2014. "Somatic Transcriptome Priming Gates Lineage-Specific Differentiation Potential of Human-Induced Pluripotent Stem Cell States." *Nature Communications* 5 (December): 5605. https://doi.org/10.1038/ncomms6605.
20. Lee, Jong-Hee, Kyle R. Salci, Jennifer C. Reid, Luca Orlando, Borko Tanasijevic, Zoya Shapovalova, and Mickie Bhatia. 2017. "Brief Report: Human Acute Myeloid Leukemia Reprogramming to Pluripotency Is a Rare Event and Selects for Patient Hematopoietic Cells Devoid of Leukemic Mutations." *Stem Cells (Dayton, Ohio)* 35 (9): 2095–2102. https://doi.org/10.1002/stem.2655.
21. Lee, Jungmin, Brad Dykstra, Joel A. Spencer, Laurie L. Kenney, Dale L. Greiner, Leonard D. Shultz, Michael A. Brehm, Charles P. Lin, Robert Sackstein, and Derrick J.

Rossi. 2017. “MRNA-Mediated Glycoengineering Ameliorates Deficient Homing of Human Stem Cell-Derived Hematopoietic Progenitors.” *The Journal of Clinical Investigation* 127 (6): 2433–37. https://doi.org/10.1172/JCI92030.

22. Mardis, Elaine R., Li Ding, David J. Dooling, David E. Larson, Michael D. McLellan, Ken Chen, Daniel C. Koboldt, et al. 2009. “Recurring Mutations Found by Sequencing an Acute Myeloid Leukemia Genome.” *The New England Journal of Medicine* 361 (11): 1058–66. https://doi.org/10.1056/NEJMoa0903840.
23. Meijering, E., M. Jacob, J.-C. F. Sarria, P. Steiner, H. Hirling, and M. Unser. 2004. “Design and Validation of a Tool for Neurite Tracing and Analysis in Fluorescence Microscopy Images.” *Cytometry. Part A: The Journal of the International Society for Analytical Cytology* 58 (2): 167–76. https://doi.org/10.1002/cyto.a.20022.
24. Melnick, Ari M. 2010. “Epigenetics in AML.” *Best Practice & Research. Clinical Haematology* 23 (4): 463–68. https://doi.org/10.1016/j.beha.2010.09.017.
25. Muñoz-López, Alvaro, Damià Romero-Moya, Cristina Prieto, Verónica Ramos-Mejía, Antonio Agraz-Doblas, Ignacio Varela, Marcus Buschbeck, et al. 2016. “Development Refractoriness of MLL-Rearranged Human B Cell Acute Leukemias to Reprogramming into Pluripotency.” *Stem Cell Reports* 7 (4): 602–18. https://doi.org/10.1016/j.stemcr.2016.08.013.
26. Nazor, Kristopher L., Gulsah Altun, Candace Lynch, Ha Tran, Julie V. Harness, Ileana Slavin, Ibon Garitaonandia, et al. 2012. “Recurrent Variations in DNA Methylation in Human Pluripotent Stem Cells and Their Differentiated Derivatives.” *Cell Stem Cell* 10 (5): 620–34. https://doi.org/10.1016/j.stem.2012.02.013.
27. Ntziachristos, Panagiotis, Omar Abdel-Wahab, and Iannis Aifantis. 2016. “Emerging Concepts of Epigenetic Dysregulation in Hematological Malignancies.” *Nature Immunology* 17 (9): 1016–24. https://doi.org/10.1038/ni.3517.
28. Ottersbach, Katrin. 2019. “Endothelial-to-Haematopoietic Transition: An Update on the Process of Making Blood.” *Biochemical Society Transactions* 47 (2): 591–601. https://doi.org/10.1042/BST20180320.
29. Reid, Jennifer C., Borko Tanasijevic, Diana Golubeva, Allison L. Boyd, Deanna P. Porras, Tony J. Collins, and Mickie Bhatia. 2018. “CXCL12/CXCR4 Signaling Enhances Human PSC-Derived Hematopoietic Progenitor Function and Overcomes Early In Vivo Transplantation Failure.” *Stem Cell Reports* 10 (5): 1625–41. https://doi.org/10.1016/j.stemcr.2018.04.003.
30. Reynolds, B. A., and S. Weiss. 1992. “Generation of Neurons and Astrocytes from Isolated Cells of the Adult Mammalian Central Nervous System.” *Science (New York, N.Y.)* 255 (5052): 1707–10. https://doi.org/10.1126/science.1553558.
31. Rodrigues, Cecilia Pessoa, Maria Shvedunova, and Asifa Akhtar. 2021. “Epigenetic Regulators as the Gatekeepers of Hematopoiesis.” *Trends in Genetics* 37 (2): 125–42. https://doi.org/10.1016/j.tig.2020.09.015.
32. Salci, Kyle R., Jong-Hee Lee, Sarah Laronde, Steve Dingwall, Rahul Kushwah, Aline Fiebig-Comyn, Brian Leber, Ronan Foley, Arianna Dal Cin, and Mickie Bhatia. 2015. “Cellular Reprogramming Allows Generation of Autologous Hematopoietic Progenitors From AML Patients That Are Devoid of Patient-Specific Genomic Aberrations.” *Stem Cells (Dayton, Ohio)* 33 (6): 1839–49. https://doi.org/10.1002/stem.1994.
33. Schindelin, Johannes, Ignacio Arganda-Carreras, Erwin Frise, Verena Kaynig, Mark Longair, Tobias Pietzsch, Stephan Preibisch, et al. 2012. “Fiji: An Open-Source Platform

for Biological-Image Analysis." *Nature Methods* 9 (7): 676–82. https://doi.org/10.1038/nmeth.2019.

34. Shih, Alan H., Omar Abdel-Wahab, Jay P. Patel, and Ross L. Levine. 2012. "The Role of Mutations in Epigenetic Regulators in Myeloid Malignancies." *Nature Reviews. Cancer* 12 (9): 599–612. https://doi.org/10.1038/nrc3343.
35. Takahashi, Kazutoshi, Koji Tanabe, Mari Ohnuki, Megumi Narita, Tomoko Ichisaka, Kiichiro Tomoda, and Shinya Yamanaka. 2007. "Induction of Pluripotent Stem Cells from Adult Human Fibroblasts by Defined Factors." *Cell* 131 (5): 861–72. https://doi.org/10.1016/j.cell.2007.11.019.
36. Takahashi, Kazutoshi, and Shinya Yamanaka. 2006. "Induction of Pluripotent Stem Cells from Mouse Embryonic and Adult Fibroblast Cultures by Defined Factors." *Cell* 126 (4): 663–76. https://doi.org/10.1016/j.cell.2006.07.024.
37. Takashima, Yasuhiro, Ge Guo, Remco Loos, Jennifer Nichols, Gabriella Ficz, Felix Krueger, David Oxley, et al. 2014. "Resetting Transcription Factor Control Circuitry toward Ground-State Pluripotency in Human." *Cell* 158 (6): 1254–69. https://doi.org/10.1016/j.cell.2014.08.029.
38. Vardiman, James W., Jüergen Thiele, Daniel A. Arber, Richard D. Brunning, Michael J. Borowitz, Anna Porwit, Nancy Lee Harris, et al. 2009. "The 2008 Revision of the World Health Organization (WHO) Classification of Myeloid Neoplasms and Acute Leukemia: Rationale and Important Changes." *Blood* 114 (5): 937–51. https://doi.org/10.1182/blood-2009-03-209262.
39. Welch, John S., Timothy J. Ley, Daniel C. Link, Christopher A. Miller, David E. Larson, Daniel C. Koboldt, Lukas D. Wartman, et al. 2012. "The Origin and Evolution of Mutations in Acute Myeloid Leukemia." *Cell* 150 (2): 264–78. https://doi.org/10.1016/j.cell.2012.06.023.
40. Wesely, Josephine, Andriana G. Kotini, Franco Izzo, Hanzhi Luo, Han Yuan, Jun Sun, Maria Georgomanoli, et al. 2020. "Acute Myeloid Leukemia IPSCs Reveal a Role for RUNX1 in the Maintenance of Human Leukemia Stem Cells." *Cell Reports* 31 (9): 107688. https://doi.org/10.1016/j.celrep.2020.107688.
41. Wouters, Bas J., and Ruud Delwel. 2016. "Epigenetics and Approaches to Targeted Epigenetic Therapy in Acute Myeloid Leukemia." *Blood* 127 (1): 42–52. https://doi.org/10.1182/blood-2015-07-604512.
42. Zhang, S. C., M. Wernig, I. D. Duncan, O. Brüstle, and J. A. Thomson. 2001. "In Vitro Differentiation of Transplantable Neural Precursors from Human Embryonic Stem Cells." *Nature Biotechnology* 19 (12): 1129–33. https://doi.org/10.1038/nbt1201-1129.

Figures

Figure 1

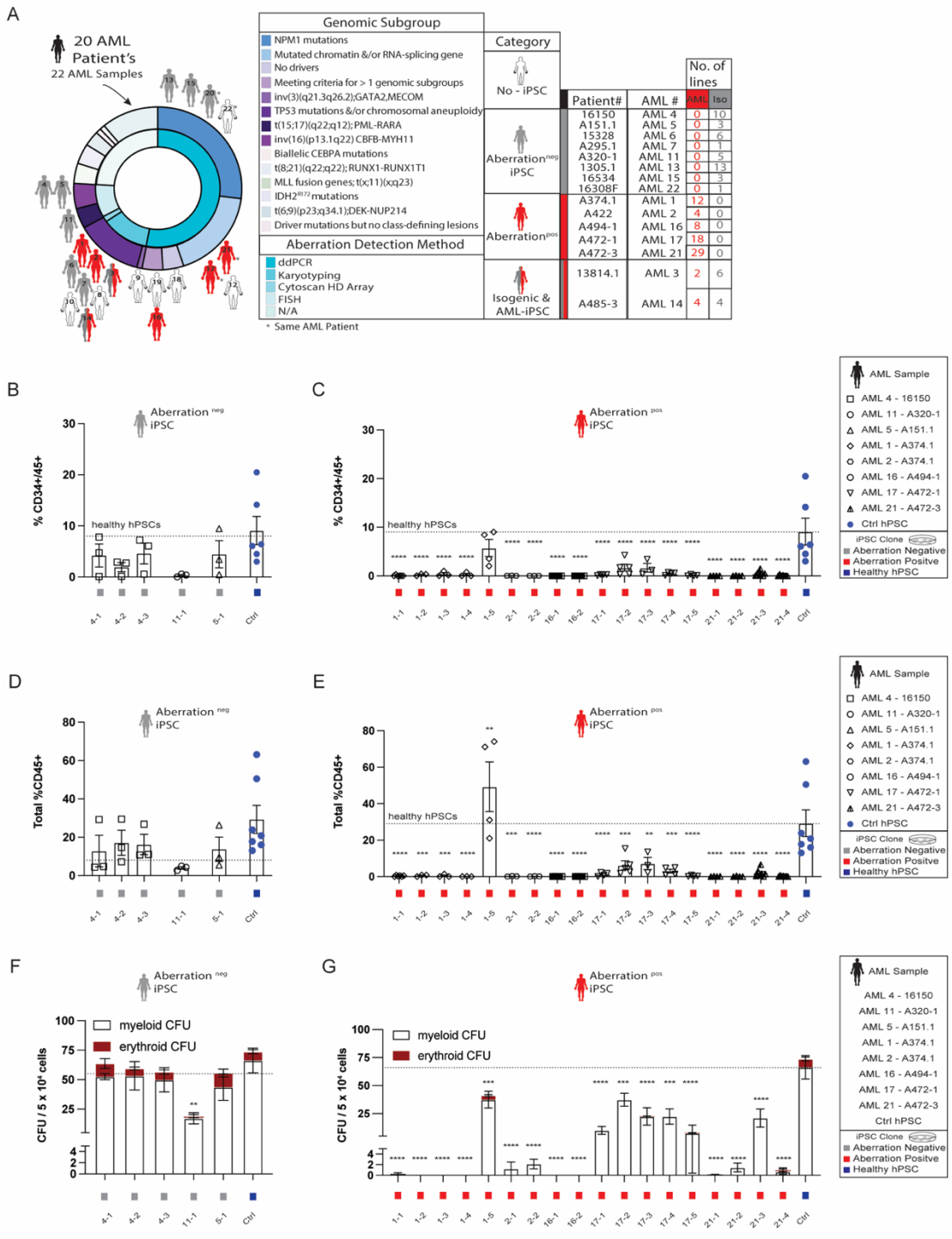

Figure 1 – Hematopoietic differentiation potential of AML patient derived iPSC library.

(A) Chart summary of AML samples reprogrammed and their respective mutations. 22 primary AML samples were reprogrammed representing 8 different genomic classifications. The size of the bar in the chart corresponds to the frequency of cytogenetic abnormalities. All clones derived were tested for primary patient aberrations using distinct methods such as FISH, karyotyping, cytoscan HD array & droplet digital PCR (ddPCR). 7/22 samples produced no iPSC colonies, 15/22 produced colonies, of which 8 produced aberration negative clones, 5 produced solely aberration positive clones (AML-iPSC), & 2/22 produced paired clones of aberration positive and negative colonies (Paired Isogenic-iPSC & AML-iPSCs respectively). Grey represents aberration negative iPSC. Red represents aberration positive iPSCs. * denotes sample from the same AML patient. **(B & C)** Phenotypic frequency of primitive hematopoietic progenitors ($CD34^+/CD45^+$) captured on day 21 & analyzed by flow cytometry across multiple aberration negative iPSC lines derived from AML 4, 5 & 11 (B) and aberration positive iPSC lines derived from AML 1, 2, 16, 17 & 21 (C). **(D & E)** Frequency of differentiated mature blood cells ($CD45^+$) captured on day 21 of hematopoietic differentiation and analyzed by flow cytometry across multiple iPSC lines, aberration negative (D) and aberration positive (E). **(F & G)** Total number of hematopoietic colony forming units (CFUs) and number of colony subtypes (myeloid CFU vs erythroid CFUs) generated by plating bulk populations into methylcellulose based medium on day 21. Dashed line represents positive hPSC control average. All data show average with error bars representing ± SEM (N=3-9). All comparison were made to healthy hPSC control lines using a one-way ANOVA and Tukey multiple comparison test. Statistically significant test results are denoted as * $p \leq 0.05$, ** $p \leq 0.01$, *** $p \leq 0.001$, **** $p \leq 0.0001$.

Figure 2

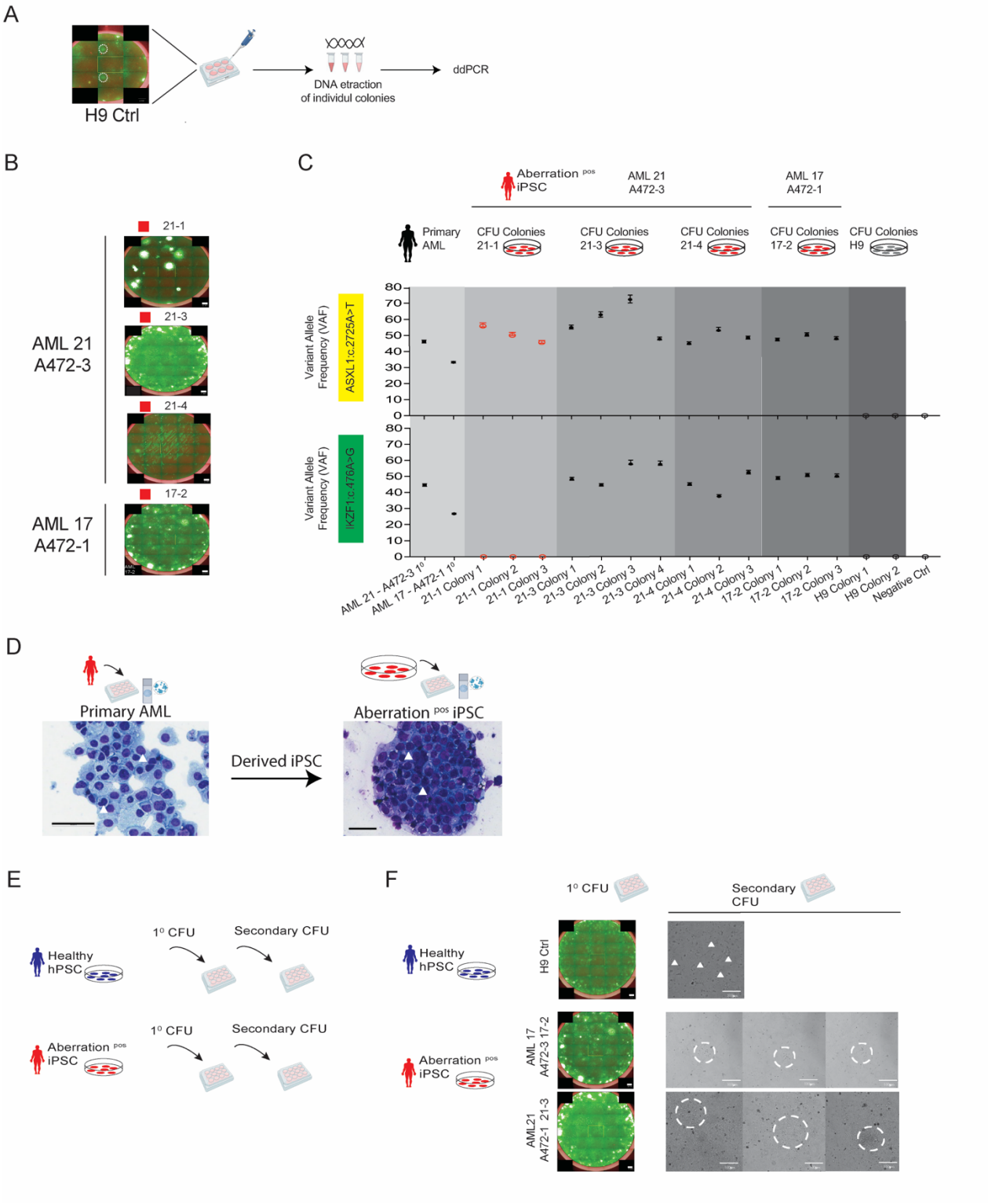

Figure 2 – AML-iPSC hematopoietic progeny retain mutations and recapitulate features of primary disease.

(A) Schematic depicting technique used to isolate individual CFU colonies for validation of mutational status. **(B)** Representative whole-well CFU images of 3 AML-iPSC clones (21-1, 21-3, 21-4) derived from AML A472-3 and 1 AML-iPSC clone (17-2) derived from A472-1. Images were acquired at 2x using Operetta High Content Screening (Perkin Elmer) by means of calcein green am staining. Whole-well images were stitched in Columbus software (Perkin Elmer). White scale bar represents 2 μm. **(C)** Droplet PCR results from individual CFU-Monocyte/macrophage colonies derived from AML A472-3 clones (21-1, 21-3, 21-4) and AML A472-1 clones (17-2) by comparison to original primary AML and healthy control (H9 CFU-M colony). Variant Allele Frequency (VAF) is displayed for droplet PCR results, probing for ASXL1:c.2725A>T and IKZF1:c.476A>G. 2-4. Individual CFU-M colonies were collected from methylcellulose after the progenitor CFU assay from each respective clone. Mutations detected in individual CFU colonies matched original mutations detected in de novo AML patient sample. **(D)** Representative image of bulk CFUs spun onto slides from Wright-Giemsa staining (cytospin) of primary AML and AML-iPSCs. Black scale bar represents 60 μm. White arrows denote blast-like morphology seen in primary AML & AML-iPSC clone. **(E)** Schematic depicting methodology of secondary CFU assay. Whole wells of primary CFU's derived from hPSCs lines were collected, recounted, and reseeded in methylcellulose-based medium for an additional 14 days. Prior to collection the total number and types of colonies were counted at the initial 14 days. **(F)** Clonogenicity potential of leukemic progenitors derived from primary CFU's of AML-iPSC lines. Representative whole-well images of primary CFU of AML 17 (A472-3) clone 17-2 and AML 21 (A472-1) clone 21-3 and H9 healthy control hESC line. Images were acquired at 2x using Operetta High Content Screening (Perkin Elmer) by means of calcein green am staining. Whole-well images were stitched in Columbus software (Perkin Elmer). White scale bar represents 2 μm. All secondary CFU colony images were collected using a phase-contrast microscope. Representative images of 3 individual CFU-M colonies from AML 17 (A472-3) clone 17-2 & AML 21 (A472-1) clone 21-3. Dashed-white circle highlights individual colonies arising from leukemic progenitors presumably originating from the primary CFU assay. Absence of secondary CFU potential is demonstrated in healthy control hESC line H9 depicted by distinct individual cells. White triangles highlight individual cells. Scale bar 100 μm. (N=1 per iPSC line).

Figure 3

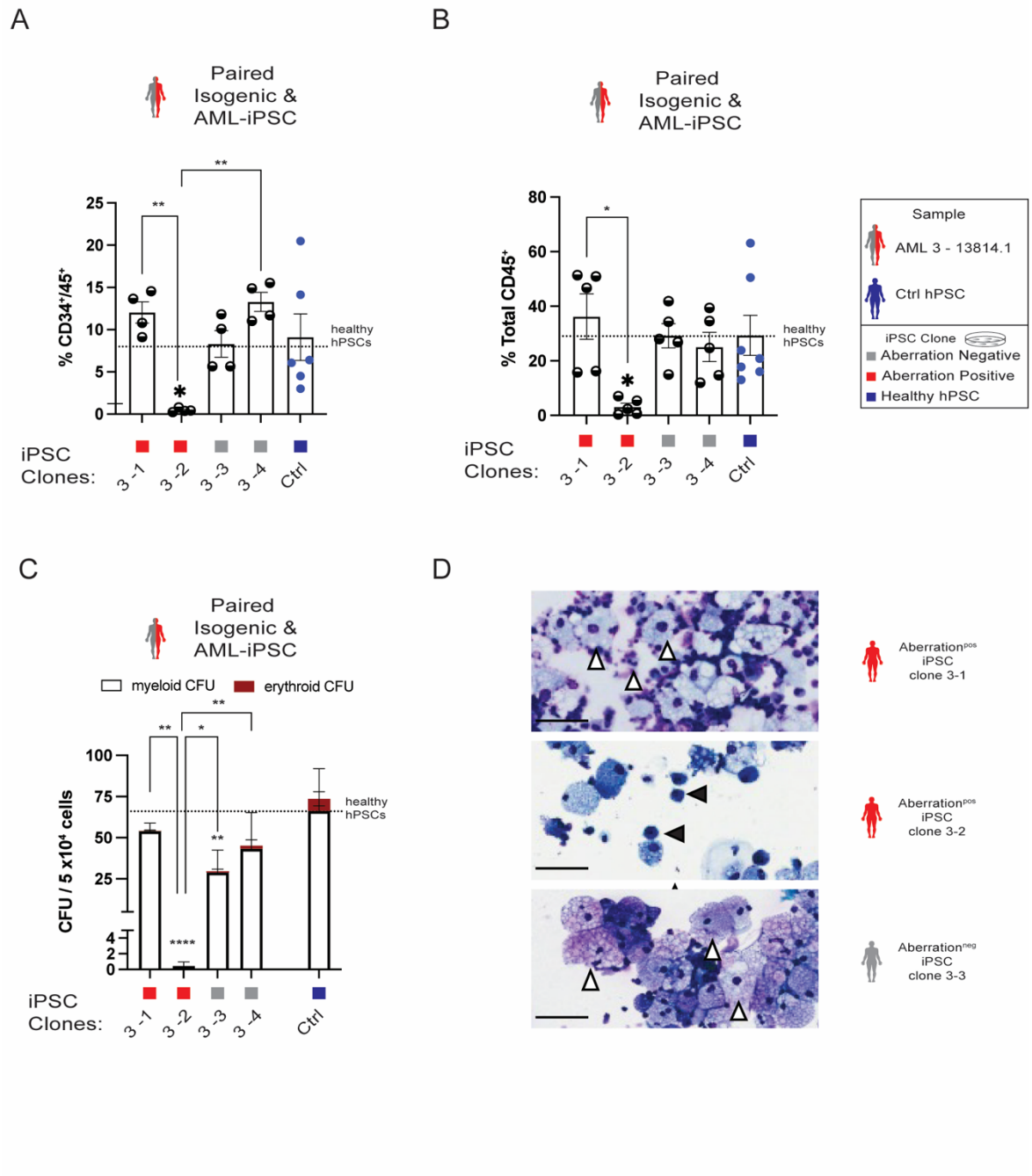

Figure 3 – Differential segregation of phenotype and functional progenitor capacity by cytogenetic status of iPSCs.

Frequency of **(A)** hematopoietic progenitors ($CD34^+/CD45^+$) **(B)** told blood cells ($CD45^+$) and **(C)** hematopoietic CFU and colony subtypes (myeloid CFU vs erythroid CFUs) of paired malignant and normal/isogenic iPSC lines derived from AML patient 13814.1 (AML 3). Malignant lines (AML-iPSC) are clone 3-1 and 3-2 versus isogenic lines are clone 3-3 and 3-4. All data are mean

± SEM (N=4-9). All comparisons were made using one-way ANOVA and Tukey multiple comparison test. Dashed line represents positive hPSC control average. Statistically significant test results are denoted as * $p \leq 0.05$, ** $p \leq 0.01$, *** $p \leq 0.001$, **** $p \leq 0.0001$. **(D)** Plucked CFUs were spun onto slides for Wright-Giemsa staining (cytospin). Black scale bar represents 60 μm. White arrows denote normal cell morphology of macrophages and neutrophil versus black arrows indicate immature blast-like cells.

Figure 4

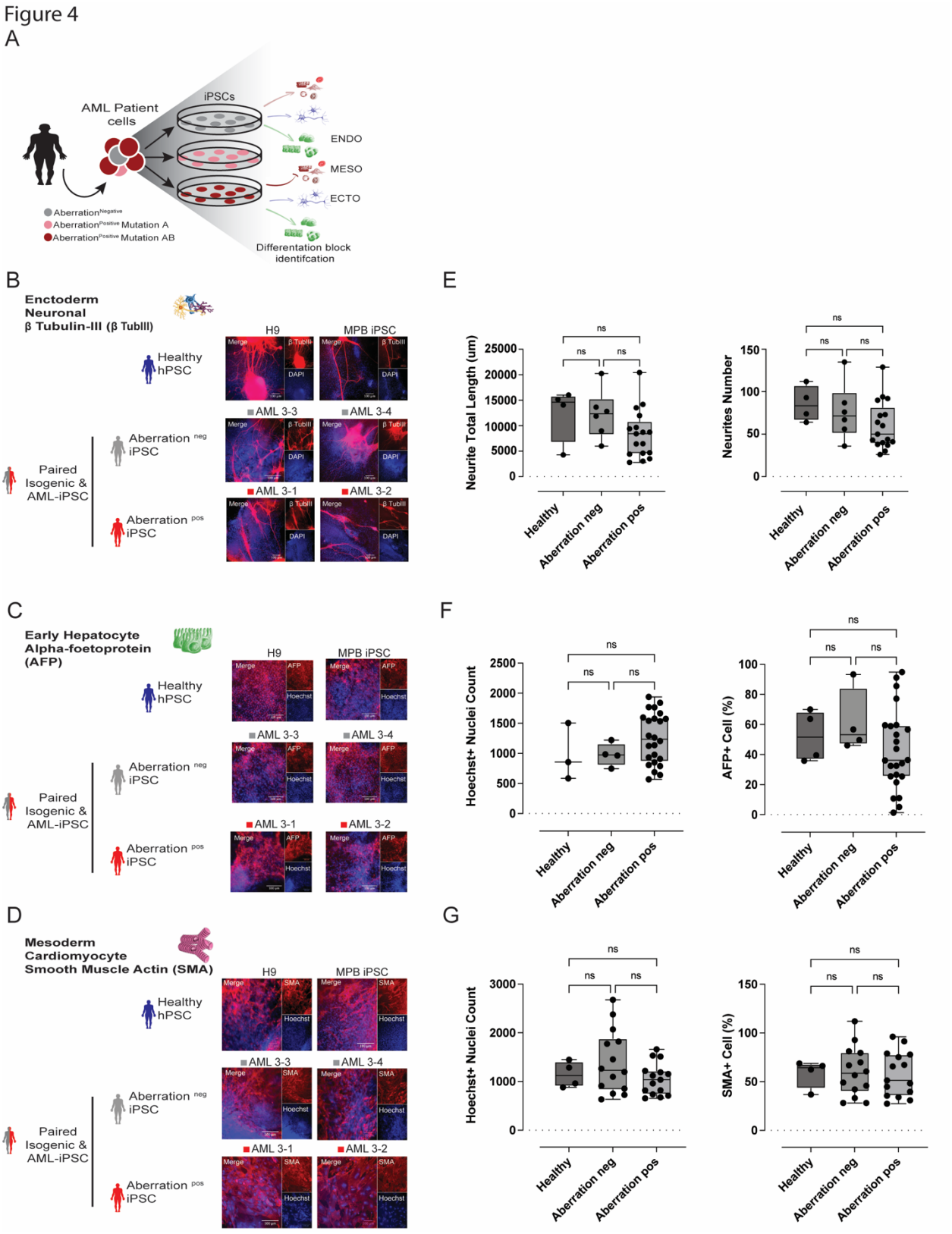
A
AML Patient cells
iPSCs
ENDO
MESO
ECTO
Aberration Negative
Aberration Positive Mutation A
Aberration Positive Mutation AB
Differentation block identifcation
B
Enctoderm
Neuronal
β Tubulin-III (β TubIII)
H9
MPB iPSC
Healthy hPSC
Paired Isogenic & AML-iPSC
Aberration neg iPSC
Aberration pos iPSC
AML 3-3
AML 3-4
AML 3-1
AML 3-2
Merge
β TubIII
DAPI
C
Early Hepatocyte
Alpha-foetoprotein
(AFP)
AFP
Hoechst
D
Mesoderm
Cardiomyocyte
Smooth Muscle Actin (SMA)
SMA
E
Neurite Total Length (um)
Neurites Number
F
Hoechst+ Nuclei Count
AFP+ Cell (%)
G
SMA+ Cell (%)
ns
Healthy
Aberration neg
Aberration pos

Figure 4 – Differentiation potential of AML patient derived iPSCs to non-hematopoietic lineages.

(A) Schematic representation of germ layer interrogation strategy on AML patient derived iPSC lines. Representative immunocytochemical images of paired isogenic & AML-iPSC lines of **(B)** βIII-Tubulin counterstained with DAPI, **(C)** early hepatocyte marker Alpha-fetoprotein (AFP) counterstained with Hoechst 33342 and of **(D)** smooth muscle actin (SMA) counterstained with Hoechst 33342. All scale bars represent 100 μm. **(E)** Quantification of neurite total length & total number amongst healthy hPSCs, aberration negative iPSCs and aberration positive iPSCs. Quantification of **(F)** AFP and **(G)** SMA counterstained with Hoechst amongst healthy hPSCs, aberration negative iPSCs and aberration positive iPSCs. Note, neurite outgrowth was analyzed using the NeuronJ plugin (Meijering et al., 2004) from the ImageJ package Fiji (Schindelin et al., 2012) and to quantify endoderm and mesoderm differentiation, the percentage of cells in a sample stained with the fluorescent probe of interest was quantified by using ImageJ Analyze Particles Measure Plugin. See methods section for further details. Data are depicted by box and whisker plot showing minimum and maximum (N=4-24). All comparison were made using a one-way ANOVA and Tukey multiple comparison test. No statistical differences were observed.

Figure 5

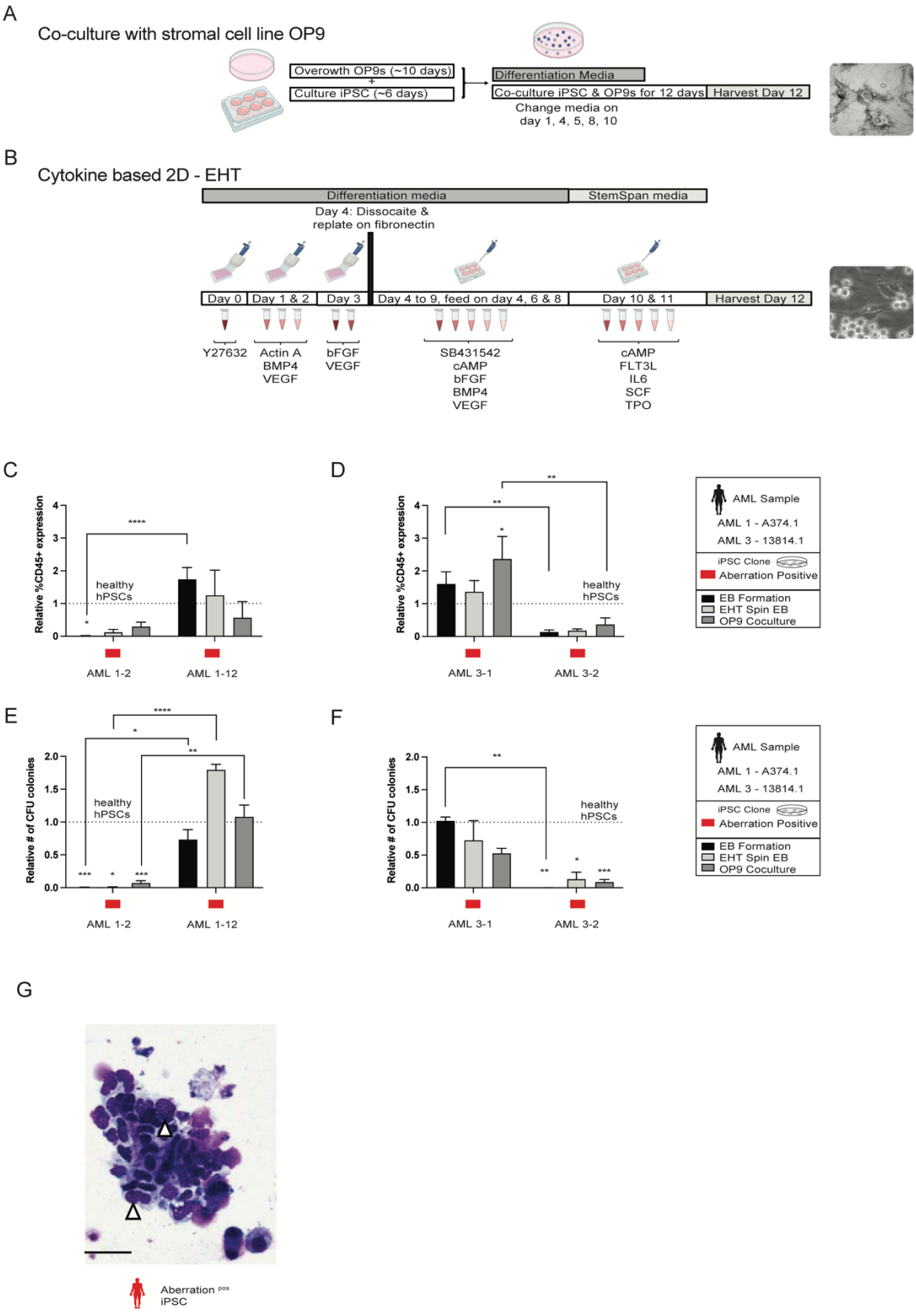
A
Co-culture with stromal cell line OP9
Overowth OP9s (~10 days)
+
Culture iPSC (~6 days)
Differentiation Media
Co-culture iPSC & OP9s for 12 days
Harvest Day 12
Change media on
day 1, 4, 5, 8, 10
B
Cytokine based 2D - EHT
Differentiation media
StemSpan media
Day 4: Dissocaite &
replate on fibronectin
Day 0
Day 1 & 2
Day 3
Day 4 to 9, feed on day 4, 6 & 8
Day 10 & 11
Harvest Day 12
Y27632
Actin A
BMP4
VEGF
bFGF
VEGF
SB431542
cAMP
bFGF
BMP4
VEGF
cAMP
FLT3L
IL6
SCF
TPO
C
Relative %CD45+ expression
healthy
hPSCs
AML 1-2
AML 1-12
D
Relative %CD45+ expression
healthy
hPSCs
AML 3-1
AML 3-2
AML Sample
AML 1 - A374.1
AML 3 - 13814.1
iPSC Clone
Aberration Positive
EB Formation
EHT Spin EB
OP9 Coculture
E
Relative # of CFU colonies
healthy
hPSCs
AML 1-2
AML 1-12
F
Relative # of CFU colonies
healthy
hPSCs
AML 3-1
AML 3-2
AML Sample
AML 1 - A374.1
AML 3 - 13814.1
iPSC Clone
Aberration Positive
EB Formation
EHT Spin EB
OP9 Coculture
G
Aberration pos
iPSC

Figure 5 – Methodology does not dictate phenotypic or functional capacity of AML-iPSCs.

(A) A flow chart depicting the 12-day OP9 coculture protocol that involves culturing undifferentiated hPSCs with overgrown OP9 cells. **(B)** A flow chart depicting the 12-day Endothelial-to-hematopoietic transition (EHT) hematopoietic methodology involving 4 days of mesoderm induction before EHT on adherent culture. Phenotypic frequency of mature blood cells ($CD45^+$) on select AML-iPSC clones derived from **(C)** patient A374.1 (AML 1) and patient 13814.1 (AML 3) normalized to control hPSCs **(D)**. The relative number of CFU colonies at day 14, normalized to control hPSCs on select AML-iPSC clones derived from **(E)** patient A374.1 (AML 1) and **(F)** patient 13814.1 (AML 3). All data displayed are mean ± standard error of mean (SEM) with N=4-9 for EB formation, N=3-5 for EHT transition, and N=4-5 for OP9 coculture. All comparisons were made using a two-way ANOVA test and Tukey's multiple comparisons test (within each column, compare rows to determine simple effects within columns). Statistically significant test results are denoted as * $p \leq 0.05$, ** $p \leq 0.01$, *** $p \leq 0.001$, **** $p \leq 0.0001$.

Supplemental Figures

Supplemental Figure 1

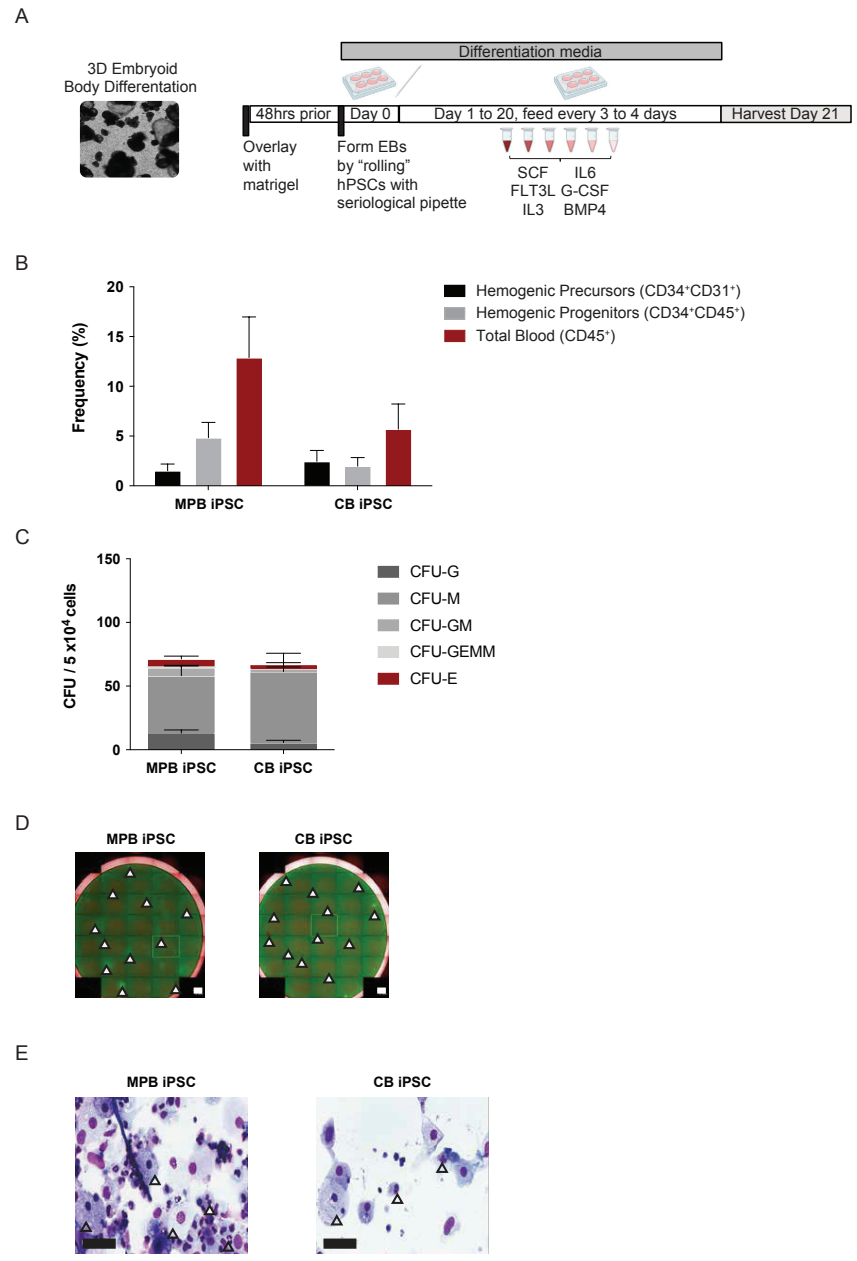

Supplemental Figure 1 - Shared Phenotypic and Progenitor Capacity of hESC and hiPSC lines in vitro.

(A) A schematic representation depicting the 21-day EB formation protocol for the non-adherent formation of 3D aggregates. **(B)** Flow cytometry analysis of EB-differentiated healthy hiPSC lines (MPB iPSC & CB iPSC) showing similar hematopoietic programs for both hemogenic precursors ($CD34^+/CD31^+$), hemogenic progenitors ($CD34^+/CD45^+$) and total blood content ($CD45^+$). All data are mean ± SEM (N=5-10). All comparisons are made using one-way ANOVA and Tukey multiple comparison test on each individual phenotypic population displayed amongst the two hiPSC lines. No statistical differences were observed. **(C)** Total number of hematopoietic colony forming units (CFUs) and number of colony subtypes CFU-Erythroid, CFU-Granulocyte, CFU-Monocyte/macrophage and CFU-GM, CFU-GEMM. All data are mean ± SEM (N=5-10). All comparisons are made using one-way ANOVA and Tukey multiple comparison test. No statistical differences were observed. **(D)** Representative whole-well CFU images of hPSC lines. Images were acquired at 2x using Operetta High Content Screening (Perkin Elmer) by means of calcein green am staining. Whole-well images were stitched in Columbus software (Perkin Elmer). White scale bar represents 2 μm. **(E)** Picked CFU were spun onto slides for Wright-Giemsa staining (cytospin). Black scale bar represents 500 μm. Arrows denote normal cell morphology of macrophages and neutrophils.

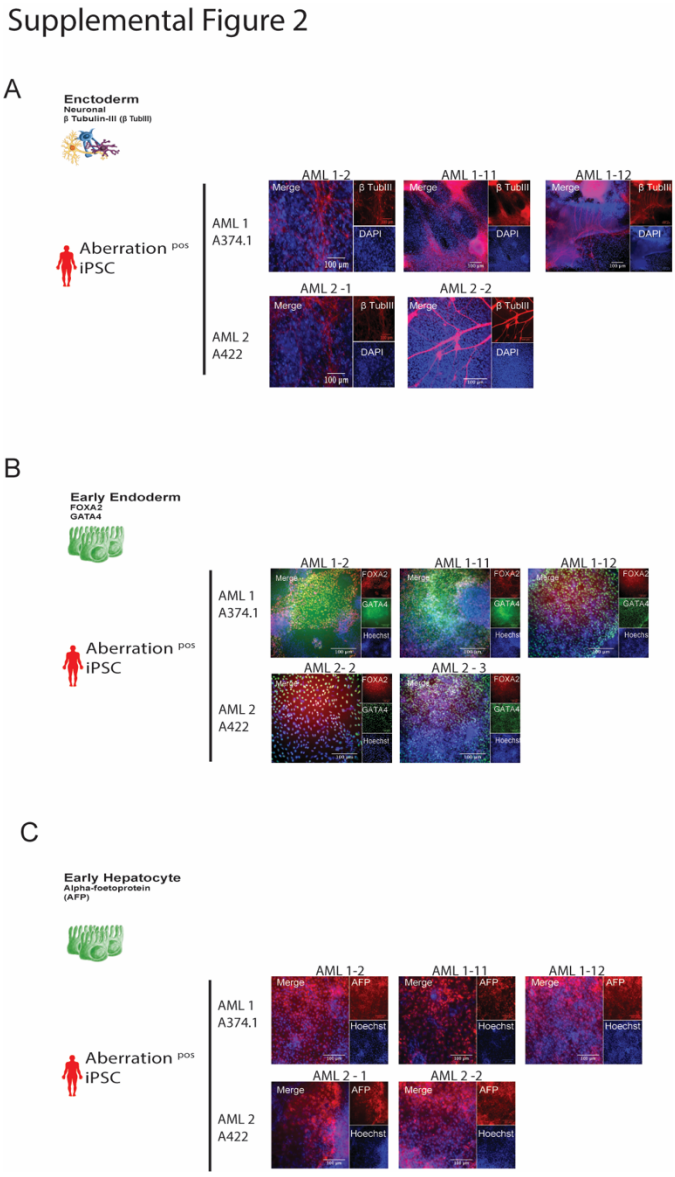

Supplemental Figure 2 – Differentiation potential of additional AML-iPSC lines into endoderm, and ectodermal lineages.

(A) Representative immunocytochemical images of βIII-Tubulin counterstained with DAPI. Scale bar 100 µm. **(B)** Representative immunocytochemical images of early ectodermal markers GATA4 and FOXA2 and **(C)** early hepatocyte marker Alpha-fetoprotein (AFP) positive cells counterstained with Hoechst 33342. Scale bar 100 µm.

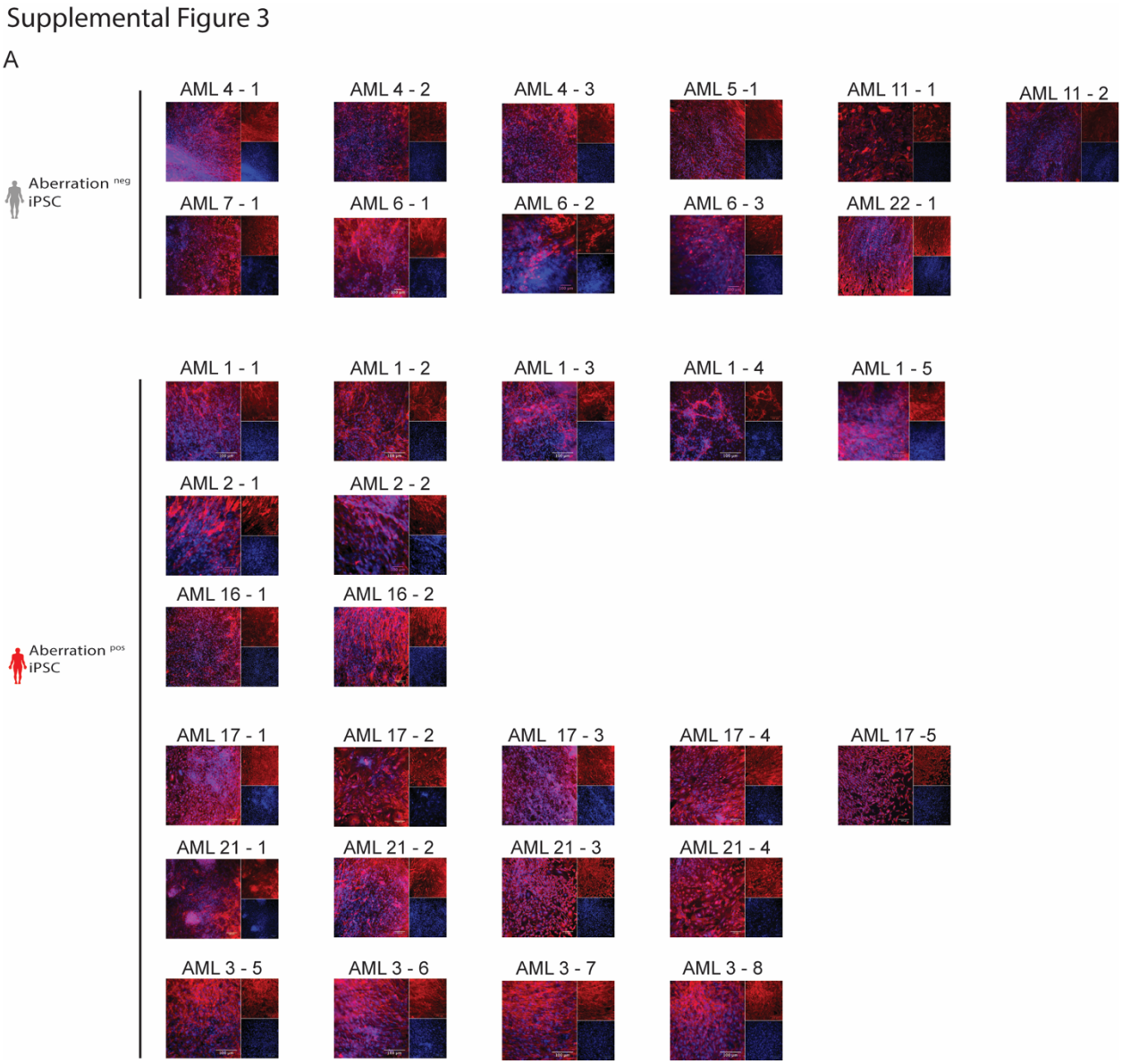

Supplementary Figure 3 – Characterization of AML-iPSC differentiation into mesoderm lineage.

(A) Representative immunocytochemical images of smooth muscle actin (SMA) counterstained with Hoechst 33342 on all AML patient derived iPSC lines tested. Scale bar 100 µm.

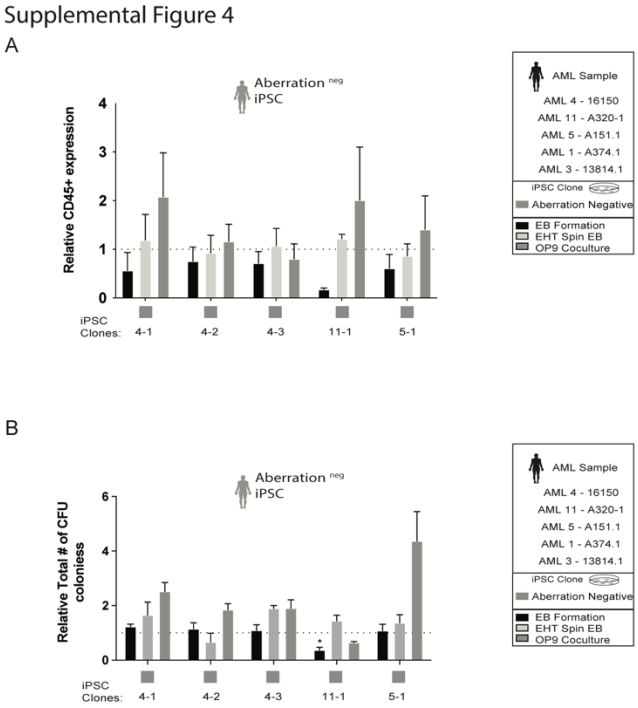

Supplementary Figure 4 – Aberration negative iPSCs derived from AML patients phenocopy healthy hPSC independent of methodology used for HSPC derivation.

(A) Flow cytometry analysis of the relative $CD45^{+}$ expression in all three methods, (I) day 21 for EB formation, (II) day 12 for EHT transition, (III) and day 12 for OP9 coculture. All aberration negative lines were normalized to the control, which consisted of MPB iPSC. All data displayed are mean ± standard error of mean (SEM) with N=4 for EB formation, N=3 for EHT transition, and N=4-5 for OP9 coculture. All comparisons were made using a two-way ANOVA test and Tukey's multiple comparisons test (within each column, compare rows to determine simple effects within columns). No statistical significance was observed.

CHAPTER 5: DISCUSSION

5.0 Preamble

Preamble

Our lab and others have previously reported on the challenges of reprogramming primary AML somatic cells. Nevertheless, this thesis set out to build on this body of work and investigate ways in which to utilize and further optimize cellular reprogramming technology to address unmet needs in the field of human AML research. Specifically, I hypothesized that an autologous source of normal HSPCs could be derived from AML-iPSC lines devoid of somatic leukemic aberrations and used to establish a healthy source of transplantable HSCs. I believed that investigating this hypothesis would provide initial proof of concepts and insights required for future development of novel sources of safe HSPCs for personalized therapeutics. Though I was successful in the derivation of HPCs in vitro, the derivation of HSCs (SRCs) from patient-specific hiPSCs, which I believe is the holy grail in regenerative medicine, was unfortunately unattainable **(Chapter 2)**.

As the major limitation preventing applications and deeper insights using AML-iPSCs is the rarity of its success, I next set out to test and refine methods in which to enhance the efficiency of reprogramming AML. Through a combination of de novo, xenografting, naïve vs prime states and immune-phenotyping of AML cells, I hypothesized an enhanced reprogramming efficiency of AML-iPSCs would be possible, capturing inter and intra heterogeneity of AML patients. While testing this hypothesis I was able to procure a novel library of 129 AML patient-derived iPSCs of which 77 were AML-iPSCs lines **(Chapter 3)**. Using fluorescence activated cell sorting, it was demonstrated that the relationship between AML and healthy reprogramming is dependent on the differentiation status of diseased tissue, where the use of the myeloid marker CD33 instead of the stem cell marker, CD34, decreases the capture of AML clones during reprogramming.

I next sought to interrogate the ability of this library for in vitro disease modeling and hypothesized that the previously reported ability of AML-iPSCs to maintain features of their cells of origin would be true. By performing hematopoietic differentiation assays, I demonstrated that majority of AML-iPSC lines display a block in differentiation measured by little to no functional progenitor capacity and fail to develop into primitive or mature blood cells **(Chapter 4)**. Moreover, these results were consistent across three distinct hematopoietic methodologies. However, some AML-iPSC clones from the same patient showed hematopoietic differentiation capacity to similar degrees as healthy iPSCs despite carrying cytogenetic mutations originating from donor patient disease cells, making them ideal controls for subsequent molecular comparison between iPSC lines.

Here I discuss the significance, limitations, and future directions of our findings, and share additional insights into other uses cellular reprogramming technologies may have in addressing novel questions in AML research.

5.1 Personalized Therapeutics – Using AML patient-specific iPSCs to derive blood products

Recently, our lab demonstrated that the generation of AML patient-specific iPSCs from dermal fibroblasts and BM was possible and allowed for derivation of CD34+CD45+ HPCs devoid of leukemia-associated aberration(s) in vitro (Salci et al., 2015). Concomitantly, the first successful derivation of HSCs from iPSCs with in vivo engraftment was reported through combined morphogen-directed differentiation recapitulating the EHT lineage transition from HE and the use

of a defined set of TF over-expression in HE cells (Sugimura et al., 2017). By combining these findings, we rationalized that the generation of normal autologous hematopoietic progenitors from AML patients would be possible. This would establish a proof of principle that iPSCs may represent a suitable source of healthy autologous cells to address the clinical shortage of blood cells required for transplantation. Though we were ultimately unsuccessful, as addressed in Chapter 2, our findings should continue to motivate efforts toward a robust and practical generation of transplantable HSPCs.

Despite the major achievement of the generation of putative HSPCs with multi-lineage engraftment potential (Sugimura et al., 2017), this approach did not yield the quantities of induced-HSPCs required clinically, and we have independently confirmed that these hPSC-derived HSPCs remain molecularly distinct from adult HSCs (Chapter 2). Additionally, it has now become apparent that HSPC generation from hPSCs can only be achieved by accessing the in vivo niche as an essential regulator coupled to TF function. Independent groups have reported the limited derivation of hPSC-HSPCs in vivo using teratoma formation (Amabile et al., 2013; Suzuki et al., 2013), and now most recently HSC engraftment of 7TF-HE cells was only achieved by in vivo programming (Sugimura et al., 2017). This suggests that extracellular cues from the in vivo BM niche are crucial. However, no studies to date have examined the interaction of the BM niche in modulating in vivo programming of hPSC-HE to HSPCs. As the 7TFs do not act in a cell-autonomous fashion and likely require niche interactions, future studies investigating changes in the BM that collaborate with the 7TF effects ought to be characterized and explored. The use of these results could enable an increase in the efficiency of this process or replacement of the TFs using niche-modulating drugs. Ultimately, the limited success in establishing differentiation conditions to generate engraftable hematopoiesis by many investigators over the past two decades suggests that future work in refining this process is still highly needed.

AML patient-specific iPSCs and derived HPCs may provide cell sources that have a more direct clinical impact, independent of the many advancements necessary for the creation of safe transplantable HSPCs. AML management requires frequent blood transfusions to prevent anemia, bleeding, and infection (Dawson et al., 2007; Perl & Carroll, 2007). To meet these demands, however, a sizable number of donors are needed per patient (Dawson et al., 2007)(Dawson et al., 2007), and many patients develop alloimmunization-related transfusion product resistance (Schiffer, 2001). As such, transplantation of autologous HPCs such as platelets or RBCs could serve as a means of providing short-term hematopoietic recovery in AML patients throughout therapy. Independent research teams have proved that human iPSCs can be used to create megakaryocyte progenitors (Feng et al., 2014; Nakamura et al., 2014). Following transfusion into mice, these megakaryocytes produce platelets that are functionally capable of aiding in the production of blood clots in vivo (Feng et al., 2014; Nakamura et al., 2014). Similarly, hESCs have been used to create enucleated RBCs that are capable of transporting oxygen, though they predominantly expressed fetal hemoglobin (Lu et al., 2008).

Considering the above discussion, I ultimately believe that AML patient-specific iPSCs have the potential to provide a novel source of autologous blood cells that circumvent obstacles associated with current sources for transplant and transfusion.

5.2 Barriers to Reprogramming – developing methods that allow for superior generation of AML patient derived iPSCs

An overarching goal of this work was to generate a pluripotent AML-iPSC library which would have the potential to capture intra and inter-AML patient heterogeneity. During our attempts to generate such a library (Chapter 3), knowing very well that AML cells are refractory to reprogramming, we rediscovered just how difficult this is to achieve. Notably, this appears to be a general feature of malignant cells, not limited to hematopoietic tissues, and manifests as a predominance of normal lines among the derived iPSCs, even in cases when the starting cell sample is overwhelmingly clonal (Chao et al., 2017; Hoffmann et al., 2016; J. Kim et al., 2013; Kotini et al., 2017b; J.-H. Lee et al., 2017; Muñoz-López et al., 2016; Raya et al., 2009; Yamasaki et al., 2019). We clearly demonstrate this by showing that 8 of 15 patient samples reprogramming solely yield iPSCs that were devoid of the primary patient mutation(s) (aberration negative iPSCs), while 7 samples were unsuccessful in reprogramming all together. Notably, a limitation in our experimental design is the lack of a control for the reprogramming process. In reprogrammed samples that did not yield any colonies, such as AML 18 (Chapter 3), it is hard to pinpoint the reason for the lack of reprogramming success. It could be due to a biological reason, such as the specific cytogenic abnormality causing a barrier to be reprogrammed. However, it could also be due to a technical error in one of the many steps of the reprogramming process or an issue with a reagent used. It would be ideal for future samples to be reprogrammed along side a well of healthy mobilized peripheral blood cells (MPB) as a control, since reprogramming efficiency tends to be higher in blood cells (Malik & Rao, 2013) than what we have seen in AML samples. If the MPB control was successfully reprogrammed but the AML sample was not, it would appear more likely that the AML sample itself is the reason for a lack of reprogramming. However, this idea is limited by the resources it would require, including the added Sendai virus, the MPB samples needed, and the additional sorting and culture time this would require.

Since our 2017 paper, in which we were the first to provide experimental insights on the difficulties of reprogramming human cancer cells by demonstrating that reprogramming blockade occurs downstream of reprogramming TF delivery and expression (J.-H. Lee et al., 2017), BM from an AML patient with the high-risk der(7)t(7;13) translocation was reprogrammed (Yamasaki et al., 2019). The iPSC lines derived did not harbour the translocation and were cytogenetically normal (Yamasaki et al., 2019). Similarly, reprogramming an AML patient sample with a t(8;21) translocation resulted in the successful reprogramming of one cytogenetically normal iPSC line (Hoffmann et al., 2016). These studies provide further evidence that particular chromosomal abnormalities and point mutations are likely selected against during reprogramming, though the basis for failure was not experimentally explored within these papers. Most recently, Yamasaki et al., attempted another round of reprogramming of AML with Sendai virus, but this time used the HL-60 leukemic cell line as opposed to a primary patient sample (Yamasaki et al., 2020). Despite using a cell line, only one iPSC line was successfully expanded in culture and successfully retained almost all of the genomic aberrations of the parental leukemic line (Yamasaki et al., 2020). Nevertheless, the exact reason for the refractory nature of reprogramming remains obscure but may involve the aberrant genetics and potentially also epigenetic states of malignant and premalignant cells. One possibility is that genes mutated in myeloid neoplasms can often involve epigenetic regulators which are required for successful reprogramming (Watanabe et al., 2013). Another possibility is that high mutation burden and aneuploidy can trigger cell stress responses such as p53 activation that impede reprogramming (Marión et al., 2009). Another potential reason is the hindered capacity of leukemic cells for ex vivo growth. Cell division is critically required both for efficient transduction with reprogramming vectors to initiate reprogramming, as well as for the epigenome remodeling required to complete reprogramming to pluripotency. Thus, the

inability to enter a proliferative state severely hampers a cell's reprogramming ability (Guo et al., 2014; Hanna et al., 2009; Ruiz et al., 2011). Notably, while this makes it more challenging to directly reprogram some malignant clones, it creates an opportunity to capture preleukemic intermediates that may be too rare to be directly detected by other approaches. Thus, approaches to optimizing the reprogramming process should continue to be investigated.

Reprogramming methods have evolved since the initial discovery by Takahashi et al. (Takahashi & Yamanaka, 2006) whereby other viruses are now used such as adenoviruses (Stadtfeld et al., 2008) and Sendai virus which do not require viral integration (Fusaki et al., 2009). Additionally, virus-free DNA and RNA-based reprogramming methods have been put forth to maximize reprogramming efficacy (Okita et al., 2010; Warren et al., 2010). For example, Anokye-Danso et al., increased reprogramming efficacy by a 2-fold magnitude by expressing a miRNA cluster, miR302/367, which has been demonstrated to play an important role in pluripotency in hESCs and during reprogramming (Anokye-Danso et al., 2011). Additionally, there has been interest in utilizing epigenetic modifiers to increase reprogramming efficiency, since reprogramming is known to alter the epigenetic landscape, to boost the transcription of pluripotency-associated genes (Buganim et al., 2013; Knaupp et al., 2017). Thus, interest has been gained in investigating post-translational histone modification enzymes to improve the process. This involves modifications to the DNA itself as well as histone markers. Modifiers may function directly or by enhancing the activity of innate epigenetic enzymes. Specifically, inhibitors of DNA methyltransferase and histone deacetylase have been shown to significantly increase the effectiveness of reprogramming (Huangfu et al., 2008). Valproic acid in particular can increase the reprogramming effectiveness of MEFs by a factor of more than 100 (Huangfu et al., 2008). Overall, it has been demonstrated that small molecule drugs can reconfigure the chromatin state with both positive and negative impacts on reprogramming effectiveness, and their long-term implications are not well understood. In the next few years, more efficient reprogramming strategies will continue to be generated which should ultimately provide enhanced methods of reprogramming refractory AML cells. This will not only provide model platforms in which to perform mechanistic and drug screening studies in AML but may also extend to other difficult-to-reprogram malignant cells.

Interestingly, to circumvent the difficulty of reprogramming AML, gene editing of iPSCs offers a unique opportunity. In 2013, the development of the CRISPR/Cas9 system as a versatile and user-friendly genome editing tool took biomedical research by storm (Ran et al., 2013), and paired with iPSC technology offers immense opportunities. Specifically, gene editing offers the ability to introduce specific mutations found in AML into normal iPSCs, or by correcting them in AML-iPSCs, or, ideally, by both strategies (Chang et al., 2018). Isogenic pairs of lines are more superior controls, as we have shown in Chapter 4, than unrelated or even patient-matched normal lines, thus, the ability to generate isogenic paired lines is highly appealing. Interestingly, it has been proposed that the CRISPR/Cas9 system could be used both to inactivate genes to model common loss-of-function mutations in leukemias through nonhomologous end joining repair of Cas9-mediated double-strand DNA breaks and to introduce hotspot mutations in oncogenic driver genes through the homology-directed repair from a donor DNA template (Papapetrou, 2019).

5.3 The Future – elucidating AML differentiation blockade through cellular reprogramming

By developing more robust reprogramming conditions in Chapter 3, we were able to establish a library of AML patient-derived iPSCs in which we could assess the ability of iPSCs to model AML. Through the successful generation of AML-iPSCs harbouring leukemia-associated aberration, we found that majority of their derivative HPCs were dysfunctional in their differentiation capacity (Chapter 4). This is reminiscent of the hematopoietic blockade observed in AML characterized by an inability to generate mature blood cells. Additionally, we observed the reestablishment of leukemic features in the cellular morphology of hPSC-derived hematopoietic cells from AML-iPSC clones, mirroring de novo AML. This supports the concept of retaining epigenetic memory of the reprogrammed AML cells and is similar to the observation of enhanced blood formation from iPSCs made from healthy hematopoietic cells (K. Kim et al., 2010; J.-H. Lee et al., 2014). Surprisingly, we also discovered that a smaller subset of AML-iPSC harbouring cytogenetic mutations originating from donor patient disease cells, demonstrate hematopoietic differentiation capacity to similar degrees as healthy iPSCs or iPSCs derived from AML patients devoid of DNA aberrations. Our findings demonstrate that despite retaining oncogenic lesions of the primary AML, paired malignant AML-iPSCs exhibit differential hematopoietic capacity. As such, I believe that any blockade in hematopoietic differentiation observed results from an aberrant chromatin landscape captured in select AML-iPSCs. Importantly, these epigenetic variations seem to be retained through epigenetic memory of primary AML cells after pluripotent reprogramming

Though more detailed comparisons between equivalent populations of iPSC derived HPCs and primary AML blasts may be encouraged to better understand how faithfully the former recapitulate the chromatin and gene expression landscape of the latter, based on our current findings, we are now in a unique position to identify specific epigenetic alternations that mark the earliest initiation events that drive the transformation to a leukemic state. Specifically, future work in our lab aims to use a multi-omic approach to capture genomic regions and changes in global patterns of gene expression crucial to leukemogenesis (i.e involved in hematopoietic blockade), to characterize distinct 'regulomes' of AML. This will be done by combining Assay for Transposase-Accessible Chromatin sequencing (ATAC-seq) in conjunction with RNA sequencing (RNAseq) from iPSC lines in the pluripotent state. Both these methodologies will be applied to paired isogenic and AML-iPSCs as well as intra-patient AML-iPSC with differential hematopoietic capacity in combination with healthy hiPSC lines that will serve as baseline 'regulome' controls. Our main focus will be to discriminate the epigenetic regulome of clones that are functionally blocked in hematopoietic differentiation (non-overlapping loci in Venn diagram segment "A" of Figure 1B), which represents the central defect of diseased AML cells. Next, we will use isogenic controls that lack disease-specific mutations as an additional filter when possible (Figure 1C). Finally, we will subtract any features that are shared with healthy iPSCs that represent epigenetic states associated with the reprogramming process itself (Figure 1B & 1C). Importantly, we have never observed functional defects in hematopoietic differentiation from any of our healthy-derived iPSC lines, reinforcing that the distinct differentiation block observed in AML-iPSCs is directly attributable to disease states. Simultaneous profiling of DNA accessibility and gene expression dynamics will provide candidate loci that have validated transcript changes and a defined 'regulome' of AML-iPSC present and absent in various clonal lines. We believe this approach will define rare concealed epigenetic abnormalities and thereby provide key insights into the evolutionary process of leukemogenesis as well as identify important regulatory programs that could be targeted toward future therapeutics.

Overall, I hope that future studies, like the one described above, will form the foundation to systematically understand the fundamental molecular drivers of AML disease, identify new targets and develop new biomarkers to predict and prevent relapse.

5.4 Concluding Remarks

In this thesis, we have carried out initial proof of concept experiments to demonstrate that cellular reprogramming of human AML patient somatic cells to pluripotency allows for the creation of normal **(Chapter 2)** and dysfunctional **(Chapter 4)** HPCs. Moreover, our efforts of refining the refractory nature of reprogramming AML provides a platform for further optimization of AML-iPSC generation, and a unique library of 129 mutant and healthy iPSCs **(Chapter 3)** derived directly from a heterogenous set of AML patients for study by the broader scientific community. These early insights should motivate additional research to identify the genetic and/or epigenetic links to aberrant hematopoiesis in AML. The AML world is a bit brighter thanks to basic research that continuous to wage war on this cancer!

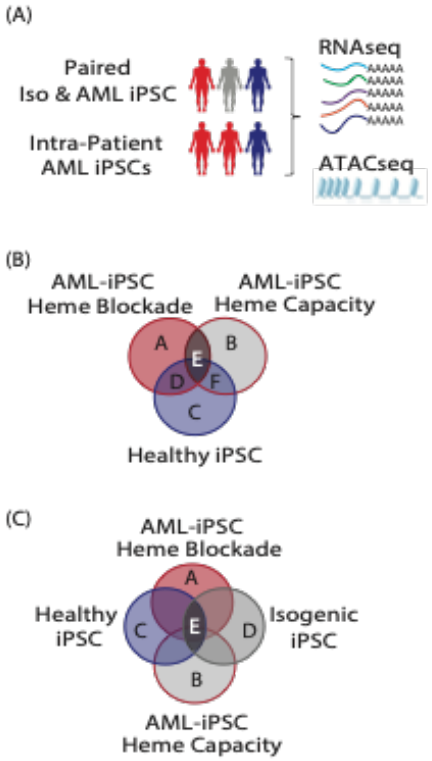

Figure 1. Integrated Genomic Analyses (A) Schematic of the methodology and comparisons to be done in future studies (B) Venn diagram showing overlap among iPSC lines in order to determine candidate genes/loci based on differentially accessible peaks/genes from AML-iPSC with differential hematopoietic capacity vs Healthy iPSCs (C) Venn diagram showing complementary pairs of iPSCs from a single patient vs healthy iPSCs. Overlap represents epigenetic landscape induced through reprogramming.

APPENDIX

Appendix I: Bibliography

Adachi, K., Suemori, H., Yasuda, S.-Y., Nakatsuji, N., & Kawase, E. (2010). Role of SOX2 in maintaining pluripotency of human embryonic stem cells. *Genes to Cells: Devoted to Molecular & Cellular Mechanisms*, *15*(5), 455–470. https://doi.org/10.1111/j.1365-2443.2010.01400.x

Akashi, K., Traver, D., Miyamoto, T., & Weissman, I. L. (2000). A clonogenic common myeloid progenitor that gives rise to all myeloid lineages. *Nature*, *404*(6774), 193–197. https://doi.org/10.1038/35004599

Amabile, G., Welner, R. S., Nombela-Arrieta, C., D'Alise, A. M., Di Ruscio, A., Ebralidze, A. K., Kraytsberg, Y., Ye, M., Kocher, O., Neuberg, D. S., Khrapko, K., Silberstein, L. E., & Tenen, D. G. (2013). In vivo generation of transplantable human hematopoietic cells from induced pluripotent stem cells. *Blood*, *121*(8), 1255–1264. https://doi.org/10.1182/blood-2012-06-434407

Anokye-Danso, F., Trivedi, C. M., Juhr, D., Gupta, M., Cui, Z., Tian, Y., Zhang, Y., Yang, W., Gruber, P. J., Epstein, J. A., & Morrisey, E. E. (2011). Highly efficient miRNA-mediated reprogramming of mouse and human somatic cells to pluripotency. *Cell Stem Cell*, *8*(4), 376–388. https://doi.org/10.1016/j.stem.2011.03.001

Araki, R., Uda, M., Hoki, Y., Sunayama, M., Nakamura, M., Ando, S., Sugiura, M., Ideno, H., Shimada, A., Nifuji, A., & Abe, M. (2013). Negligible immunogenicity of terminally differentiated cells derived from induced pluripotent or embryonic stem cells. *Nature*, *494*(7435), 100–104. https://doi.org/10.1038/nature11807

Arber, D. A., Orazi, A., Hasserjian, R., Thiele, J., Borowitz, M. J., Le Beau, M. M., Bloomfield, C. D., Cazzola, M., & Vardiman, J. W. (2016). The 2016 revision to the World Health Organization classification of myeloid neoplasms and acute leukemia. *Blood*, *127*(20), 2391–2405. https://doi.org/10.1182/blood-2016-03-643544

Atashzar, M. R., Baharlou, R., Karami, J., Abdollahi, H., Rezaei, R., Pourramezan, F., & Zoljalali Moghaddam, S. H. (2020). Cancer stem cells: A review from origin to therapeutic implications. *Journal of Cellular Physiology*, *235*(2), 790–803. https://doi.org/10.1002/jcp.29044

Avilion, A. A., Nicolis, S. K., Pevny, L. H., Perez, L., Vivian, N., & Lovell-Badge, R. (2003). Multipotent cell lineages in early mouse development depend on SOX2 function. *Genes & Development*, *17*(1), 126–140. https://doi.org/10.1101/gad.224503

Bain, B. J. (2001). Bone marrow trephine biopsy. *Journal of Clinical Pathology*, *54*(10), 737–742. https://doi.org/10.1136/jcp.54.10.737

Ballen, K. K. (2015). Is there a best graft source of transplantation in acute myeloid leukemia? *Best Practice & Research. Clinical Haematology*, *28*(2–3), 147–154. https://doi.org/10.1016/j.beha.2015.10.012

Batta, K., Florkowska, M., Kouskoff, V., & Lacaud, G. (2014). Direct reprogramming of murine fibroblasts to hematopoietic progenitor cells. *Cell Reports*, *9*(5), 1871–1884. https://doi.org/10.1016/j.celrep.2014.11.002

Bauman, J. G., Wiegant, J., Borst, P., & van Duijn, P. (1980). A new method for fluorescence microscopical localization of specific DNA sequences by in situ hybridization of fluorochromelabelled RNA. *Experimental Cell Research*, *128*(2), 485–490. https://doi.org/10.1016/0014-4827(80)90087-7

Becker, A. J., McCULLOCH, E. A., & Till, J. E. (1963). Cytological demonstration of the clonal nature of spleen colonies derived from transplanted mouse marrow cells. *Nature*, *197*, 452–454. https://doi.org/10.1038/197452a0

Bejar, R. (2014). Clinical and genetic predictors of prognosis in myelodysplastic syndromes. *Haematologica*, *99*(6), 956–964. https://doi.org/10.3324/haematol.2013.085217

Bendall, S. C., Stewart, M. H., Menendez, P., George, D., Vijayaragavan, K., Werbowetski-Ogilvie, T., Ramos-Mejia, V., Rouleau, A., Yang, J., Bossé, M., Lajoie, G., & Bhatia, M. (2007). IGF and FGF cooperatively establish the regulatory stem cell niche of pluripotent human cells in vitro. *Nature*, *448*(7157), 1015–1021. https://doi.org/10.1038/nature06027

Bennett, J. M., Catovsky, D., Daniel, M. T., Flandrin, G., Galton, D. A., Gralnick, H. R., & Sultan, C. (1976). Proposals for the classification of the acute leukaemias. French-American-British (FAB) co-operative group. *British Journal of Haematology*, *33*(4), 451–458. https://doi.org/10.1111/j.1365-2141.1976.tb03563.x

Bertrand, J. Y., Chi, N. C., Santoso, B., Teng, S., Stainier, D. Y. R., & Traver, D. (2010). Haematopoietic stem cells derive directly from aortic endothelium during development. *Nature*, *464*(7285), 108–111. https://doi.org/10.1038/nature08738

Bhatia, M., Wang, J. C., Kapp, U., Bonnet, D., & Dick, J. E. (1997). Purification of primitive human hematopoietic cells capable of repopulating immune-deficient mice. *Proceedings of the National Academy of Sciences of the United States of America*, *94*(10), 5320–5325. https://doi.org/10.1073/pnas.94.10.5320

Bibikova, M., Chudin, E., Wu, B., Zhou, L., Garcia, E. W., Liu, Y., Shin, S., Plaia, T. W., Auerbach, J. M., Arking, D. E., Gonzalez, R., Crook, J., Davidson, B., Schulz, T. C., Robins, A., Khanna, A., Sartipy, P., Hyllner, J., Vanguri, P., … Fan, J.-B. (2006). Human

embryonic stem cells have a unique epigenetic signature. *Genome Research*, *16*(9), 1075–1083. https://doi.org/10.1101/gr.5319906

Bird, A. (2002). DNA methylation patterns and epigenetic memory. *Genes & Development*, *16*(1), 6–21. https://doi.org/10.1101/gad.947102

Blau, H. M., & Daley, G. Q. (2019). Stem Cells in the Treatment of Disease. *New England Journal of Medicine*, *380*(18), 1748–1760. https://doi.org/10.1056/NEJMra1716145

Boisset, J.-C., van Cappellen, W., Andrieu-Soler, C., Galjart, N., Dzierzak, E., & Robin, C. (2010). In vivo imaging of haematopoietic cells emerging from the mouse aortic endothelium. *Nature*, *464*(7285), 116–120. https://doi.org/10.1038/nature08764

Bone-marrow transplant from an unrelated donor for chronic granulomatous disease. (1977). *Lancet (London, England)*, *1*(8005), 210–213.

Bonnet, D., & Dick, J. E. (1997). Human acute myeloid leukemia is organized as a hierarchy that originates from a primitive hematopoietic cell. *Nature Medicine*, *3*(7), 730–737.

Borsatti, A., & Nacheva, E. P. (2019). Molecular Karyotyping Combined with FISH Offers an Alternative to Chromosome Banding Analysis for Diagnostic Evaluation of Genome Complexity in Acute Myeloid Leukemia. *Blood*, *134*(Supplement_1), 5188. https://doi.org/10.1182/blood-2019-131983

Boyd, A. L., Aslostovar, L., Reid, J., Ye, W., Tanasijevic, B., Porras, D. P., Shapovalova, Z., Almakadi, M., Foley, R., Leber, B., Xenocostas, A., & Bhatia, M. (2018). Identification of Chemotherapy-Induced Leukemic-Regenerating Cells Reveals a Transient Vulnerability of Human AML Recurrence. *Cancer Cell*, *34*(3), 483-498.e5. https://doi.org/10.1016/j.ccell.2018.08.007

Boyer, L. A., Lee, T. I., Cole, M. F., Johnstone, S. E., Levine, S. S., Zucker, J. P., Guenther, M. G., Kumar, R. M., Murray, H. L., Jenner, R. G., Gifford, D. K., Melton, D. A., Jaenisch, R., & Young, R. A. (2005). Core transcriptional regulatory circuitry in human embryonic stem cells. *Cell*, *122*(6), 947–956. https://doi.org/10.1016/j.cell.2005.08.020

Bradley, T. R., & Metcalf, D. (1966). The growth of mouse bone marrow cells in vitro. *The Australian Journal of Experimental Biology and Medical Science*, *44*(3), 287–299. https://doi.org/10.1038/icb.1966.28

Briggs, R., & King, T. J. (1952). Transplantation of Living Nuclei From Blastula Cells into Enucleated Frogs' Eggs. *Proceedings of the National Academy of Sciences of the United States of America*, *38*(5), 455–463. https://doi.org/10.1073/pnas.38.5.455

Briggs, R., & King, T. J. (1957). Changes in the nuclei of differentiating endoderm cells as revealed by nuclear transplantation. *Journal of Morphology*, *100*(2), 269–311. https://doi.org/10.1002/jmor.1051000204

Brinster, R. L. (1974). The effect of cells transferred into the mouse blastocyst on subsequent development. *The Journal of Experimental Medicine*, *140*(4), 1049–1056. https://doi.org/10.1084/jem.140.4.1049

Broxmeyer, H. E., Douglas, G. W., Hangoc, G., Cooper, S., Bard, J., English, D., Arny, M., Thomas, L., & Boyse, E. A. (1989). Human umbilical cord blood as a potential source of transplantable hematopoietic stem/progenitor cells. *Proceedings of the National Academy of Sciences of the United States of America*, *86*(10), 3828–3832. https://doi.org/10.1073/pnas.86.10.3828

Buganim, Y., Faddah, D. A., & Jaenisch, R. (2013). Mechanisms and models of somatic cell reprogramming. *Nature Reviews. Genetics*, *14*(6), 427–439. https://doi.org/10.1038/nrg3473

Bursen, A., Schwabe, K., Rüster, B., Henschler, R., Ruthardt, M., Dingermann, T., & Marschalek, R. (2010). The AF4.MLL fusion protein is capable of inducing ALL in mice without requirement of MLL.AF4. *Blood*, *115*(17), 3570–3579. https://doi.org/10.1182/blood-2009-06-229542

Cai, S. F., & Levine, R. L. (2019). Genetic and epigenetic determinants of AML pathogenesis. *Seminars in Hematology*, *56*(2), 84–89. https://doi.org/10.1053/j.seminhematol.2018.08.001

Cancer Genome Atlas Research Network. (2013). Genomic and epigenomic landscapes of adult de novo acute myeloid leukemia. *The New England Journal of Medicine*, *368*(22), 2059–2074. https://doi.org/10.1056/NEJMoa1301689

Carette, J. E., Pruszak, J., Varadarajan, M., Blomen, V. A., Gokhale, S., Camargo, F. D., Wernig, M., Jaenisch, R., & Brummelkamp, T. R. (2010). Generation of iPSCs from cultured human malignant cells. *Blood*, *115*(20), 4039–4042. https://doi.org/10.1182/blood-2009-07-231845

Chabannon, C., Kuball, J., Bondanza, A., Dazzi, F., Pedrazzoli, P., Toubert, A., Ruggeri, A., Fleischhauer, K., & Bonini, C. (2018). Hematopoietic stem cell transplantation in its 60s: A platform for cellular therapies. *Science Translational Medicine*, *10*(436), eaap9630. https://doi.org/10.1126/scitranslmed.aap9630

Chadwick, K., Wang, L., Li, L., Menendez, P., Murdoch, B., Rouleau, A., & Bhatia, M. (2003). Cytokines and BMP-4 promote hematopoietic differentiation of human embryonic stem cells. *Blood*, *102*(3), 906–915. https://doi.org/10.1182/blood-2003-03-0832

Chambers, I., Colby, D., Robertson, M., Nichols, J., Lee, S., Tweedie, S., & Smith, A. (2003). Functional expression cloning of Nanog, a pluripotency sustaining factor in embryonic stem cells. *Cell*, *113*(5), 643–655. https://doi.org/10.1016/s0092-8674(03)00392-1

Chang, C.-J., Kotini, A. G., Olszewska, M., Georgomanoli, M., Teruya-Feldstein, J., Sperber, H., Sanchez, R., DeVita, R., Martins, T. J., Abdel-Wahab, O., Bradley, R. K., & Papapetrou, E. P. (2018). Dissecting the Contributions of Cooperating Gene Mutations to Cancer Phenotypes and Drug Responses with Patient-Derived iPSCs. *Stem Cell Reports*, *10*(5), 1610–1624. https://doi.org/10.1016/j.stemcr.2018.03.020

Chao, M. P., Gentles, A. J., Chatterjee, S., Lan, F., Reinisch, A., Corces, M. R., Xavy, S., Shen, J., Haag, D., Chanda, S., Sinha, R., Morganti, R. M., Nishimura, T., Ameen, M., Wu, H., Wernig, M., Wu, J. C., & Majeti, R. (2017). Human AML-iPSCs Reacquire Leukemic Properties after Differentiation and Model Clonal Variation of Disease. *Cell Stem Cell*, *20*(3), 329-344.e7. https://doi.org/10.1016/j.stem.2016.11.018

Chen, G., Gulbranson, D. R., Hou, Z., Bolin, J. M., Ruotti, V., Probasco, M. D., Smuga-Otto, K., Howden, S. E., Diol, N. R., Propson, N. E., Wagner, R., Lee, G. O., Antosiewicz-Bourget, J., Teng, J. M. C., & Thomson, J. A. (2011). Chemically defined conditions for human iPSC derivation and culture. *Nature Methods*, *8*(5), 424–429. https://doi.org/10.1038/nmeth.1593

Constantinides, P. G., Jones, P. A., & Gevers, W. (1977). Functional striated muscle cells from non-myoblast precursors following 5-azacytidine treatment. *Nature*, *267*(5609), 364–366. https://doi.org/10.1038/267364a0

Copelan, E. A. (2006). Hematopoietic stem-cell transplantation. *The New England Journal of Medicine*, *354*(17), 1813–1826. https://doi.org/10.1056/NEJMra052638

Corral, J., Lavenir, I., Impey, H., Warren, A. J., Forster, A., Larson, T. A., Bell, S., McKenzie, A. N., King, G., & Rabbitts, T. H. (1996). An Mll-AF9 fusion gene made by homologous recombination causes acute leukemia in chimeric mice: A method to create fusion oncogenes. *Cell*, *85*(6), 853–861. https://doi.org/10.1016/s0092-8674(00)81269-6

Davis, R. L., Weintraub, H., & Lassar, A. B. (1987). Expression of a single transfected cDNA converts fibroblasts to myoblasts. *Cell*, *51*(6), 987–1000.

Dawson, M. A., Avery, S., McQuilten, Z. K., Bailey, M. J., Shortt, J., Polizzotto, M. N., Wood, E. M., & Cole-Sinclair, M. F. (2007). Blood transfusion requirements for patients undergoing chemotherapy for acute myeloid leukemia how much is enough? *Haematologica*, *92*(7), 996–997. https://doi.org/10.3324/haematol.11019

Degos, L., & Wang, Z. Y. (2001). All trans retinoic acid in acute promyelocytic leukemia. *Oncogene*, *20*(49), 7140–7145. https://doi.org/10.1038/sj.onc.1204763

Di Croce, L., Raker, V. A., Corsaro, M., Fazi, F., Fanelli, M., Faretta, M., Fuks, F., Lo Coco, F., Kouzarides, T., Nervi, C., Minucci, S., & Pelicci, P. G. (2002). Methyltransferase recruitment and DNA hypermethylation of target promoters by an oncogenic transcription factor. *Science (New York, N.Y.)*, *295*(5557), 1079–1082. https://doi.org/10.1126/science.1065173

Döhner, H., Estey, E., Grimwade, D., Amadori, S., Appelbaum, F. R., Büchner, T., Dombret, H., Ebert, B. L., Fenaux, P., Larson, R. A., Levine, R. L., Lo-Coco, F., Naoe, T., Niederwieser, D., Ossenkoppele, G. J., Sanz, M., Sierra, J., Tallman, M. S., Tien, H.-F., … Bloomfield, C. D. (2017). Diagnosis and management of AML in adults: 2017 ELN recommendations from an international expert panel. *Blood*, *129*(4), 424–447. https://doi.org/10.1182/blood-2016-08-733196

Doulatov, S., Vo, L. T., Chou, S. S., Kim, P. G., Arora, N., Li, H., Hadland, B. K., Bernstein, I. D., Collins, J. J., Zon, L. I., & Daley, G. Q. (2013). Induction of multipotential hematopoietic progenitors from human pluripotent stem cells via respecification of lineage-restricted precursors. *Cell Stem Cell*, *13*(4), 459–470. https://doi.org/10.1016/j.stem.2013.09.002

Dührsen, U., Villeval, J. L., Boyd, J., Kannourakis, G., Morstyn, G., & Metcalf, D. (1988). Effects of recombinant human granulocyte colony-stimulating factor on hematopoietic progenitor cells in cancer patients. *Blood*, *72*(6), 2074–2081.

Dzierzak, E., & Speck, N. A. (2008). Of lineage and legacy: The development of mammalian hematopoietic stem cells. *Nature Immunology*, *9*(2), 129–136. https://doi.org/10.1038/ni1560

Ebert, A. D., Yu, J., Rose, F. F., Mattis, V. B., Lorson, C. L., Thomson, J. A., & Svendsen, C. N. (2009). Induced pluripotent stem cells from a spinal muscular atrophy patient. *Nature*, *457*(7227), 277–280. https://doi.org/10.1038/nature07677

Eilken, H. M., Nishikawa, S.-I., & Schroeder, T. (2009). Continuous single-cell imaging of blood generation from haemogenic endothelium. *Nature*, *457*(7231), 896–900. https://doi.org/10.1038/nature07760

Eliopoulos, N., Stagg, J., Lejeune, L., Pommey, S., & Galipeau, J. (2005). Allogeneic marrow stromal cells are immune rejected by MHC class I- and class II-mismatched recipient mice. *Blood*, *106*(13), 4057–4065. https://doi.org/10.1182/blood-2005-03-1004

Evans, M. J. (1972). The isolation and properties of a clonal tissue culture strain of pluripotent mouse teratoma cells. *Journal of Embryology and Experimental Morphology*, *28*(1), 163–176.

Evans, M. J., & Kaufman, M. H. (1981). Establishment in culture of pluripotential cells from mouse embryos. *Nature*, *292*(5819), 154–156. https://doi.org/10.1038/292154a0

Feng, Q., Shabrani, N., Thon, J. N., Huo, H., Thiel, A., Machlus, K. R., Kim, K., Brooks, J., Li, F., Luo, C., Kimbrel, E. A., Wang, J., Kim, K.-S., Italiano, J., Cho, J., Lu, S.-J., & Lanza, R. (2014). Scalable generation of universal platelets from human induced pluripotent stem cells. *Stem Cell Reports*, *3*(5), 817–831. https://doi.org/10.1016/j.stemcr.2014.09.010

Figueroa, M. E., Lugthart, S., Li, Y., Erpelinck-Verschueren, C., Deng, X., Christos, P. J., Schifano, E., Booth, J., van Putten, W., Skrabanek, L., Campagne, F., Mazumdar, M., Greally, J. M., Valk, P. J. M., Löwenberg, B., Delwel, R., & Melnick, A. (2010). DNA methylation signatures identify biologically distinct subtypes in acute myeloid leukemia. *Cancer Cell*, *17*(1), 13–27. https://doi.org/10.1016/j.ccr.2009.11.020

Figueroa, M. E., Skrabanek, L., Li, Y., Jiemjit, A., Fandy, T. E., Paietta, E., Fernandez, H., Tallman, M. S., Greally, J. M., Carraway, H., Licht, J. D., Gore, S. D., & Melnick, A. (2009). MDS and secondary AML display unique patterns and abundance of aberrant DNA methylation. *Blood*, *114*(16), 3448–3458. https://doi.org/10.1182/blood-2009-01-200519

Fouse, S. D., Shen, Y., Pellegrini, M., Cole, S., Meissner, A., Van Neste, L., Jaenisch, R., & Fan, G. (2008). Promoter CpG methylation contributes to ES cell gene regulation in parallel with Oct4/Nanog, PcG complex, and histone H3 K4/K27 trimethylation. *Cell Stem Cell*, *2*(2), 160–169. https://doi.org/10.1016/j.stem.2007.12.011

Fu, S., Consoli, U., Hanania, E. G., Zu, Z., Claxton, D. F., Andreeff, M., & Deisseroth, A. B. (1995). PML/RARalpha, a fusion protein in acute promyelocytic leukemia, prevents growth factor withdrawal-induced apoptosis in TF-1 cells. *Clinical Cancer Research: An Official Journal of the American Association for Cancer Research*, *1*(6), 583–590.

Fusaki, N., Ban, H., Nishiyama, A., Saeki, K., & Hasegawa, M. (2009). Efficient induction of transgene-free human pluripotent stem cells using a vector based on Sendai virus, an RNA virus that does not integrate into the host genome. *Proceedings of the Japan Academy. Series B, Physical and Biological Sciences*, *85*(8), 348–362. https://doi.org/10.2183/pjab.85.348

Gandre-Babbe, S., Paluru, P., Aribeana, C., Chou, S. T., Bresolin, S., Lu, L., Sullivan, S. K., Tasian, S. K., Weng, J., Favre, H., Choi, J. K., French, D. L., Loh, M. L., & Weiss, M. J. (2013). Patient-derived induced pluripotent stem cells recapitulate hematopoietic abnormalities of juvenile myelomonocytic leukemia. *Blood*, *121*(24), 4925–4929. https://doi.org/10.1182/blood-2013-01-478412

Gatti, R. A., Meuwissen, H. J., Allen, H. D., Hong, R., & Good, R. A. (1968). Immunological reconstitution of sex-linked lymphopenic immunological deficiency. *Lancet (London, England)*, *2*(7583), 1366–1369. https://doi.org/10.1016/s0140-6736(68)92673-1

Gluckman, E., Broxmeyer, H. A., Auerbach, A. D., Friedman, H. S., Douglas, G. W., Devergie, A., Esperou, H., Thierry, D., Socie, G., & Lehn, P. (1989). Hematopoietic reconstitution

in a patient with Fanconi's anemia by means of umbilical-cord blood from an HLA-identical sibling. *The New England Journal of Medicine*, *321*(17), 1174–1178. https://doi.org/10.1056/NEJM198910263211707

Goldberg, A. D., Allis, C. D., & Bernstein, E. (2007). Epigenetics: A landscape takes shape. *Cell*, *128*(4), 635–638. https://doi.org/10.1016/j.cell.2007.02.006

Graf, T. (2011). Historical origins of transdifferentiation and reprogramming. *Cell Stem Cell*, *9*(6), 504–516. https://doi.org/10.1016/j.stem.2011.11.012

Graf, T., & Enver, T. (2009). Forcing cells to change lineages. *Nature*, *462*(7273), 587–594. https://doi.org/10.1038/nature08533

Gragert, L., Eapen, M., Williams, E., Freeman, J., Spellman, S., Baitty, R., Hartzman, R., Rizzo, J. D., Horowitz, M., Confer, D., & Maiers, M. (2014). HLA match likelihoods for hematopoietic stem-cell grafts in the U.S. registry. *The New England Journal of Medicine*, *371*(4), 339–348. https://doi.org/10.1056/NEJMsa1311707

Grassi, S., Guerrini, F., Ciabatti, E., Puccetti, R., Salehzadeh, S., Metelli, M. R., Di Vita, A., Domenichini, C., Caracciolo, F., Orciuolo, E., Pelosini, M., Mazzantini, E., Rossi, P., Mazziotta, F., Petrini, M., & Galimberti, S. (2020). Digital Droplet PCR is a Specific and Sensitive Tool for Detecting IDH2 Mutations in Acute Myeloid LeuKemia Patients. *Cancers*, *12*(7), 1738. https://doi.org/10.3390/cancers12071738

Gratwohl, A., Baldomero, H., Aljurf, M., Pasquini, M. C., Bouzas, L. F., Yoshimi, A., Szer, J., Lipton, J., Schwendener, A., Gratwohl, M., Frauendorfer, K., Niederwieser, D., Horowitz, M., Kodera, Y., & Worldwide Network of Blood and Marrow Transplantation. (2010). Hematopoietic stem cell transplantation: A global perspective. *JAMA*, *303*(16), 1617–1624. https://doi.org/10.1001/jama.2010.491

Greaves, M. (2016). Leukaemia “firsts” in cancer research and treatment. *Nature Reviews. Cancer*, *16*(3), 163–172. https://doi.org/10.1038/nrc.2016.3

Griffin, J. D., & Löwenberg, B. (1986). Clonogenic cells in acute myeloblastic leukemia. *Blood*, *68*(6), 1185–1195.

Grimwade, D., Ivey, A., & Huntly, B. J. P. (2016). Molecular landscape of acute myeloid leukemia in younger adults and its clinical relevance. *Blood*, *127*(1), 29–41. https://doi.org/10.1182/blood-2015-07-604496

Grimwade, D., Walker, H., Oliver, F., Wheatley, K., Harrison, C., Harrison, G., Rees, J., Hann, I., Stevens, R., Burnett, A., & Goldstone, A. (1998). The importance of diagnostic cytogenetics on outcome in AML: Analysis of 1,612 patients entered into the MRC AML 10 trial. The Medical Research Council Adult and Children’s Leukaemia Working Parties. *Blood*, *92*(7), 2322–2333.

Guenechea, G., Gan, O. I., Dorrell, C., & Dick, J. E. (2001). Distinct classes of human stem cells that differ in proliferative and self-renewal potential. *Nature Immunology*, *2*(1), 75–82. https://doi.org/10.1038/83199

Guha, P., Morgan, J. W., Mostoslavsky, G., Rodrigues, N. P., & Boyd, A. S. (2013). Lack of immune response to differentiated cells derived from syngeneic induced pluripotent stem cells. *Cell Stem Cell*, *12*(4), 407–412. https://doi.org/10.1016/j.stem.2013.01.006

Guo, S., Zi, X., Schulz, V. P., Cheng, J., Zhong, M., Koochaki, S. H. J., Megyola, C. M., Pan, X., Heydari, K., Weissman, S. M., Gallagher, P. G., Krause, D. S., Fan, R., & Lu, J. (2014). Nonstochastic reprogramming from a privileged somatic cell state. *Cell*, *156*(4), 649–662. https://doi.org/10.1016/j.cell.2014.01.020

Gurdon, J. B. (1960). The developmental capacity of nuclei taken from differentiating endoderm cells of Xenopus laevis. *Journal of Embryology and Experimental Morphology*, *8*, 505–526.

Gurdon, J. B. (1962). The developmental capacity of nuclei taken from intestinal epithelium cells of feeding tadpoles. *Journal of Embryology and Experimental Morphology*, *10*, 622–640.

Gurdon, J. B. (2006). From nuclear transfer to nuclear reprogramming: The reversal of cell differentiation. *Annual Review of Cell and Developmental Biology*, *22*, 1–22. https://doi.org/10.1146/annurev.cellbio.22.090805.140144

Gurdon, J. B., Elsdale, T. R., & Fischberg, M. (1958). Sexually mature individuals of Xenopus laevis from the transplantation of single somatic nuclei. *Nature*, *182*(4627), 64–65. https://doi.org/10.1038/182064a0

Gurdon, J. B., & Uehlinger, V. (1966). "Fertile" intestine nuclei. *Nature*, *210*(5042), 1240–1241. https://doi.org/10.1038/2101240a0

Hanna, J., Saha, K., Pando, B., van Zon, J., Lengner, C. J., Creyghton, M. P., van Oudenaarden, A., & Jaenisch, R. (2009). Direct cell reprogramming is a stochastic process amenable to acceleration. *Nature*, *462*(7273), 595–601. https://doi.org/10.1038/nature08592

Hanna, J., Wernig, M., Markoulaki, S., Sun, C.-W., Meissner, A., Cassady, J. P., Beard, C., Brambrink, T., Wu, L.-C., Townes, T. M., & Jaenisch, R. (2007). Treatment of sickle cell anemia mouse model with iPS cells generated from autologous skin. *Science (New York, N.Y.)*, *318*(5858), 1920–1923. https://doi.org/10.1126/science.1152092

Harris, H., Miller, O. J., Klein, G., Worst, P., & Tachibana, T. (1969). Suppression of malignancy by cell fusion. *Nature*, *223*(5204), 363–368. https://doi.org/10.1038/223363a0

Harris, H., & Watkins, J. F. (1965). HYBRID CELLS DERIVED FROM MOUSE AND MAN: ARTIFICIAL HETEROKARYONS OF MAMMALIAN CELLS FROM DIFFERENT SPECIES. *Nature*, *205*, 640–646. https://doi.org/10.1038/205640a0

Hentze, H., Soong, P. L., Wang, S. T., Phillips, B. W., Putti, T. C., & Dunn, N. R. (2009). Teratoma formation by human embryonic stem cells: Evaluation of essential parameters for future safety studies. *Stem Cell Research*, *2*(3), 198–210. https://doi.org/10.1016/j.scr.2009.02.002

Hoffman, G. E., Hartley, B. J., Flaherty, E., Ladran, I., Gochman, P., Ruderfer, D. M., Stahl, E. A., Rapoport, J., Sklar, P., & Brennand, K. J. (2017). Transcriptional signatures of schizophrenia in hiPSC-derived NPCs and neurons are concordant with post-mortem adult brains. *Nature Communications*, *8*(1), 2225. https://doi.org/10.1038/s41467-017-02330-5

Hoffmann, D., Göhring, G., Heuser, M., Ganser, A., Schambach, A., & Morgan, M. A. (2016). Letter to the Editor: Production of Mature Healthy Hematopoietic Cells from Induced Pluripotent Stem Cells Derived from an AML Diagnostic Sample Containing the t(8;21) Translocation. *Stem Cells (Dayton, Ohio)*, *34*(3), 797–799. https://doi.org/10.1002/stem.2207

Hope, K. J., Jin, L., & Dick, J. E. (2004). Acute myeloid leukemia originates from a hierarchy of leukemic stem cell classes that differ in self-renewal capacity. *Nature Immunology*, *5*(7), 738–743. https://doi.org/10.1038/ni1080

Hosoi, M., Kumano, K., Taoka, K., Arai, S., Kataoka, K., Ueda, K., Kamikubo, Y., Takayama, N., Otsu, M., Eto, K., Nakauchi, H., & Kurokawa, M. (2014). Generation of induced pluripotent stem cells derived from primary and secondary myelofibrosis patient samples.

Experimental Hematology, *42*(9), 816–825. https://doi.org/10.1016/j.exphem.2014.03.010

Hsu, T. C., & Moorhead, P. S. (1957). Mammalian chromosomes in vitro. VII. Heteroploidy in human cell strains. *Journal of the National Cancer Institute*, *18*(3), 463–471.

Hu, K., Yu, J., Suknuntha, K., Tian, S., Montgomery, K., Choi, K.-D., Stewart, R., Thomson, J. A., & Slukvin, I. I. (2011). Efficient generation of transgene-free induced pluripotent stem cells from normal and neoplastic bone marrow and cord blood mononuclear cells. *Blood*, *117*(14), e109-119. https://doi.org/10.1182/blood-2010-07-298331

Huangfu, D., Maehr, R., Guo, W., Eijkelenboom, A., Snitow, M., Chen, A. E., & Melton, D. A. (2008). Induction of pluripotent stem cells by defined factors is greatly improved by small molecule compounds. *Nature Biotechnology*, *26*(7), 795–797. https://doi.org/10.1038/nbt1418

International Stem Cell Initiative, Adewumi, O., Aflatoonian, B., Ahrlund-Richter, L., Amit, M., Andrews, P. W., Beighton, G., Bello, P. A., Benvenisty, N., Berry, L. S., Bevan, S., Blum, B., Brooking, J., Chen, K. G., Choo, A. B. H., Churchill, G. A., Corbel, M., Damjanov, I., Draper, J. S., … Zhang, W. (2007). Characterization of human embryonic stem cell lines by the International Stem Cell Initiative. *Nature Biotechnology*, *25*(7), 803–816. https://doi.org/10.1038/nbt1318

Ito, R., Takahashi, T., Katano, I., & Ito, M. (2012). Current advances in humanized mouse models. *Cellular & Molecular Immunology*, *9*(3), 208–214. https://doi.org/10.1038/cmi.2012.2

Kahan, B. W., & Ephrussi, B. (1970). Developmental potentialities of clonal in vitro cultures of mouse testicular teratoma. *Journal of the National Cancer Institute*, *44*(5), 1015–1036.

Kamel-Reid, S., & Dick, J. E. (1988). Engraftment of immune-deficient mice with human hematopoietic stem cells. *Science (New York, N.Y.)*, *242*(4886), 1706–1709. https://doi.org/10.1126/science.2904703

Kim, D.-S., Ross, P. J., Zaslavsky, K., & Ellis, J. (2014). Optimizing neuronal differentiation from induced pluripotent stem cells to model ASD. *Frontiers in Cellular Neuroscience*, *8*, 109. https://doi.org/10.3389/fncel.2014.00109

Kim, J., Hoffman, J. P., Alpaugh, R. K., Rhim, A. D., Rhimm, A. D., Reichert, M., Stanger, B. Z., Furth, E. E., Sepulveda, A. R., Yuan, C.-X., Won, K.-J., Donahue, G., Sands, J., Gumbs, A. A., & Zaret, K. S. (2013). An iPSC line from human pancreatic ductal adenocarcinoma undergoes early to invasive stages of pancreatic cancer progression. *Cell Reports*, *3*(6), 2088–2099. https://doi.org/10.1016/j.celrep.2013.05.036

Kim, K., Doi, A., Wen, B., Ng, K., Zhao, R., Cahan, P., Kim, J., Aryee, M. J., Ji, H., Ehrlich, L. I. R., Yabuuchi, A., Takeuchi, A., Cunniff, K. C., Hongguang, H., Mckinney-Freeman, S., Naveiras, O., Yoon, T. J., Irizarry, R. A., Jung, N., … Daley, G. Q. (2010). Epigenetic memory in induced pluripotent stem cells. *Nature*, *467*(7313), 285–290. https://doi.org/10.1038/nature09342

Kitala, D., Kawecki, M., Klama-Baryła, A., Łabuś, W., Kraut, M., Glik, J., Ryszkiel, I., Kawecki, M. P., & Nowak, M. (2016). Allogeneic vs. Autologous Skin Grafts in the Therapy of Patients with Burn Injuries: A Restrospective, Open-label Clinical Study with Pair Matching. *Advances in Clinical and Experimental Medicine: Official Organ Wroclaw Medical University*, *25*(5), 923–929. https://doi.org/10.17219/acem/61961

Kleinsmith, L. J., & Pierce, G. B. (1964). MULTIPOTENTIALITY OF SINGLE EMBRYONAL CARCINOMA CELLS. *Cancer Research*, *24*, 1544–1551.

Knaupp, A. S., Buckberry, S., Pflueger, J., Lim, S. M., Ford, E., Larcombe, M. R., Rossello, F. J., de Mendoza, A., Alaei, S., Firas, J., Holmes, M. L., Nair, S. S., Clark, S. J., Nefzger, C. M., Lister, R., & Polo, J. M. (2017). Transient and Permanent Reconfiguration of Chromatin and Transcription Factor Occupancy Drive Reprogramming. *Cell Stem Cell*, *21*(6), 834-845.e6. https://doi.org/10.1016/j.stem.2017.11.007

Kohli, R. M., & Zhang, Y. (2013). TET enzymes, TDG and the dynamics of DNA demethylation. *Nature*, *502*(7472), 472–479. https://doi.org/10.1038/nature12750

Kondo, M., Weissman, I. L., & Akashi, K. (1997). Identification of clonogenic common lymphoid progenitors in mouse bone marrow. *Cell*, *91*(5), 661–672.

Kotini, A. G., Chang, C.-J., Chow, A., Yuan, H., Ho, T.-C., Wang, T., Vora, S., Solovyov, A., Husser, C., Olszewska, M., Teruya-Feldstein, J., Perumal, D., Klimek, V. M., Spyridonidis, A., Rampal, R. K., Silverman, L., Reddy, E. P., Papaemmanuil, E., Parekh, S., … Papapetrou, E. P. (2017a). Stage-Specific Human Induced Pluripotent Stem Cells Map the Progression of Myeloid Transformation to Transplantable Leukemia. *Cell Stem Cell*, *20*(3), 315-328.e7. https://doi.org/10.1016/j.stem.2017.01.009

Kotini, A. G., Chang, C.-J., Chow, A., Yuan, H., Ho, T.-C., Wang, T., Vora, S., Solovyov, A., Husser, C., Olszewska, M., Teruya-Feldstein, J., Perumal, D., Klimek, V. M., Spyridonidis, A., Rampal, R. K., Silverman, L., Reddy, E. P., Papaemmanuil, E., Parekh, S., … Papapetrou, E. P. (2017b). Stage-Specific Human Induced Pluripotent Stem Cells Map the Progression of Myeloid Transformation to Transplantable Leukemia. *Cell Stem Cell*, *20*(3), 315-328.e7. https://doi.org/10.1016/j.stem.2017.01.009

Kotini, A. G., & Papapetrou, E. P. (2020). Engineering of targeted megabase-scale deletions in human induced pluripotent stem cells. *Experimental Hematology*, *87*, 25–32. https://doi.org/10.1016/j.exphem.2020.06.001

Kulessa, H., Frampton, J., & Graf, T. (1995). GATA-1 reprograms avian myelomonocytic cell lines into eosinophils, thromboblasts, and erythroblasts. *Genes & Development*, *9*(10), 1250–1262. https://doi.org/10.1101/gad.9.10.1250

Kumano, K., Arai, S., Hosoi, M., Taoka, K., Takayama, N., Otsu, M., Nagae, G., Ueda, K., Nakazaki, K., Kamikubo, Y., Eto, K., Aburatani, H., Nakauchi, H., & Kurokawa, M. (2012). Generation of induced pluripotent stem cells from primary chronic myelogenous leukemia patient samples. *Blood*, *119*(26), 6234–6242. https://doi.org/10.1182/blood-2011-07-367441

Lapidot, T., Pflumio, F., Doedens, M., Murdoch, B., Williams, D. E., & Dick, J. E. (1992). Cytokine stimulation of multilineage hematopoiesis from immature human cells engrafted in SCID mice. *Science (New York, N.Y.)*, *255*(5048), 1137–1141. https://doi.org/10.1126/science.1372131

Lapidot, T., Sirard, C., Vormoor, J., Murdoch, B., Hoang, T., Caceres-Cortes, J., Minden, M., Paterson, B., Caligiuri, M. A., & Dick, J. E. (1994). A cell initiating human acute myeloid leukaemia after transplantation into SCID mice. *Nature*, *367*(6464), 645–648. https://doi.org/10.1038/367645a0

Larochelle, A., Vormoor, J., Hanenberg, H., Wang, J. C., Bhatia, M., Lapidot, T., Moritz, T., Murdoch, B., Xiao, X. L., Kato, I., Williams, D. A., & Dick, J. E. (1996). Identification of primitive human hematopoietic cells capable of repopulating NOD/SCID mouse bone

marrow: Implications for gene therapy. *Nature Medicine*, *2*(12), 1329–1337. https://doi.org/10.1038/nm1296-1329

Lassar, A. B., Paterson, B. M., & Weintraub, H. (1986). Transfection of a DNA locus that mediates the conversion of 10T1/2 fibroblasts to myoblasts. *Cell*, *47*(5), 649–656. https://doi.org/10.1016/0092-8674(86)90507-6

Lee, J., Dykstra, B., Spencer, J. A., Kenney, L. L., Greiner, D. L., Shultz, L. D., Brehm, M. A., Lin, C. P., Sackstein, R., & Rossi, D. J. (2017). MRNA-mediated glycoengineering ameliorates deficient homing of human stem cell-derived hematopoietic progenitors. *The Journal of Clinical Investigation*, *127*(6), 2433–2437. https://doi.org/10.1172/JCI92030

Lee, J.-H., Lee, J. B., Shapovalova, Z., Fiebig-Comyn, A., Mitchell, R. R., Laronde, S., Szabo, E., Benoit, Y. D., & Bhatia, M. (2014). Somatic transcriptome priming gates lineage-specific differentiation potential of human-induced pluripotent stem cell states. *Nature Communications*, *5*, 5605. https://doi.org/10.1038/ncomms6605

Lee, J.-H., Salci, K. R., Reid, J. C., Orlando, L., Tanasijevic, B., Shapovalova, Z., & Bhatia, M. (2017). Brief Report: Human Acute Myeloid Leukemia Reprogramming to Pluripotency Is a Rare Event and Selects for Patient Hematopoietic Cells Devoid of Leukemic Mutations. *Stem Cells (Dayton, Ohio)*, *35*(9), 2095–2102. https://doi.org/10.1002/stem.2655

Legrand, N., Weijer, K., & Spits, H. (2006). Experimental models to study development and function of the human immune system in vivo. *Journal of Immunology (Baltimore, Md.: 1950)*, *176*(4), 2053–2058. https://doi.org/10.4049/jimmunol.176.4.2053

Levenstein, M. E., Ludwig, T. E., Xu, R.-H., Llanas, R. A., VanDenHeuvel-Kramer, K., Manning, D., & Thomson, J. A. (2006). Basic fibroblast growth factor support of human

embryonic stem cell self-renewal. *Stem Cells (Dayton, Ohio)*, *24*(3), 568–574. https://doi.org/10.1634/stemcells.2005-0247

Levsky, J. M., & Singer, R. H. (2003). Fluorescence in situ hybridization: Past, present and future. *Journal of Cell Science*, *116*(Pt 14), 2833–2838. https://doi.org/10.1242/jcs.00633

Li, E., Beard, C., & Jaenisch, R. (1993). Role for DNA methylation in genomic imprinting. *Nature*, *366*(6453), 362–365. https://doi.org/10.1038/366362a0

Li, E., Bestor, T. H., & Jaenisch, R. (1992). Targeted mutation of the DNA methyltransferase gene results in embryonic lethality. *Cell*, *69*(6), 915–926. https://doi.org/10.1016/0092-8674(92)90611-f

Liao, J., Karnik, R., Gu, H., Ziller, M. J., Clement, K., Tsankov, A. M., Akopian, V., Gifford, C. A., Donaghey, J., Galonska, C., Pop, R., Reyon, D., Tsai, S. Q., Mallard, W., Joung, J. K., Rinn, J. L., Gnirke, A., & Meissner, A. (2015). Targeted disruption of DNMT1, DNMT3A and DNMT3B in human embryonic stem cells. *Nature Genetics*, *47*(5), 469–478. https://doi.org/10.1038/ng.3258

Lu, S.-J., Feng, Q., Park, J. S., Vida, L., Lee, B.-S., Strausbauch, M., Wettstein, P. J., Honig, G. R., & Lanza, R. (2008). Biologic properties and enucleation of red blood cells from human embryonic stem cells. *Blood*, *112*(12), 4475–4484. https://doi.org/10.1182/blood-2008-05-157198

Ludwig, T. E., Bergendahl, V., Levenstein, M. E., Yu, J., Probasco, M. D., & Thomson, J. A. (2006). Feeder-independent culture of human embryonic stem cells. *Nature Methods*, *3*(8), 637–646. https://doi.org/10.1038/nmeth902

Ludwig, T. E., Levenstein, M. E., Jones, J. M., Berggren, W. T., Mitchen, E. R., Frane, J. L., Crandall, L. J., Daigh, C. A., Conard, K. R., Piekarczyk, M. S., Llanas, R. A., &

Thomson, J. A. (2006). Derivation of human embryonic stem cells in defined conditions. *Nature Biotechnology*, *24*(2), 185–187. https://doi.org/10.1038/nbt1177

Malik, N., & Rao, M. S. (2013). A Review of the Methods for Human iPSC Derivation. In U. Lakshmipathy & M. C. Vemuri (Eds.), *Pluripotent Stem Cells* (Vol. 997, pp. 23–33). Humana Press. https://doi.org/10.1007/978-1-62703-348-0_3

Mandai, M., Kurimoto, Y., & Takahashi, M. (2017). Autologous Induced Stem-Cell-Derived Retinal Cells for Macular Degeneration. *The New England Journal of Medicine*, *377*(8), 792–793. https://doi.org/10.1056/NEJMc1706274

Marchetto, M. C. N., Carromeu, C., Acab, A., Yu, D., Yeo, G. W., Mu, Y., Chen, G., Gage, F. H., & Muotri, A. R. (2010). A model for neural development and treatment of Rett syndrome using human induced pluripotent stem cells. *Cell*, *143*(4), 527–539. https://doi.org/10.1016/j.cell.2010.10.016

Marión, R. M., Strati, K., Li, H., Murga, M., Blanco, R., Ortega, S., Fernandez-Capetillo, O., Serrano, M., & Blasco, M. A. (2009). A p53-mediated DNA damage response limits reprogramming to ensure iPS cell genomic integrity. *Nature*, *460*(7259), 1149–1153. https://doi.org/10.1038/nature08287

Martin, G. R. (1981). Isolation of a pluripotent cell line from early mouse embryos cultured in medium conditioned by teratocarcinoma stem cells. *Proceedings of the National Academy of Sciences of the United States of America*, *78*(12), 7634–7638. https://doi.org/10.1073/pnas.78.12.7634

Matin, M. M., Walsh, J. R., Gokhale, P. J., Draper, J. S., Bahrami, A. R., Morton, I., Moore, H. D., & Andrews, P. W. (2004). Specific knockdown of Oct4 and beta2-microglobulin expression by RNA interference in human embryonic stem cells and embryonic

carcinoma cells. *Stem Cells (Dayton, Ohio)*, *22*(5), 659–668. https://doi.org/10.1634/stemcells.22-5-659

McCulloch, E. A. (1983). Stem cells in normal and leukemic hemopoiesis (Henry Stratton Lecture, 1982). *Blood*, *62*(1), 1–13.

McCune, J. M., Namikawa, R., Kaneshima, H., Shultz, L. D., Lieberman, M., & Weissman, I. L. (1988). The SCID-hu mouse: Murine model for the analysis of human hematolymphoid differentiation and function. *Science (New York, N.Y.)*, *241*(4873), 1632–1639. https://doi.org/10.1126/science.241.4873.1632

McNeish, J., Gardner, J. P., Wainger, B. J., Woolf, C. J., & Eggan, K. (2015). From Dish to Bedside: Lessons Learned While Translating Findings from a Stem Cell Model of Disease to a Clinical Trial. *Cell Stem Cell*, *17*(1), 8–10. https://doi.org/10.1016/j.stem.2015.06.013

Medeiros, B. C., Fathi, A. T., DiNardo, C. D., Pollyea, D. A., Chan, S. M., & Swords, R. (2017). Isocitrate dehydrogenase mutations in myeloid malignancies. *Leukemia*, *31*(2), 272–281. https://doi.org/10.1038/leu.2016.275

Medinger, M., & Passweg, J. R. (2017). Acute myeloid leukaemia genomics. *British Journal of Haematology*, *179*(4), 530–542. https://doi.org/10.1111/bjh.14823

Medvinsky, A., & Dzierzak, E. (1996). Definitive hematopoiesis is autonomously initiated by the AGM region. *Cell*, *86*(6), 897–906.

Melnick, A., & Licht, J. D. (1999). Deconstructing a disease: RARalpha, its fusion partners, and their roles in the pathogenesis of acute promyelocytic leukemia. *Blood*, *93*(10), 3167–3215.

Metcalf, D., Moore, M. A., & Warner, N. L. (1969). Colony formation in vitro by myelomonocytic leukemic cells. *Journal of the National Cancer Institute*, *43*(4), 983–1001.

Miller, L. W. (2002). Cardiovascular toxicities of immunosuppressive agents. *American Journal of Transplantation: Official Journal of the American Society of Transplantation and the American Society of Transplant Surgeons*, *2*(9), 807–818. https://doi.org/10.1034/j.1600-6143.2002.20902.x

Mitsui, K., Tokuzawa, Y., Itoh, H., Segawa, K., Murakami, M., Takahashi, K., Maruyama, M., Maeda, M., & Yamanaka, S. (2003). The homeoprotein Nanog is required for maintenance of pluripotency in mouse epiblast and ES cells. *Cell*, *113*(5), 631–642. https://doi.org/10.1016/s0092-8674(03)00393-3

Moore, M. A., Williams, N., & Metcalf, D. (1973). In vitro colony formation by normal and leukemic human hematopoietic cells: Characterization of the colony-forming cells. *Journal of the National Cancer Institute*, *50*(3), 603–623. https://doi.org/10.1093/jnci/50.3.603

Morrison, S. J., Wandycz, A. M., Hemmati, H. D., Wright, D. E., & Weissman, I. L. (1997). Identification of a lineage of multipotent hematopoietic progenitors. *Development (Cambridge, England)*, *124*(10), 1929–1939.

Morrison, S. J., & Weissman, I. L. (1994). The long-term repopulating subset of hematopoietic stem cells is deterministic and isolatable by phenotype. *Immunity*, *1*(8), 661–673.

Mosier, D. E., Gulizia, R. J., Baird, S. M., & Wilson, D. B. (1988). Transfer of a functional human immune system to mice with severe combined immunodeficiency. *Nature*, *335*(6187), 256–259. https://doi.org/10.1038/335256a0

Müller, A. M. S., Kohrt, H. E. K., Cha, S., Laport, G., Klein, J., Guardino, A. E., Johnston, L. J., Stockerl-Goldstein, K. E., Hanania, E., Juttner, C., Blume, K. G., Negrin, R. S., Weissman, I. L., & Shizuru, J. A. (2012). Long-term outcome of patients with metastatic breast cancer treated with high-dose chemotherapy and transplantation of purified autologous hematopoietic stem cells. *Biology of Blood and Marrow Transplantation: Journal of the American Society for Blood and Marrow Transplantation*, *18*(1), 125–133. https://doi.org/10.1016/j.bbmt.2011.07.009

Muñoz-López, A., Romero-Moya, D., Prieto, C., Ramos-Mejía, V., Agraz-Doblas, A., Varela, I., Buschbeck, M., Palau, A., Carvajal-Vergara, X., Giorgetti, A., Ford, A., Lako, M., Granada, I., Ruiz-Xivillé, N., Rodríguez-Perales, S., Torres-Ruíz, R., Stam, R. W., Fuster, J. L., Fraga, M. F., … Menendez, P. (2016). Development Refractoriness of MLL-Rearranged Human B Cell Acute Leukemias to Reprogramming into Pluripotency. *Stem Cell Reports*, *7*(4), 602–618. https://doi.org/10.1016/j.stemcr.2016.08.013

Nagai, K., Ishii, H., Miyoshi, N., Hoshino, H., Saito, T., Sato, T., Tomimaru, Y., Kobayashi, S., Nagano, H., Sekimoto, M., Doki, Y., & Mori, M. (2010). Long-term culture following ES-like gene-induced reprogramming elicits an aggressive phenotype in mutated cholangiocellular carcinoma cells. *Biochemical and Biophysical Research Communications*, *395*(2), 258–263. https://doi.org/10.1016/j.bbrc.2010.03.176

Nagase, R., Inoue, D., Pastore, A., Fujino, T., Hou, H.-A., Yamasaki, N., Goyama, S., Saika, M., Kanai, A., Sera, Y., Horikawa, S., Ota, Y., Asada, S., Hayashi, Y., Kawabata, K. C., Takeda, R., Tien, H.-F., Honda, H., Abdel-Wahab, O., & Kitamura, T. (2018). Expression of mutant Asxl1 perturbs hematopoiesis and promotes susceptibility to

leukemic transformation. *The Journal of Experimental Medicine*, *215*(6), 1729–1747. https://doi.org/10.1084/jem.20171151

Nagy, A., Rossant, J., Nagy, R., Abramow-Newerly, W., & Roder, J. C. (1993). Derivation of completely cell culture-derived mice from early-passage embryonic stem cells. *Proceedings of the National Academy of Sciences of the United States of America*, *90*(18), 8424–8428. https://doi.org/10.1073/pnas.90.18.8424

Nakamura, S., Takayama, N., Hirata, S., Seo, H., Endo, H., Ochi, K., Fujita, K., Koike, T., Harimoto, K., Dohda, T., Watanabe, A., Okita, K., Takahashi, N., Sawaguchi, A., Yamanaka, S., Nakauchi, H., Nishimura, S., & Eto, K. (2014). Expandable megakaryocyte cell lines enable clinically applicable generation of platelets from human induced pluripotent stem cells. *Cell Stem Cell*, *14*(4), 535–548. https://doi.org/10.1016/j.stem.2014.01.011

Nakanishi, M., Mitchell, R. R., Benoit, Y. D., Orlando, L., Reid, J. C., Shimada, K., Davidson, K. C., Shapovalova, Z., Collins, T. J., Nagy, A., & Bhatia, M. (2019). Human Pluripotency Is Initiated and Preserved by a Unique Subset of Founder Cells. *Cell*, *177*(4), 910-924.e22. https://doi.org/10.1016/j.cell.2019.03.013

Nichols, J., Zevnik, B., Anastassiadis, K., Niwa, H., Klewe-Nebenius, D., Chambers, I., Schöler, H., & Smith, A. (1998). Formation of pluripotent stem cells in the mammalian embryo depends on the POU transcription factor Oct4. *Cell*, *95*(3), 379–391. https://doi.org/10.1016/s0092-8674(00)81769-9

Niwa, H., Miyazaki, J., & Smith, A. G. (2000). Quantitative expression of Oct-3/4 defines differentiation, dedifferentiation or self-renewal of ES cells. *Nature Genetics*, *24*(4), 372–376. https://doi.org/10.1038/74199

Notta, F., Doulatov, S., Laurenti, E., Poeppl, A., Jurisica, I., & Dick, J. E. (2011). Isolation of single human hematopoietic stem cells capable of long-term multilineage engraftment. *Science (New York, N.Y.)*, *333*(6039), 218–221. https://doi.org/10.1126/science.1201219

Ogawa, S. (2019). Genetics of MDS. *Blood*, *133*(10), 1049–1059. https://doi.org/10.1182/blood-2018-10-844621

Ogle, B. M., Cascalho, M., & Platt, J. L. (2005). Biological implications of cell fusion. *Nature Reviews. Molecular Cell Biology*, *6*(7), 567–575. https://doi.org/10.1038/nrm1678

Okita, K., Hong, H., Takahashi, K., & Yamanaka, S. (2010). Generation of mouse-induced pluripotent stem cells with plasmid vectors. *Nature Protocols*, *5*(3), 418–428. https://doi.org/10.1038/nprot.2009.231

Orkin, S. H., & Zon, L. I. (2002). Hematopoiesis and stem cells: Plasticity versus developmental heterogeneity. *Nature Immunology*, *3*(4), 323–328. https://doi.org/10.1038/ni0402-323

Orkin, S. H., & Zon, L. I. (2008). Hematopoiesis: An evolving paradigm for stem cell biology. *Cell*, *132*(4), 631–644. https://doi.org/10.1016/j.cell.2008.01.025

Osborn, T. M., Hallett, P. J., Schumacher, J. M., & Isacson, O. (2020). Advantages and Recent Developments of Autologous Cell Therapy for Parkinson's Disease Patients. *Frontiers in Cellular Neuroscience*, *14*, 58. https://doi.org/10.3389/fncel.2020.00058

Papaemmanuil, E., Gerstung, M., Bullinger, L., Gaidzik, V. I., Paschka, P., Roberts, N. D., Potter, N. E., Heuser, M., Thol, F., Bolli, N., Gundem, G., Van Loo, P., Martincorena, I., Ganly, P., Mudie, L., McLaren, S., O'Meara, S., Raine, K., Jones, D. R., … Campbell, P. J. (2016). Genomic Classification and Prognosis in Acute Myeloid Leukemia. *The New England Journal of Medicine*, *374*(23), 2209–2221. https://doi.org/10.1056/NEJMoa1516192

Papapetrou, E. P. (2019). Modeling Leukemia with Human Induced Pluripotent Stem Cells. *Cold Spring Harbor Perspectives in Medicine*, *9*(12), a034868. https://doi.org/10.1101/cshperspect.a034868

Pereira, C.-F., Chang, B., Qiu, J., Niu, X., Papatsenko, D., Hendry, C. E., Clark, N. R., Nomura-Kitabayashi, A., Kovacic, J. C., Ma'ayan, A., Schaniel, C., Lemischka, I. R., & Moore, K. (2013). Induction of a hemogenic program in mouse fibroblasts. *Cell Stem Cell*, *13*(2), 205–218. https://doi.org/10.1016/j.stem.2013.05.024

Perl, A. E., & Carroll, M. (2007). Exploiting signal transduction pathways in acute myelogenous leukemia. *Current Treatment Options in Oncology*, *8*(4), 265–276. https://doi.org/10.1007/s11864-007-0043-z

Petit, I., Szyper-Kravitz, M., Nagler, A., Lahav, M., Peled, A., Habler, L., Ponomaryov, T., Taichman, R. S., Arenzana-Seisdedos, F., Fujii, N., Sandbank, J., Zipori, D., & Lapidot, T. (2002). G-CSF induces stem cell mobilization by decreasing bone marrow SDF-1 and up-regulating CXCR4. *Nature Immunology*, *3*(7), 687–694. https://doi.org/10.1038/ni813

Piccolo, F. M., Pereira, C. F., Cantone, I., Brown, K., Tsubouchi, T., Soza-Ried, J., Merkenschlager, M., & Fisher, A. G. (2011). Using heterokaryons to understand pluripotency and reprogramming. *Philosophical Transactions of the Royal Society of London. Series B, Biological Sciences*, *366*(1575), 2260–2265. https://doi.org/10.1098/rstb.2011.0004

Pierce, G. B., & Dixon, F. J. (1959). Testicular teratomas. II. Teratocarcinoma as an ascitic tumor. *Cancer*, *12*(3), 584–589. https://doi.org/10.1002/1097-0142(195905/06)12:3<584::aid-cncr2820120317>3.0.co;2-f

Pike, B. L., & Robinson, W. A. (1970). Human bone marrow colony growth in agar-gel. *Journal of Cellular Physiology*, *76*(1), 77–84. https://doi.org/10.1002/jcp.1040760111

Pineault, N., & Abu-Khader, A. (2015). Advances in umbilical cord blood stem cell expansion and clinical translation. *Experimental Hematology*, *43*(7), 498–513. https://doi.org/10.1016/j.exphem.2015.04.011

Pogosova-Agadjanyan, E. L., Moseley, A., Othus, M., Appelbaum, F. R., Chauncey, T. R., Chen, I.-M. L., Erba, H. P., Godwin, J. E., Jenkins, I. C., Fang, M., Huynh, M., Kopecky, K. J., List, A. F., Naru, J., Radich, J. P., Stevens, E., Willborg, B. E., Willman, C. L., Wood, B. L., … Stirewalt, D. L. (2020). AML risk stratification models utilizing ELN-2017 guidelines and additional prognostic factors: A SWOG report. *Biomarker Research*, *8*, 29. https://doi.org/10.1186/s40364-020-00208-1

Ran, F. A., Hsu, P. D., Wright, J., Agarwala, V., Scott, D. A., & Zhang, F. (2013). Genome engineering using the CRISPR-Cas9 system. *Nature Protocols*, *8*(11), 2281–2308. https://doi.org/10.1038/nprot.2013.143

Raya, A., Rodríguez-Pizà, I., Guenechea, G., Vassena, R., Navarro, S., Barrero, M. J., Consiglio, A., Castellà, M., Río, P., Sleep, E., González, F., Tiscornia, G., Garreta, E., Aasen, T., Veiga, A., Verma, I. M., Surrallés, J., Bueren, J., & Izpisúa Belmonte, J. C. (2009). Disease-corrected haematopoietic progenitors from Fanconi anaemia induced pluripotent stem cells. *Nature*, *460*(7251), 53–59. https://doi.org/10.1038/nature08129

Riddell, J., Gazit, R., Garrison, B. S., Guo, G., Saadatpour, A., Mandal, P. K., Ebina, W., Volchkov, P., Yuan, G.-C., Orkin, S. H., & Rossi, D. J. (2014). Reprogramming committed murine blood cells to induced hematopoietic stem cells with defined factors. *Cell*, *157*(3), 549–564. https://doi.org/10.1016/j.cell.2014.04.006

Robertson, J. A. (2010). Embryo stem cell research: Ten years of controversy. *The Journal of Law, Medicine & Ethics: A Journal of the American Society of Law, Medicine & Ethics*, *38*(2), 191–203. https://doi.org/10.1111/j.1748-720X.2010.00479.x

Rosenthal, M. D., Wishnow, R. M., & Sato, G. H. (1970). In vitro growth and differetiation of clonal populations of multipotential mouse clls derived from a transplantable testicular teratocarcinoma. *Journal of the National Cancer Institute*, *44*(5), 1001–1014.

Ruiz, S., Panopoulos, A. D., Herrerías, A., Bissig, K.-D., Lutz, M., Berggren, W. T., Verma, I. M., & Izpisua Belmonte, J. C. (2011). A high proliferation rate is required for cell reprogramming and maintenance of human embryonic stem cell identity. *Current Biology: CB*, *21*(1), 45–52. https://doi.org/10.1016/j.cub.2010.11.049

Sabitha, K. R., Shetty, A. K., & Upadhya, D. (2021). Patient-derived iPSC modeling of rare neurodevelopmental disorders: Molecular pathophysiology and prospective therapies. *Neuroscience and Biobehavioral Reviews*, *121*, 201–219. https://doi.org/10.1016/j.neubiorev.2020.12.025

Sachs, L. (1987). Cell differentiation and bypassing of genetic defects in the suppression of malignancy. *Cancer Research*, *47*(8), 1981–1986.

Salci, K. R., Lee, J.-H., Laronde, S., Dingwall, S., Kushwah, R., Fiebig-Comyn, A., Leber, B., Foley, R., Dal Cin, A., & Bhatia, M. (2015). Cellular Reprogramming Allows Generation of Autologous Hematopoietic Progenitors From AML Patients That Are Devoid of Patient-Specific Genomic Aberrations. *Stem Cells (Dayton, Ohio)*, *33*(6), 1839–1849. https://doi.org/10.1002/stem.1994

Salehzadeh, S., Guerrini, F., Pizzano, U., Grassi, S., Ciabatti, E., Iovino, L., Buda, G., Caracciolo, F., Benedetti, E., Orciuolo, E., Pelosini, M., Consani, G., Carulli, G., Metelli,

M. R., Martini, F., Mazziotta, F., Mazzantini, E., Rossi, P., Tavarozzi, R., … Galimberti, S. (2019). The assessment of minimal residual disease versus that of somatic mutations for predicting the outcome of acute myeloid leukemia patients. *Cancer Cell International*, *19*, 83. https://doi.org/10.1186/s12935-019-0807-0

Salomoni, P., & Pandolfi, P. P. (2002). The role of PML in tumor suppression. *Cell*, *108*(2), 165–170. https://doi.org/10.1016/s0092-8674(02)00626-8

Sawyers, C. L., Gishizky, M. L., Quan, S., Golde, D. W., & Witte, O. N. (1992). Propagation of human blastic myeloid leukemias in the SCID mouse. *Blood*, *79*(8), 2089–2098.

Schiffer, C. A. (2001). Management of patients refractory of platelet transfusion. *Leukemia*, *15*(4), 683–685. https://doi.org/10.1038/sj.leu.2402075

Schweitzer, J. S., Song, B., Herrington, T. M., Park, T.-Y., Lee, N., Ko, S., Jeon, J., Cha, Y., Kim, K., Li, Q., Henchcliffe, C., Kaplitt, M., Neff, C., Rapalino, O., Seo, H., Lee, I.-H., Kim, J., Kim, T., Petsko, G. A., … Kim, K.-S. (2020). Personalized iPSC-Derived Dopamine Progenitor Cells for Parkinson's Disease. *The New England Journal of Medicine*, *382*(20), 1926–1932. https://doi.org/10.1056/NEJMoa1915872

Shultz, L. D., Ishikawa, F., & Greiner, D. L. (2007). Humanized mice in translational biomedical research. *Nature Reviews. Immunology*, *7*(2), 118–130. https://doi.org/10.1038/nri2017

Shultz, L. D., Lyons, B. L., Burzenski, L. M., Gott, B., Chen, X., Chaleff, S., Kotb, M., Gillies, S. D., King, M., Mangada, J., Greiner, D. L., & Handgretinger, R. (2005). Human lymphoid and myeloid cell development in NOD/LtSz-scid IL2R gamma null mice engrafted with mobilized human hemopoietic stem cells. *Journal of Immunology (Baltimore, Md.: 1950)*, *174*(10), 6477–6489. https://doi.org/10.4049/jimmunol.174.10.6477

Simaria, A. S., Hassan, S., Varadaraju, H., Rowley, J., Warren, K., Vanek, P., & Farid, S. S. (2014). Allogeneic cell therapy bioprocess economics and optimization: Single-use cell expansion technologies. *Biotechnology and Bioengineering*, *111*(1), 69–83. https://doi.org/10.1002/bit.25008

Siminovitch, L., Mcculloch, E. A., & Till, J. E. (1963). THE DISTRIBUTION OF COLONY-FORMING CELLS AMONG SPLEEN COLONIES. *Journal of Cellular and Comparative Physiology*, *62*, 327–336. https://doi.org/10.1002/jcp.1030620313

Slukvin, I. I. (2013). Hematopoietic specification from human pluripotent stem cells: Current advances and challenges toward de novo generation of hematopoietic stem cells. *Blood*, *122*(25), 4035–4046. https://doi.org/10.1182/blood-2013-07-474825

Smith, A. R., & Wagner, J. E. (2009). Alternative haematopoietic stem cell sources for transplantation: Place of umbilical cord blood. *British Journal of Haematology*, *147*(2), 246–261. https://doi.org/10.1111/j.1365-2141.2009.07828.x

Song, B., Cha, Y., Ko, S., Jeon, J., Lee, N., Seo, H., Park, K.-J., Lee, I.-H., Lopes, C., Feitosa, M., Luna, M. J., Jung, J. H., Kim, J., Hwang, D., Cohen, B. M., Teicher, M. H., Leblanc, P., Carter, B. S., Kordower, J. H., … Kim, K.-S. (2020). Human autologous iPSC-derived dopaminergic progenitors restore motor function in Parkinson's disease models. *The Journal of Clinical Investigation*, *130*(2), 904–920. https://doi.org/10.1172/JCI130767

Speicher, M. R., & Carter, N. P. (2005). The new cytogenetics: Blurring the boundaries with molecular biology. *Nature Reviews. Genetics*, *6*(10), 782–792. https://doi.org/10.1038/nrg1692

Stadtfeld, M., Nagaya, M., Utikal, J., Weir, G., & Hochedlinger, K. (2008). Induced pluripotent stem cells generated without viral integration. *Science (New York, N.Y.)*, *322*(5903), 945–949. https://doi.org/10.1126/science.1162494

Stevens, L. C. (1958). Studies on transplantable testicular teratomas of strain 129 mice. *Journal of the National Cancer Institute*, *20*(6), 1257–1275. https://doi.org/10.1093/jnci/20.6.1257

Stevens, L. C. (1960). Embryonic potency of embryoid bodies derived from a transplantable testicular teratoma of the mouse. *Developmental Biology*, *2*, 285–297. https://doi.org/10.1016/0012-1606(60)90010-5

Stevens, L. C. (1970). The development of transplantable teratocarcinomas from intratesticular grafts of pre- and postimplantation mouse embryos. *Developmental Biology*, *21*(3), 364–382. https://doi.org/10.1016/0012-1606(70)90130-2

Stevens, L. C., & Hummel, K. P. (1957). A description of spontaneous congenital testicular teratomas in strain 129 mice. *Journal of the National Cancer Institute*, *18*(5), 719–747.

Stevens, L. C., & Little, C. C. (1954). Spontaneous Testicular Teratomas in an Inbred Strain of Mice. *Proceedings of the National Academy of Sciences of the United States of America*, *40*(11), 1080–1087. https://doi.org/10.1073/pnas.40.11.1080

Stricker, S. H., Feber, A., Engström, P. G., Carén, H., Kurian, K. M., Takashima, Y., Watts, C., Way, M., Dirks, P., Bertone, P., Smith, A., Beck, S., & Pollard, S. M. (2013). Widespread resetting of DNA methylation in glioblastoma-initiating cells suppresses malignant cellular behavior in a lineage-dependent manner. *Genes & Development*, *27*(6), 654–669. https://doi.org/10.1101/gad.212662.112

Sturgeon, C. M., Ditadi, A., Awong, G., Kennedy, M., & Keller, G. (2014). Wnt signaling controls the specification of definitive and primitive hematopoiesis from human pluripotent stem cells. *Nature Biotechnology*, *32*(6), 554–561. https://doi.org/10.1038/nbt.2915

Subramanyam, D., Belair, C. D., Barry-Holson, K. Q., Lin, H., Kogan, S. C., Passegué, E., & Blelloch, R. (2010). PML-RAR{alpha} and Dnmt3a1 cooperate in vivo to promote acute promyelocytic leukemia. *Cancer Research*, *70*(21), 8792–8801. https://doi.org/10.1158/0008-5472.CAN-08-4481

Sugimura, R., Jha, D. K., Han, A., Soria-Valles, C., da Rocha, E. L., Lu, Y.-F., Goettel, J. A., Serrao, E., Rowe, R. G., Malleshaiah, M., Wong, I., Sousa, P., Zhu, T. N., Ditadi, A., Keller, G., Engelman, A. N., Snapper, S. B., Doulatov, S., & Daley, G. Q. (2017). Haematopoietic stem and progenitor cells from human pluripotent stem cells. *Nature*, *545*(7655), 432–438. https://doi.org/10.1038/nature22370

Sullivan, S., Stacey, G. N., Akazawa, C., Aoyama, N., Baptista, R., Bedford, P., Bennaceur Griscelli, A., Chandra, A., Elwood, N., Girard, M., Kawamata, S., Hanatani, T., Latsis, T., Lin, S., Ludwig, T. E., Malygina, T., Mack, A., Mountford, J. C., Noggle, S., … Song, J. (2018). Quality control guidelines for clinical-grade human induced pluripotent stem cell lines. *Regenerative Medicine*, *13*(7), 859–866. https://doi.org/10.2217/rme-2018-0095

Suzuki, N., Yamazaki, S., Yamaguchi, T., Okabe, M., Masaki, H., Takaki, S., Otsu, M., & Nakauchi, H. (2013). Generation of engraftable hematopoietic stem cells from induced pluripotent stem cells by way of teratoma formation. *Molecular Therapy: The Journal of*

the American Society of Gene Therapy, *21*(7), 1424–1431. https://doi.org/10.1038/mt.2013.71

Szabo, E., Rampalli, S., Risueño, R. M., Schnerch, A., Mitchell, R., Fiebig-Comyn, A., Levadoux-Martin, M., & Bhatia, M. (2010). Direct conversion of human fibroblasts to multilineage blood progenitors. *Nature*, *468*(7323), 521–526. https://doi.org/10.1038/nature09591

Tada, M., Takahama, Y., Abe, K., Nakatsuji, N., & Tada, T. (2001). Nuclear reprogramming of somatic cells by in vitro hybridization with ES cells. *Current Biology: CB*, *11*(19), 1553–1558. https://doi.org/10.1016/s0960-9822(01)00459-6

Takagi, S., Mandai, M., Gocho, K., Hirami, Y., Yamamoto, M., Fujihara, M., Sugita, S., Kurimoto, Y., & Takahashi, M. (2019). Evaluation of Transplanted Autologous Induced Pluripotent Stem Cell-Derived Retinal Pigment Epithelium in Exudative Age-Related Macular Degeneration. *Ophthalmology. Retina*, *3*(10), 850–859. https://doi.org/10.1016/j.oret.2019.04.021

Takahashi, K., Tanabe, K., Ohnuki, M., Narita, M., Ichisaka, T., Tomoda, K., & Yamanaka, S. (2007). Induction of Pluripotent Stem Cells from Adult Human Fibroblasts by Defined Factors. *Cell*, *131*(5), 861–872. https://doi.org/10.1016/j.cell.2007.11.019

Takahashi, K., & Yamanaka, S. (2006). Induction of Pluripotent Stem Cells from Mouse Embryonic and Adult Fibroblast Cultures by Defined Factors. *Cell*, *126*(4), 663–676. https://doi.org/10.1016/j.cell.2006.07.024

Talib, S., & Shepard, K. A. (2020). Unleashing the cure: Overcoming persistent obstacles in the translation and expanded use of hematopoietic stem cell-based therapies. *Stem Cells Translational Medicine*, *9*(4), 420–426. https://doi.org/10.1002/sctm.19-0375

Tanaka, A., Yuasa, S., Node, K., & Fukuda, K. (2015). Cardiovascular Disease Modeling Using Patient-Specific Induced Pluripotent Stem Cells. *International Journal of Molecular Sciences*, *16*(8), 18894–18922. https://doi.org/10.3390/ijms160818894

Taylor, S. M., & Jones, P. A. (1979). Multiple new phenotypes induced in 10T1/2 and 3T3 cells treated with 5-azacytidine. *Cell*, *17*(4), 771–779.

Tefferi, A. (2008). The history of myeloproliferative disorders: Before and after Dameshek. *Leukemia*, *22*(1), 3–13. https://doi.org/10.1038/sj.leu.2404946

Thomas, E. D., Lochte, H. L., Cannon, J. H., Sahler, O. D., & Ferrebee, J. W. (1959). Supralethal whole body irradiation and isologous marrow transplantation in man. *The Journal of Clinical Investigation*, *38*, 1709–1716. https://doi.org/10.1172/JCI103949

Thomas, E. D., Lochte, H. L., Lu, W. C., & Ferrebee, J. W. (1957). Intravenous infusion of bone marrow in patients receiving radiation and chemotherapy. *The New England Journal of Medicine*, *257*(11), 491–496. https://doi.org/10.1056/NEJM195709122571102

Thomson, J. A., Itskovitz-Eldor, J., Shapiro, S. S., Waknitz, M. A., Swiergiel, J. J., Marshall, V. S., & Jones, J. M. (1998). Embryonic stem cell lines derived from human blastocysts. *Science (New York, N.Y.)*, *282*(5391), 1145–1147. https://doi.org/10.1126/science.282.5391.1145

Till, J. E., & McCULLOCH, E. A. (1961). A direct measurement of the radiation sensitivity of normal mouse bone marrow cells. *Radiation Research*, *14*, 213–222.

Till, J. E., & McCulloch, E. A. (2012). A direct measurement of the radiation sensitivity of normal mouse bone marrow cells. 1961. *Radiation Research*, *178*(2), AV3-7. https://doi.org/10.1667/rrav01.1

van Gils, N., Denkers, F., & Smit, L. (2021). Escape From Treatment; the Different Faces of Leukemic Stem Cells and Therapy Resistance in Acute Myeloid Leukemia. *Frontiers in Oncology*, *11*, 659253. https://doi.org/10.3389/fonc.2021.659253

Vodyanik, M. A., Bork, J. A., Thomson, J. A., & Slukvin, I. I. (2005). Human embryonic stem cell-derived CD34+ cells: Efficient production in the coculture with OP9 stromal cells and analysis of lymphohematopoietic potential. *Blood*, *105*(2), 617–626. https://doi.org/10.1182/blood-2004-04-1649

Wang, J. C., Doedens, M., & Dick, J. E. (1997). Primitive human hematopoietic cells are enriched in cord blood compared with adult bone marrow or mobilized peripheral blood as measured by the quantitative in vivo SCID-repopulating cell assay. *Blood*, *89*(11), 3919–3924.

Wang, L., Li, L., Shojaei, F., Levac, K., Cerdan, C., Menendez, P., Martin, T., Rouleau, A., & Bhatia, M. (2004). Endothelial and hematopoietic cell fate of human embryonic stem cells originates from primitive endothelium with hemangioblastic properties. *Immunity*, *21*(1), 31–41. https://doi.org/10.1016/j.immuni.2004.06.006

Wang, L., Menendez, P., Shojaei, F., Li, L., Mazurier, F., Dick, J. E., Cerdan, C., Levac, K., & Bhatia, M. (2005). Generation of hematopoietic repopulating cells from human embryonic stem cells independent of ectopic HOXB4 expression. *The Journal of Experimental Medicine*, *201*(10), 1603–1614. https://doi.org/10.1084/jem.20041888

Warren, L., Manos, P. D., Ahfeldt, T., Loh, Y.-H., Li, H., Lau, F., Ebina, W., Mandal, P. K., Smith, Z. D., Meissner, A., Daley, G. Q., Brack, A. S., Collins, J. J., Cowan, C., Schlaeger, T. M., & Rossi, D. J. (2010). Highly efficient reprogramming to pluripotency

and directed differentiation of human cells with synthetic modified mRNA. *Cell Stem Cell*, *7*(5), 618–630. https://doi.org/10.1016/j.stem.2010.08.012

Watanabe, A., Yamada, Y., & Yamanaka, S. (2013). Epigenetic regulation in pluripotent stem cells: A key to breaking the epigenetic barrier. *Philosophical Transactions of the Royal Society of London. Series B, Biological Sciences*, *368*(1609), 20120292. https://doi.org/10.1098/rstb.2012.0292

Watanabe-Okochi, N., Kitaura, J., Ono, R., Harada, H., Harada, Y., Komeno, Y., Nakajima, H., Nosaka, T., Inaba, T., & Kitamura, T. (2008). AML1 mutations induced MDS and MDS/AML in a mouse BMT model. *Blood*, *111*(8), 4297–4308. https://doi.org/10.1182/blood-2007-01-068346

Welch, J. S., Ley, T. J., Link, D. C., Miller, C. A., Larson, D. E., Koboldt, D. C., Wartman, L. D., Lamprecht, T. L., Liu, F., Xia, J., Kandoth, C., Fulton, R. S., McLellan, M. D., Dooling, D. J., Wallis, J. W., Chen, K., Harris, C. C., Schmidt, H. K., Kalicki-Veizer, J. M., … Wilson, R. K. (2012). The Origin and Evolution of Mutations in Acute Myeloid Leukemia. *Cell*, *150*(2), 264–278. https://doi.org/10.1016/j.cell.2012.06.023

Wesely, J., Kotini, A. G., Izzo, F., Luo, H., Yuan, H., Sun, J., Georgomanoli, M., Zviran, A., Deslauriers, A. G., Dusaj, N., Nimer, S. D., Leslie, C., Landau, D. A., Kharas, M. G., & Papapetrou, E. P. (2020). Acute Myeloid Leukemia iPSCs Reveal a Role for RUNX1 in the Maintenance of Human Leukemia Stem Cells. *Cell Reports*, *31*(9), 107688. https://doi.org/10.1016/j.celrep.2020.107688

Wiseman, D. H., & Somervaille, T. C. P. (2017). Nanofluidic Allele-Specific Digital PCR Method for Quantifying IDH1 and IDH2 Mutation Burden in Acute Myeloid Leukemia.

Methods in Molecular Biology (Clifton, N.J.), *1633*, 235–255. https://doi.org/10.1007/978-1-4939-7142-8_15

Wognum, B., Yuan, N., Lai, B., & Miller, C. L. (2013). Colony forming cell assays for human hematopoietic progenitor cells. *Methods in Molecular Biology (Clifton, N.J.)*, *946*, 267–283. https://doi.org/10.1007/978-1-62703-128-8_17

Xie, H., Ye, M., Feng, R., & Graf, T. (2004). Stepwise reprogramming of B cells into macrophages. *Cell*, *117*(5), 663–676. https://doi.org/10.1016/s0092-8674(04)00419-2

Xie, W., Schultz, M. D., Lister, R., Hou, Z., Rajagopal, N., Ray, P., Whitaker, J. W., Tian, S., Hawkins, R. D., Leung, D., Yang, H., Wang, T., Lee, A. Y., Swanson, S. A., Zhang, J., Zhu, Y., Kim, A., Nery, J. R., Urich, M. A., … Ren, B. (2013). Epigenomic analysis of multilineage differentiation of human embryonic stem cells. *Cell*, *153*(5), 1134–1148. https://doi.org/10.1016/j.cell.2013.04.022

Xu, C., Rosler, E., Jiang, J., Lebkowski, J. S., Gold, J. D., O'Sullivan, C., Delavan-Boorsma, K., Mok, M., Bronstein, A., & Carpenter, M. K. (2005). Basic fibroblast growth factor supports undifferentiated human embryonic stem cell growth without conditioned medium. *Stem Cells (Dayton, Ohio)*, *23*(3), 315–323. https://doi.org/10.1634/stemcells.2004-0211

Xu, R.-H., Sampsell-Barron, T. L., Gu, F., Root, S., Peck, R. M., Pan, G., Yu, J., Antosiewicz-Bourget, J., Tian, S., Stewart, R., & Thomson, J. A. (2008). NANOG is a direct target of TGFbeta/activin-mediated SMAD signaling in human ESCs. *Cell Stem Cell*, *3*(2), 196–206. https://doi.org/10.1016/j.stem.2008.07.001

Yamanaka, S. (2013). The winding road to pluripotency (Nobel Lecture). *Angewandte Chemie (International Ed. in English)*, *52*(52), 13900–13909. https://doi.org/10.1002/anie.201306721

Yamanaka, S. (2020). Pluripotent Stem Cell-Based Cell Therapy-Promise and Challenges. *Cell Stem Cell*, *27*(4), 523–531. https://doi.org/10.1016/j.stem.2020.09.014

Yamasaki, A. E., King, N. E., Matsui, H., Jepsen, K., & Panopoulos, A. D. (2019). Two iPSC lines generated from the bone marrow of a relapsed/refractory AML patient display normal karyotypes and myeloid differentiation potential. *Stem Cell Research*, *41*, 101587. https://doi.org/10.1016/j.scr.2019.101587

Yamasaki, A. E., Warshaw, J. N., Kyalwazi, B. L., Matsui, H., Jepsen, K., & Panopoulos, A. D. (2020). An iPSC line derived from a human acute myeloid leukemia cell line (HL-60-iPSC) retains leukemic abnormalities and displays myeloid differentiation defects. *Stem Cell Research*, *49*, 102096. https://doi.org/10.1016/j.scr.2020.102096

Yu, J., Vodyanik, M. A., Smuga-Otto, K., Antosiewicz-Bourget, J., Frane, J. L., Tian, S., Nie, J., Jonsdottir, G. A., Ruotti, V., Stewart, R., Slukvin, I. I., & Thomson, J. A. (2007). Induced pluripotent stem cell lines derived from human somatic cells. *Science (New York, N.Y.)*, *318*(5858), 1917–1920. https://doi.org/10.1126/science.1151526

Zhang, B., Duan, Z., & Zhao, Y. (2009). Mouse models with human immunity and their application in biomedical research. *Journal of Cellular and Molecular Medicine*, *13*(6), 1043–1058. https://doi.org/10.1111/j.1582-4934.2008.00347.x

Zhang, S. C., Wernig, M., Duncan, I. D., Brüstle, O., & Thomson, J. A. (2001). In vitro differentiation of transplantable neural precursors from human embryonic stem cells. *Nature Biotechnology*, *19*(12), 1129–1133. https://doi.org/10.1038/nbt1201-1129

Zhao, T., Zhang, Z.-N., Rong, Z., & Xu, Y. (2011). Immunogenicity of induced pluripotent stem cells. *Nature*, *474*(7350), 212–215. https://doi.org/10.1038/nature10135

Zhou, Q., Brown, J., Kanarek, A., Rajagopal, J., & Melton, D. A. (2008). In vivo reprogramming of adult pancreatic exocrine cells to beta-cells. *Nature*, *455*(7213), 627–632. https://doi.org/10.1038/nature07314

Zhu, X., Tang, B., & Sun, Z. (2021). Umbilical cord blood transplantation: Still growing and improving. *Stem Cells Translational Medicine*, *10 Suppl 2*, S62–S74. https://doi.org/10.1002/sctm.20-0495

Zovein, A. C., Hofmann, J. J., Lynch, M., French, W. J., Turlo, K. A., Yang, Y., Becker, M. S., Zanetta, L., Dejana, E., Gasson, J. C., Tallquist, M. D., & Iruela-Arispe, M. L. (2008). Fate tracing reveals the endothelial origin of hematopoietic stem cells. *Cell Stem Cell*, *3*(6), 625–636. https://doi.org/10.1016/j.stem.2008.09.018

Appendix II: Copyrights and permissions to reprint published material

Chapter 2: Challenges in cell fate acquisition to Scid-Repopulating Activity from hemogenic endothelium of hiPSCs derived from AML patients using forced transcription factor expression

Cells 2022, 11(12), 1915; https://doi.org/10.3390/cells11121915

Received: 27 March 2022 / Revised: 5 June 2022 / Accepted: 8 June 2022 / Published: 13 June 2022 (This article belongs to the Special Issue Generation of Hematopoietic Stem/Progenitor Cells from Pluripotent Stem Cells for Cellular Therapy)

Appendix III: List of Scientific Publications

Published Referred Papers

1. **Porras DP**, Reid JC, Tanasijevic B, Golubeva D, Boyd AL, Bhatia M. Challenges in Cell Fate Acquisition to Scid-Repopulating Activity from Hemogenic Endothelium of hiPSCs Derived from AML Patients Using Forced Transcription Factor Expression. *Cells* 11(12):1915 (2022). PMID: 35741044.
2. Vojnits K, Nakanishi M, **Porras DP**, Kim Y, Feng Z, Golubeva D, Bhatia M. Developing CRISPR/Cas9-Mediated Fluorescent Reporter Human Pluripotent Stem-Cell Lines for High-Content Screening. *Molecules* 27(8):2434 (2022). PMID: 35458632.
3. Aslostovar L, Boyd AL, Benoit YD, Di Lu J, Garcia Rodriguez JL, Nakanishi M, **Porras DP**, Reid JC, Mitchell RR, Leber B, Xenocostas A, Foley R, Bhatia M. Abnormal dopamine receptor signaling allows selective therapeutic targeting of neoplastic progenitors in AML patients. *Cell Rep Med* 2(2):100202 (2021). PMID: 33665638.
4. Orlando L, Tanasijevic B, Nakanishi M, Reid JC, García-Rodríguez JL, Chauhan KD, **Porras DP**, Aslostovar L, Lu JD, Shapovalova Z, Mitchell RR, Boyd AL, Bhatia M. Phosphorylation state of the histone variant H2A.X controls human stem and progenitor cell fate decisions. *Cell Rep* 34(10):108818 (2021). PMID: 33691101.
5. Benoit YD, Mitchell RR, Wang W, Orlando L, Boyd AL, Tanasijevic B, Aslostovar L, Shapovalova Z, Doyle M, Bergin CJ, Vojnits K, Casado FL, Di Lu J, **Porras DP**, García-Rodriguez JL, Russell J, Zouggar A, Masibag AN, Caba C, Koteva K, Kinthada LK, Patel JS, Andres SN, Magolan J, Collins TJ, Wright GD, Bhatia M. Targeting SUMOylation dependency in human cancer stem cells through a unique SAE2 motif revealed by chemical genomics. *Cell Chem Biol* 28(10):1394-1406 (2021). PMID: 33979648.
6. Boyd AL, Aslostovar L, Reid J, Ye W, Tanasijevic B, **Porras DP**, Shapovalova Z, Almakadi M, Foley R, Leber B, Xenocostas A, Bhatia M. Identification of Chemotherapy-Induced Leukemic-Regenerating Cells Reveals a Transient Vulnerability of Human AML Recurrence. *Cancer Cell* 34(3):483-498.e5 (2018). PMID: 30205048.
7. Reid JC, Tanasijevic B, Golubeva D, Boyd AL, **Porras DP**, Collins TJ, Bhatia M. CXCL12/CXCR4 Signaling Enhances Human PSC-Derived Hematopoietic Progenitor Function and Overcomes Early In Vivo Transplantation Failure. *Stem Cell Reports* 10(5):1625-1641 (2018). PMID: 29742393.
8. **Porras DP**, Abbaszadeh M, Bhattacharya D, D'Souza NC, Edjiu NR, Perry CGR, Scimè A. p107 Determines a Metabolic Checkpoint Required for Adipocyte Lineage Fates. *Stem Cells* 35(5):1378-1391 (2017). PMID: 28233396.
9. Boyd AL, Reid JC, Salci KR, Aslostovar L, Benoit YD, Shapovalova Z, Nakanishi M, **Porras DP**, Almakadi M, Campbell CJV, Jackson MF, Ross CA, Foley R, Leber B, Allan DS, Sabloff M, Xenocostas A, Collins TJ, Bhatia M. Acute myeloid leukaemia disrupts endogenous myelo-erythropoiesis by compromising the adipocyte bone marrow niche. *Nat Cell Biol* 19(11):1336-1347 (2017). PMID: 29035359.
10. Teich T, Pivovarov JA, **Porras DP**, Dunford EC, Riddell MC. Curcumin limits weight gain, adipose tissue growth, and glucose intolerance following the cessation of exercise and caloric restriction in rats. *J Appl Physiol (1985)* 123(6):1625-1634 (2017). PMID: 28839007.
11. Teich T, Dunford EC, **Porras DP**, Pivovarov JA, Beaudry JL, Hunt H, Belanoff JK, Riddell MC. Glucocorticoid antagonism limits adiposity rebound and glucose intolerance in young male rats following the cessation of daily exercise and caloric restriction. *Am J Physiol Endocrinol Metab* 311(1):E56-68 (2016). PMID: 27143556.

12. De Sousa M, **Porras DP**, Perry CG, Seale P, Scimè A. p107 is a crucial regulator for determining the adipocyte lineage fate choices of stem cells. *Stem Cells* 32(5):1323-36 (2014). PMID: 24449206.

Manuscripts Under Peer Review

1. Diana Golubeva*, **Deanna P Porras***, Meaghan Doyle, Jennifer C Reid, Borko Tanasijevic, Allison L Boyd and Mickie Bhatia. Reprogramming of Acute Myeloid Leukemia Patients Cells Harboring Cancer Mutations Requires Targeting of AML hierarchy. *Stem Cells Transl Med* 2022. ***Co-first author**
2. Allison L. Boyd, Justin Lu, Wendy Ye, Cameron G. Hollands, Jennifer C. Reid, Lili Alsostovar, **Deanna P Porras**, Dimetri Xenocostas, Andrew Leber, Shiva Murali, Maria Ines Pinto Sanchez, Ronan Foley, Brian Leber, Michael Trus, Eri Kawata, Anargyros Xenocostas, and Mickie Bhatia. Leukemic progenitor compartment serves as a measure of stemness that is prognostic for AML patient outcome. Cell Rep Med 2022.

Manuscripts awaiting submission

1. **Deanna P Porras**, Meaghan Doyle, Amy Qiao, Kinga Vojnits, Diana Golubeda, Amro Elrafie and Mickie Bhatia. Pluripotent reprogramming of acute myeloid leukemia from heterogenous patient specific DNA mutations demonstrates an exclusive block in hematopoietic lineage specification. Stem Cell Reports 2022.